THE BELL SYSTEM

Technical Journal

DEVOTED TO THE SCIENTIFIC AND ENGINEERING ASPECTS OF ELECTRICAL COMMUNICATION

VOLUME XXXI JULY 1952 NUMBER 4

THE BELL SYSTEM TECHNICAL JOURNAL

PUBLISHED SIX TIMES A YEAR BY THE

AMERICAN TELEPHONE AND TELEGRAPH COMPANY

195 BROADWAY, NEW YORK 7, N.Y.

CLEO F. CRAIG, *President*

CARROLL O. BICKELHAUPT, *Secretary*

DONALD R. BELCHER, *Treasurer*

SUBSCRIPTIONS

Subscriptions are accepted at $3.00 per year. Single copies are 75 cents each.

The foreign postage is 65 cents per year or 11 cents per copy.

PRINTED IN U.S.A.

The Bell System Technical Journal

Volume XXXI July 1952 Number 4

Thirtieth Anniversary

Thirty years ago this month THE BELL SYSTEM TECHNICAL JOURNAL began publication. Suggested by Dr. George A. Campbell, it had been under discussion for some years. Dr. R. W. King, who had been one of its most active advocates, became its editor when the staff of the JOURNAL was established. Except for a six-year period following 1928, while he was in England, Dr. King continued as editor until he retired in 1949.

By July, 1922, when No. 1, Vol. 1 of the JOURNAL appeared, research and development was a long established practice in the Bell System. The high-vacuum electronic tube, which had already begun to revolutionize electrical communication, was itself a product of Bell System research. Since electrical communication was a still comparatively new field of study, however, its publications were widely scattered. There seemed a need for a magazine that would serve the communication engineers exclusively, and it was largely to meet this need that THE BELL SYSTEM TECHNICAL JOURNAL was launched.

In the thirty years since that time, the art and science of communication has advanced and ramified beyond anything likely to have been then foreseen. A very substantial part of this increase has originated within the Bell System, and this progress has been reflected in the pages of the TECHNICAL JOURNAL. There seems little reason to doubt that the next three decades will witness an advance at least comparable with that of the past three, and it is planned to have the JOURNAL present the work of the coming years, with perhaps even greater effectiveness than in the past. Abstracts or titles of all Bell System technical and scientific papers appearing in other publications are listed in the JOURNAL and reprints of many of these papers are available and may be obtained by subscribers. In one way or another, therefore, JOURNAL readers have access to essentially all the technical papers published by the Bell System. With this increased coverage, it is hoped that the JOURNAL will prove increasingly useful to a growing circle of readers.

Lee de Forest and William Shockley Discuss Electronics

Dr. de Forest is the inventor of the Audion from which the modern vacuum tube in its many forms and types has sprung. Dr. Shockley is the leader of the research group at Bell Telephone Laboratories whose members invented the transistor. Standing side by side these two men seem to epitomize the basic change in the pattern of our technical life which has taken place during the first half of the present century—the change from the struggling individual inventor to the great industrial scientific laboratory as the source of much of our technological advance.

Network Synthesis Using Tchebycheff Polynomial Series†

By SIDNEY DARLINGTON

(Manuscript received April 17, 1952)

A general method is developed for finding functions of frequency which approximate assigned gain or phase characteristics, within the special class of functions which can be realized exactly as the gain or phase of finite networks of linear lumped elements. The method is based upon manipulations of two Tchebycheff polynomial series, one of which represents the assigned characteristic, and the other the approximating network function. The wide range of applicability is illustrated with a number of examples.

1. INTRODUCTION

Network synthesis is the opposite of network analysis—namely, the design of a network to have assigned characteristics, as opposed to the evaluation of the characteristics of an assigned network. In general, there are specifications on the internal constitution of the network, as well as requirements relating to its external performance. A common form of the general problem is the design of a finite network of linear lumped elements, to produce an assigned gain or phase characteristic over a prescribed interval of useful frequencies. The present paper relates to this particular form.

In general, the restrictions on the network are such that the assigned performance cannot be matched exactly. This gives rise to an approximation or interpolation problem. For present purposes, the problem is: to choose a function of frequency which matches the assigned gain or phase to a satisfactory accuracy, from that special class of functions which can be realized exactly with physical finite networks of linear lumped elements. The function of frequency may be defined in terms of network singularities (natural modes and infinite loss points). The

† Presented orally, in briefer form, at the 1951 Western Convention of the Institute of Radio Engineers, and at the Symposium on *Modern Network Synthesis* sponsored by the Polytechnic Institute of Brooklyn and The Office of Naval Research, New York City, April, 1952.

interpolation problem may then be regarded as solved when a suitable set of network singularities has been obtained; for quite different techniques are used to design actual networks with these singularities.

The interpolation problem may be attacked in a number of different ways; and a variety of different techniques are, in fact, needed to cover the wide diversity of practical applications. The present topic is a fairly general way of attacking the problem, based upon manipulations of two series of Tchebycheff polynomials. The two series represent expansions of two functions of frequency—one, the ideal assigned gain or phase, the other, the network approximation to the ideal. The interpolation problem may be solved in this way because it is feasible, as will be shown, to determine network singularities from arbitrarily assigned values of coefficients in the corresponding Tchebycheff polynomial series.

The techniques to be described were derived originally from studies of the so-called potential analogy; but they can now be developed most easily without reference thereto.† In a sense they may be regarded as extensions of familiar filter theory, using Tchebycheff polynomials, to more general gain and phase functions. The extensions, however, depend upon a number of new principles. Extensions of the filter theory applied to more general problems have been noted in published papers; but those noted have not used the specific general approach employed here.‡ The wide applicability of this general approach will be illustrated by specific examples.

2. NETWORK AND TRANSMISSION FUNCTION

It will be sufficient for our present purposes to limit the discussion to the general 4-pole shown in Fig. 1. The 4-pole may be active or passive, but it must be a stable finite network of linear lumped elements. E and V are steady state ac voltages, E the driving voltage and V the response. The gain α and phase β are here defined as the real and imaginary parts of $\log V/E$.

For a finite network of lumped elements, $\alpha + i\beta$ always has the following form:

$$\alpha + i\beta = \log K \frac{(p - p_1')(p - p_2') \cdots}{(p - p_1'')(p - p_2'') \cdots} \tag{1}$$

† Tchebycheff polynomials are related to potential analogue charges on ellipses, as described in the author's paper "The Potential Analogue Method of Network Synthesis"[1], Section 15.

‡ For the most part, they have used the potential analogy, in such a way that Tchebycheff polynomials do not appear at all in general applications. For examples, see methods of Matthaei[2], Bashkow[3], and Kuh[4].

The "frequency variable" p represents, of course, $i\omega$. The zeros p'_σ of the rational fraction are those values of p at which there is infinite loss. The poles p''_σ are the so-called natural modes, or values of p at which response V can exist in the absence of driving voltage E. The scale factor K determines the average level of transmission. The zeros, poles, and scale factor together determine the gain and phase completely.

For a physical stable network, the zeros and poles must meet certain well known restrictions, which are commonly stated in terms of locations in the complex plane for frequency variable p. Within these restrictions, the zeros and poles can be subject to arbitrary choice, say for purposes of network synthesis.

$\alpha + i\beta = \text{LOG } V/E$

Fig. 1—A general 4-pole.

The symmetries required by the physical restrictions permit α and β to be represented separately as follows:†

$$2\alpha = \log K^2 \frac{(p_1'^2 - p^2)(p_2'^2 - p^2)\cdots}{(p_1''^2 - p^2)(p_2''^2 - p^2)\cdots}$$
$$i2\beta = \log \frac{(p_1' - p)\cdots(p_1'' + p)\cdots}{(p_1' + p)\cdots(p_1'' - p)\cdots} \qquad (2)$$

These expressions hold at all real frequencies, but only at real frequencies.

3. TCHEBYCHEFF POLYNOMIALS

It is functions of these special types which we are to synthesize with the help of Tchebycheff polynomials. More generally, Tchebycheff polynomials come in various forms, and may be analyzed in various ways. For our special purposes, however, they take somewhat special forms (a little different from textbook definitions); and they are best analyzed in quite special ways.‡ It will be simplest to start with arbitrary definitions, to be justified later on by demonstrations of usefulness.

† The phase equation omits a possible 180° phase reversal, which is trivial for present purposes.

‡ For discussions of Tchebycheff polynomials from other viewpoints, see Courant and Hilbert[5], and also a paper by Lanczos[6] on trigonometric interpolation.

Actually, the definitions must vary with the nature of the useful frequency interval. For the present, however, it will be assumed that the useful interval extends from $\omega = 0$ to ω_c; or more precisely, from $\omega = -\omega_c$ to $+\omega_c$ (in accordance with the symmetries of gain and phase functions). Useful intervals which do not include $\omega = 0$ require changes in the definitions, which will be taken up in Section 28.

For our present purposes, Tchebycheff polynomials T_k may be defined as follows:

$$\begin{aligned} p &= i\omega = i\omega_c \sin \phi \\ T_k &= \cos k\phi, \quad k \text{ even} \\ T_k &= i \sin k\phi, \quad k \text{ odd} \end{aligned} \tag{3}$$

The first equation defines an auxiliary angle variable, ϕ, in terms of which T_k is especially simple. The imaginary scale factor i, associated with polynomials of odd order, simplifies later analysis. In addition, it

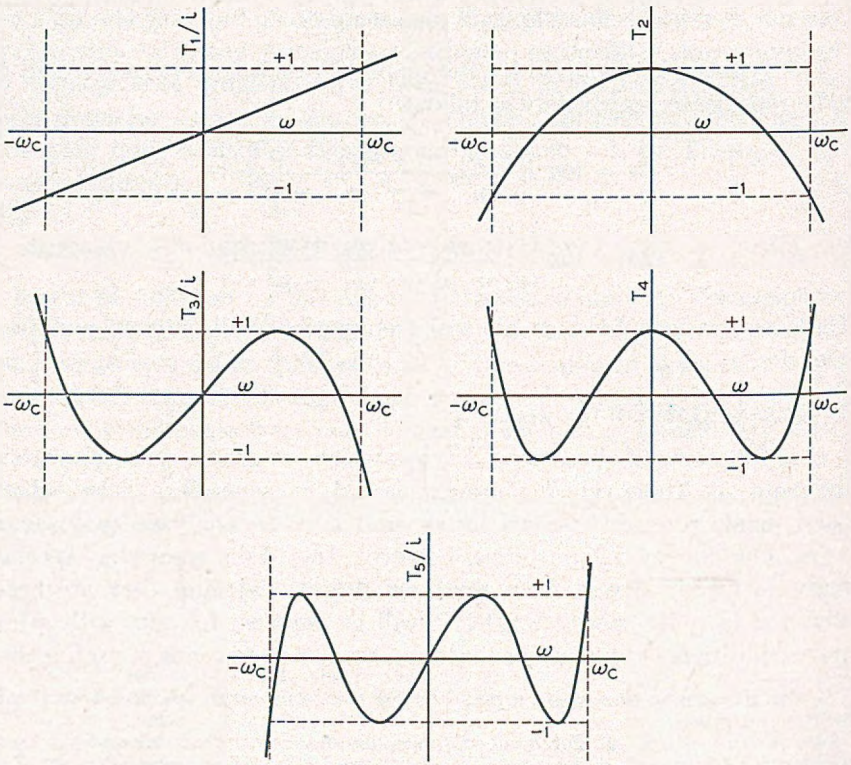

Fig. 2—Tchebycheff polynomials.

is especially appropriate for general network applications, because the odd ordered polynomials contribute to the imaginary parts of complex network functions—such as $i\beta$ in $\alpha + ib$.†

It is apparent from (3) that the Tchebycheff polynomials become simply Fourier harmonics, if they are plotted against a *distorted* frequency scale—that is, against ϕ. This means that they must be orthogonal, over that particular range of frequencies which corresponds to real values of ϕ. From the relation between ϕ and ω, it is clear that real values of ϕ cover the frequency interval between $-\omega_c$ and $+\omega_c$, which is our useful interval. In other words, the interval of orthogonality coincides with the useful frequency interval. The corresponding interval of p is of course $p = -i\omega_c$ to $+i\omega_c$.

If a given function is plotted against ϕ, instead of ω, it may be expanded in a Fourier series. Each term in the series may be replaced by a Tchebycheff polynomial, to obtain an expansion of a given function in terms of polynomials, for the specific useful interval $\omega = -\omega_c$ to $+\omega_c$. Established techniques are available for expanding experimental, or other numerical data, in Fourier series, as well as actual analytic functions.

In Fig. 2, some of the Tchebycheff polynomials are plotted against ω. The frequencies $-\omega_c$ and $+\omega_c$ are also indicated. Frequencies between these limits correspond to real values of the angle variable ϕ. If this part of the frequency scale is stretched, in the proper non-uniform way, the various "loops" not only have the same maximum values, but also the same shapes. In other words, they become periodic. More specifically, a stretch which changes the frequency scale into a ϕ scale changes the plots into $\sin k\phi$ or $\cos k\phi$.

4. TRANSFORMATION OF VARIABLE

An alternate to (3) may be obtained by relating a new variable, z, to ϕ by

$$z = e^{i\phi} \tag{4}$$

Substituting z in the exponential equivalent of $\sin \phi$, in the first equation of (3), gives an alternative definition of z directly in terms of p, namely:

$$p = \frac{\omega_c}{2}\left(z - \frac{1}{z}\right) \tag{5}$$

† A small change in the definition of ϕ would bring the definitions closer to convention, by replacing both sines by cosines (without altering T_k as a function of p). This however, would complicate our later analysis.

Substitutions in the exponential equivalents of the other sine and cosine in (3) give:

$$T_k = \frac{1}{2}\left(z^k + \frac{1}{z^k}\right), \quad k \text{ even}$$
$$T_k = \frac{1}{2}\left(z^k - \frac{1}{z^k}\right), \quad k \text{ odd} \tag{6}$$

Network applications depend upon the nature of the relationship between the variable p, and the variable z. The relationship is illustrated in Fig. 3, which indicates corresponding contours in the p and z planes.

Since angle ϕ is real in the useful interval, z, as defined by (4), has unit magnitude. In equivalent conformal mapping terms, the unit circle in the z plane maps onto a segment of the axis of real frequencies in the p plane—namely the segment extending from $p = -i\omega_c$ to $+i\omega_c$. Hereafter, we shall say merely that the useful interval in the z plane is the unit circle, or $|z| = 1$. The real frequency intervals outside the useful interval map onto the imaginary axis in the z-plane.

z-plane circles with radii other than unity map onto p-plane ellipses, all with foci at $p = \pm i\omega_c$. This is reminiscent of filter theory using Tchebycheff polynomials, and in fact such a filter may be obtained by spacing z-plane mappings of natural modes uniformly around such a circle.†

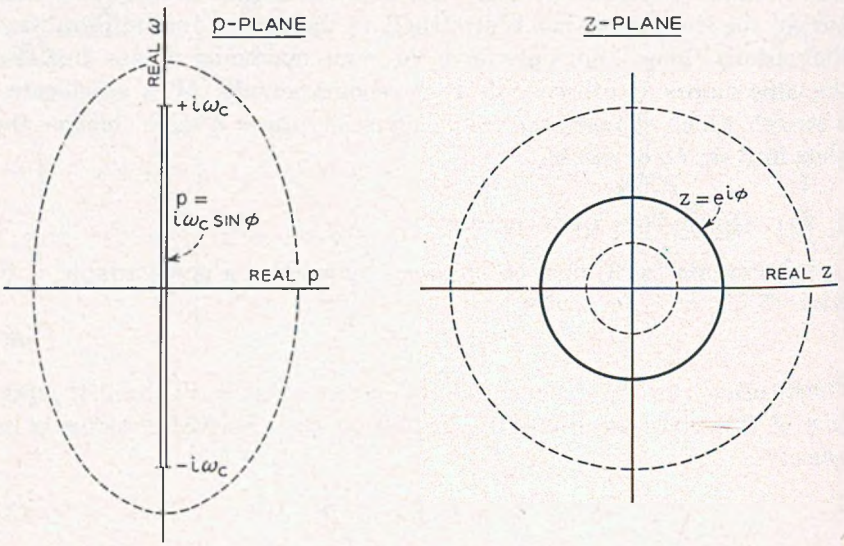

Fig. 3—The complex planes for p and z.

† The filter theory is developed in detail in a monograph by Wheeler[7], which also includes an extensive bibliography.

5. Z-PLANE MAPPINGS OF NETWORK SINGULARITIES

z-plane mappings of network singularities are also an essential part of synthesis applications. The mapping z_σ of a typical zero or pole p_σ is illustrated in Fig. 4. From (5), the analytic relation must be:

$$p_\sigma = \frac{\omega_c}{2}\left(z_\sigma - \frac{1}{z_\sigma}\right) \tag{7}$$

By its quadratic nature, there must be exactly *two* values of z_σ, corresponding to one p_σ. The relation is such that replacing z_σ by $-1/z_\sigma$ leaves p_σ unchanged; and hence the two values of z_σ must be negative reciprocals, each of the other. Thus, one mapping of p_σ falls outside the unit z-plane circle, and the other inside.

A unique definition of z_σ may be obtained by requiring that z_σ must be the mapping *outside* the unit circle. Then $|z_\sigma| > 1$ by definition, and the complete definition of z_σ may be:

$$p_\sigma = \frac{\omega_c}{2}\left(z_\sigma - \frac{1}{z_\sigma}\right) \qquad |z_\sigma| > 1 \tag{8}$$

This definition is unique provided network singularities p_σ are excluded from that very special line segment of the real frequency axis which corresponds to the useful frequency interval, $-\omega_c < \omega < +\omega_c$ (where $|z_\sigma|$ would be exactly 1).

We are going to solve the interpolation problem by choosing the z_σ first, instead of the p-plane singularities p_σ, after formulating the interpolation problem in suitable z-plane terms. For this, however, we must

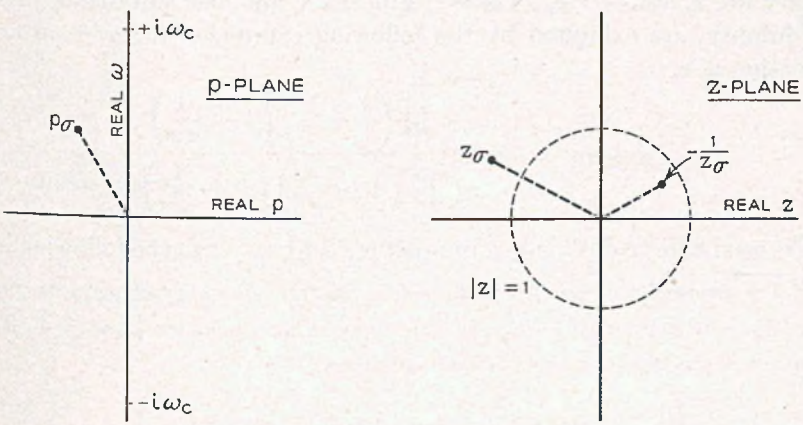

Fig. 4—Mappings of a network singularity.

know what further conditions must be imposed upon the z_σ, so that the corresponding p_σ will meet the special conditions necessary for physical networks. A simple analysis of the definition (8) of z_σ, and of the well known restrictions on the p_σ, leads to the following assertion;

The physical restrictions on z_σ are exactly the same as those on p_σ.

It is obvious, for example, that conjugate complex z_σ are necessary for conjugate complex p_σ. Also, because $|z_\sigma| > 1$, z_σ dominates $-1/z_\sigma$. Then the sign of Re p_σ is the same as that of the Re z_σ, and p_σ with negative real parts require z_σ with negative real parts, and so on.

Thus the direct choice of z_σ is restricted in exactly the same way as the choice of p_σ, except for the additional general requirement $|z_\sigma| > 1$. The last condition imposes no important restriction on the corresponding p_σ. Initially, it was adopted to make z_σ unique for any p_σ (not at a useful real frequency); but this condition does also play an essential role in the z-plane formulation of the interpolation problem.

6. NETWORK GAIN AND PHASE IN TERMS OF z

A first step in the z-plane formulation of the interpolation problem is the formulation of the network gain and phase functions, (1) and (2), in terms of z. This is most usefully examined as a transformation of functional form, rather than as a conformal mapping.

The gain and phase function (1) transforms as follows: The analytic relation between p and z is regular in the neighborhood of the singularities p_σ of the network function. Therefore, there will be similar singularities of the transformed function at the z-plane mappings of p_σ, which are z_σ and $-1/z_\sigma$. These singularities, and also suitable behavior at infinity, are exhibited by the following expression for $\alpha + i\beta$ as a function of z.

$$\alpha + i\beta = \log K_z' \frac{\prod \left(1 - \frac{z}{z_\sigma'}\right)\left(1 + \frac{1}{z_\sigma' z}\right)}{\prod \left(1 - \frac{z}{z_\sigma''}\right)\left(1 + \frac{1}{z_\sigma'' z}\right)} \tag{9}$$

$\prod$ is used here to designate a product of factors of the type following it.†

† The expression is readily confirmed in the following very elementary manner: For every factor $\left(1 - \frac{z}{z_\sigma}\right)$, in (9), there is also a factor $\left(1 + \frac{1}{z_\sigma z}\right)$. The product of the two may be expanded as follows:

$$\left(1 - \frac{z}{z_\sigma}\right)\left(1 + \frac{1}{z_\sigma z}\right) = \frac{1}{z_\sigma}\left[\left(z_\sigma - \frac{1}{z_\sigma}\right) - \left(z - \frac{1}{z}\right)\right] \tag{10}$$

If we define a new scale factor K_z by $K_z' = K_z^2$, we may write (9) as follows:

$$\alpha + i\beta = \log \left\{ K_z \frac{\prod \left(1 - \frac{z}{z_\sigma'}\right)}{\prod \left(1 - \frac{z}{z_\sigma''}\right)} \right\} \left\{ \begin{matrix} \text{Same Rational} \\ \text{Function in } -1/z \end{matrix} \right\} \tag{13}$$

Similar expressions for the separate gain and phase functions may be derived from (2):

$$2\alpha = \log \left\{ K_z^2 \frac{\prod \left(1 - \frac{z^2}{z_\sigma'^2}\right)}{\prod \left(1 - \frac{z^2}{z_\sigma''^2}\right)} \right\} \left\{ \begin{matrix} \text{Same Rational} \\ \text{Function in } -1/z \end{matrix} \right\}$$

$$i2\beta = \log \left\{ \prod \frac{1 - \frac{z}{z_\sigma'}}{1 + \frac{z}{z_\sigma'}} \prod \frac{1 + \frac{z}{z_\sigma'}}{1 - \frac{z}{z_\sigma''}} \right\} \left\{ \begin{matrix} \text{Same Rational} \\ \text{Function in } -1/z \end{matrix} \right\} \tag{14}$$

Equation (13) holds at all values of p and z, while (14) holds at all real frequencies. Simplifications of (14) should be noted, good for the useful interval only. When $|z| = 1$, $1/z = z^*$. Recalling also that $\log |x|^2$ is $2 \log |x|$, and similar elementary relations, one obtains from (14):

When $|z| = 1$,

$$\alpha = \log \left| K_z^2 \frac{\prod \left(1 - \frac{z^2}{z_\sigma'^2}\right)}{\prod \left(1 - \frac{z^2}{z_\sigma''^2}\right)} \right|$$

$$\beta = \text{Phase} \prod \frac{1 - \frac{z}{z_\sigma'}}{1 + \frac{z}{z_\sigma'}} \prod \frac{1 + \frac{z}{z_\sigma''}}{1 - \frac{z}{z_\sigma''}} \tag{15}$$

Comparison with (5) and (7) gives:

$$\left(1 - \frac{z}{z_\sigma}\right)\left(1 + \frac{1}{z_\sigma z}\right) = -\frac{2}{\omega_c z_\sigma} (p - p_\sigma) \tag{11}$$

Thus (9) is equivalent to (1) provided

$$K_z' = K \frac{\prod \left(-\frac{z_\sigma' \omega_c}{2}\right)}{\prod \left(-\frac{z_\sigma'' \omega_c}{2}\right)} \tag{12}$$

7. THE POWER SERIES IN z

Our applications to network synthesis depend upon a correspondence which may be shown to exist between certain functions of z and certain power series in z. The functions of z may be formulated in terms of network singularities. The power series in z may be derived from the Tchebycheff polynomial series in p representing the corresponding gain and phase.

The Tchebycheff polynomial expansion of a gain and phase function may be written:

$$\alpha + i\beta = \sum C_k T_k \tag{16}$$

If $\alpha + i\beta$ corresponds to a finite network, it may be represented by the function of z in (13). At the same time, T_k may be represented by the function of z in (6). With these changes, (16) becomes:

$$\log \left\{ K_z \frac{\prod \left(1 - \frac{z}{z'_\sigma}\right)}{\prod \left(1 - \frac{z}{z''_\sigma}\right)} \right\} \left\{ \begin{matrix} \text{Same Rational} \\ \text{Function in } -1/z \end{matrix} \right\} = \sum C_k \frac{1}{2} \left[z^k + \left(\frac{-1}{z} \right)^k \right] \tag{17}$$

The logarithm of the product of the two rational functions, in z and $-1/z$ respectively, may be written as the sum of two logarithms. The series in sums of z^k and $(-1/z)^k$ may be written as the sum of two series. Then

$$\log \left\{ K_z \frac{\prod \left(1 - \frac{z}{z'_\sigma}\right)}{\prod \left(1 - \frac{z}{z''_\sigma}\right)} \right\} + \log \left\{ \begin{matrix} \text{Same Rational} \\ \text{Function in } -1/z \end{matrix} \right\} = \sum \frac{C_k}{2} z^k + \sum \frac{C_k}{2} \left(\frac{-1}{z} \right)^k \tag{18}$$

The above expression equates the sum of two similar functions, in z and $-1/z$ respectively, to the sum of two power series, also respectively in z and $-1/z$. The theorem on which the synthesis methods are based asserts that the functions and power series in z and $-1/z$ may be equated separately, throughout the useful interval. That is:

When $|z| = 1$,

$$\log\left\{K_z \frac{\prod\left(1-\frac{z}{z'_\sigma}\right)}{\prod\left(1-\frac{z}{z''_\sigma}\right)}\right\} = \tfrac{1}{2}\sum C_k z^k$$

$$\log\left\{\begin{matrix}\text{Same Rational} \\ \text{Function in } -1/z\end{matrix}\right\} = \tfrac{1}{2}\sum C_k\left(\frac{-1}{z}\right)^k \tag{19}$$

The relation (18) does not, by itself, *require* (19) to be true. (19) follows from (18) if and only if the function of z has a power series expansion involving only positive powers of z, and the function in $-1/z$ has a power series expansion in $-1/z$, with the same coefficients. This added condition, however, is readily established for the useful interval.†

Combining (19) and (16) yields a most useful relationship connecting the z-plane mappings z_σ, of the network singularities p_σ, and the coefficients C_k, of the Tchebycheff polynomial expansion of $\alpha + i\beta$:

$$\alpha + i\beta = \sum C_k T_k$$

$$\sum \tfrac{1}{2} C_k z^k = \log K_z \frac{\prod\left(1-\frac{z}{z'_\sigma}\right)}{\prod\left(1-\frac{z}{z''_\sigma}\right)} \tag{20}$$

In more qualitative terms:

> *The transformation from variable p to variable z converts an expansion in Tchebycheff polynomials in p into an expansion in a power series in z.*

Thus, by working with the z_σ, in place of the p_σ, one may use a power series sort of analysis in calculating, or in choosing, the coefficients C_k in the Tchebycheff polynomial series.

The relations (20) refer to the combined gain and phase function. Exactly similar relations can readily be obtained, however, for gain and

† As defined in (8), $|z_\sigma| > 1$. In the useful interval, $|z| = 1$. Hence $|z/z_\sigma| < 1$. It follows that $\log(1 - z/z_\sigma)$ has a power (MacClauren) series expansion in positive powers of z, convergent on and within the circle $|z| = 1$. Finally the first logarithm in (19) may be expressed as a sum of logarithms of this simple type, each of which may be expanded separately. Substituting $-1/z$ for z maps the unit circle onto itself. It follows that the second logarithm in (19) has an expansion in positive powers of $-1/z$, in the useful interval, provided the first logarithm has an expansion in positive powers of z; and the coefficients in the two series will be the same.

phase separately. These may be derived from (14), and take the form:

$$\left.\begin{aligned} \alpha &= \sum C_k T_k \\ \sum C_k z^k &= \log K_z^2 \frac{\prod\left(1 - \frac{z^2}{z_\sigma'^2}\right)}{\prod\left(1 - \frac{z^2}{z_\sigma''^2}\right)} \end{aligned}\right\} k, \quad \text{even}$$

$$\left.\begin{aligned} i\beta &= \sum C_k T_k \\ \sum C_k z^k &= \log \prod \frac{1 - \frac{z}{z_\sigma'}}{1 + \frac{z}{z_\sigma'}} \prod \frac{1 + \frac{z}{z_\sigma''}}{1 - \frac{z}{z_\sigma''}} \end{aligned}\right\} k, \quad \text{odd} \tag{21}$$

(The absence of factors $\frac{1}{2}$ in $\sum C_k z^k$, as compared with (20), reflects the factors 2 associated with α and β in (14).)

8. REPRESENTATION OF ASSIGNED GAIN AND PHASE

In synthesis problems, the network gain or phase, α or β, is to approximate an assigned (ideal) gain or phase, say $\bar{\alpha}$ or $\bar{\beta}$. To make effective use of the z-plane analysis, in network synthesis, we need to describe $\bar{\alpha}$ and $\bar{\beta}$ by relations analogous to (20) and (21), which express α and β in z-plane terms. These relations, while similar to (20) and (21), must take a more general form (since $\bar{\alpha}$ or $\bar{\beta}$ need only be approximately the gain or phase of a finite network). For our present purposes, the appropriate relations are those noted below.

Let $\bar{\alpha} + i\bar{\beta}$ be any function of p which has the following properties: It must be analytic throughout the useful interval. Further, there are to be no singularities within a (p-plane) distance ϵ of the useful interval, where ϵ is *finite* (but may be small). Finally, at real frequencies, $\bar{\alpha}$ and $i\bar{\beta}$ are to equal respectively the even and odd parts of $\bar{\alpha} + i\bar{\beta}$.

Under the conditions stated, $\bar{\alpha} + i\bar{\beta}$ may always be expanded in terms of our Tchebycheff polynomials T_k. Let $\sum \bar{C}_k T_k$ be the expansion. To obtain a parallel to (20), we may form (arbitrarily) a power series $\sum \frac{1}{2}\bar{C}_k z^k$. Then we may *define* a function $\bar{R}(z)$ by identifying $\log \bar{R}(z)$ with the power series. All this adds up to the following, comparable to (20):

$$\begin{aligned} \bar{\alpha} + i\bar{\beta} &= \sum \bar{C}_k T_k \\ \sum \tfrac{1}{2}\bar{C}_k z^k &= \log \bar{R}(z) \end{aligned} \tag{22}$$

The functions of z have the following properties: Because of the mild restrictions, which we have imposed on the singularities of $\bar{\alpha} + i\bar{\beta}$, the series $\sum \bar{C}_k z^k$ defines a function which is analytic within, and on the circle $|z| = 1$. Then $\bar{R}(z)$, also, is analytic within, and on the circle. Further, $\bar{R}(z)$ has no zeros anywhere in the same region. ($\bar{R}(z)$, however, may be more general than the rational fraction in (20).) Finally, because of the even and odd symmetries, required of $\bar{\alpha}$ and $i\bar{\beta}$, (22) may be broken into the following parallels of the equations (21):

$$\left.\begin{aligned} \bar{\alpha} &= \sum \bar{C}_k T_k \\ \sum \bar{C}_k z^k &= \log [\bar{R}(z)\bar{R}(-z)] \end{aligned}\right\} k, \quad \text{even}$$

$$\left.\begin{aligned} i\bar{\beta} &= \sum \bar{C}_k T_k \\ \sum \bar{C}_k z^k &= \log \left[\frac{\bar{R}(z)}{\bar{R}(-z)}\right] \end{aligned}\right\} k, \quad \text{odd} \tag{23}$$

In some applications, it is possible to express $\bar{R}(z)$ in closed form. In all applications, it is possible to expand $\bar{R}(z)$ as a power series, convergent in the region $|z| \leqq 1$. The same is true of $1/\bar{R}(z)$, since there are no zeros in the region. Coefficients of either series ($\bar{R}(z)$ or $1/\bar{R}(z)$) may readily be calculated by means which we shall examine a little later. For the present we shall say merely that $\bar{R}(z)$ is a *known* function, corresponding to an assigned $\bar{\alpha} + i\bar{\beta}$.

9. A DESIGN CRITERION

When the gain and phase function, $\alpha + i\beta$, is to approximate $\bar{\alpha} + i\bar{\beta}$, the error in the approximation is $(\alpha - \bar{\alpha}) + i(\beta - \bar{\beta})$. The error may be expressed in terms of z by taking the difference of corresponding equations in (20), (22). The difference of the logarithms may be expressed as a single logarithm of a ratio. Alternatively, and also more conveniently for our later purposes, it may be expressed as the negative of the logarithm of the reciprocal ratio. When this is done,

$$(\alpha - \bar{\alpha}) + i(\beta - \bar{\beta}) = \sum (C_k - \bar{C}_k) T_k$$

$$\sum \tfrac{1}{2}(C_k - \bar{C}_k) z^k = -\log \left\{ \frac{1}{K_z} \frac{\prod \left(1 - \frac{z}{z_\sigma}\right)}{\prod \left(1 - \frac{z}{z_\sigma}\right)} \cdot \bar{R}(z) \right\} \tag{24}$$

Consider the following arbitrary requirement, as a design criterion: The series $\sum C_k T_k$ is to match exactly the series $\sum \bar{C}_k T_k$, through

terms of order m. If both series have converged to small remainders when $k = m$, this criterion will surely make $\alpha + i\beta$ a good approximation to $\bar{\alpha} + i\bar{\beta}$.† In terms of the coefficients, the criterion requires:

$$C_k = \bar{C}_k , \qquad k \leqq m \qquad (25)$$

If (25) is applied to the second equation of (24), the power series is zero through terms of order m. In other words, the logarithm, equated to the series, will approximate zero in the power series, or "maximally flat" manner, to order m. The logarithm is zero when the expression in brackets is unity. Further, the logarithm will approximate zero in the maximally flat manner when, and only when the bracket approximates unity in the maximally flat manner. Thus a condition which is equivalent to (25) is the following:

$$\frac{1}{K_z} \frac{\prod \left(1 - \frac{z}{z_\sigma''}\right)}{\prod \left(1 - \frac{z}{z_\sigma'}\right)} \cdot \bar{R}(z) = 1 + \epsilon_{m+1} z^{m+1} + \epsilon_{m+2} z^{m+2} \cdots \qquad (26)$$

This may be represented symbolically by

$$\frac{1}{K_z} \frac{\prod \left(1 - \frac{z}{z_\sigma''}\right)}{\prod \left(1 - \frac{z}{z_\sigma'}\right)} \cdot \bar{R}(z) \overset{m}{=} 1 \qquad (27)$$

where $\overset{m}{=}$ is used to indicate equality through power series terms of order m.

When (27) is applied to network synthesis, the singularities z_σ, and scale factor K_z are the unknowns, while $\bar{R}(z)$ is known. If m is equal to the total number of z_σ, (27) will determine the network function completely. When m is smaller, (27) will furnish $m + 1$ relations between the network parameters (including the zero order condition), which may be combined with specifications of other sorts. Since (27) is equivalent to (25), this procedure amounts to the determination of network parameters which will yield assigned values of the coefficients, $C_k = \bar{C}_k$, $k \leqq m$, in the Tchebycheff polynomial expansion of $\alpha + i\beta$.

Equation (27) applies when both gain and phase are to be approximated. For approximation to gain only, or to phase only, similar relations may be derived from (21) and (23). Only even ordered Tchebycheff

† When both residues are relatively large, the approximation *may* still be good, for the remainders may be quite similar, and the error will be their difference. In practical applications, this is a not uncommon situation.

polynomials contribute to gain. The following condition turns out to be the equivalent of $C_{2k} = \bar{C}_{2k}$, $k \leqq m$:

$$\frac{1}{K_z^2} \frac{\prod \left(1 - \frac{z^2}{z_\sigma''^2}\right)}{\prod \left(1 - \frac{z^2}{z_\sigma'^2}\right)} \cdot \bar{R}(z)\bar{R}(-z) \overset{me}{=} 1 \tag{28}$$

where $\overset{me}{=}$ means approximation in accordance with a power series of even ordered terms, through order $2m$. Correspondingly, only odd ordered Tchebycheff polynomials contribute to phase. The following condition is equivalent to $C_{2k-1} = \bar{C}_{2k-1}$, $k = 1$ to m:

$$\prod \frac{1 - \frac{z}{z_\sigma''}}{1 + \frac{z}{z_\sigma''}} \prod \frac{1 + \frac{z}{z_\sigma'}}{1 - \frac{z}{z_\sigma'}} \cdot \frac{\bar{R}(z)}{\bar{R}(-z)} \overset{2m}{=} 1 \tag{29}$$

The remaining sections (except the last) develop in more detail the application of z-plane techniques to more specific synthesis problems, of various sorts. Most of these (but not quite all) are based directly on (27), (28), or (29). The exceptions use a modification of (28), in which the function of z on the left is retained, but with the zeros and poles adjusted for a different kind of approximation to unity, $\cong$ but not $\overset{me}{=}$.

In all cases, unity is approximated with one of the functions appearing in (27), (28), (29). It will be convenient to use $H(z)$ to represent the error in the approximation, or departure from unity. When gain only is of interest, the function in (28) is used, and $H(z)$ is defined by:

$$\frac{1}{K_z^2} \frac{\prod \left(1 - \frac{z^2}{z_\sigma''^2}\right)}{\prod \left(1 - \frac{z^2}{z_\sigma'^2}\right)} \cdot \bar{R}(z)\bar{R}(-z) = 1 + H(z) \tag{30}$$

In developing the specific techniques, we shall start with a very definite, rather special example, in order to illustrate the techniques with specific operations. This will be discussed in considerable detail in Sections 10 through 14. Thereafter we shall examine how these specific operations may be generalized, in a number of different respects.

10. AN INTRODUCTORY EXAMPLE

The example which has been chosen for detailed discussion is the equalization of the gain distortion produced by two resistance-capacity

type cut-offs. The equalization is to be accomplished with a network which has n natural modes, but no finite frequencies of infinite loss. (This is simply one of the arbitrary specifications which define this problem.)

The two cut-offs may be due to circuits or devices at two different points in a communication system, which may be represented schematically as in Fig. 5. Their effect can be described in terms of two assigned natural modes. Two assigned modes are assumed, instead of only one, because a single mode would make the problem too simple. Our present purposes will be served well, however, if we simplify the problem by requiring the two assigned modes to be *identical*, say at $p = \bar{p}_0$.

Fig. 5—A system with two resistance-capacity type cut-offs.

The two natural modes would be cancelled completely by two infinite loss points at the same location in the p plane. A network with two infinite loss points, however, is not physically possible unless it has also at least two natural modes; and the natural modes will have to introduce distortion of their own. Thus no finite network will give *perfect* equalization of unwanted natural modes. Sometimes it is desirable, in practice, to use an equalizer configuration which produces *no* finite frequencies of infinite loss, the entire equalization being accomplished by a suitable choice of its n modes. Configurations of this sort are illustrated in Fig. 6. Thus, our simple illustrative problem, though chosen to introduce principles, is also of some practical interest.

The exclusion of finite frequencies of infinite loss simplifies the repre-

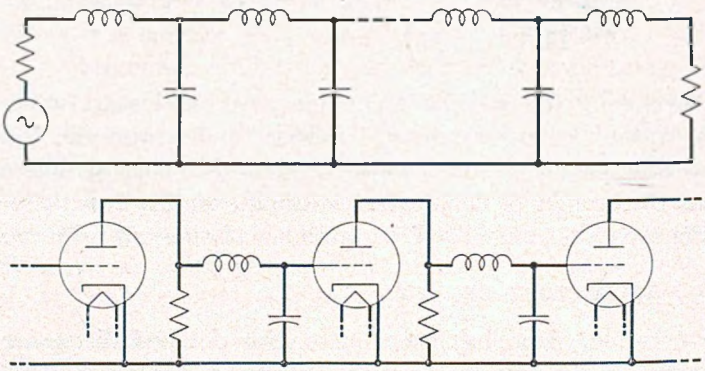

Fig. 6—Configurations which produce no finite frequencies of infinite loss.

sentation of the network gain α. In (21), the z'_σ correspond to finite frequencies of infinite loss, and are to be omitted when there are to be natural modes only. What is left is the logarithm of the reciprocal of a polynomial, which is of course the negative of the logarithm of the polynomial itself. Thus α may be described as follows, for this particular application:

$$\alpha = \sum C_{2k} T_{2k}$$

$$\sum C_{2k} z^{2k} = -\log K_z^2 \prod \left(1 - \frac{z^2}{z_\sigma^2}\right), \qquad \sigma = 1, \cdots, n \tag{31}$$

(For convenience, z_σ has been written for z''_σ, and K_z has been redefined to avoid the $1/K_z$ required if it is defined as in (21).)

The assigned gain $\bar{\alpha}$ is even more special. In this particular problem, $\bar{\alpha}$ has most of the properties of a network gain α. Specifically, it is the negative of the gain to be equalized, which in fact corresponds to a finite network. As a result, $\bar{R}(z)$ of (22) may be expressed in closed (rational) form. (Later on, we shall modify the methods appropriate for this very special situation, so that $\bar{R}(z)$ need be representable only by series.)

The specific representation of our present $\bar{\alpha}$ may be very similar to the representation of α in (31), as follows:

$$\bar{\alpha} = \sum \bar{C}_{2k} T_{2k}$$

$$\sum \bar{C}_{2k} z^{2k} = +\log \bar{K}_z^2 \left(1 - \frac{z^2}{\bar{z}_0^2}\right)^2 \tag{32}$$

(Both (31) and (32) apply only to the useful interval, $|z| = 1$.)

The constant $\bar{z}_0$ is the z-plane mapping of the assigned unwanted natural modes at $p = \bar{p}_0$, and may be calculated therefrom by (8). In (32), $\bar{z}_0$ determines the $\bar{C}_{2k}$, which in turn determine $\bar{\alpha}$. The constants z_σ, in (31), are the z-plane mappings of the arbitrary natural modes of the equalizer. They are to be adjusted to make α approximate $\bar{\alpha}$. Then the network natural modes p_σ may be calculated from them, by means of (8).

Taking the difference of corresponding equations in (31) and (32) gives the following, analogous to (24):

$$\alpha - \bar{\alpha} = \sum (C_{2k} - \bar{C}_{2k}) T_{2k}$$

$$\sum (C_{2k} - \bar{C}_{2k}) z^{2k} = -\log \left\{ K_z^2 \bar{K}_z^2 \left(1 - \frac{z^2}{\bar{z}_0^2}\right)^2 \prod \left(1 - \frac{z^2}{z_\sigma^2}\right) \right\} \tag{33}$$

This differs from (24) in two regards. It relates to the gain error, $(\alpha - \bar{\alpha})$,

without regard to phase. It reflects the more specific functional forms of our present α and $\bar{\alpha}$.

The formulas show that the coefficients in the Tchebycheff polynomial expansion of our present $\alpha - \bar{\alpha}$ are fixed by the logarithm of a polynomial in z^2, of degree $n + 2$. Since the Tchebycheff polynomial series is simply one representation of the function $\alpha - \bar{\alpha}$, this means that $\alpha - \bar{\alpha}$ itself is determined by the polynomial in z^2. Out of the $n + 2$ zeros, in terms of z^2, n are subject to arbitrary choice, but the other two are required to be at $z^2 = \bar{z}_0^2$.

To arrive at a useful choice of the zeros, one may start with the expanded form of the polynomial, which replaces the second equation of (33) by:

$$\sum (C_{2k} - \bar{C}_{2k}) z^{2k} = -\log \{\hat{K}_0 + \hat{K}_1 z^2 + \cdots \hat{K}_{n+2} z^{2n+4}\} \qquad (34)$$

All but two of the coefficients $\hat{K}_k$ may be assigned arbitrary values, provided the remaining two are then adjusted to give the required two zeros at $z^2 = \bar{z}_0^2$. The corresponding zeros z_σ^2 may then be found by ordinary root extraction methods.

The coefficients may be chosen in such a way that the complex polynomial approximates unity, when $| z | = 1$. Then the logarithm approximates zero, the coefficients in the power series (34) are small, and since these are also the coefficients in the Tchebycheff polynomial series in (33), $\alpha - \bar{\alpha}$ is small.

11. Tchebycheff Polynomial Series Matched Through n Terms

A special choice of coefficients, which meets these requirements fairly well, is the choice determined by (28), with $m = n$. The function on the left side of (28) is here the polynomial in (34). For our present purposes, therefore, (28) becomes:

$$\{\hat{K}_0 + \hat{K}_1 z^2 + \cdots \hat{K}_{n+2} z^{2n+4}\}^{ne} = 1 \qquad (35)$$

This requires $\hat{K}_0 = 1$, and $\hat{K}_k = 0$ for $k = 1$ to n. Then $\hat{K}_{n+1}$ and $\hat{K}_{n+2}$ must be adjusted to give the two required zeros at $z^2 = \bar{z}_0^2$. This gives:

$$\hat{K}_0 + \cdots \hat{K}_{n+2} z^{2n+4} = 1 - (n+2)\left(\frac{z}{\bar{z}_0}\right)^{2n+2} + (n+1)\left(\frac{z}{\bar{z}_0}\right)^{2n+4} \qquad (36)$$

In accordance with Section 9, this special choice of coefficients corresponds to a match of Tchebycheff polynomial series, α to $\bar{\alpha}$, through terms of order $2n$:

$$C_{2k} = \bar{C}_{2k}, \qquad k \leqq n \qquad (37)$$

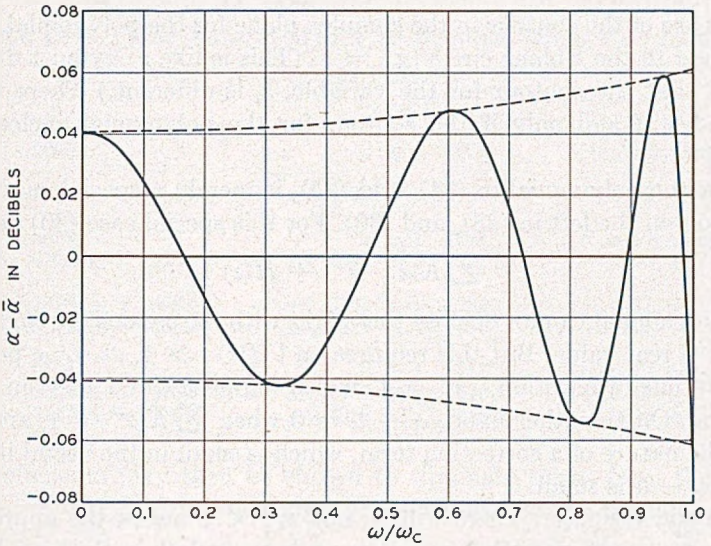

Fig. 7—Error when four natural modes equalize two natural modes at $\bar{p}_0 = -0.75\omega_c$.

The actual accuracy may be calculated from the final zeros and poles, from non-zero terms in the expansion of $\alpha - \bar{\alpha}$, or by an analysis in terms of z which will be described later.

A sample plot of $\alpha - \bar{\alpha}$ is shown in Fig. 7. This corresponds to an equalizer of four natural modes, compensating for an initial loss which rises to about 8 db at the top useful frequency, or a distortion of ± 4 db about the median loss. Residual errors are order of ± 0.06 db.

A little later we shall return to the question of accuracy, to take up methods of estimating what can be done with other numbers of arbitrary natural modes, and other values of the assigned modes. First, however, we should investigate whether the network singularities z_σ determined by (36) meet the other necessary conditions.

12. PROPERTIES OF z_σ

In the first place, $| z_\sigma |$ must be > 1. Otherwise, the function of z in (31) will have no power series expansion over the useful interval $| z | = 1$; and (31) will not, in fact, determine the gain α over the useful interval. It turns out, however, that the condition does not give trouble in the synthesis of natural modes, when there are no arbitrary frequencies of infinite loss. This may be demonstrated by the argument outlined below.

The z_σ are zeros of the polynomial in (34), which we have given the special form (36), by applying (35). A function theoretic test for $| z_\sigma | < 1$

makes use of the contour in the complex plane for the polynomial, corresponding to the z-plane circle $| z | = 1$. (This is like a Nyquist diagram except that the contour for the variable, z, is different.) There will be $| z_\sigma | < 1$ if and only if the contour for the polynomial encloses the origin.

Now the polynomial in (34), and (35), is merely a special case of the function on the left in (28), and (30). For this special case (30) becomes

$$\sum \hat{K}_k z^{2k} = 1 + H(z) \tag{38}$$

The polynomial cannot enclose the origin without passing through some negative real value. But this requires an $| H(z) | > 1$, at some point on the contour in question, $| z | = 1$, which happens to be also our useful interval. On the other hand, $\alpha - \bar{\alpha} = 0$ when $\sum \hat{K}_k z^{2k} = 1$, and $H(z)$ is in the nature of a correction term, which is small in the useful interval when $\alpha - \bar{\alpha}$ is small.

The conclusion is: There will be no $| z_\sigma | < 1$ unless the approximation, α to $\bar{\alpha}$, is so poor that $\alpha - \bar{\alpha}$ exceeds several db in the useful interval.

Besides the requirement $| z_\sigma | > 1$, the z_σ must meet physical restrictions, which we found to be the same as those limiting the natural modes p_σ. The z_σ may be calculated as follows: The z_σ^2 are roots of the polynomial in (35), in terms of z^2. All the roots in terms of z^2 are z_σ^2, except the two required roots at $\bar{z}_0^2$, which correspond to assigned gain $\bar{\alpha}$. Each z_σ is a square root of a z_σ^2. There are two possible square roots, however, differing only as to sign. As far as gain α is concerned, either choice of sign is permissible; for α depends only on z_σ^2. For a physical network, however, the choice must be such that Re $z_\sigma < 0$. This choice is possible if, and only if $\sqrt{z_\sigma^2}$ has a finite real part. A pure imaginary z_σ corresponds to a negative real z_σ^2, and thus negative real roots in terms of z^2 are excluded by physical considerations.

Table I lists both z_σ^2 and z_σ for a number of values of n. When n is even, all roots are physical. On the other hand, when n is odd, one root is always non-physical. In a sense, an odd n is not really appropriate for the present illustrative problem, with any physical design. An odd n must necessarily bring in a real natural mode, which merely increases the sort of distortion we are trying to equalize—that is the distortion due to unwanted real modes.

The following argument substantiates the suggestion, and also illustrates manipulations of a sort which are frequently useful in more general applications: The highest order coefficient in (34), $\hat{K}_{n+2}$, may be set aside for adjustments to satisfy physical requirements. The rest of

TABLE I—*Z-Plane Natural Modes for Equalization of Two Identical Unwanted Modes*

n	$z_\sigma^2/\bar{z}_0^2$	$\sqrt{z_\sigma^2/\bar{z}_0^2}$	$z_\sigma/\lvert\bar{z}_0\rvert$
1	$-.5000$	$0 \pm i\ .7071$	Non Physical
2	$-.3333 \pm i\ .4714$	$\pm(.3492 \pm i\ .6747)$	$-.3492 \pm i\ .6747$
3	$-.6059$	$0 \pm i\ .7784$	Non Physical
	$-.0720 \pm i\ .6384$	$\pm(.5340 \pm i\ .5977)$	$-.5340 \pm i\ .5977$
4	$+.1378 \pm i\ .6782$	$\pm(.6441 \pm i\ .5264)$	$-.6441 \pm i\ .5264$
	$-.5378 \pm i\ .3582$	$\pm(.2328 \pm i\ .7695)$	$-.2328 \pm i\ .7695$
5	$-.6703$	$0 \pm i\ .8187$	Non Physical
	$+.2942 \pm i\ .6684$	$\pm(.7157 \pm i\ .4670)$	$-.7157 \pm i\ .4670$
	$-.3757 \pm i\ .5701$	$\pm(.3918 \pm i\ .7275)$	$-.3918 \pm i\ .7275$

the coefficients may then be chosen to eliminate terms from the series $\sum (C_{2k} - \bar{C}_{2k})T_{2k}$, representing $\alpha - \bar{\alpha}$, subject to the previous condition that two zeros must be $z^2 = \bar{z}_0^2$. This replaces $\overset{ne}{=}$ by $\overset{(n-1)e}{=}$, in (35), and changes (36) to:

$$\sum \hat{K}_k z^{2k} = 1 - (n+1)\left(\frac{z}{\bar{z}_0}\right)^{2n} + n\left(\frac{z}{\bar{z}_0}\right)^{2n+2} + \hat{K}_{n+2} z^{2n} (\bar{z}_0^2 - z^2)^2 \tag{39}$$

If n is odd, all the roots z_σ can be physical only if $\hat{K}_{n+2}$ is negative. On the other hand, any finite negative $\hat{K}_{n+2}$ leads to a larger error, $\alpha - \bar{\alpha}$, than $\hat{K}_{n+2} = 0$. Reducing $\hat{K}_{n+2}$ to zero is the same as reducing the degree of the polynomial by one, which amounts to reducing n by 1, from an odd to the next smaller even integer. In other words, a *physical* design with an odd number of natural modes is less effective, for the present application, than a simpler network, with the next smaller even number of modes.

Note that the z_σ in Table I are proportional to $\bar{z}_0$. This means that root extraction methods need be used only once for each value of n, after which the roots may be quickly adjusted for any value of $\bar{z}_0$, corresponding to any assigned value of the two identical modes, $\bar{p}_0$.

13. ACCURACY

The accuracy of a completed design can be checked by calculating α from the natural modes p_σ, and comparing α with $\bar{\alpha}$. It is important, however, to have at least some information about accuracy in advance

of the detailed calculation of the p_σ. Otherwise, it may be necessary to carry out several designs, in all detail, in order to obtain one satisfactory design.

The needed information about accuracy can in fact be obtained from the error function $H(z)$, which we formulated for general gain applications in (30), and for the present application in (38). The analysis which yields (15) may be used to obtain a very similar expression for $\alpha - \bar{\alpha}$, in which $\bar{R}(z)\bar{R}(-z)$ appears in combination with the rational function of z from (15). It may be expressed in terms of the error function $H(z)$ of (30), as follows:

$$\alpha - \bar{\alpha} = -\log | 1 + H(z) | \tag{40}$$

When $H(z)$ is zero, $\alpha - \bar{\alpha}$ is zero. When $H(z)$ is small, $\alpha - \bar{\alpha}$ depends on phase $H(z)$ as much as on $| H(z) |$. When $H(z)$ is a positive real, $\alpha - \bar{\alpha}$ is negative. When $H(z)$ is imaginary, $\alpha - \bar{\alpha}$ is very small. When $H(z)$ is a negative real, $\alpha - \bar{\alpha}$ is positive. When $H(z)$ is complex, $| \alpha - \bar{\alpha} |$ is always smaller than with a real $H(z)$ of the same magnitude. The last statement may be expressed as follows:

$$-\log \{1 + | H(z) |\} \leqq \alpha - \bar{\alpha} \leqq -\log \{1 - | H(z) |\} \tag{41}$$

The left hand relation is an equality when phase $H(z)$ is an even number of π radians; the right hand side, when it is an odd number of π radians.

In the useful interval, where $z = e^{i\phi}$, the $H(z)$ corresponding to (36) is as follows:

$$\begin{aligned} H(z) &= -(n+2)\left(\frac{z}{\bar{z}_0}\right)^{2n+2} + (n+1)\left(\frac{z}{\bar{z}_0}\right)^{2n+4} \\ |H(z)| &= \frac{n+2}{\bar{z}_0^{2n+2}}\left| 1 - \frac{n+1}{(n+2)\bar{z}_0^2}\, e^{i\phi} \right| \\ \text{phase } H(z) &= \pi + (2n+2)\phi + \text{phase}\left\{1 - \frac{n+1}{(n+2)\bar{z}_0^2}\, e^{2i\phi}\right\} \end{aligned} \tag{42}$$

As ω varies from 0 to ω_c, ϕ varies by $\frac{\pi}{2}$ radians. The corresponding phase of $H(z)$ varies by $(n+1)\pi$ radians, which means that $H(z)$ is successively positive real, imaginary, negative real, imaginary, through $n+1$ half cycles. This accounts for the oscillatory nature of the $\alpha - \bar{\alpha}$ curve, illustrated in Fig. 7.

The amplitudes of the oscillations are fixed by $| H(z) |$, which varies relatively slowly. Specifically, the two logarithms in (41) determine

envelopes, between which the actual error curve oscillates. These are the dashed lines in Fig. 7.

The maximum error, in the useful interval, is determined by the maximum value of the envelopes, i.e.,

$$(\alpha - \bar{\alpha})_{\max.} \cong \frac{n+2}{\bar{z}_0^{2n+2}} \left[1 + \frac{n+1}{n+2} \frac{1}{\bar{z}_0^2} \right] \tag{43}$$

This function is plotted in Fig. 8, for various values of n. The abscissae "distortion before equalization" represent distortion relative to the median loss in the useful interval, or one half the total variation in the interval. (This is a function of the top useful frequency ω_c, relative to the assigned natural mode $\bar{p}_0$; and (7) makes $\omega_c/\bar{p}_0$ a simple function of $\bar{z}_0$.) The figure is convenient for estimating the values of n needed for specific applications.

The various ripples in $\alpha - \bar{\alpha}$ do not all have the same amplitude, (43). For some values of n and $\bar{z}_0$, the amplitudes are almost uniform; for others they are quite variable. A measure of the variability in ripple

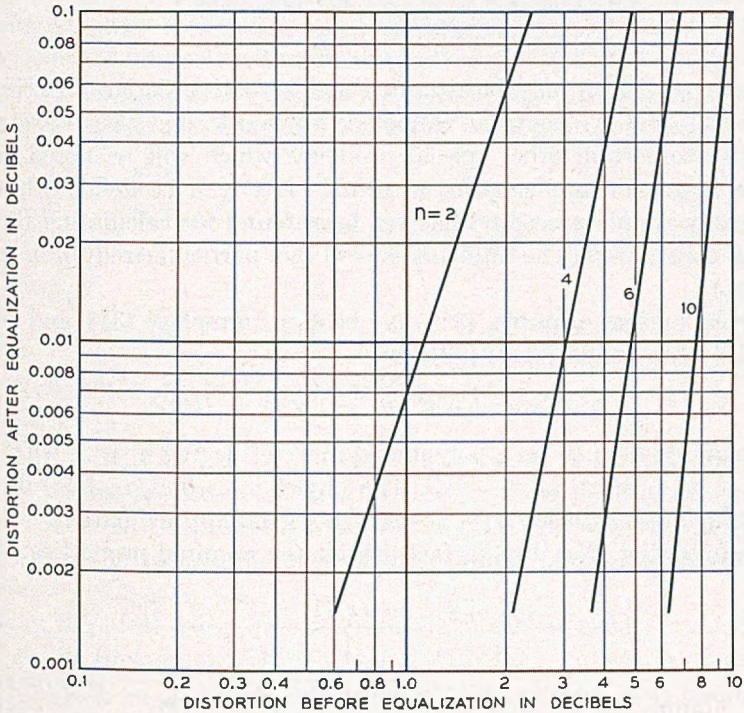

Fig. 8—Distortion before and after equalization—n natural modes equalizing 2 identical natural modes.

amplitude, across the useful interval, is:

$$\frac{|H(z)|_{\max.}}{|H(z)|_{\min.}} = \frac{(n+2)\bar{z}_0^2 + (n+1)}{(n+2)\bar{z}_0^2 - (n+1)} \tag{44}$$

14. APPROXIMATION IN THE TCHEBYCHEFF SENSE

The above analysis suggests a way of improving the design determined by (37) (or the equivalent, (36)). An *optimum* $\alpha - \bar{\alpha}$ is commonly one which has the following properties, in the useful interval:

A maximum number of "ripples,"
all maxima of $|\alpha - \bar{\alpha}|$ *equal.*

(This usually minimizes the largest departure in the useful interval, thereby yielding an "approximation in the Tchebycheff Sense.") Since the variation in phase $H(z)$ determines the number of ripples, while $|H(z)|$ determines the amplitudes of the ripples, the above conditions will be met if $H(z)$ has the following properties, in the useful interval:

Phase $H(z)$ *as variable as possible,*
$|H(z)|$ *constant.* (45)

These conditions may be regarded as alternative design criteria, replacing $C_{2k} = \bar{C}_{2k}$. They can in fact be applied to our special example, and also to certain other special problems which will be noted later. For more general applications, a suitable $H(z)$ can be defined, but no reasonably simple procedure has yet been found for calculating the required constants. (The difficulties will be particularized in a later section.)

For the present example, (38) may be used to replace (34), and hence also the second equation of (33), by:

$$\sum (C_{2k} - \bar{C}_{2k}) z^{2k} = -\log [1 + H(z)] \tag{46}$$

(33) requires $H(z)$ to be a polynomial in z^2, of degree $n + 2$, with two zeros of $[1 + H(z)]$ at $z^2 = \bar{z}_0^2$. The object is to find an $H(z)$ of this sort, which also satisfies (45), at least to a good approximation.

The following $H(z)$ does in fact exhibit the required properties:

$$H(z) = Gz^{2n+2} \frac{[1 - Jz^2][1 - J^{n+2}/z^{2n+4}]}{[1 - J/z^2]} \tag{47}$$

The function is a polynomial because the factor $[1 - J^{n+2}/z^{2n+4}]$ is divisible by $(1 - J/z^2)$. The constants J and G are to be chosen to

give the required double zero of $[1 + H(z)]$ at $z^2 = \bar{z}_0^2$. One value of J, so determined, is real and of order $1/\bar{z}_0^2$. This is the appropriate solution. Then $| J^{n+2}/z^{2n+4} |$ is of order $1/\bar{z}_0^{2n+4}$, when $| z | \geqq 1$. This suggests the following approximation in place of (47):

$$H(z) \cong\cong Gz^{2n+2} \frac{1 - Jz^2}{1 - J/z^2} \tag{48}$$

The approximation is at least as good as $1/\bar{z}_0^{2n+4}$, compared with unity, both in the useful interval and in the neighborhood of the singularities $\bar{z}_0$, and z_σ. This means that the approximation can be used: in estimating the error $\alpha - \bar{\alpha}$ (in the useful interval), in calculating J and G, and in finding the roots z_σ.

In the useful interval, $| z | = 1$, and therefore $1/z = z^*$. Then $(1 - J/z^2)$ is $(1 - Jz^2)^*$; and their ratio has magnitude unity. Thus $| H(z) | = | G |$, in the useful interval, to order of $1/\bar{z}_0^{2n+4}$ compared with unity†. With $| J | < 1$, phase $H(z)$ varies over the useful interval to the same extent as the phase of z^{2n+2}.‡ Fig. 9 illustrates the difference in $\alpha - \bar{\alpha}$, as determined by (42) and (48). These curves, however, are for single values of n and $\bar{z}_0$; and the improvement obtained by using (48) would be different with different values of n or $\bar{z}_0$.

The values of J and G, determined from (48), and the requirement that $[1 + H(z)]$ must have two zeros at $z^2 = \bar{z}_0^2$, turn out to be:

$$J = \frac{n+1}{n+2}\frac{1}{\bar{z}_0^2} \frac{2}{1 + \frac{1}{\bar{z}_0^4} + \sqrt{\left(1 - \frac{1}{\bar{z}_0^4}\right)^2 + \frac{4}{(n+2)^2\bar{z}_0^4}}}$$

$$G = -\frac{1}{\bar{z}_0^{2n+2}} \frac{1 - J/\bar{z}_0^2}{1 - J\bar{z}_0^2} \tag{49}$$

Note that this J is in fact smaller than $1/\bar{z}_0^2$.

15. GENERALIZATION

The several sections preceding describe a quite specific example, as an introduction to synthesis applications. The next several sections describe how the specific methods of the example may be generalized, in several respects.

First, the ideal gain, $\bar{\alpha}$, is generalized, so that it need not even have the sort of functional form associated with finite networks. Then, the

† The $| H(z) |$ determined by (42) is constant only to order $1/\bar{z}_0^2$.

‡ This is the most we can expect, when we have n singularities, which can prevent the dominance of only lower order terms, through z^{2n}.

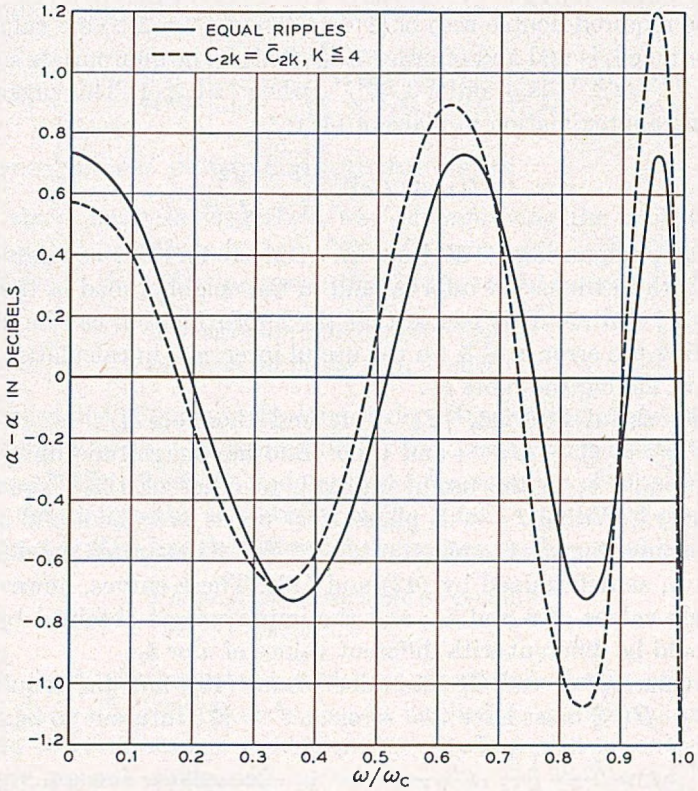

Fig. 9—Comparison of design procedures—four natural modes equalizing two natural modes at $\bar{p}_0 = -\frac{5}{12}\,\omega_c$.

approximating network gain is generalized, by introducing arbitrary frequencies of infinite loss, in addition to the arbitrary natural modes. The methods are also modified for approximation to an assigned phase, instead of gain, or to phase and gain simultaneously. Finally, the analysis is modified to permit useful intervals of the "high-pass" type, or (in the case of gain simulation) of the "band-pass" type.

16. Approximation to a General Assigned Gain $\bar{\alpha}$

If we now permit the assigned gain $\bar{\alpha}$ to be general, in the sense of Section 8, we must return to the formulation:

$$\begin{aligned} \bar{\alpha} &= \sum \bar{C}_{2k} T_{2k} \\ \sum \bar{C}_{2k} z^{2k} &= \log [\bar{R}(z)\bar{R}(-z)] \end{aligned} \tag{50}$$

If we retain simulation with a network which has n natural modes, and no frequencies of infinite loss, we must retain the formulation:

$$\begin{aligned} \alpha &= \sum C_{2k} T_{2k} \\ \sum C_{2k} z^{2k} &= -\log K_z^2 \prod \left(1 - \frac{z^2}{z_\sigma^2}\right), \qquad \sigma = 1, \cdots, n \end{aligned} \tag{51}$$

The corresponding formulation of the error is (in place of (33)):

$$\begin{aligned} \alpha - \bar{\alpha} &= \sum (C_{2k} - \bar{C}_{2k}) T_{2k} \\ \sum (C_{2k} - \bar{C}_{2k}) z^{2k} &= -\log \left[K_z^2 \prod \left(1 - \frac{z^2}{z_\sigma^2}\right) \cdot \bar{R}(z) \bar{R}(-z) \right] \end{aligned} \tag{52}$$

For $C_{2k} = \bar{C}_{2k}$, $k \leqq m$, the following special case of (28) is now required:

$$K_z^2 \prod \left(1 - \frac{z^2}{z_\sigma^2}\right) \cdot \bar{R}(z) \bar{R}(-z) \overset{me}{=} 1 \tag{53}$$

Now the reciprocal of $\bar{R}(z)\bar{R}(-z)$ has a power series expansion, in the region of interest. (Recall Section 8.)

It follows that (53) may be multiplied by this quantity, without damaging the equality of power series coefficients. In other words (53) is equivalent to:

$$K_z^2 \prod \left(1 - \frac{z^2}{z_\sigma^2}\right) \overset{me}{=} \frac{1}{\bar{R}(z)\bar{R}(-z)} \tag{54}$$

Let K_k be the coefficient of z^{2k} in the polynomial expansion of the left hand side; and let $\bar{K}_k$ be the coefficient of z^{2k} in the infinite series expansion of the right hand side. Then,

$$\begin{aligned} K_z^2 \prod \left(1 - \frac{z^2}{z_\sigma^2}\right) &= K_0 + K_1 z^2 + \cdots K_n z^{2n} \\ \frac{1}{\bar{R}(z)\bar{R}(-z)} &= \sum \bar{K}_k z^{2k}, \qquad k = 0, ---, \infty \end{aligned} \tag{55}$$

Substitution in (54) gives

$$K_0 + K_1 z^2 + \cdots K_n z^{2n} \overset{me}{=} \sum \bar{K}_k z^{2k} \tag{56}$$

In other words,

$$K_k = \bar{K}_k, \qquad k \leqq m \tag{57}$$

These relations are directly applicable to network synthesis, provided

the coefficients $\bar{K}_k$ can be calculated. Formulae for their calculation may be derived in the following way:

If (55) is substituted in (50), the result is:†

$$\begin{aligned} \bar{\alpha} &= \sum \bar{C}_{2k} T_{2k} \\ \sum \bar{C}_{2k} z^{2k} &= -\log \sum \bar{K}_k z^{2k} \end{aligned} \tag{58}$$

When $z = 0$, the second equation reduces to:

$$\bar{K}_0 = e^{-\bar{C}_0} \tag{59}$$

If the functions of z are differentiated, a simple rearrangement gives:

$$\sum k\bar{K}_k z^{2k-2} = [-\sum k\bar{C}_{2k} z^{2k-2}][\sum \bar{K}_k z^{2k}] \tag{60}$$

The right hand side may be expanded as a single power series, and then like powers on the two sides may be equated separately. The result is:

$$\begin{aligned} \bar{K}_1 &= -\bar{C}_2\bar{K}_0 \\ 2\bar{K}_2 &= -\bar{C}_2\bar{K}_1 - 2\bar{C}_4\bar{K}_0 \\ 3\bar{K}_3 &= -\bar{C}_2\bar{K}_2 - 2\bar{C}_4\bar{K}_1 - 3\bar{C}_6\bar{K}_0 \end{aligned} \tag{61}$$

Synthesis calculations may now be carried out in the following stages. The assigned gain $\bar{\alpha}$ is expanded as a Tchebycheff polynomial series, to determine coefficients $\bar{C}_{2k}$, say through order $k = n$. The equations (61) are then used to calculate coefficients $\bar{K}_k$, also through order n. Each successive coefficient is computed in terms of those previously determined. Note that the $\bar{K}_k$, $k \leqq n$, are fixed by the same number of $\bar{C}_{2k}$—that is, orders $k \leqq n$.

Equation (57) is now applied to identify K_k with $\bar{K}_k$, $k \leqq m$. If all the network degrees of freedom are to be used to get $C_{2k} = \bar{C}_{2k}$, index $m = n$, and (57) determines the polynomial in (55) completely. Otherwise, $m < n$, and coefficients K_{m+1} to K_n are to be adjusted in accordance with specifications of other kinds. When all the K_k have been determined, the singularities z_σ are found by root extraction methods, applied to the right hand side of the first equation of (55).

The previous example might have been carried out in these terms, but happened to be simpler in the terms used. If (32) is regarded as a special case of (50), and if (32) is simplified (for purposes illustration) by using $\bar{K}_z = 1$, the corresponding $\bar{R}(z)\bar{R}(-z)$ becomes simply $\left(1 - \frac{z^2}{z_0^2}\right)^2$. Then $\sum \bar{K}_k z^{2k}$ is

† We may think of these equations as defining an *infinite* network, with natural modes only, which would match the assigned gain $\bar{\alpha}$ exactly.

$$\sum \bar{K}_k z^{2k} = \frac{1}{(1 - z^2/\bar{z}_0^2)^2} = \sum (k+1)\left(\frac{z^2}{\bar{z}_0^2}\right)^k \tag{62}$$

thus $\bar{K}_k$ and K_k become

$$\begin{aligned} \bar{K}_k &= \frac{k+1}{\bar{z}_0^{2k}}, \qquad k = 0 \text{ to } \infty \\ K_k &= \frac{k+1}{\bar{z}_0^{2k}}, \qquad k = 0 \text{ to } n \end{aligned} \tag{63}$$

If these K_k are used to evaluate the polynomial on the left hand side of (53), in accordance with (55), and if the polynomial is then multiplied by the above special $\bar{R}(z)\bar{R}(-z)$, the result is exactly (36).

The error function $H(z)$, of (30) and (42), may now be defined as follows:

$$K_z^2 \prod \left(1 - \frac{z^2}{z_\sigma^2}\right) R(z)R(-z) = 1 + H(z) \tag{64}$$

The error $\alpha - \tilde{\alpha}$ is again:

$$\alpha - \tilde{\alpha} = -\log |\, 1 + H(z) \,| \tag{65}$$

If (64) is used to express (53) in terms of $H(z)$, a "1" may be subtracted from each side of the relation, to get

$$H(z) \overset{m\bullet}{=} 0 \tag{66}$$

When $m = n$, this requires an $H(z)$ of the following form, in terms of the coefficients $\bar{K}_k$ derived from $\bar{R}(z)\bar{R}(-z)$:

$$H(z) = -\frac{\bar{K}_{n+1}z^{2n+2} + \bar{K}_{n+2}z^{2n+4} + \cdots}{\sum \bar{K}_k z^{2k}} \tag{67}$$

17. CHARACTERISTICS OF z_σ

As in the previous example, $|\, z_\sigma \,| > 1$ when the approximation, α to $\tilde{\alpha}$, is at all reasonable. The z_σ are again zeros of $1 + H(z)$; but now $H(z)$ is defined by (64). If $|\, H(z) \,| < 1$, when $|\, z \,| = 1$, there will be the same number of zeros of $1 + H(z)$ as poles, in the region $|\, z \,| < 1$. Any poles would have to be poles of $\bar{R}(z)\bar{R}(-z)$. In Section 8, we noted that this function is regular in the region $|\, z \,| \leqq 1$. Hence, there will be no poles, and there will be no $|\, z_\sigma \,| < 1$, under ordinary accuracy conditions.

As before, the z_σ can be chosen in accordance with the physical con-

ditions, provided none are pure imaginaries. Since an imaginary z_σ is a negative real z_σ^2 :

There must be no negative real z_σ^2 .

There will be no negative real z_σ^2 if the polynomial $\sum K_k z^{2k}$ in (55) is non-zero at all negative real z^2. If the requirement is violated, initially, one or more K_k , of the highest orders, must be modified. Graphical methods are likely to be useful for this, combining plots of the original polynomial, and proposed changes. An approximation of the form $C_{2k} = \bar{C}_{2k}$, $k \leqq m$, will still be realized, but with $m < n$.

The error function corresponding to $m < n$ is as follows, in place of (67):

$$H(z) = \frac{(K_{m+1} - \bar{K}_{m+1})z^{2m+2} \cdots - \bar{K}_{n+1}z^{2n+2} \cdots}{\sum \bar{K}_k z^{2k}} \tag{68}$$

18. ACCURACY

The accuracy of match again may be estimated by the means of (41), using $H(z)$ of (67) or (68). $H(z)$, however, may not be so easily calculated as for the previous example.

A simpler but less reliable estimate of accuracy is furnished by the error in the first unmatched coefficient in the Tchebycheff polynomial series. If $K_k = \bar{K}_k$ through $k = m$, the leading terms in various series are as follows. First, from (64) and (68),

$$K_z^2 \prod \left(1 - \frac{z^2}{z_\sigma^2}\right) R(z)R(-z) = 1 + \frac{K_{m+1} - \bar{K}_{m+1}}{K_0} z^{2m+2} \cdots \tag{69}$$

using this in (52) gives:

$$\sum (C_{2k} - \bar{C}_{2k})z^{2k} = -\log\left[1 + \left(\frac{K_{m+1} - \bar{K}_{m+1}}{\bar{K}_0}\right) z^{2m+2} \cdots\right] \tag{70}$$

Then, from the properties of logarithms,

$$\sum (C_{2k} - \bar{C}_{2k})z^{2k} = -\frac{K_{m+1} - \bar{K}_{m+1}}{\bar{K}_0} z^{2m+2} \cdots \tag{71}$$

Consequently (also from (52)):

$$\alpha - \bar{\alpha} = \frac{\bar{K}_{m+1} - K_{m+1}}{\bar{K}_0} T_{2m+2} \cdots \tag{72}$$

This is the same as the leading term of $H(z)$, except that z^{2m+2} is replaced by $-T_{2m+2}$. If $m = n$, the same equation holds with $K_{m+1} = 0$.

The coefficient $\frac{\bar{K}_{m+1} - K_{m+1}}{K_0}$ in (72) is a sort of average of the envelopes of the ripples in $\alpha - \bar{\alpha}$. The variability of the envelopes, across the useful interval, depends upon higher order coefficients, in comparison with the leading term. Calculation of higher order coefficients is relatively complicated.

19. APPROXIMATION IN THE TCHEBYCHEFF SENSE

The criteria (45) carry over to general assigned gains, as conditions on $H(z)$ which, if realized, are usually sufficient to establish approximation in the Tchebycheff sense. For this purpose we must use the $H(z)$ of (64), rather than (67) or (68) (which correspond explicitly to $C_{2k} = \bar{C}_{2k}$, $k \leqq m$). In terms of the polynomial and series representations of (55), the $H(z)$ of (64) becomes:

$$H(z) = \frac{K_0 + K_1 z^2 \cdots K_n z^{2n}}{\sum \bar{K}_k z^{2k}} - 1 \tag{73}$$

The following somewhat special problem is easily solved, in these terms, and has a direct bearing on various quite different synthesis techniques: A network is to be designed which combines the functions of an equalizer or simulator, with those of a filter, or selective network. In the useful interval, an assigned gain variation $\bar{\alpha}$ is to be approximated in the Tchebycheff sense. At higher frequencies, there is to be a rapidly increasing loss, or "sharp filter cut-off." The number of natural modes, n, is to be more than sufficient to match $\bar{\alpha}$ to the required accuracy, in the absence of a selectivity requirement, the latitude being used to produce the required sharp cut-off. In particular, n is to be large enough so that an n term match of Tchebycheff coefficients produces errors that are negligible compared with those accepted as a price of the sharp cut-off.

On the above assumption of an ample n, the infinite series $\sum \bar{K}_k z^{2k}$ in (73) may be truncated after the term of order n, *and the errors due to the truncation may be neglected in calculating the design error* $\alpha - \bar{\alpha}$.† Then (73) becomes

$$H(z) = \frac{K_0 + K_1 z^2 \cdots K_n z^{2n}}{\bar{K}_0 + \bar{K}_1 z^2 \cdots \bar{K}_n z^{2n}} - 1 \tag{74}$$

† The truncated series is merely the polynomial on the left side of (56) which *would* be obtained if the filter selectivity were ignored, and m were given the maximum value, n.

If a sharp cut-off were not required, this approximate $H(z)$ could be made exactly zero, by using $K_k = \bar{K}_k$ for all coefficients. Then the actual design error would be determined by the approximation inherent in the use of (74) in place of (73). For high selectivity, however, K_n should be much larger than $\bar{K}_n$, as large as possible within assigned limits on $\alpha - \bar{\alpha}$ in the useful range. (It is readily established that $K_n z^n$ will determine α at asymptotically high frequencies.) The other K_k are then to be adjusted so that $\alpha - \bar{\alpha}$ exhibits the desired "equal ripples."

The following $H(z)$ has the functional form (74), and also meets conditions (45):

$$H(z) = Gz^{2n} \frac{\bar{K}_0 + \frac{\bar{K}_1}{z^2} \cdots \frac{\bar{K}_n}{z^{2n}}}{\bar{K}_0 + \bar{K}_1 z^2 \cdots \bar{K}_n z^{2n}} \tag{75}$$

Multiplying Gz^{2n} into the numerator gives a rational fraction which is obviously consistent with (74). The coefficients K_k of (74) which correspond to (75) are:

$$K_k = \bar{K}_k + G\bar{K}_{n-k} \tag{76}$$

In the useful interval $[\sum \bar{K}_k/z^{2k}]$ is $[\sum \bar{K}_k z^{2k}]^*$. Hence the polynomials in z and $1/z$ have identical magnitudes, in the useful interval; and, since also $|z| = 1$, $|H(z)| = |G|$ in (75). The phase variation, over the useful interval, is the same for $H(z)$ as for z^{2n}, which yields the same number of ripples in $\alpha - \bar{\alpha}$ as an ordinary Tchebycheff filter of like degree.†

The constant G is arbitrary, except that its sign must be properly chosen to avoid non-physical natural modes. Increasing G increases the filter selectivity, but also increases $\alpha - \bar{\alpha}$ in the useful interval. G and n are to be chosen together, to realize an assigned selectivity within an assigned limit on distortion.

The above analysis may be related to the following filter problem: Required to design a filter which has flat gain, in the useful interval, but which has m *assigned* frequencies of infinite loss, in addition to n arbitrary natural modes ($m \leqq n$). The n arbitrary natural modes may be regarded as compensating for gain variations due to the assigned frequencies of infinite loss, in the useful interval, while reinforcing their effects at other frequencies. *Compensation* of effects of the infinite loss points is the same as *simulation* of the effects of natural modes at the same (assigned) frequencies. The approximation in the useful interval

† This assumes an $\bar{\alpha}$ with the general characteristics described in Section 8, which are such that the numerator and denominator of the fraction in (75) will each have a net phase shift of *zero*, across the useful interval.

is to be no better than necessary, so that there may be a maximum reinforcing of losses at other frequencies. In these terms, (58), and $\sum \bar{K}_k z^{2k}$ in (73), correspond to the assigned natural modes (at the same locations as the assigned frequencies of infinite loss). Then the ideal $\sum \bar{K}_k z^{2k}$ is itself a polynomial, of degree $m \leqq n$, and (74) is exact, rather than an approximation to (73). Then (76) determines the n arbitrary modes in such a way that the net filter gain approximates zero in the Tchebycheff sense, over the useful interval.

A different procedure for obtaining the same result is described in the author's paper "Synthesis of Reactance 4-Poles".[8] The above analysis of the filter problem is of interest in relating the more general synthesis techniques, in terms of Tchebycheff polynomial series, to previous filter theory.

Similar filters have also been obtained by Matthaei[2], on a potential analogy basis. He includes, however, somewhat more general filter characteristics, for which he obtains only approximately equal ripple errors. Analysis of the sort described above may be used to clarify Matthaei's analysis of the conditions under which he obtains exactly equal-ripples.

Equation (75) may be related to work of Bashkow[3]. The (arbitrary) amplitude of the (equal) maxima of $|\alpha - \bar{\alpha}|$, computed from $H(z)$ of (75), depends only on $|G|$. The frequencies at which the maxima occur correspond to phase $H(z) = s\pi$, which is independent of $|G|$. Thus, the locations of the maxima are invariant to the arbitrary amplitude, *within the range where* (75) *applies*. (75) applies only when (74) may be used in place of (73). Generally, (74) only approximates (73), and the approximation introduces small variations in the maxima of $|\alpha - \bar{\alpha}|$ (when α corresponds to (76)). If the maxima themselves are sufficiently small, the small variations will be large *percentage* variations; and the adjustments to compensate for the variations will yield significant shifts in the location of the maxima. In other words, the locations of the maxima of $|a - \bar{\alpha}|$, required for *equal* amplitudes, are largely invariant to the magnitude of the equal amplitudes, but only to an approximation which becomes worse as the amplitudes are decreased.

Bashkow states the invariance of the frequencies of maximum $|\alpha - \bar{\alpha}|$, as a more or less empirical conclusion, based on a quite different approach to the same synthesis problem.

Equation (75) may be related also to work of Kuh.[4] The natural modes z_σ are zeros of $1 + H(z)$. In other words, $H(z_\sigma) = -1$. Using the $H(z)$ of (75) gives the following:

$$K_0 + K_1 z_\sigma^2 + \cdots K_n z_\sigma^{2n} = -G z_\sigma^{2n} \left\{ \bar{K}_0 + \frac{\bar{K}_1}{z_\sigma^2} + \cdots \frac{\bar{K}_n}{z_\sigma^{2n}} \right\} \qquad (77)$$

It must be remembered, however, that this formulation is permissible only if the approximations, inherent in (75), are justified when $z = z_\sigma$ (as well as in the useful interval). Taking the logarithm of each side gives:

$$\log \{\bar{K}_0 + \cdots \bar{K}_n z_\sigma^{2n}\} = \log (-G) + 2n \log z_\sigma + \log \left\{\bar{K}_0 + \cdots \frac{\bar{K}_n}{z_\sigma^{2n}}\right\} \tag{78}$$

Equation (58) may now be applied, to replace the logarithms by power series, provided the truncation of the series is again justified, and provided the convergence of $\sum \bar{C}_{2k} z^{2k}$ is also proper, at both $z = z_\sigma$ and $z = 1/z_\sigma$. This gives

$$-\sum \bar{C}_{2k} z_\sigma^{2k} = -\sum \bar{C}_{2k}/z_\sigma^{2k} + 2n \log z_\sigma + \log (-G) \tag{79}$$

(Summations $\sum$ are all with respect to k; and there is one equation for each σ.) This is a suitable rule, for obtaining an $|\alpha - \bar{\alpha}|$ with equal maxima, whenever the approximations are in fact unimportant. It is not at all clear, however, just when the approximations become significant.

Kuh uses the potential analogy approach for the same sort of synthesis problem. He spaces the natural modes along a p-plane contour defined in fairly complicated potential analogy terms. It can be shown, however, that mapping his potentials from p plane to z plane leads to (79).

When the network is to approximate $\bar{\alpha}$ in the useful interval, but is *not* required to supply selectivity at other frequencies, the approximation (74) is usually untenable. It is generally necessary to retain the exact formulation (73).

When selectivity is not required, the phase excursion of $H(z)$, in the useful interval, can usually be increased to that of z^{2n+2} (as in (67), corresponding to $C_{2k} = \bar{C}_{2k}$, $k \leqq n$). As a step toward meeting the first condition of (45), one may then write (73) as follows:

$$H(z) = -\bar{K}_{n+1} z^{2n+2} \frac{\sum \frac{\bar{K}_{n+1+k}}{\bar{K}_{n+1}} z^{2k} + \sum_1^{n+1} Q_k \frac{1}{z^{2k}}}{\sum \bar{K}_k z^{2k}} \tag{80}$$

$$Q_k = \frac{\bar{K}_{n+1-k} - K_{n+1-k}}{\bar{K}_{n+1}}, \qquad k = 1, \cdots, n+1$$

The coefficients $\bar{K}_k$ and $\frac{\bar{K}_{n+1+k}}{\bar{K}_{n+1}}$ are fixed by $\bar{\alpha}$. The only arbitrary

design constants are the Q_k. They are to be small enough so that they do not affect the total phase excursion $H(z)$, when $|z| = 1$. Their specific values are to make $|H(z)|$ approximately constant, when $|z| = 1$. In general the (required) series in z^2 in the numerator makes it extremely difficult to determine the required values for the Q_k. No reasonably simple general procedure has yet been found.

20. ARBITRARY RATIONAL FRACTIONS

The preceding sections were devoted to the approximation α to $\bar{\alpha}$, using n arbitrary natural modes, but no arbitrary frequencies of infinite loss. Similar techniques may be used when there are n'' arbitrary natural modes and n' arbitrary frequencies of infinite loss. As the applications become more involved, however, routine calculations must be supplemented increasingly with an element of art.

For simultaneous design of natural modes and frequencies of infinite loss, we must go back from (31) to the α formulation in (21). This we shall now write:

$$\begin{aligned} \alpha &= \sum C_{2k} T_{2k} \\ \sum C_{2k} z^{2k} &= -\log \frac{N}{D} \end{aligned} \tag{81}$$

The functions N and D are polynomials. The coefficients will be defined as follows:

$$\begin{aligned} N &= K_0'' + K_1'' z^2 \cdots K_{n''}'' z^{2n''} \\ D &= 1 + K_1' z^2 \cdots K_{n'}' z^{2n'} \end{aligned} \tag{82}$$

By comparison with (21), the zeros of N, in terms of z^2, are the $z_\sigma''^2$. (Note the minus sign in 81.) The zeros of D are then the $z_\sigma'^2$. For physical networks, $n'' \geqq n'$.

Equations (50), describing $\bar{\alpha}$, may be retained as they stand. Combining (50) and (81) gives, in place of (52):

$$\begin{aligned} \alpha - \bar{\alpha} &= \sum (C_{2k} - \bar{C}_{2k}) T_{2k} \\ \sum (C_{2k} - \bar{C}_{2k}) z^{2k} &= -\log \left[\frac{N}{D} \bar{R}(z) \bar{R}(-z) \right] \end{aligned} \tag{83}$$

The function $\bar{R}(z)\bar{R}(-z)$ is exactly the same as before. The reciprocal of the function will still be $\sum \bar{K}_k z^{2k}$, with the $\bar{K}_k$ related to $\bar{C}_{2k}$ by (58), (59), (61). The new rational fraction N/D will appear where previously we had the polynomial $K_0 + \cdots K_n z^{2n}$.

Accordingly, the rule for $C_{2k} = \bar{C}_{2k}$, $k \leqq m$, now becomes, in place of (56),

$$\frac{N}{D} \overset{me}{=} \sum \bar{K}_k z^{2k} \tag{84}$$

This condition may be used to determine the coefficients K_k'', K_k' of N and D (in combination with conditions of other sorts, when $m < n'' + n'$). When the coefficients have been calculated, the (z-plane) natural modes z_σ'' may be determined from the roots of N, exactly as the z_σ of previous sections. The infinite loss points z_σ' may be calculated from the roots of D, in exactly the same way except that Re z_σ' need not be negative. Signs of the z_σ' must be such that complex *and imaginary* z_σ' are in conjugate pairs. Note that there can be *conjugate* imaginary z_σ' only if D has a corresponding *double* negative real zero.

When $m = n'' + n'$, the following method may be used to calculate the K_k'' and K_k' determined by (84). The relation is first multiplied by D, to get:

$$N \overset{(n''+n')}{=} D \sum \bar{K}_k z^{2k} \tag{85}$$

Then algebraic manipulation is used to evaluate the power series equivalent of the right hand side, through terms of order $n'' + n'$, using the known values of the $\bar{K}_k$, but general values of the K_k' of D. Each coefficient is a linear function of the unknowns, K_k'.

Now the polynomial N, in (85), has no terms of order $k > n''$. Therefore (85) requires zero coefficients in the expansion of the right hand side, from order $n'' + 1$ to order $n'' + n'$. Equating these coefficients to zero gives n' linear equations in the n' unknown K_k'. Solving for the K_k' determines polynomial D. The values calculated for the K_k' may then be used in lower order coefficients of the expansion of the right hand side of (85), which are exactly the coefficients K_k'' of N.

When $n'' - n' = 0$ or 1, a continued fraction method is likely to be preferable. Various established techniques† may be used to convert the series $\sum \bar{K}_k z^{2k}$ into a continued fraction of the form:

$$\sum \bar{K}_k z^{2k} = a_0 + \cfrac{1}{\cfrac{a_1}{z^2} + \cfrac{1}{a_2 + \cfrac{1}{\cfrac{a_3}{z^2} + \cfrac{1}{a_4 \cdots}}}} \tag{86}$$

† See, for example, Fry's applications of continued fractions to network design.[9]

If the continued fraction is truncated after the term of order m, and is rearranged as a rational fraction N/D, it will obey equation (84). The degrees of N and D will be such that $n'' + n' = m$, and $n'' - n' = 0$ or 1. The continued fraction may be associated with the hypothetical ladder network shown in Fig. 10, with variable impedance shunt branches proportional to z^2. The impedance of the (truncated) ladder is N/D.

21. ACCURACY

The accuracy of match, $\alpha - \bar{\alpha}$, may again be evaluated from the final network singularities; or by (41), with $H(z)$ as in (30), before the singularities have been determined from roots of N and D. A rougher estimate may again be obtained from the error in the first unmatched term in the Tchebycheff polynomial series. As before, (equation (72)), this is equal to the leading term in $H(z)$, with z^{2m+2} replaced by $-T_{2m+2}$.

The rational fraction in (30) is the same as our present N/D. In terms of N/D, (30) becomes:

$$\frac{N}{D}\bar{R}(z)\bar{R}(-z) = 1 + H(z) \tag{87}$$

If (86), or Fig. (10), is used to determine N and D, the leading term in $H(z)$ turns out to be:

$$H(z) = \frac{(-)^{m+1}z^{2m+2}}{(a_1a_2 \cdots a_m)^2 a_{m+1}\bar{K}_0} \cdots \tag{88}$$

The corresponding mismatch in Tchebycheff polynomial terms is:

$$C_{2m+2} - \bar{C}_{2m+2} = \frac{(-)^m}{(a_1a_2 \cdots a_m)^2 a_{m+1}\bar{K}_0} \tag{89}$$

22. ZEROS AND POLES

When frequencies of infinite loss are to be chosen, as well as natural modes, the situation in regard to $|z_\sigma| < 1$ is somewhat less favorable.

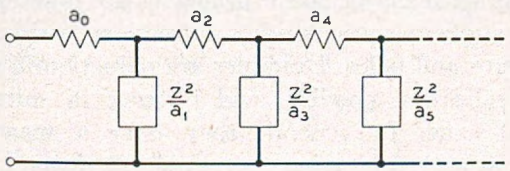

Fig. 10—A ladder network representation of the continued fraction (86).

It is still true that $1 + H(z)$ will have the same number of zeros as poles in the region $|z| < 1$, so long as $\alpha - \bar{\alpha}$ is reasonably small in the interval $|z| = 1$. In equation (87), however, the poles of $1 + H(z)$ include the zeros z'_σ of D (the arbitrary infinite loss points), as well as the poles of $\bar{R}(z)\bar{R}(-z)$. When the coefficients of D are to be chosen as in the previous section, the contour rule merely says that any z'_σ and z''_σ in the region $|z| < 1$ will occur in like numbers.

Fortunately, the frequent occurrence of $|z_\sigma| < 1$ is softened by the following curious circumstance. Almost always, any $|z'_\sigma|$ and $|z''_\sigma| < 1$ are so nearly identical that factors $(z - z'_\sigma)$ and $(z - z''_\sigma)$ may be cancelled out without any important effect on $H(z)$, or $\alpha - \bar{\alpha}$. Cancellations of this sort were encountered a number of times before an explanation was discovered. Actually the explanation is quite simple.

At any zero of $1 + H(z)$, $H(z) = -1$. On the other hand, $H(z)$ is small when $|z| = 1$. Generally, it is much *smaller* in most of the interval $|z| < 1$. For instance, when $C_{2k} = \bar{C}_{2k}$ through $k = m$, $H(z)$ is proportional to z^{2m+2}, in the neighborhood of $z = 0$. As a result, $|H(z)|$ rarely becomes as large as 1, in the region $|z| < 1$, except in the very close proximity of a pole. In other words, in the region $|z| < 1$, any zero z''_σ is usually very close to a pole z'_σ—usually so close that the corresponding factors $z - z_\sigma$ may be cancleled out without significant effect on $\alpha - \bar{\alpha}$.

The occurrence of non-physical natural modes ($Re z''_\sigma = 0$) is the same as before; but adjustments to correct for these, in an efficient manner, are much more complicated. In addition, there may be non-physical infinite loss points, z'_σ. To correct for non-physical singularities, the *simplest* procedure would be to change one or both of the highest order coefficients in N and D of (82), that is $K''_{n''}$ and $K'_{n'}$. This would be inefficient, however, for it would spoil the match of $C_{n''}$ to $\bar{C}_{n''}$, or $C_{n'}$ to $\bar{C}_{n'}$. The unmodified design, defined by (84), can match terms through order $n'' + n'$, and it is desirable to change only the highest order terms in adjusting the design.

More efficient adjustments are in fact feasible. They sometimes require an increased element of art; but the art may be based on specific principles. Some particularly useful principles are described in the next section. These apply to various other corrections besides correction of non-physical zeros and poles. Examples are reduction in phase to make two-terminal realization possible, and increase in shunt capacity in two-terminal designs. In general, they offer a means of making $m < n' + n''$ in (84), and using the remaining degrees of freedom to meet other conditions.

23. MODIFICATION OF N/D

Suppose N_1/D_1 and N_2/D_2 are two rational fractions, representing special choices of N and D in (82), such that:

$$\frac{N_1}{D_1} \overset{m_1 e}{=} \sum \bar{K}_k z^{2k}$$
$$\frac{N_2}{D_2} \overset{m_2 e}{=} \sum \bar{K}_k z^{2k} \tag{90}$$

Then suppose F is a function of z^2 such that

$$F \overset{\mu e}{=} 0 \tag{91}$$

The following combination represents an approximation to $\sum \bar{K}_k z^{2k}$, of the order indicated:†

$$\frac{N_1 + FN_2}{D_1 + FD_2} \overset{me}{=} \sum \bar{K}_k z^{2k} \tag{92}$$

$m = m_1$, or $m_2 + \mu$, whichever is the smaller.

The left hand side of (92) may be used as N/D in (84), to match C_{2k} to $\bar{C}_{2k}$ through $k = m$. Adjustment of the function F may be used to satisfy other requirements, in addition to accuracy specifications.

Frequently, N_1/D_1 may be the rational fraction corresponding to truncation of the continued fraction, (86), after the term in $a_{n''+n'}$. Then N_2/D_2 is likely to be a truncation of order $m < n'' + n'$. The corresponding F is likely to be proportional to $z^{2\mu}$, or at most a simple polynomial in z^2. When F is a constant, and $m = n'' + n' - 1$, the use of these particular rational functions in (92), to determine N/D, corresponds to matching C_{2k} to $\bar{C}_{2k}$ through $k = n'' + n' - 1$, but leaving $C_{2(n''+n')}$ subject to adjustment. Specifically, $C_{2(n''+n')}$ depends on the choice of F, which may hinge upon such special conditions as the elimination of non-physical singularities.

Problems which call for more complicated combinations are by no means uncommon. Skill may be needed in the choice of specific combinations which will solve specific problems. Computations may be

† The relationship is easily established by noting that:

$$\frac{N_1 + FN_2}{D_1 + FD_2} - \Sigma \bar{K}_k z^{2k} = \frac{\dfrac{N_1}{D_1} - \Sigma \bar{K}_k z^{2k}}{1 + F\dfrac{D_2}{D_1}} + F\frac{\dfrac{N_2}{D_2} - \Sigma \bar{K}_k z^{2k}}{\dfrac{D_1}{D_2} + F} \tag{93}$$

systematized, to a considerable extent, by using the error formula (88), and other relations between the coefficients of the continued fraction, and the rational fraction truncations of various orders.†

24. APPROXIMATION TO BOTH GAIN AND PHASE

The applications described in previous sections relate to approximations to prescribed gain, $\bar{\alpha}$, without regard to the associated phase. Quite similar methods apply, however, to the simultaneous approximation of gain and phase.

The starting point is equation (20). Replacing products of factors by polynomials gives, in place of (81):

$$\begin{aligned} \alpha + i\beta &= \sum C_k T_k , \qquad k \text{ even and odd} \\ \sum \tfrac{1}{2} C_k z^k &= -\log \frac{N}{D} . \end{aligned} \tag{94}$$

The polynomials are now as follows, in place of (82):

$$\begin{aligned} N &= K_0'' + K_1'' z \cdots K_{n''}'' z^{n''} \\ D &= 1 + K_1' z \cdots K_{n'}' z^{n'} \end{aligned} \tag{95}$$

(If only natural modes are to be used, the suitable replacement for the first equation or (55) is here obtained merely by using $D = 1$, and K_s, z, z_σ, in place of their squares.)

A comparable expression is needed for the assigned gain and phase $\bar{\alpha} + i\bar{\beta}$. In place of (50), we now repeat (22), and redefine the coefficients $\bar{K}_k$ in accordance with

$$\begin{aligned} \bar{\alpha} + i\bar{\beta} &= \sum \bar{C}_k T_k , \qquad k \text{ even and odd} \\ \sum \tfrac{1}{2} \bar{C}_k z^k &= \log \bar{R}(z) = -\log \sum \bar{K}_k z^k \end{aligned} \tag{96}$$

The definition of $\bar{K}_k$ has been changed in such a way that it is now related to $\bar{C}_k/2$ exactly as it was previously (in 58) related to $\bar{C}_{2k}$. Equations (59), (61) may be applied to calculating the $\bar{K}_k$ by merely substituting therein a $\bar{C}_k/2$ for every $\bar{C}_{2k}$.

† For example, a simple recursion formula may be used to assemble the polynomials N and D which correspond to truncation of the continued fraction (86) at a number of different points. Specifically, $P_n = P_{n-1} + \dfrac{z^2}{a_n a_{n-1}} P_{n-2}$, where P is either N or D and P_n corresponds to truncation of the continued fraction after the term in a_n. The formula holds for $n \geqq 2$.

Equations (84), (85), (86) may now be modified, for the new N, D and $\bar{K}_k$, by merely using z in place of z^2 wherever it occurs (including z^k in place of z^{2k}).† The modifications of equations (84), (85), and the truncation of (86) after a_m now lead to $C_k = \bar{C}_k$, $k \leqq m$, instead of the previous $C_{2k} = \bar{C}_{2k}$. This means that m must be twice as great to match coefficients out to the same actual orders. This is to be expected since now one half of our design parameters are used to approximate phase $\bar{\beta}$, leaving only half for approximating gain $\bar{\alpha}$. Equation (89) must be changed not only in regard to the orders of C_k, $\bar{C}_k$, but also in regard to the factors $\frac{1}{2}$ in (94), (96). This gives

$$\frac{C_{m+1} - \bar{C}_{m+1}}{2} = \frac{(-)^m}{(a_1 a_2 \cdots a_m)^2 \, a_{m+1} \bar{K}_0} \tag{97}$$

The most important change is in regard to the zeros and poles z_σ. The polynomials N and D now determine z_σ'' and z_σ' directly, instead of their squares. There is no opportunity to adjust the sign of Re z_σ'' by choosing the correct sign of $\sqrt{z_\sigma''^2}$. When non-physical singularities appear, adjustments of high order coefficients may be tried. Section 23 applies provided z^2 is replaced by z. If the specification of the problem permits added delay, linear phase may be added to $\bar{\alpha} + i\bar{\beta}$ to increase the probability of physical singularities‡. (Addition of linear phase changes only $\bar{C}_1$, in $\sum \bar{C}_k T_k$. A *negative* change in $\bar{C}_1$ *increases* the delay.)

25. APPROXIMATION TO AN ASSIGNED PHASE $\bar{\beta}$§

Sometimes it is required to approximate an assigned phase, without regard to gain. More commonly, it is required to approximate an assigned phase, using an "all-pass" network, which has a theoretically zero gain. These two problems, however, are very nearly identical, due to circumstances explained at the end of this section.

For approximation to phase only, we go back to the β equation in (21). As before, products of factors $(z - z_\sigma)$ are replaced by polynomial

† and $\overset{m}{=}$ in place of $\overset{m_e}{=}$.

‡ The well known relation between the gain and phase of any physical network (See for instance Bode[10]) may give some information regarding the reasonableness of $\bar{\beta}$. It must be remembered, however, that departures of network gain α, from the assigned gain $\bar{\alpha}$, outside the useful interval, may affect the permissible phase β, within the interval.

§ Up to the present, applications to phase problems have not been developed to the same extent as for gain. Techniques have been explored, however, to determine how such applications may in fact be carried out.

equivalents. Then, in place of (81) or (94), we have

$$\left.\begin{aligned} i\beta &= \sum C_k T_k \\ \sum C_k z^k &= -\log \frac{N}{D} \end{aligned}\right\} k \text{ odd} \tag{98}$$

Using n to represent $n'' + n'$, the total number of network singularities, we may write N and D as follows, in place of (82) or (95):

$$\begin{aligned} N &= 1 + K_1 z + K_2 z^2 + K_3 z^3 \cdots + K_n z^n \\ D &= 1 - K_1 z + K_2 z^2 - K_3 z^3 \cdots (-)^n K_n z^n \end{aligned} \tag{99}$$

Notice that N and D are related by

$$D(z) = N(-z), \tag{100}$$

which is required by the form of the β equation in (21).

To arrive at *a* design procedure most easily (but not the simplest design procedure), one may express the *assigned* gain $\bar{\beta}$ in the following way (comparable to (58) and (96)):

$$\begin{aligned} i\bar{\beta} &= \sum \bar{C}_k T_k , \qquad k \text{ odd} \\ \sum \bar{C}_k z^k &= -\log \sum \bar{K}_k z^k \end{aligned} \tag{101}$$

Coefficients $\bar{K}_k$ may again be calculated by a modification of (61). This time $\bar{C}_{2k}$ is replaced by $\bar{C}_k$, wherever it appears in (61), and then all even ordered $\bar{C}_k$ are made zero (since only odd terms appears in $\sum \bar{C}_k z^k$ of (101)). Note that even ordered $\bar{K}_k$ are *not* usually zero, even though even ordered $\bar{C}_k$ are.

The degrees of N and D, in (99), are such that we can make $C_k = \bar{C}_k$ through terms of order $k = 2n$. This requires merely:

$$\frac{N}{D} \overset{2n}{=} \sum \bar{K}_k z^k \tag{102}$$

As stated, the condition applies to C_k of both even and odd orders. Since even ordered $\bar{C}_k$ are zero, it means that at least n even ordered C_k will be zero, in addition to the match between n odd orders. (102) is sufficient to determine an N and a D without reference to (100). If the (equal) degrees n of (99) are assumed, however, the N and D determined by (102) will be found to obey (100) automatically (provided $\sum \bar{K}_k z^k$ corresponds to an *odd* series $\sum \bar{C}_k z^k$, as here assumed).†

A simpler method for computing the same N and D takes advantage

† This was discovered by Mrs. M. D. Stoughton.

of the known relation (100), connecting N and D. Let E and O be respectively the sums of even and odd terms in N. Then N is $E + O$ and (100) requires D to be $E - O$. The ratio O/E may be related to $\sum C_k z^k$ of (98) as follows:

$$\frac{O}{E} = -\tanh \tfrac{1}{2} \sum C_k z^k \tag{103}$$

Now let two convergent series, respectively even and odd, be such that:

$$\frac{\bar{O}}{\bar{E}} = -\tanh \tfrac{1}{2} \sum \bar{C}_k z^k \tag{104}$$

Let coefficients $\bar{K}'_k$ be defined by:

$$\bar{E} + \bar{O} = \sum \bar{K}'_k z^k \tag{105}$$

Then $\bar{E}$ and $\bar{O}$ are respectively the sums of the even and odd terms. The complete series may now be related to the (odd) series $\sum \bar{C}_k z^k$ as follows:

$$\sum \tfrac{1}{2} \bar{C}_k z = -\log \sum \bar{K}'_k z^k \tag{106}$$

This fixes the $\bar{K}'_k$ of $\bar{E} + \bar{O}$ in terms of the $\bar{C}_k$.

To make $C_k = \bar{C}_k$ through m odd orders, (102) is now replaced by

$$\frac{O}{E} \overset{mo}{=} \frac{\bar{O}}{\bar{E}} \tag{107}$$

The symbol $\overset{mo}{=}$ designates equality of power series through *m odd* orders. (*All* even terms are now zero on both sides.) The right hand side may be expressed as a continued fraction of the following form, comparable to (86):

$$\frac{\bar{O}}{\bar{E}} = \cfrac{1}{\cfrac{a_1}{z} + \cfrac{1}{\cfrac{a_2}{z} + \cfrac{1}{\cfrac{a_3}{z} \cdots}}} \tag{108}$$

Truncation after only the m^{th} term gives the O/E of (107).

The coefficients of $\bar{O}$ and $\bar{E}$ may be calculated by an appropriate modification of (61). (Calculate like $\bar{K}_k$ of (101), after dividing all $\bar{C}_k$ by 2). After O and E have been evaluated, by truncating the continued fraction (108), their sum gives polynomial N of (99).

The natural modes and frequencies of infinite loss are determined from the zeros of the polynomial N. By (21), each zero is either a (z-plane) natural mode, z_σ'', or the negative of an infinite loss point $-z_\sigma'$. If gain variations are inconsequential, there is likely to be some latitude in designating each zero as a z_σ'', or as a $-z_\sigma'$.

A zero of N with a *positive* real part would make a non-physical natural mode, and hence it *must* be a $-z_\sigma'$, corresponding to an infinite loss point. A zero of N with a *negative* real part *can* be a natural mode z_σ'', but this may not be *required*. It may be either a z_σ'' or a $-z_\sigma'$, provided conjugate zeros are assigned in the same way, and provided the total number of $-z_\sigma'$ does not exceed the total number of z_σ''. The latter condition requires:

At least half the zeros of N
must have negative real parts.

The continued fraction (108) shows how many zeros will have negative real parts, before any zeros have been calculated. The following theorem makes this easy:

The number of zeros of N which have negative real parts is equal to the number of positive coefficients in the truncation of the continued fraction (108) *which determined N.*

When gain is not to be disregarded, but is to be exactly zero, the synthesis technique needs few changes. The phase of an "all-pass" network is related to the natural modes z_σ'' as follows:

$$i\beta = \sum C_k T_k, \qquad k \text{ odd}$$

$$\sum \frac{C_k z^k}{2} = -\log \frac{\prod \left(1 - \frac{z}{z_\sigma''}\right)}{\prod \left(1 + \frac{z}{z_\sigma''}\right)} \tag{109}$$

This may be regarded as a special case of (20) for $\alpha = 0$ (which makes $C_k = 0$ for k even, and also happens to require $z_\sigma' = -z_\sigma''$). In functional form however, it is more like $i\beta$ of (21). It differs in only two regards. In the power series in z, each C_k is divided by two. In the rational fraction in z, all the zeros correspond to natural modes, and the poles correspond to frequencies of infinite loss; but the poles are also exactly the negatives of the zeros, as in the $i\beta$ equations of (21).

Accordingly, the phase synthesis technique which ignores gain variations may be applied to the zero gain form of the problem by cutting

every $\bar{C}_k$ in two. All zeros of $N = E + O$ must be construed as natural modes z_σ''. Finally, the network must have as many infinite loss points as natural modes, such that $z_\sigma' = -z_\sigma''$. (Integer n is now the number of natural modes, rather than the total number of singularities.)

For physical networks, all the first n terms of the continued fraction (108) must now be positive. To meet this condition it may be necessary to add linear phase to the assigned phase (by adding a *negative* correction to $\bar{C}_1$). It appears that sufficient linear phase will always lead to a physical design, provided the number of modes n is increased to retain a reasonable accuracy.

26. LINEAR PHASE

When the assigned phase $\bar{\beta}$ is linear, the calculations are relatively simple.

If a delay D is to be approximated over a frequency interval extending to $\omega = \omega_c$,

$$i\bar{\beta} = -D\omega_c T_1 \tag{110}$$

If delay D is to be realized without regard to gain variations, the appropriate $\bar{O}/\bar{E}$ is

$$\frac{\bar{O}}{\bar{E}} = \tanh \frac{D\omega_c z}{2} \tag{111}$$

A known continued fraction expansion of $\tanh X$ may be applied to (111), to obtain the coefficients of (108) without bothering with (105).† The result may be arranged as follows:

$$\frac{\bar{O}}{\bar{E}} = \cfrac{1}{\cfrac{2}{D\omega_c z} + \cfrac{1}{\cfrac{3\cdot 2}{D\omega_c z} + \cfrac{1}{\cfrac{5\cdot 2}{D\omega_c z} \cdots}}}} \tag{112}$$

Truncation of the continued fraction gives O/E, and then $O + E$. The zeros z_σ turn out to be proportional to $\frac{1}{D}$, and therefore root extraction techniques are required only for one D, for each n. The zeros are tabulated for sample n's, in Table II.

† For the expansion of $\tanh X$, reference may be made to a text on continued fractions by Wall[11], page 349, equation 91.6.

TABLE II—*Z-Plane Natural Modes for Linear Phase*

n	$D\omega_c z_\sigma$
1	-2
2	$-3 \pm i\sqrt{3}$
3	-4.64438 $-3.67782 \pm i\ 3.50876$
4	$-5.79242 \pm i\ 1.73446$ $-4.20758 \pm i\ 5.31484$
5	-7.29348 $-6.70392 \pm i\ 3.48532$ $-4.64934 \pm i\ 7.14204$
6	$-8.49668 \pm i\ 1.73510$ $-7.47142 \pm i\ 5.25256$ $-5.03190 \pm i\ 8.98532$

The error in the first mismatched Tchebycheff coefficient is a rough measure of accuracy. It may be shown to be

$$C_{2n+1} - \bar{C}_{2n+1} = \frac{(-)^n (D\omega_c)^{2n+1}}{4^n[1 \cdot 3 \cdot 5 \cdots (2n-1)]^2(2n+1)} \tag{113}$$

This measure of accuracy is plotted in Fig. 11, for various numbers of natural modes n. A sample detailed curve of $\beta - \bar{\beta}$ is shown in Fig. 12, with dotted lines corresponding to the estimated error (113).

If delay D is such that the error is reasonable, all the zeros may be natural modes. If these are combined with a like number of infinite loss points, such that $z'_\sigma = -z''_\sigma$, an all-pass network will be obtained, instead of one which approximates D without regard to gain. The all pass network will produce twice the delay, and twice the nonlinearity of phase. In other words, for an all pass network, both coördinates in Fig. 11 must be doubled.

27. SIMPLIFICATION OF SINGULARITY ARRAYS

In complex communication systems, a single equalizer may be required to correct for a number of effects. In a coaxial cable system, for instance, a single network in the standard repeater may be required to compensate for the following: Cable attenuation, characteristics of input and output networks, effects of interstages (significant because the feedback is limited), and distortion due to variable controls at mean settings. Tchebycheff polynomial methods may not be efficient when applied

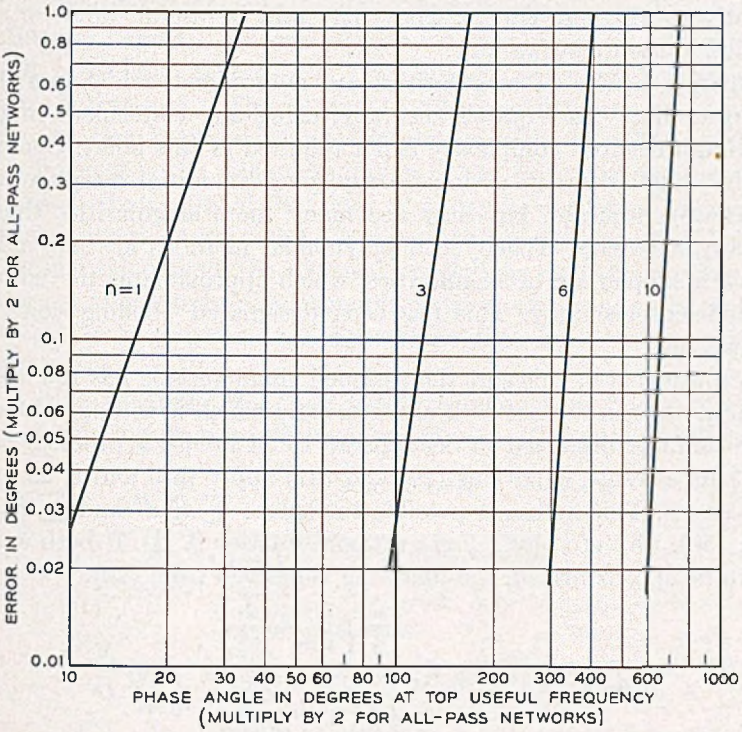

Fig. 11—Estimated error for n natural modes approximating linear phase.

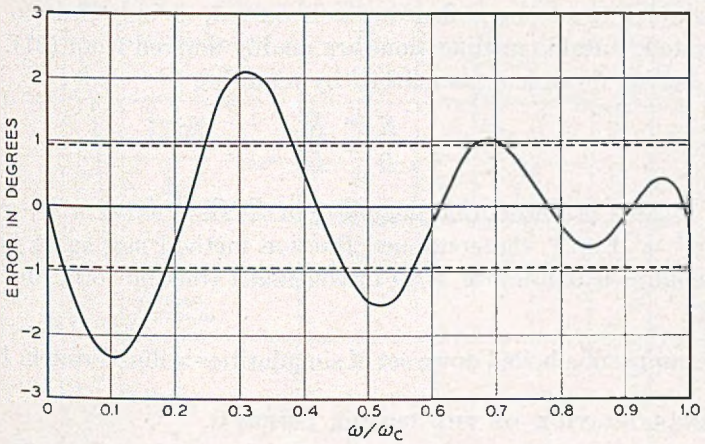

Fig. 12—Error when six natural modes approximate a linear phase, with a slope giving 402° at top useful frequency.

directly to all these effects. They may still be useful, however, when applied in the following way:

Separate arrays of singularities are determined, which match the separate effects to required accuracy, using any convenient methods. Minimum network complexity is not required at this point. Combining all the singularities in a single array gives an initial design which is sufficiently accurate, but may use many more singularities than are actually necessary. Tchebycheff polynomial methods are now used to obtain a simpler set of singularities, which approximates the initial set to sufficient accuracy. This has been designated "boiling down" the original set.

In a problem of this sort the assigned characteristic has the network form, as well as the network characteristic which is to approximate it. (The example discussed in Sections 10 to 14 is also a problem of this sort.) As a result, equations (20) and (21) apply to $\bar{\alpha}$ and $\bar{\beta}$, as well as to α and β. This makes it possible to replace $\sum \bar{K}_k z^{2k}$ and $\sum \bar{K}_k z^k$, of (55), (56), (96) etc., by a finite rational fraction $\bar{N}/\bar{D}$. If both $\bar{\alpha}$ and $\bar{\beta}$ are to be approximated, the following is derived from (20).

$$\sum \tfrac{1}{2}\bar{C}_k z^k = \log \bar{K}_z \frac{\prod \left(1 - \frac{z}{\bar{z}'_\sigma}\right)}{\prod \left(1 - \frac{z}{\bar{z}''_\sigma}\right)} = -\log \frac{\bar{N}}{\bar{D}} \tag{114}$$

The singularities $\bar{z}''_\sigma$, $\bar{z}'_\sigma$ correspond, of course, to the network singularities which are to be boiled down. If only $\bar{\alpha}$, or only $\bar{\beta}$, is to be approximated, suitable modifications are readily derived from (21).

The boiling down is accomplished by requiring

$$\frac{N}{D} \overset{m}{=} \frac{\bar{N}}{\bar{D}} \tag{115}$$

where N/D is of lower total degree than $\bar{N}/\bar{D}$. If $m = n'' + n'$, and $n'' - n' = 0$ or 1, the continued fraction method can again be used. This requires expansion of $\bar{N}/\bar{D}$ in continued fraction form, instead of $\sum \bar{K}_k z^k$.

An example of a boiled down set of singularities is illustrated in Fig. 13.

28. GENERALIZATION OF THE USEFUL INTERVAL

All the previous analysis applies to a useful frequency interval $-\omega_c < \omega < +\omega_c$. Its important characteristics are as follows: It is a single continuous interval, with $\omega = 0$ at its center. Useful intervals with other

other characteristics may be obtained, within limits, by changing the definitions of z and z_σ, in terms of p and p_σ (equations (5) and (8)).

In all cases, the definition of Tchebycheff polynomial T_k remains the same in terms of z. The interval of orthogonality remains $|z| = 1$; and the relation between p and z is always such that the useful frequency interval is the p-plane mapping of $|z| = 1$. The relation must also be such that rational functions of p may be expressed as products of rational functions, in z and $1/z$ respectively, corresponding to (13), (14). At the same time, the physical restrictions on network singularities p_σ must translate into manageable restrictions on the z-plane singularities z_σ. It is restrictions such as these that limit the manageable useful intervals.

It is easy to apply the "low-pass" techniques to "high-pass" intervals, extending from ω_c, through ∞, to $-\omega_c$. The appropriate trans-

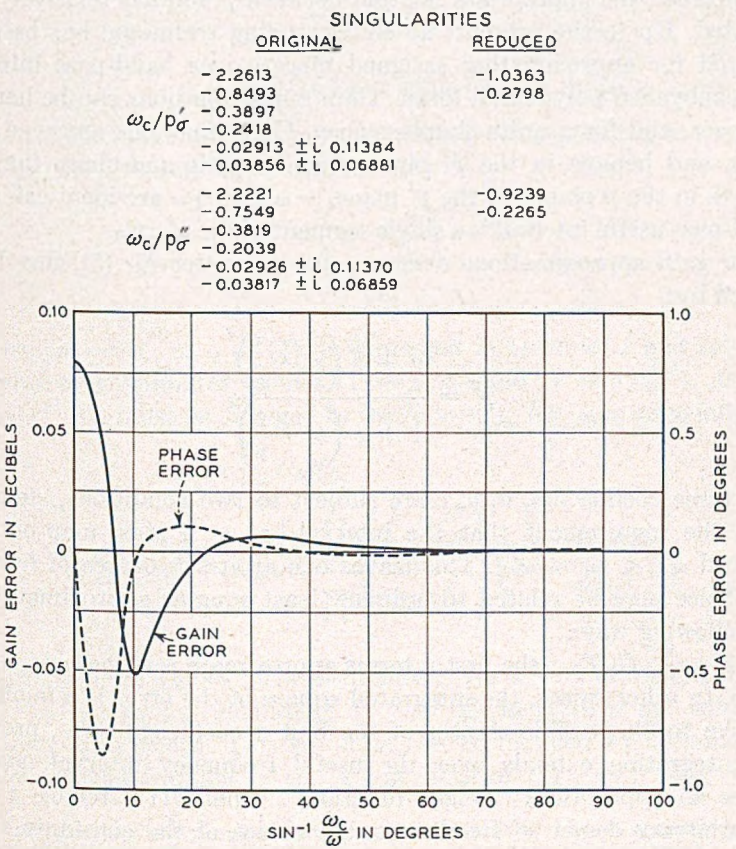

Fig. 13—An example of reduction in complexity.

formation, replacing (5), is:

$$p = \frac{2\omega_c}{z - \frac{1}{z}} \tag{116}$$

With this transformation, the whole of the previous z-plane analysis may be applied at once to high-pass useful intervals, except where linear phase is involved.

The situation is more complicated in regard to "band-pass" intervals. If the useful interval includes the frequencies between ω_{c1} and ω_{c2}, the *complete* useful interval (p-plane mapping of $|z| = 1$) must include also the "image" frequencies, between $-\omega_{c1}$ and $-\omega_{c2}$. Otherwise, conjugate complex z-plane singularities z_σ will not lead to conjugate network singularities p_σ. When there are two disjoint parts of the useful interval, the appropriate relation between p and z is relatively complicated. Up to the present, no corresponding technique has been discovered for approximating assigned phases over band-pass intervals, in Tchebycheff polynomial terms. Gain approximations can be handled, however, and for a quite simple reason. Gain functions are even functions, and behave in the p^2 plane much as gain-and-phase functions behave in the p plane. In the p^2 plane, $-\omega$ and $+\omega$ are identical, and a band-pass useful interval is a single segment of the ω^2 axis.

For gain approximations over a band-pass interval, (5) may be replaced by:

$$p^2 = \frac{a + b\left(z - \frac{1}{z}\right)^2}{1 + c\left(z - \frac{1}{z}\right)^2} \tag{117}$$

The three coefficients, a, b, c are subject to two conditions, stemming from the requirement that the interval $|z| = 1$ must map onto the interval $\omega_{c1}^2 < \omega^2 < \omega_{c2}^2$. This leaves one arbitrary degree of freedom. Its choice may be related to ordinary least squares approximations in the following way:

If $\alpha = \sum C_{2k} T_{2k}$, the first n terms approximate α in the least squares sense. In other words, the integrated square of the error is a minimum, relative to all possible choices of the first n coefficients C_{2k}, provided the integration extends over the useful frequency interval, and includes an appropriate "weight function". When (117) relates z to p, the arbitrary degree of freedom in the choice of the constants a, b, c permits selection of any one of a *family* of weight functions. Conventional

least squares analysis may be applied to determine these functions.†

In applying least squares analysis, it must be borne in mind that the network gain α does not approximate the assigned gain $\bar{\alpha}$ in the simple least squares sense. When $C_{2k} = \bar{C}_{2k}$ for $k \leqq n$, $\alpha - \bar{\alpha}$ depends upon *two* least squares approximations. The first n terms of $\sum C_{2k}T_{2k}$ represent a least squares approximation to α, and are made identical with the first n terms of $\sum \bar{C}_{2k}T_{2k}$, which represent a least squares approximation to $\bar{\alpha}$.

When (117) relates p to z, z-plane singularities z_σ may be defined by:

$$p_\sigma^2 = \frac{a + b\left(z_\sigma - \dfrac{1}{z_\sigma}\right)^2}{1 + c\left(z_\sigma - \dfrac{1}{z_\sigma}\right)^2} \tag{118}$$

$$|z_\sigma| > 1,$$

Re z_σ to have same sign as Re p_σ

An additional singularity, z_0^2, is also needed, corresponding to the finite poles of (117). It may be defined as follows:

$$1 + c\left(z_0 - \frac{1}{z_0}\right)^2 = 0 \tag{119}$$

$$|z_0| > 1$$

When $p_\sigma^2 - p^2$, in α of (2), is expressed in terms of z and z_σ, (117) introduces denominator factors $(1 - z^2/z_0^2)$ and $(1 - 1/z_0^2z^2)$. As a result, α of (21) must be changed to the following, for band-pass intervals:

$$\alpha = \sum C_{2k}T_{2k}$$

$$\sum C_{2k}z^{2k} = \log K_z^2 \frac{\prod\left(1 - \dfrac{z^2}{z_\sigma'^2}\right)}{\prod\left(1 - \dfrac{z^2}{z_\sigma''^2}\right)}\left(1 - \frac{z^2}{z_0^2}\right)^{n''-n'} \tag{120}$$

When definite values have been chosen for a, b, c of (117) (in order that the $\bar{C}_k$ may be calculated), $(1 - z^2/z_0^2)$ in (120) is not subject to arbitrary adjustment. This situation can be handled by defining N/D as the rational fraction in the α equations of (21), as before, but re-

† For general discussions of orthogonal functions and least squares approximations, see Courant and Hilbert[5], and also a short text by Jackson.[12]

placing (84) by

$$\frac{N}{D}^{m\sigma} = \left(1 - \frac{z^2}{z_0^2}\right)^{n''-n'} \sum \bar{K}_k z^{2k} \tag{121}$$

Fig. 14 illustrates an application of the technique to the simulation of a coaxial cable attenuation (which is nearly proportional to $\sqrt{\omega}$).

29. RECAPITULATION

Tchebycheff polynomial series may be applied advantageously to a very wide range of network synthesis applications. The scope of their usefulness may depend upon the skill of the designer, as with any synthesis tools, but the underlying principles are reasonably simple. The most important principles are perhaps the following:

A Tchebycheff polynomial series in frequency may be related to a power series in a new variable z. When the Tchebycheff polynomial series corresponds to a finite network gain or phase, the power series corresponds to an analytic function of z, quite similar in form to the network function of p, with singularities at z-plane mappings of the

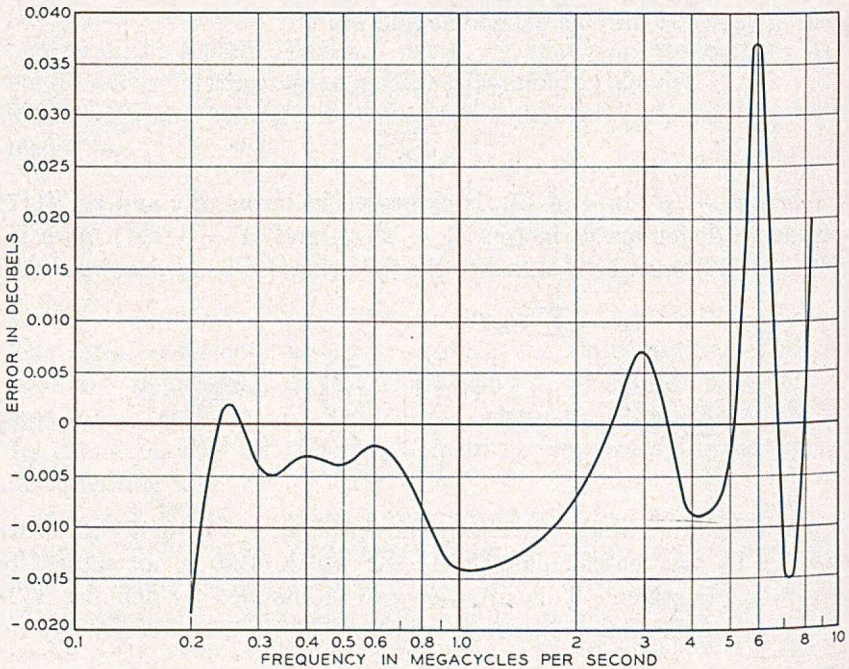

Fig. 14—Simulation of a coaxial cable attenuation—Attenuation at top useful frequency = 46 db; Network = four constant-resistance sections.

network singularities. This makes it possible to apply power series approximation methods, in terms of z, to obtain approximations based on Tchebycheff polynomial series, in terms of frequency.

"Maximally flat" approximations in terms of z may be used to match the first m terms in the Tchebycheff polynomial series representing network gain or phase to the corresponding terms in the series representing assigned gain or phase. In this way, a Tchebycheff polynomial type of least squares approximation to the network function is made identical to the corresponding least squares approximation to the ideal function. The overall error, network function minus ideal function, is then the difference between the two least squares errors.

The z-plane analysis may also be manipulated, in a quite different way, to approach an equal ripple type of approximation (which usually represents approximation in the Tchebycheff sense). The complications are such that applications have been limited to problems of certain quite special types. On the other hand, analysis of this sort has been found useful in clarifying various other ways of seeking equal ripple approximations.

REFERENCES

1. S. Darlington, "The Potential Analogue Method of Network Synthesis," Bell System Tech. J., **30**, pp. 315–365, Apr. 1951.
2. G. L. Matthaei, "A General Method for Synthesis of Filter Transfer Functions as Applied to L-C and R-C Filter Examples," *Stanford University Electronics Laboratory Technical Report No. 39*, Aug. 31, 1951 (for Office of Naval Research, NR-078-360).
3. T. R. Bashkow, "A Contribution to Network Synthesis by Potential Analogy," *Stanford University Electronics Laboratory Technical Report No. 25*, June 30, 1950 (for Office of Naval Research, NR-078-360).
4. E. S. Kuh, "A Study of the Network-Synthesis Approximation Problem for Arbitrary Loss Functions," *Stanford University Electronics Laboratory Technical Report No. 44*, Feb. 14, 1952 (for Office of Naval Research, NR-078-360).
5. R. Courant and D. Hilbert, *Methoden der Mathematischen Physik*, Vol. I, Chap. 2, Julius Springer, Berlin, 1931.
6. C. Lanczos, "Trigonometric Interpolation of Empirical and Analytic Functions," *J. of Math. and Phys.*, **17**, pp. 123–199, 1938–39.
7. H. A. Wheeler, "Potential Analog for Frequency Selectors with Oscillating Peaks," *Wheeler Monograph No. 15*, Wheeler Laboratories, Great Neck, N. Y., 1951.
8. S. Darlington, "Synthesis of Reactance 4-Poles," *J. of Math. and Phys.*, **18**, pp. 257–353, Sept., 1939.
9. T. C. Fry, "Use of Continued Fractions in Design of Electrical Networks," *American Math. Soc. Bulletin*, **35**, pp. 463–498, July-Aug., 1929.
10. H. W. Bode, *Network Analysis and Feedback Amplifier Design*, D. Van Nostrand Co., New York, 1945.
11. H. S. Wall, *Analytic Theory of Continued Fractions*, D. Van Nostrand Co., New York, 1948.
12. Dunham Jackson, *Fourier Series and Orthogonal Polynomials*, The Mathematical Association of America, Oberlin, Ohio, 1941.

A Carrier Telegraph System for Short-Haul Applications

By J. L. HYSKO, W. T. REA and L. C. ROBERTS

(Manuscript received May 14, 1952)

A compact frequency-shift carrier telegraph system is described which provides channels in the voice range and above the voice. The channel terminal unit incorporates arrangements for handling TWX supervisory signals and employs no electro-magnetic relays.

INTRODUCTION

Most short Bell System telegraph circuits, particularly those in the less-densely populated areas of the country, have customarily been operated over direct-current facilities obtained by compositing or simplexing physical telephone circuits. Many of these extend from a telegraph repeater in a central office to another arranged as a subscriber set and mounted in the knee-well of the customer's teletypewriter table. Thus, for example, circuits are extended to Teletypewriter Exchange Service (TWX) subscribers located far from the switchboard. The TWX facilities are arranged to handle supervision as well as transmission. The form of supervision is identical to that obtained when local facilities are employed and hence uniform operating procedures are obtained at TWX switchboards for all subscriber stations without regard to their geographical location.

During and immediately following World War II, the growth of the Bell System's telegraph business resulted in some shortage of dc facilities. It was foreseen that this shortage would be rapidly intensified by the use of new short-haul carrier telephone systems, such as type N1,[1] in providing telephone circuits without adding physical conductors. Moreover, many of the existing direct-current facilities would be absorbed to meet signaling needs for the rapid expansion of telephone toll dialing. It therefore became evident that carrier telegraph methods must be adopted for relatively short hauls in fringe areas.

The existing 40C1 voice-frequency carrier telegraph system[2, 3] was

designed for application in large groups at telegraph central offices and for trunk-service operation over toll telephone circuits employing standard levels. It has proved very economical in this field. However, the very features which make for economy in large installations (such as amplitude modulation, common carrier supply and testing equipment, and standardized operating conditions) cause this equipment to be costly when it is applied a few channels at a time in outlying offices; these may not be equipped with either telegraph battery supplies or telegraph boards. Moreover, the 40Cl equipment, being a carrier-on-for-mark and carrier-off-for-space system, does not lend itself to the provision of TWX toll subscriber line supervision identical to that of local stations without the addition of rather complex and expensive supervisory applique circuits. Where TWX supervision is involved these supervisory circuits are required to generate and recognize supervisory signal patterns capable of being distinguished from transmission space signals and communication breaks, which are long space signals.

Consequently, it was decided to develop a new carrier telegraph system especially aimed at the needs of fringe areas. One of the problems to which much thought was given concerned the choice between amplitude-modulation and frequency-shift operation. A frequency-shift system provides some reduction in the effect of noise and other interference on transmission and it is also less affected by rapid level changes. Although these advantages were attractive, it was not clear that they were sufficient to justify the added complexity and cost entailed by the adoption of this type of transmission, in view of the quiet and stable circuits encountered in the Bell System plant. What finally swung the balance to a frequency-shift system was its advantage in handling TWX supervisory signals. With transmission accomplished by shifting the carrier frequency, supervisory signals could be sent by turning the carrier on and off. A cheap and simple circuit might then be used to distinguish between transmission and supervision.

From the foregoing discussion it will be evident that during the twelve years since the 40Cl system was developed the needs of the Bell System have changed. Fortunately, the designer's art has concurrently made great strides in making available new miniature apparatus and electronic techniques such as have been exploited so successfully in the 143A type electronic telegraph regenerative repeater,[4] the V3 telephone repeater[5] and the N-1 carrier telephone system. As a result, the channel terminal of the new 43A1 carrier telegraph system, being small, inexpensive, self-contained and all-electronic with no electro-mechanical

relays, is almost ideally suited to the needs of the smaller central offices and TWX stations.

FREQUENCY ALLOCATIONS

The 43A1 system provides two groups of channel-frequency allocations, as follows:

a—A three-channel high-frequency allocation, using frequencies between the upper edge of the voice-frequency band and the lower edge of the type-C carrier telephone band. This allocation is primarily for operation on open-wire lines but can also be operated on cable circuits where the loading provides a suitably high cut-off.

b—A voice-frequency allocation capable of providing six channels on two-wire circuits or twelve channels on four-wire circuits. The channels of this allocation are for operation over telephone speech channels on any of the standard facilities, including broad-band carrier and cable or open-wire physical circuits.

The present frequency allocations are shown in Fig. 1. The voice-frequency system is based on twelve nominal midband frequencies spaced 170 cycles apart from 595 cycles to 2635 cycles, omitting 1615 cycles. The carrier frequency is shifted ±35 cycles about midband, and either the higher or the lower frequency may be used for marking sig-

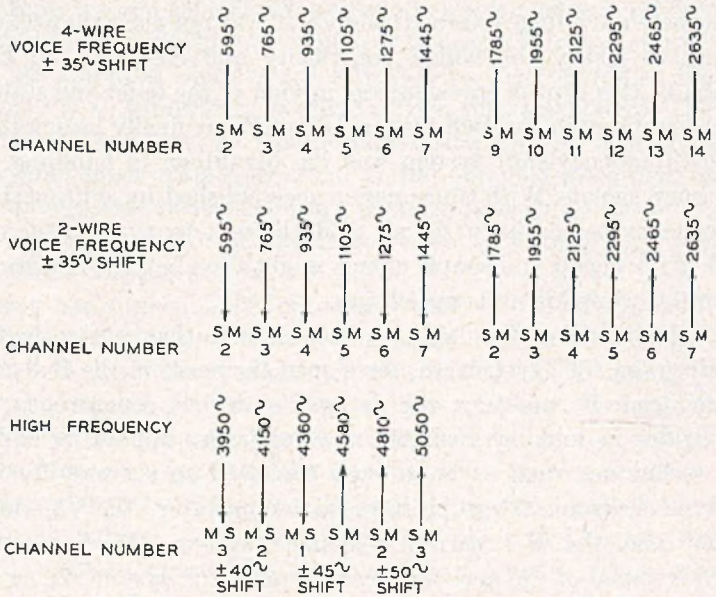

Fig. 1—Frequency allocations.

nals. The high-frequency system is based on six midband frequencies spaced from 200 to 240 cycles apart. The frequency shift ranges from ±40 cycles in the lowest channel to ±50 cycles in the highest. These wider spacings and shifts were adopted to ease the problem of designing inexpensive filters and oscillators for the higher frequencies.

Channel 1 of the high-frequency system employs adjacent frequency assignments for the two directions of transmission. The lower frequency path employs a downward shift for marking signals and the higher-frequency path an upward shift for marking signals. In half-duplex operation this minimizes interference from the strong signals at the transmitter output to the weak signals at the receiver input. The steady marking frequency, which is being sent against the flow of traffic, is shifted away from the band over which the message is passing.

CHANNEL TERMINAL CIRCUIT

Sending Circuit

The sending portion of the channel terminal circuit is shown in the upper part of Fig. 2. When the teletypewriter sending contacts open the loop to send a spacing signal, the sending triode is cut off. When the contacts close the loop to send a marking signal, the grid is made positive with respect to the cathode, the tube conducts and the potential at the plate is decreased. A varistor bridge modulator is connected between this plate and a source of potential having a value lying midway between the marking and spacing plate potentials. Thus, the potential applied across the modulator during marking signals is opposite in polarity to that applied during spacing signals. When the voltage across the varistor bridge is in the conducting direction, the varistors provide a low impedance path to alternating currents. Thus additional capacitance is coupled to the oscillator tank circuit and the oscillator operates at the lower of its two signal frequencies. When the voltage across the bridge is in the non-conducting direction, the varistors are biased to a high-impedance portion of their characteristic, the capacitor is effectively disconnected from the tank circuit and the oscillator operates at its higher signal frequency.

The reversing switch in the driving circuit of the modulator permits either the higher or the lower frequency to be used for marking signals.

The oscillator output power is adjusted by the SEND LEVEL potentiometer and passed through a buffer amplifier and a band pass filter to the send bus and line.

The filter is an impedance transforming structure which contains a

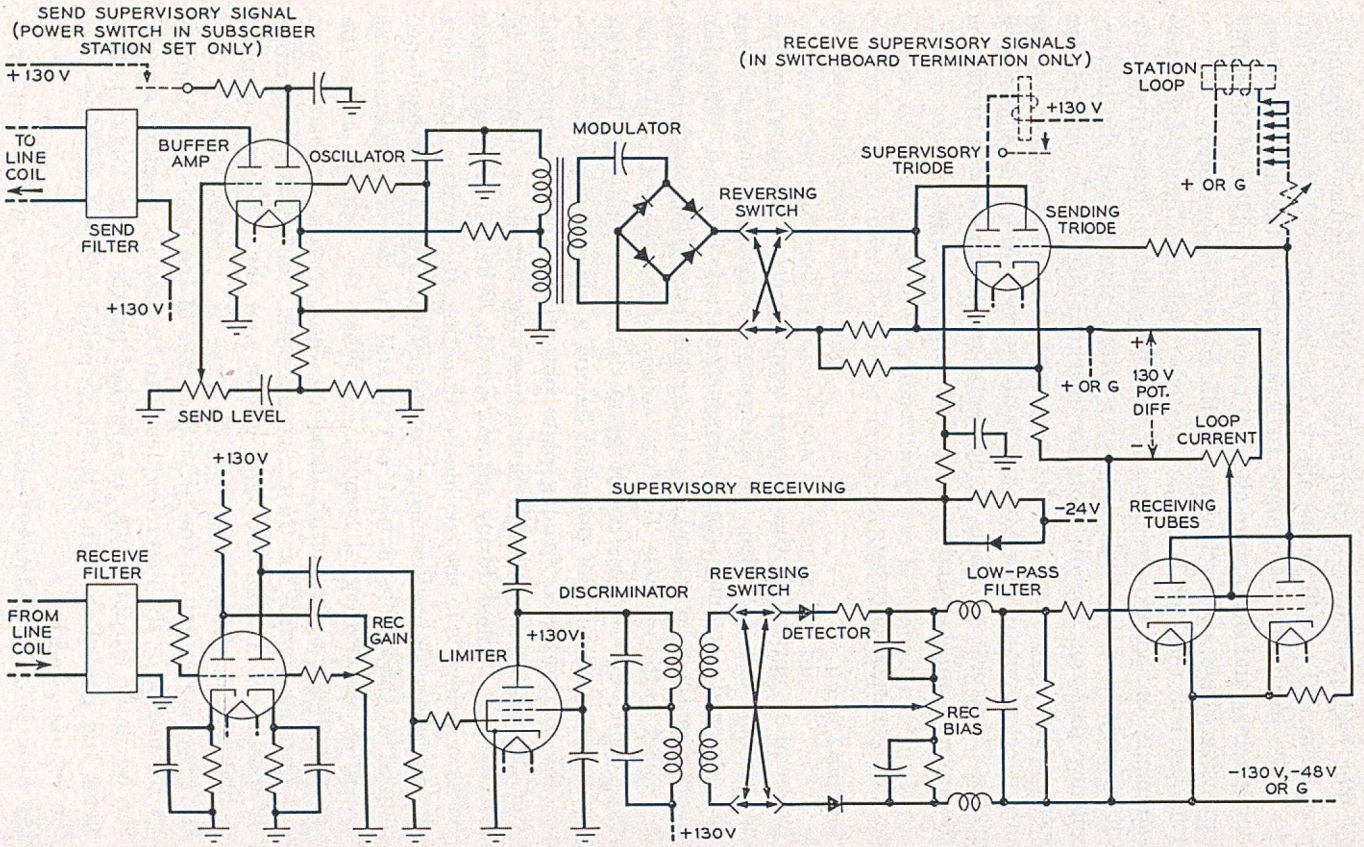

Fig. 2—Simplified diagram of channel terminal circuit, half-duplex.

downward transformation (7500:600) from the impedance of the buffer amplifier to that of the line so that no amplifier output transformer is required.

Either unity-ratio line coils or a hybrid coil may be used to connect the unbalanced sending and receiving filters to a balanced line. The hybrid coil is used with a two-wire line when the send and receive frequencies occupy adjacent bands.

Receiving Circuit

The receiving circuit, shown in the lower part of Fig. 2, is equipped with a filter which selects a narrow band of frequencies centered about the mark and space frequencies of the channel to be received. The receiving band filter has characteristics similar to those of the sending filter, except that it has a greater discrimination against unwanted frequencies and provides an upward transformation (600:140,000) from the line impedance to a value suitable for driving the grid of the first amplifier stage.

The frequency-loss characteristics of a typical receiving filter used in the voice band and of the corresponding sending filter are given in Fig. 3.

The carrier signals selected by the receiving filter are passed through a three stage amplifier limiter. Most of the limiting action is provided by the third stage; the first and second stages act as amplifiers only for weak signals but limit strong signals. An adjustment for receiving gain

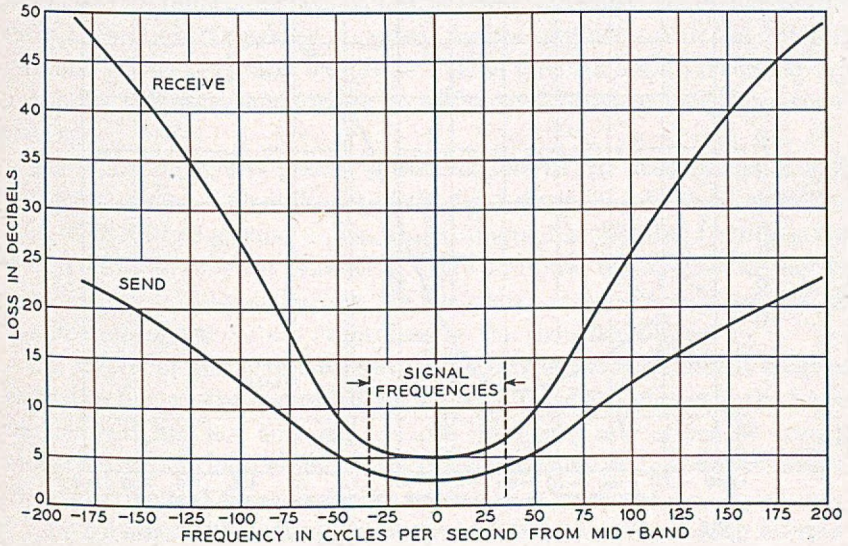

Fig. 3—Send and receive filter characteristics, VF allocation.

is provided between the first and second stages. With the REC GAIN control at maximum the third stage is driven to full output when the input to the receiving filter is greater than about −50 dbm*. Where it is not necessary to detect the presence or absence of carrier for supervision as described below, the control is generally set for maximum gain.

The limiter output is passed through a frequency discriminator consisting of two anti-resonant circuits in series, tuned so that one has a parallel resonance at the low frequency edge and the other at the high frequency edge of the channel band. The voltages appearing across the anti-resonant circuits are rectified separately by germanium varistor diodes and the resultant d-c output voltages are added algebraically, filtered and applied to the control grids of the output tubes.

Since at normal receiving levels the limiter removes all magnitude variations, the output from the discriminator detector circuit is dependent in magnitude and sign only on the signaling frequency. A negative voltage from the detector causes cut-off of the amplifier tubes and a positive voltage causes plate current to flow. A switch between the discriminator and the detector provides means for reversing the output connections of the discriminator so that a positive voltage from the detector can be obtained with either the higher or the lower signaling frequency. Fig. 4 shows the dc voltage output versus frequency characteristic obtained with a typical discriminator.

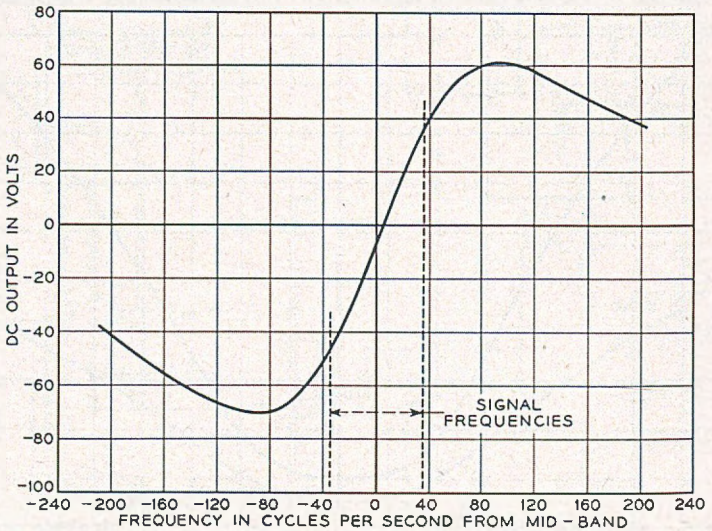

Fig. 4—Frequency characteristic of typical discriminator.

* "dbm" is an abbreviation for "decibels with respect to one milliwatt."

The low pass filter between the detector and last stage serves to remove carrier ripple and to decrease the effects of noise and other interference having demodulated frequency components greater than about 40 cps, which is slightly higher than the "dotting" frequency of 100-word per minute signals. In order to prevent a change in the tuning of the discriminator when the reversing switch is operated, a balanced low-pass filter structure without mutual inductance is employed. This presents high and nearly equal impedances to ground from the positive and negative sides of the detector circuit.

Nearly all the voltage gain of the receiver appears ahead of the detector. Since the detector output voltage applied to the grids of the beam power tetrodes is high enough to give an approximately square signal wave shape in the loop, no intermediate stage of dc amplification is needed following the detector. For unbiased signal reception, the demodulated signals should be centered on the grid characteristic of the receiving tubes; that is, the marking and spacing voltages applied to the grid circuit should be symmetrical about a potential a few volts negative with respect to the receiving tube cathodes. To obviate the need for a voltage source negative with respect to the cathodes, the signals are prebiased by unbalancing the detector so that the mean of the mark and space output voltages from the low pass filter is about −5 volts. Further adjustment of the mean signal value may be made by means of the REC BIAS potentiometer to compensate for bias of signals received from the line due to deviations in the mark and space frequencies from their theoretical values or to other causes originating at the sending terminal of the telegraph circuit as well as for bias due to discrepancies in the discriminator network or to differences between mark and space levels.

These arrangements permit great freedom in the assignment of loop battery voltages. The cathodes of the final stage may be fixed at −130-volt, −48-volt or ground potential and the plates operated from ground, +48-volt or +130-volt potential. The remainder of the circuit may be powered by +130-volt battery for the plates and −24-volt battery for the heaters of the tubes, regardless of the loop conditions.

By means of the reversing switch mentioned above, current may be caused to flow in the loop during the reception of the higher or the lower frequency. Thus not only can various frequency allocations be accommodated, but the local circuit may be operated neutral (current for mark) or inverse neutral (no current for mark).

One tube is used in the final stage for 20 ma or 30 ma loop current, and two for 60 ma loop current.

Supervisory Circuit

When the channel is used in TWX service as a toll subscriber line, the subscriber calls the operator to initiate a call by closing the power switch on his teletypewriter. This connects power to the teletypewriter motor, closes the transmission circuit to the teletypewriter and applies plate battery voltage to the transmitting oscillator in the channel terminal, resulting in the transmission of carrier current over the line. At the distant (switchboard) terminal the receipt of carrier current energizes a supervisory signal receiving circuit which is responsive to carrier-on and carrier-off conditions in the receive band. In this circuit, carrier voltage appearing at the plate of the limiter tube is rectified and applied to the grid of the supervisory triode. The operation of a relay in the plate circuit of this tube causes a line lamp at the switchboard to light.

A disconnect signal is sent by the subscriber at the end of a call by opening the teletypewriter power switch. This removes the oscillator plate voltage. At the central office, the receipt of the resulting no-carrier signal de-energizes the supervisory receiving circuit and causes the supervisory lamp in the operator's cord circuit to light steadily. To recall the operator during a call the subscriber opens and recloses his power switch. This causes the cord lamp at the switchboard to flash.

An RC circuit slows the rise of current in the supervisory receiving tube to guard against false operation of the switchboard line lamp due to noise impulses during the carrier-off, that is, the idle condition.

DC Circuits

On the dc side of the channel terminal, provision is made for optional wiring arrangements to connect to the circuits of the various telegraph test boards, service boards and TWX switchboards, as well as to local teletypewriter loops, using telegraph voltages of either 130 or 48 volts. In offices where a negative 130-volt battery is not provided, operation with a single positive 130-volt battery is possible.

The loop connections are made to an electronic circuit in the channel terminal which is similar to that employed in a recently-developed electronic loop repeater used in telegraph offices and which possesses several interesting features. Fig. 5 compares the action of this circuit, in transmitting toward the subscriber station, with that of more conventional arrangements:

(a) shows a conventional open-and-close circuit and the wave shapes which it produces at the central office end and at the far end of a capaci-

tative loop. As is well known, the asymmetrical wave shape causes positive signal bias.

(b) shows an "effective polar" circuit along with the wave shapes it delivers. This is the circuit conventionally used to drive subscriber loops. It presents a constant low impedance to the loop and might therefore be considered a "close-and-close" circuit.

(c) shows the electronic loop circuit. The driving tetrodes are operated in their high-impedance region, above the knee of the plate-current plate-voltage curve. They deliver a highly symmetrical rectangular wave to the loop and little or no bias results. This circuit presents a nearly constant high impedance to the loop and might be considered an "open-and-open" circuit.

Although the rectangular wave is inferior to a peaked wave in that less average power is delivered for the same values of steady-state current and voltage, it provides entirely acceptable transmission for 19-gauge cable loops up to about 20 to 25 miles in length. Inasmuch as 80 volts potential is absorbed in the electron tube plate circuits, this is almost the maximum length over which 62.5 ma can be supplied when loop battery of 260 volts is used.

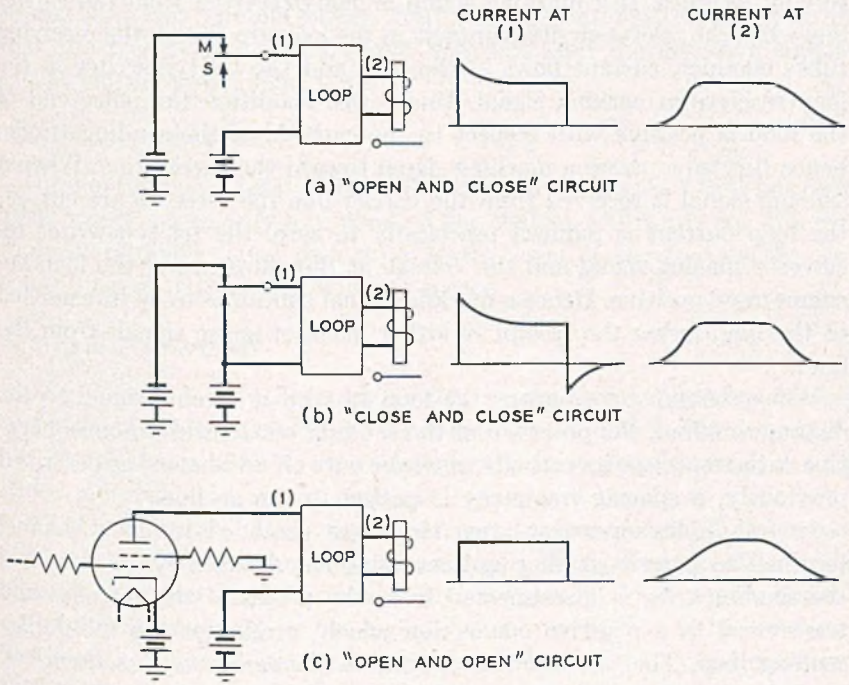

Fig. 5—Explanation of electronic loop circuit.

During open-and-close transmission by the subscriber, the high impedance termination of the loop at the tetrode plate circuits causes the current at the central office end of the loop to change very slowly—too slowly for good transmission at teletypewriter speeds. However, the voltage wave is very well shaped, and this is what is used to drive the grid of the transmitting tube. One noteworthy fact is that the bias of the signals repeated from loop to line is nearly independent of loop length; consequently no inductive wave shaping is required at the subscriber station, even in the longest operable loops.

Because of the high impedance termination, loop current is insensitive to circuit resistance. The loop padding rheostat is, therefore, adjusted to build out the loop resistance to a standard value and the amount of loop current required for proper operation of the station teletypewriter is obtained by varying the screen grid potential of the tetrode tubes.

Duplex Feature

In half-duplex operation, one dc loop at each channel terminal serves for both sending and receiving. The central office end of this loop is connected to the grid of the sending triode and to the plates of the receiving tetrodes. If a marking signal is being received from the carrier line while the teletypewriter contacts in the loop are closed, the receiving tubes conduct, current flows in the loop and the teletypewriter in the loop receives a marking signal. Under this condition the office end of the loop is positive with respect to the cathode of the sending triode; hence this tube passes a marking signal toward the carrier line. When a spacing signal is received from the carrier line the tetrodes are cut off, the loop current is reduced practically to zero, the teletypewriter receives a spacing signal and the voltage at the office end of the loop becomes more positive. Hence a marking signal continues to be transmitted to the line during the receipt of either mark or space signals from the line.

When the subscriber opens the loop to send a spacing signal to the distant terminal, the potential of the sending triode grid becomes negative with respect to its cathode, the tube cuts off and hence, as described previously, a spacing frequency is passed to the ac line.

In full-duplex operation, two loops are provided at each channel terminal to permit sending and receiving simultaneously. The grid of the sending tube is disconnected from the plates of the tetrodes and transferred to a resistive connection which terminates the full-duplex sending loop. The loop circuits operate in the same way as described for half-duplex operation except that no break action is provided.

Break Feature

When the subscriber opens the loop at the teletypewriter to break transmission coming from the distant terminal, a clean-cut space should be transmitted to the line regardless of any incoming signals. The resistor shunted between the plates and cathodes of the receiving tubes causes the central office end of the open loop to assume the same potential as the tetrode cathodes. This insures that a steady spacing potential will be applied to the send tube even though the tetrodes are cut off by an incoming space. This provides a rapid, clean break. However, if a large leakage exists across the loop conductors, the resistor will not be able to keep the sending tube in a cut-off condition and a break by the subscriber will result in the incoming transmission being reflected in an inverted condition to the distant carrier terminal. In such a case the distant sending subscriber would be broken by a "bust-up" of local copy or by operation of the keyboard break lock. This would normally be caused only by a trouble condition in cable loops.

If a break signal is received over the line from the distant end while the near end subscriber is sending, his loop current is reduced to practically zero. This operates the keyboard break lock thus breaking the subscriber. This circuit differs from the conventional loop circuit in that the receipt of a break signal does not stop the outgoing signals except via the break lock.

TELEGRAPH DISTORTION

On quiet circuits, total distortion per section averages 1 to 2 per cent at 60 words per minute and about 5 per cent at 100 words per minute. Plots of received signal distortion versus level of received carrier are shown on Fig. 6 for both signaling speeds.

EQUIPMENT FEATURES

The channel terminal employs a formed sheet-metal framework and occupies a space $10\frac{1}{2}$ inches high, $5\frac{1}{4}$ inches wide and $7\frac{3}{4}$ inches deep overall. Fig. 7 shows a 43A1 channel terminal. It is plug-terminated, and hence removable for maintenance or repair at a bench.

The basic portion of the channel terminal is common to all frequency allocations. The oscillator network and send filter, which constitute the elements determining the transmitted frequency, form a plug-terminated sub-assembly $7\frac{3}{4}$ inches high, $5\frac{3}{8}$ inches wide, and $1\frac{1}{2}$ inches deep. The receive filter and discriminator, which select the received frequency, form a plug-terminated sub-assembly of the same size.

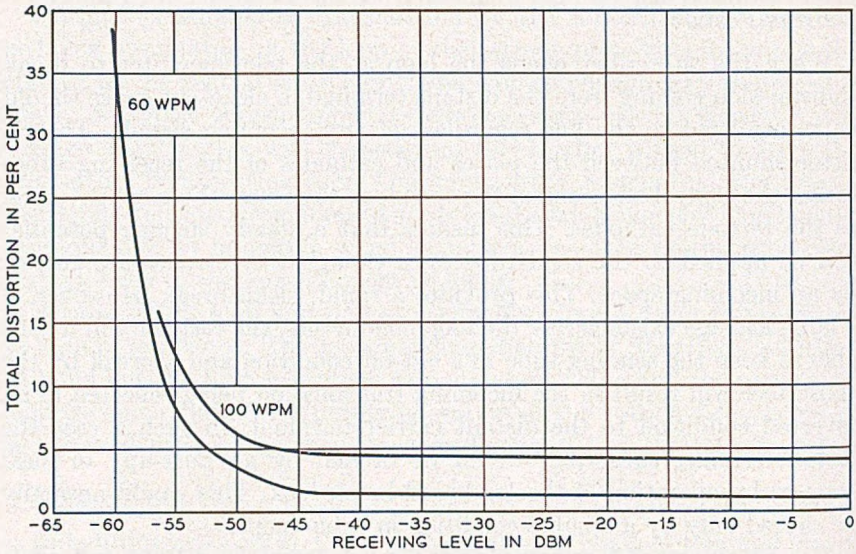

Fig. 6—Telegraph distortion vs receiving level.

A rear view of the channel terminal with the send frequency unit removed is shown in Fig. 8. With both frequency units in place, the rear of the channel terminal is almost completely enclosed. When they are removed, the wiring and apparatus terminals of the basic channel terminal are readily accessible for test and repair.

Tube sockets, potentiometers, test points, switches and the inductor of the low-pass filter are mounted on the front panel. Small resistors, capacitors, and germanium diodes are assembled on a plastic "ladder" which is mounted vertically in the space between the frequency units.

As shown in Fig. 9, three channel terminals may be mounted abreast on a welded metal frame which is fastened to any of the standard bay frameworks designed to accommodate 19-inch mounting plates. The unit mounting frame carries the multicontact receptacles into which the channel terminals are plugged. Twenty-four channel terminals may be mounted on an 11½-foot relay rack, with line coils and certain auxiliary equipment.

Where arrangements for switching between half and full-duplex operation are required, duplex switches for a number of channel terminals are mounted on a narrow plate between the channel terminal mounting frameworks.

Loop rheostats, when required, may be mounted adjacent to the channel terminals or in a loop pad bay along with other loop rheostats that may be associated with electronic loop repeaters. The latter arrange-

ment concentrates the heat dissipated by these rheostats at a place where it will not be harmful.

Subscriber Set

A channel terminal may also be mounted in a station set box appearing in the knee-well of a subscriber's teletypewriter table. This, called a 130B1 teletypewriter subscriber set, is illustrated in Fig. 10. It contains a line or hybrid coil and balancing network, as well as local circuit resistors and other miscellaneous apparatus. When so mounted, the

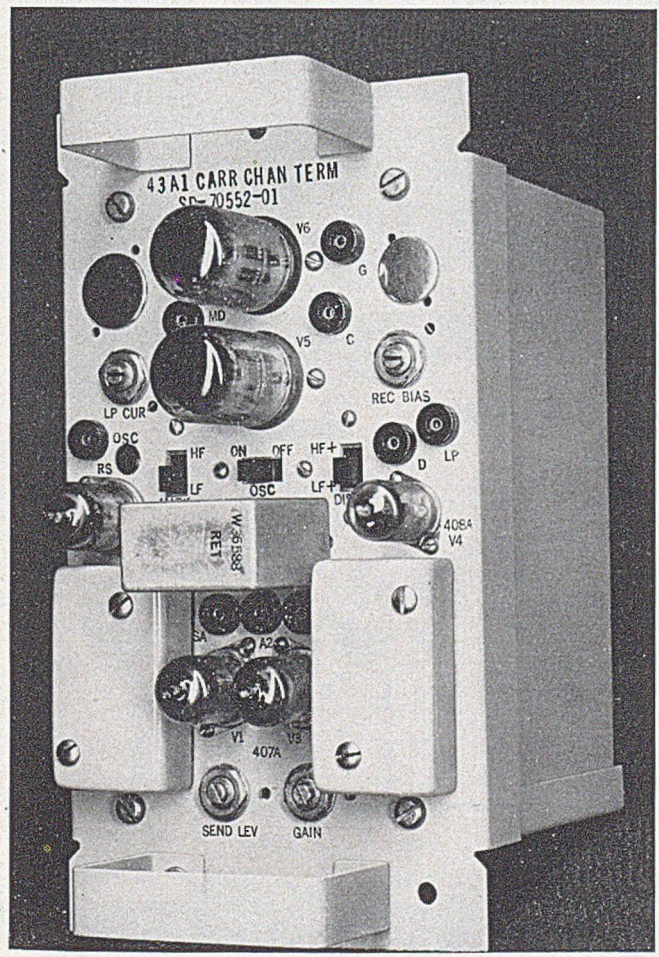

Fig. 7—Channel terminal, front view.

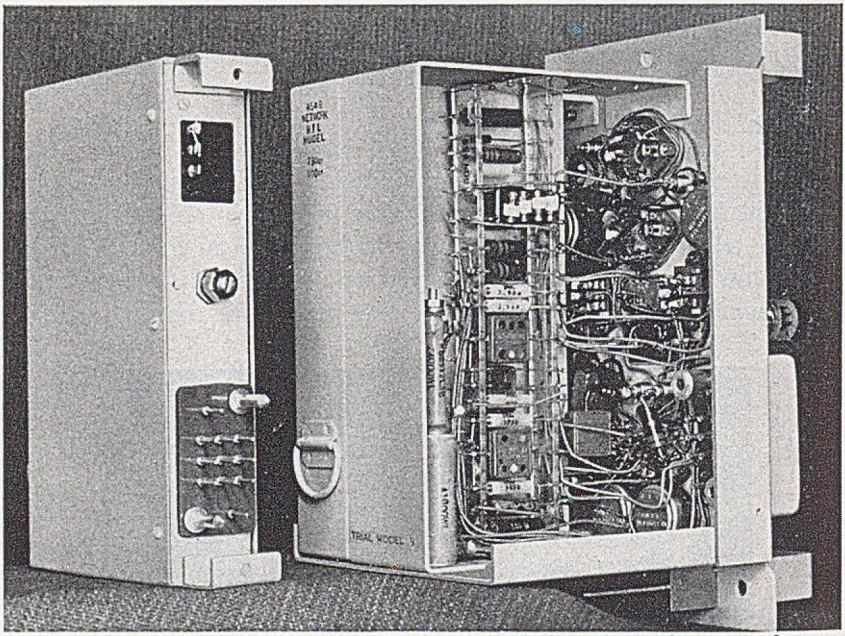

Fig. 8—Channel terminal, rear view, sending network removed.

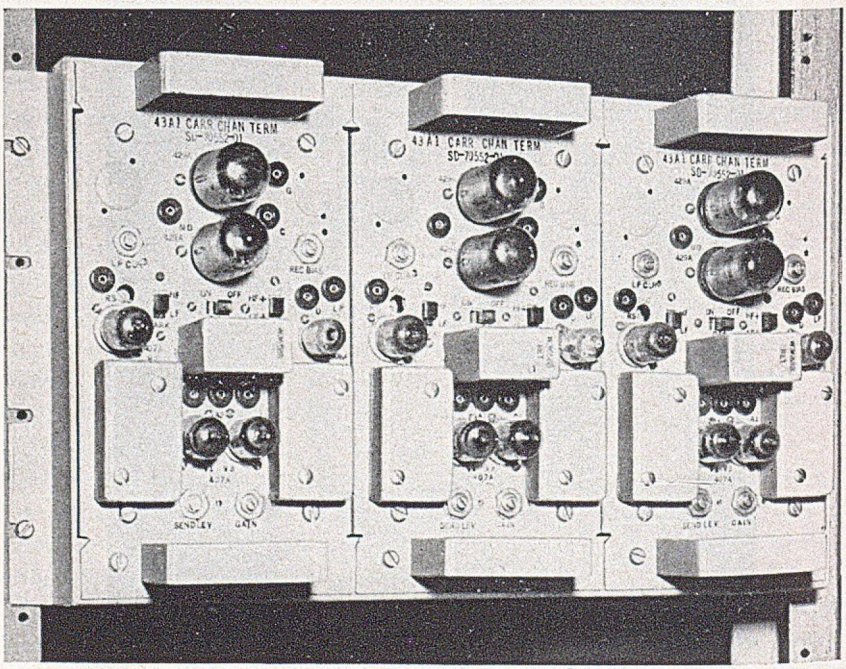

Fig. 9—Three channel terminals mounted on relay rack.

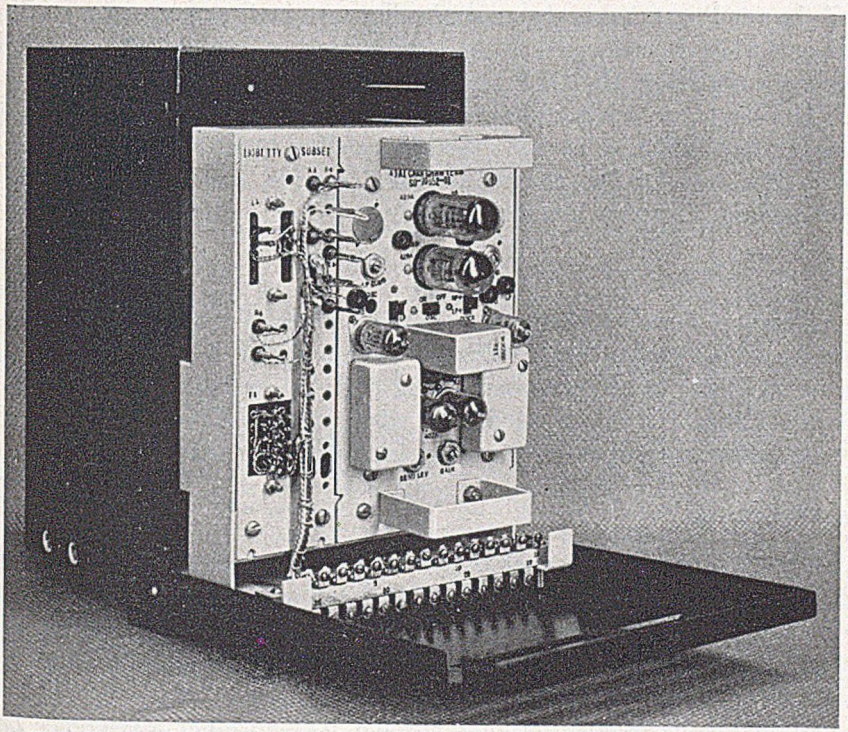

Fig. 10—130B1 teletypewriter subscriber set including channel terminal.

channel terminal is powered by the teletypewriter rectifier, which furnishes 130-volt dc and 20-volt ac power.

The 130B1 set may be employed in private-line or TWX service. In the latter, the application and removal of oscillator plate battery is controlled as described above by the teletypewriter power switch, so that the equivalent of telephone "switch-hook" supervision is attained.

Supervision and transmission are largely independent. The telegraph receiving circuit at the central office terminal remains marking during recall and disconnect signals; hence these supervisory signals do not pass through the cord-circuit repeater to the TWX toll line. Since there is no frequency discrimination in the supervisory receiving circuit, either marking or spacing carrier from the station energizes the supervisory circuit. Hence a communication break (spacing) signal from the subscriber station is transmitted through the operator's cord without any effect on the supervision.

On a TWX call to the subscriber station, a series of alternate marks and spaces, generated by applying 20-cycle ringing voltage to the grid

of the sending tube at the central office terminal, actuates the station ringer, which is connected to the local loop whenever the teletypewriter power switch is in the OFF position.

The circuit which terminates the TWX toll subscriber line at the switchboard office is operable with all existing types of TWX cord circuit repeater. All the features of TWX service, including unattended service, are therefore available.

POWER DRAINS

A channel terminal dissipates about 25 watts. Tube heaters consume about half an ampere at 24 volts and the remainder of the channel terminal, exclusive of its loop-terminating portion, consumes 50 ma at 130 volts. The loop terminating portion dissipates 20, 30 or 62.5 ma at 80 volts, depending upon the type of local circuit employed.

LINE LEVELS

The 43A1 system is capable of working with a great variety of line levels. The send level may be adjusted for any value from +6 dbm downward. The receiving equipment operates satisfactorily with −45 dbm or even −50 dbm. But the levels actually used are controlled by crosstalk and noise conditions in the line.

Receiving levels are normally limited by lightning interference on open wire and by noise on cable circuits. The minimum tolerable levels are about −40 dbm on open wire, −45 dbm on four-wire cable circuits and −35 dbm on two-wire cable.

In Fig. 11, a comparison is made of the effects of static on the 43A1 system and on the 40C amplitude-modulation system. It gives the results of simultaneous tests on the 2465-cycle bands of the two systems, using the static from a record made at Madison, Florida. The 43A1 channel could tolerate about 4 db stronger static than the 40C.

SYSTEM LAYOUTS

A typical circuit layout of the 43A1 system working in the frequency band between the voice and type-C carrier on an open-wire line is shown in Fig. 12. The telegraph circuits extend from 43A1 channel terminals located in a central office, at the left, to 130B1 sets in subscriber stations, at the right. In the central office, the send and receive paths of the channel terminal are combined in a hybrid coil. With the moderate degree of balance provided by the network of this hybrid coil, the allowable difference between send and receive levels of the middle channel may be

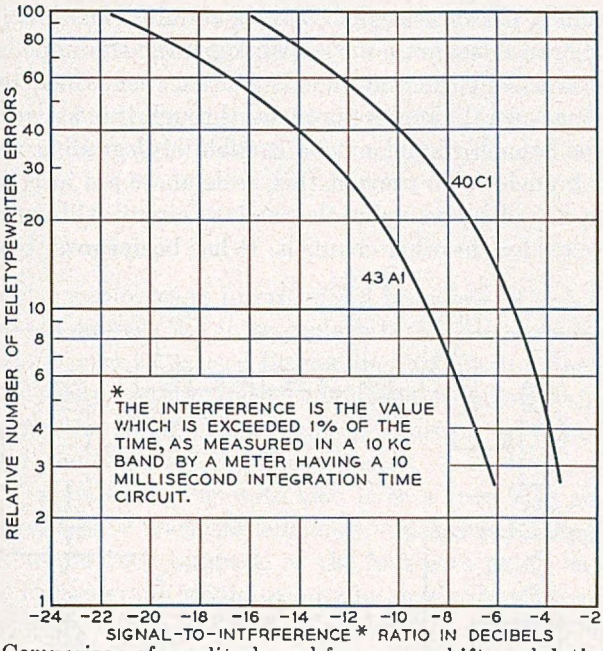

Fig. 11—Comparison of amplitude and frequency shift modulation with static interference.

35 db or more. The telegraph channels are next combined with the voice frequency circuit by means of a 150A filter, and are connected to the composite set and line through the low-pass section of the 121A (type -C) carrier line filter. As a result of the cut-offs of the 150A high-pass and 121A low-pass filter components, the pass band of the telegraph is about 3.7 to 5.4kc. At the outlying terminal of the open-wire line, the telegraph is separated from the voice and type-C carrier circuits by similar filters and connected to the individual subscriber stations by a branching network and branch lines.

The typical arrangement on a two-wire circuit in the voice frequency range is shown in Fig. 13. Six channels are available, using six of the twelve frequency bands for transmission east to west and the other six bands west to east. As in the high frequency case, a branching network and branch lines at the outlying end connect the circuits to the subscribers. Fig. 14 shows a layout in which branch lines are connected at intermediate points in the telephone circuit. At these intermediate points the impedance of the branching network is made high, in order to keep the balance at the telephone repeater from being harmed excessively. Though the network attenuates greatly the signals through it, the telegraph level is usually sufficiently high so that this loss can be tolerated.

The branching network at the outlying terminal has low impedance. Taps on the transformers in the network permit the impedance ratios to be adjusted to suit the line impedances between which the network operates. Since several circuits may pass through this network, a short-circuit on one branch should not be capable of degrading transmission in the other branches. To prevent this, resistances are inserted in series with each branch of such a value that a short circuit will not cause more than 3 db excess loss in other channels. It has been shown by tests that,

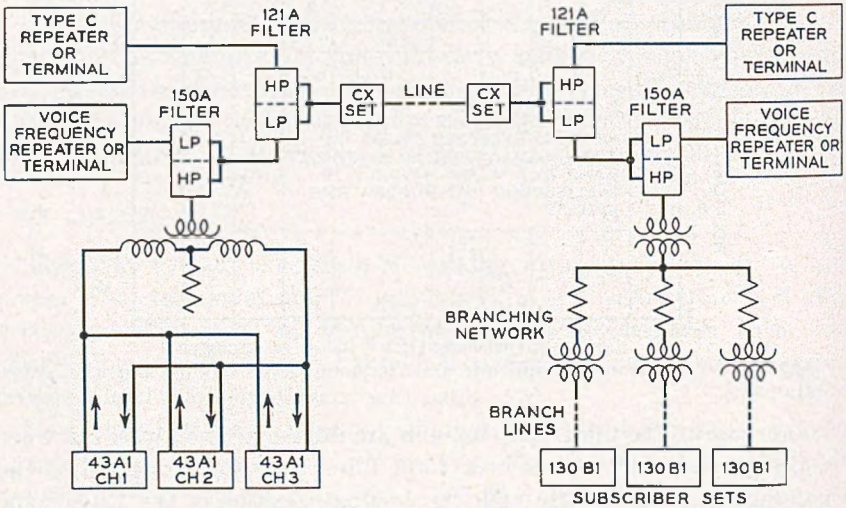

Fig. 12—System layout, above the voice.

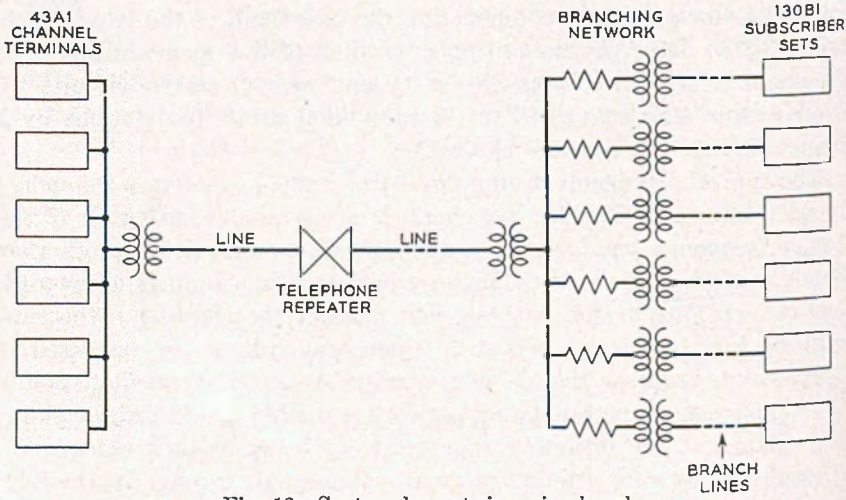

Fig. 13—System layout, in voice band.

in this frequency-modulation system, a sudden loss of 3 db causes little distortion. The series resistances may serve another purpose besides protecting against short circuits. If one branch has a much greater attenuation than the others, the resistance values in series with the shorter branches may be increased so that more energy is directed into the longer branch.

Emergency Circuits

If a circuit containing no intermediate branches fails, a regular message circuit can be patched in to replace it until the trouble is cleared. Fig. 15 shows trunks to be used for making this patch in the case of two-wire circuits. They contain 3 db pads which reduce the signal level to compensate for the change from 0 db transmission level on the regular line to +3 db level on the message circuit.

The 43A1 system may operate also over a four-wire circuit, which accommodates twelve telegraph channels. A patch to an emergency message circuit would then be made at the four-wire patch bay. Since the circuit used for telegraph would usually be similar to those used for telephone message service, no pads to adjust levels would be required for this

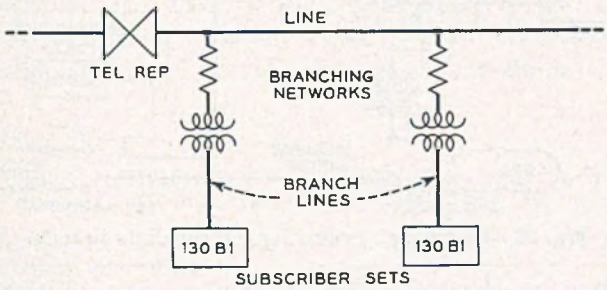

Fig. 14—Intermediate branch lines.

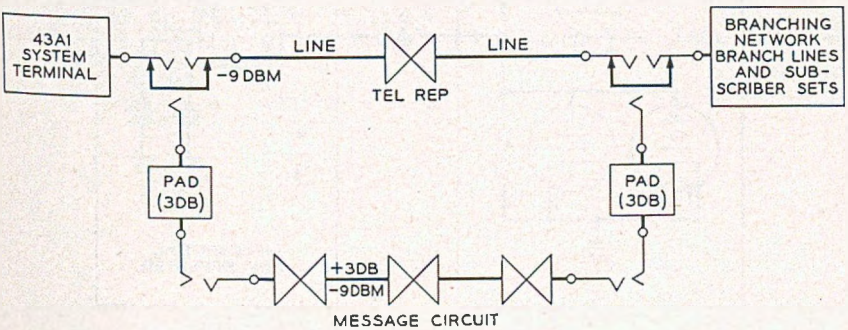

Fig. 15—Emergency circuit.

patch. Obviously echo suppressors must be disabled when a message circuit is used for telegraph.

When the telegraph circuit contains one or more branches at intermediate points, it would be difficult and often impractical to use an ordinary message circuit to replace the telegraph stem in emergencies. The branching location frequently will not be manned and so no one will be available to patch the branch line to the message circuit. In such cases each intermediate branch circuit may be made good over a separate message circuit which is individual to it. Fig. 16 shows this arrangement. A patch trunk is provided between the 43A1 channel terminal at the central office and the telephone switchboard. At the switchboard which is nearest to the intermediate branch subscriber, the branch line is

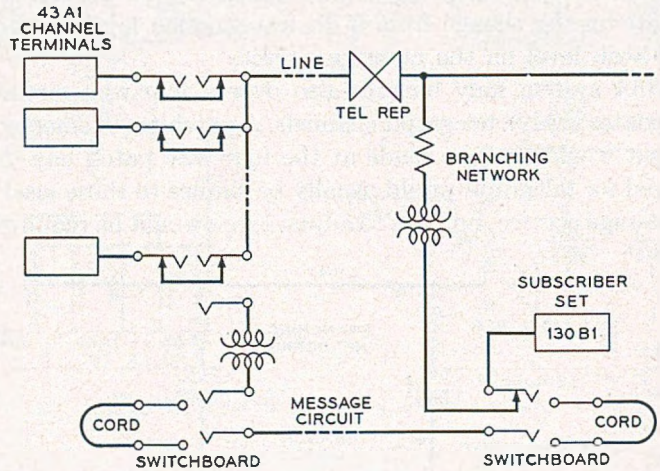

Fig. 16—Emergency circuit for intermediate branch.

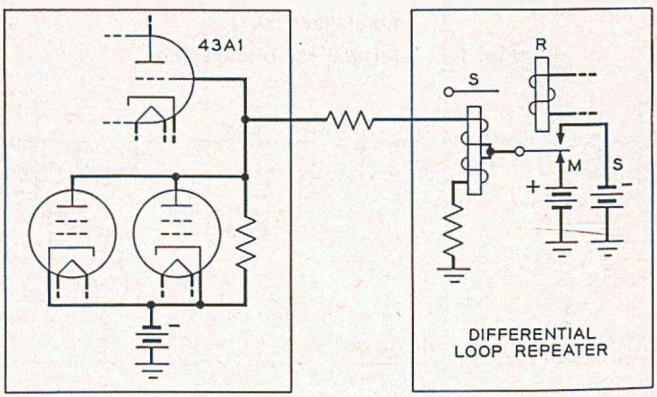

Fig. 17–Connection to other telegraph repeaters.

carried through a cut-off jack. The toll operators then can patch the circuit to the subscriber, thus by-passing the main line when it is in trouble. Since the telegraph energy from only one channel is impressed on the emergency circuit, no adjustment of levels is required.

The channel terminals which are at the central office, shown at the left of Figs. 12 to 16, may be connected to subscribers over dc loops or they may be connected to other types of telegraph repeaters. Fig. 17 indicates the latter connection schematically. Since the loop circuit must supply positive potential to the 43A1 channel terminal, the connecting repeater must be arranged to supply positive battery for marking signals.

FUTURE EXTENSIONS

It is expected that the field of application of the 43A1 system will be broadened by further development over the next few years. More frequencies will be provided, both in and above the voice band. Means will be designed for passing TWX supervisory signals over a direct-current loop from a subscriber station to a channel terminal installed in a nearby central office. The built-in supervisory arrangements of the 43A1 equipment will be exploited to obtain inexpensive straightforward trunks for use both between TWX switchboards and from switchboards to Line Concentrating Units. The supervisory feature will also be employed in private line service to provide an open circuit alarm.

REFERENCES

1. R S. Caruthers, H, R. Huntley, W. E. Kahl, L. Pedersen, "A New Telephone Carrier System for Medium-Haul Circuits," *Elec. Eng.*, **70**, pp. 692–697, Aug. 1951.
2. B. P. Hamilton, "Carrier Telegraphy in the Bell System," *Bell Labs. Record*, **26**, pp. 58–62, Feb. 1948.
3. J. A. Duncan, R. D. Parker and R. E. Pierce, "Telegraphy in the Bell System," A.I.E.E. Transactions, **63**, pp. 1032–1044, 1944.
4. B. Ostendorf, Jr., "New Electronic Telegraph Regenerative Repeater," *Elec. Eng.*, **69**, pp. 237–240, March, 1950.
5. R. L. Case, "Transmission Features of V3 Repeaters," *Bell Labs. Record*, **27**, pp. 94–95, March, 1949.

The Type-O Carrier System

BY PAUL G. EDWARDS AND L. R. MONTFORT

(Manuscript received June 11, 1952)

INTRODUCTION

While the sight of an open-wire toll line is a rarity in many parts of the East, considerable use is made of open-wire facilities in other sections of the country to provide toll and exchange service. At the present time there are about 170,000-route-miles of open-wire in the Bell System which carry some 1,400,000 pair-miles of wire used for toll service. It is estimated that about 60 per cent of this pair-mileage is used for carrier, although only about 10 per cent carries the full fifteen carrier channels, which is possible by employing type-C and type-J carrier systems. It is obvious that some of the remaining line pairs are available for additional carrier growth, provided, of course, the demand for additional circuits exists, and there are carrier systems which can meet these demands economically. Type O is a multi-channel, open-wire carrier system which has been designed to provide, economically, additional circuits in the range from a minimum of about 15 up to a maximum of 150 miles, or more. The type-O system is the open-wire counterpart of the type N short-haul cable system.

Present open-wire toll lines vary from a single-arm line, with one or two pairs of wires, up to lines with five or six arms carrying thirty pairs. These lines may carry long-haul toll circuits up to about 1000 miles in length, short-haul toll circuits up to 150 miles, as well as tributary trunks and exchange circuits. Growth in the past of toll and tributary circuits on these lines has been provided by the addition of single-channel D or H systems, three-channel C systems, twelve-channel J systems or by other similar carrier systems.

The full development of a line for open-wire carrier has, in the past, required expensive line rearrangements. For instance, most lines reach terminal and repeater offices over entrance cables which may be several miles in length. Impedance matching at the junction of the open-wire and cable is required, and is provided by loading the cable at both voice and carrier frequencies, by employing junction line filters using non-

loaded carrier pairs, or by the use of autotransformers. In addition, transposition schemes are needed to reduce the crosstalk coupling between open-wire pairs to tolerable amounts, and longitudinal and metallic filtering is necessary at repeater points to control interaction crosstalk. The C and J carriers have been designed essentially for long-haul use, and when the line transposition costs are added, these systems are likely to be more expensive than adding wire for providing relief for the shorter circuits, which are required in increasing number as the length decreases.

In contrast to the heavy back-bone toll lead carrying both long and short haul circuits is the one or two arm line which may be a secondary route, or a line which terminates in a small town. The demands along this line are for short-haul toll service, trunks between tributary offices and their toll centers, and for exchange service. Because growth has been relatively slow, carrier has been employed only to a limited extent. Single-channel D or H systems may be found on these lines, or an adaptation of the M system for toll service, and possibly other miscellaneous systems. Only minor rearrangements of the line and entrance cables has been necessary because of the small percentage of circuits equipped with carrier facilities.

A typical need for expansion on this type of line occurs when a manual tributary office is cut over to dial operation, and the operators are moved to the toll center. Additional circuits are immediately needed from the toll center to the tributary office because of certain factors introduced when the operators are moved some miles away. Experience has shown the desirability of being able to reach an operator a fairly large percentage of the time because of special services, such as directory information, reports on the availability of toll circuits, service complaints, etc. This requires a substantial increase in the number of circuits to the tributary office in such instances. Development of this line, then, proceeds by adding single-channel carrier systems, until a point is reached where it is necessary to string more copper wire, which is costly and may be in short supply, or to add multi-channel carrier systems.

The situation in Iowa is typical of many areas in the Southern and Western parts of the country. Fig. 1 shows the principal open-wire and cable routes in Iowa used by the Bell System for toll business. The type-K transcontinental cable crosses the state, passing through Davenport and Des Moines on its way to Omaha. Small branch cables serve Muscatine, Cedar Rapids and Atlantic, where the circuits are extended by open-wire facilities. In general, the transcontinental TD-2 radio relay system follows the K carrier route. A coaxial cable route extends north from Des Moines to Minneapolis, connecting at Iowa Falls with short

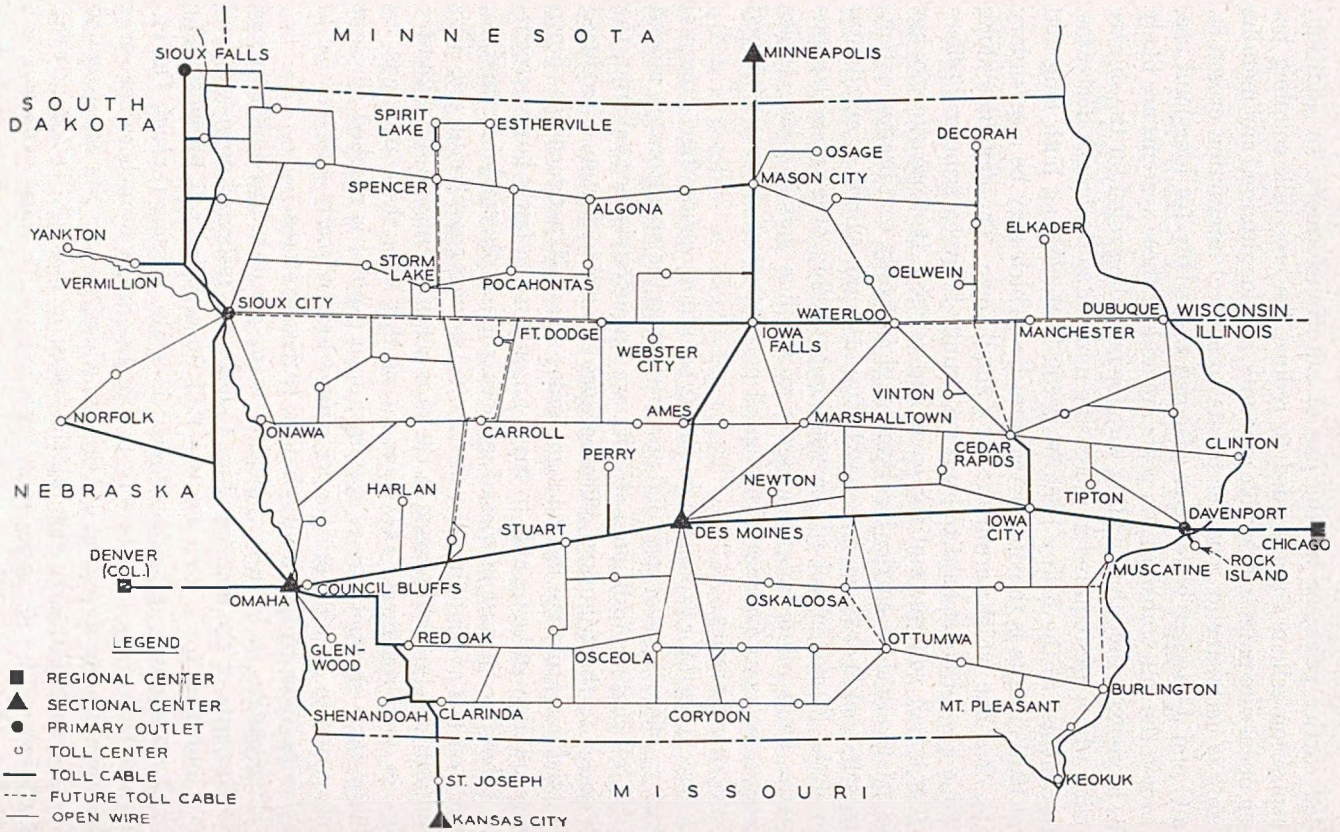

Fig. 1—Principal open-wire and cable routes in Iowa.

K cables to Fort Dodge and Waterloo. Eventually a second cable route will extend across the state through Waterloo and Fort Dodge, as shown by the dashed lines. A second coaxial route cuts across the southwestern corner on its way to Kansas City and a third coaxial route connects Sioux City with Omaha. The rest of the state is served by open-wire lines.

Fig. 2 shows the distribution with length of the Bell System open-wire short-haul toll and tributary circuits in Iowa in 1950, including both voice-frequency and carrier facilities. It will be noted that 95 per cent of the circuits are less than 100 miles in length, while 90 per cent are less than 70 miles, the point where type C systems just become economical. For tributary circuits 98 per cent are less than 30 miles in length. There are a total of some 2700 toll and tributary circuits in Iowa. In addition, there is also a sizable connecting company development. Fig. 3 is a distribution of the number of circuits per group, where a group is composed of the circuits used for via or terminating business between two towns. There are about four circuits per group for short-haul toll and two circuits per group for tributary service in the median case. As the dial conversion program proceeds the average number of circuits per tributary group is expected to increase.

Because of the short distances involved, and the small number of circuits per group, carrier development in Iowa has been restricted, to a large extent, to single-channel systems, and type M. Only four or five M channels can be operated on a given open-wire line, and while these systems have some transmission disadvantages, they have been employed to a large extent. However, further M development is blocked because of the expense of isolating M systems from adjacent lines. There are a few C systems on such routes as Sioux City-Spencer-Mason City, Waterloo-Dubuque, Muscatine-Keokuk, and Atlantic-Spencer.

The type-O system, therefore, is being made available to provide short-haul toll and tributary circuits on open-wire lines in the range from 15 to 150 miles. When completely developed it will provide four four-channel systems in the frequency range from 2 to 156 kc, as shown on Fig. 4. The use for separate channels of both sidebands of a single carrier, called a "twin-channel," results in economical use of the frequency space. The four channel systems are designated OA, OB, OC, and OD respectively, and cover substantially the same frequency range as the C and J systems.

Considerable attention has been given to keeping the line rearrangements as simple as possible. The use of non-loaded entrance cable is proposed, and simple arrangements are available for adding O groups

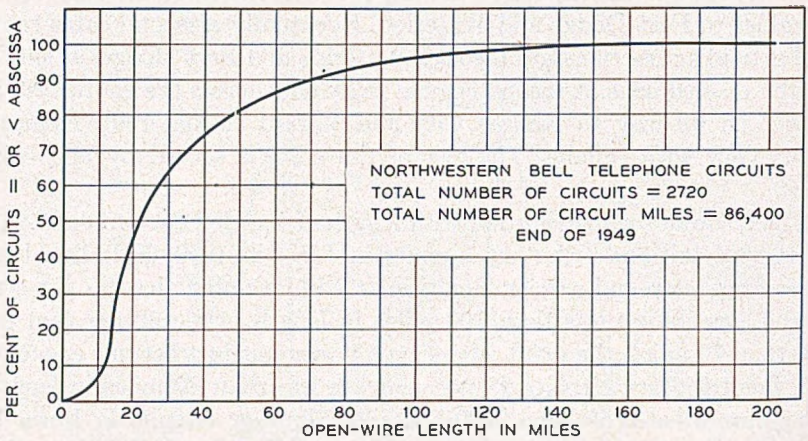

Fig. 2—Distribution of circuit lengths in Iowa in 1950.

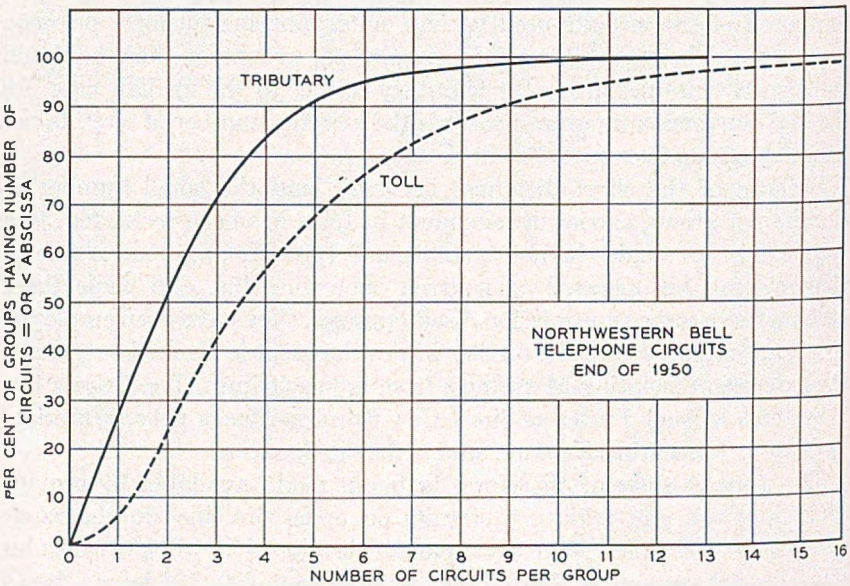

Fig. 3—Distribution of circuits per group in Iowa in 1950.

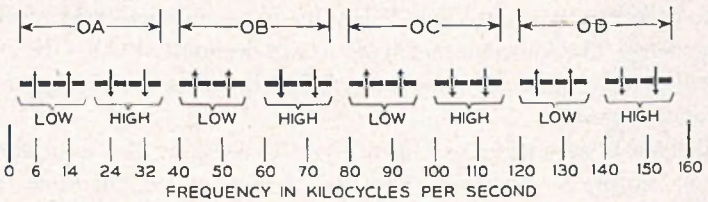

Fig. 4—O carrier telephone—frequency allocation.

above existing carrier systems, such as C, which has a top frequency of 30 kc. With the aid of the compandor, it is possible to apply the OB system to practically any open-wire pair transposed for C carrier operation, thus nearly doubling the number of circuits without additional line rearrangements. Transposition arrangements which are expected to be less expensive to apply are being made available where the higher-frequency type-O groups are involved. Line losses of the order of 35 to 40 db can be spanned under normal wet weather conditions, and 50 db loss under sleet conditions with some transmission impairment, since sleet is relatively infrequent in occurrence. This will result in repeater spacings of the order of 50 miles in sleet areas for the OB group, and 100 miles in other areas. For the higher frequency groups (OC and OD) these spacings will be approximately halved.

CHOICE OF DEVELOPMENT APPROACH

The type-O carrier system followed the type-N system closely in time, and, in effect, covers the same range of circuit lengths for open wire lines that N provides for cables. It was both natural and expedient that many of the N features were carried over directly into the O design. It was necessary, however, to make important distinctions as well. These similarities and differences will be discussed in some detail.

The transmitting and receiving voice frequency subassemblies are reused with substantially no modification. This provides the O system with the same compandor and the same 3700 cycle signaling system as used in N.

An important difference between the two systems is concerned with the use of single sideband in the O rather than double sideband as in the N. This choice is an economic one. The double sideband system is relatively easier to design and less expensive than the single sideband arrangement. The use of double sideband in cables is practicable in many cables because of the relative abundance of conductors as compared with open wire pairs. In some cases the use of single sideband in cables may be attractive as compared with the cost of new outside plant for certain length ranges.

Another distinction between the two systems is the provision of circuits in smaller groups in O. In N the basic group is 12, although systems may in some instances be partially equipped. In O, the desire to furnish smaller circuits groups resulted in the choice of a basic four-channel group. The full complement per pair for O, including a channel replacing the voice circuit, is sixteen channels.

The regulation problem is more severe in the O design. It is necessary

to provide sufficient regulator range to accommodate line variations due to wet or icy lines. The repeater and receiving group regulator range common to four channels is in the order of 40 to 50 db, or approximately four times the regulating range of an N repeater. The range of the twin-channel regulator is comparable to the N individual channel regulator, but the O regulator is shared by two channels forming adjacent sidebands of the same carrier.

The use of a single sideband imposes more severe requirements on channel band filters. The use of a material called ferrite, in combination with a crystal, affords an efficient channel band filter in a small space when compared to previous single sideband channel filters employing air-core coils. Ferrite coils are employed in a coil-condenser type of filter to provide separation for the various four-channel groups. While the N system employs only receiving channel band filters, O has filters in both the transmitting and receiving terminals.

The O system employs the double modulation principle for all groups. This arrangement permits the use of only four channel band filter designs for all of the 32 channel frequency allocations. The frequency range for these basic channel bands has been selected to provide the most economical overall filter design.

The use of die-castings has been extended in a number of ways. Notable among these is a die-cast framework, used in both the terminal and the repeater. The plug-in technique has been expanded to provide plug-in filters for channel and group band filters.

DESCRIPTION OF THE SYSTEM

The system will be described first by block schematics, second, by transmission characteristics, and finally by photographs. This description will show representative features rather than describe the system completely.

While the description will cover the complete O plan, it should be pointed out that the OB system is the first to be made available. It will be followed by the other O systems.

In the schematic description, where a unit is common to all systems the designation is "Type O." Where the arrangement is different for the several systems, a particular designation is used, such as "Type OB," etc.

Schematics

The O modulation plan is shown on Fig. 5. The single-sideband channel filters for all groups are in the frequency range from 180 to 196 kc.

By the use of different group carrier frequencies the several four-channel groups are placed in their various locations. As indicated by Figs. 4 and 5, high and low group assignments are used for the two directions of each four-channel system. A repeater is provided for each four-channel system and, except in the case of OA, the high and low frequency groups are "frogged" at each repeater, as in the N system.

Figure 6 shows a block diagram of a complete O system. On this figure, and in general on other figures showing filters, a letter code is assigned to designate the kind of filter, with a subscript letter to indicate the particular system in which the filter is used. The several filter designations and number codes are collected for reference in Table I. Much of the apparent complexity of the system, particularly as regards filters, arises out of the use of a single pair for both directions of transmission. Another complexity is occasioned by the requirement that a complete complement of O systems will not always be provided. For example, OB, OC, and OD systems may be used above an existing C system, or similar systems.

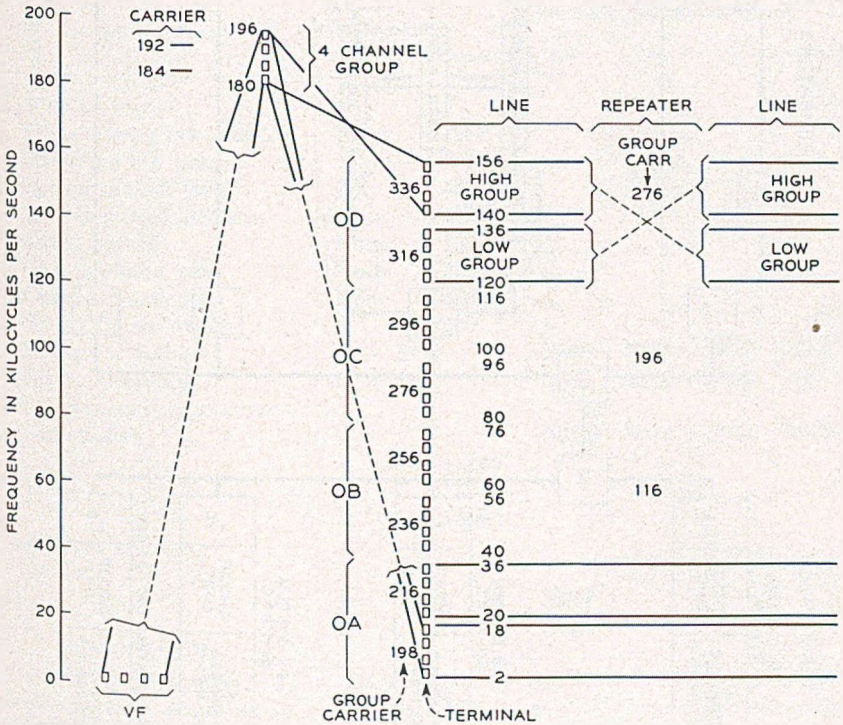

Fig. 5—Type-O modulation plan.

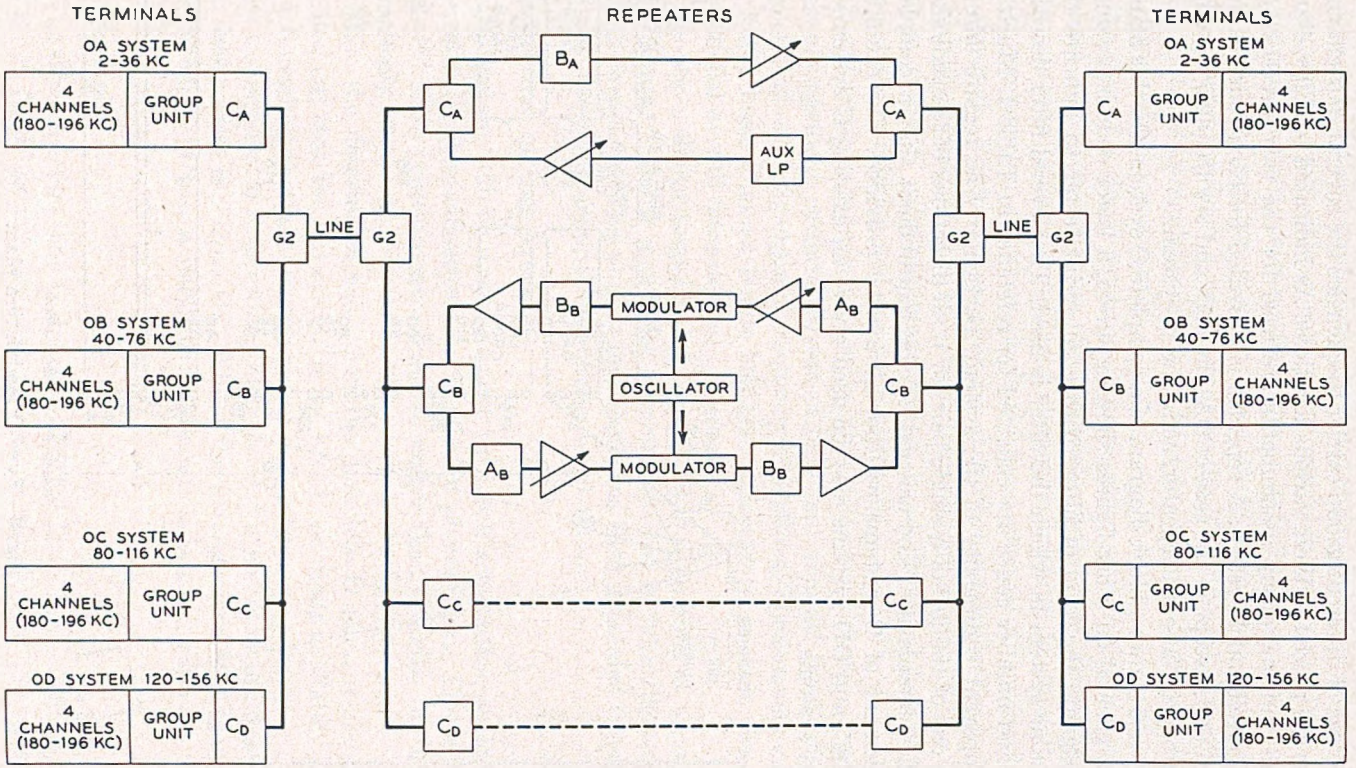

Fig. 6—Type-O carrier system.

Line filters (G) are provided to separate the OB, OC, and OD Systems from the OA frequency ranges. Because of the lower attenuation and slope in the OA frequency range, and the better line coupling factors, the repeaters do not "frog" the high and low groups.

The OB Carrier Terminal

A block diagram of a typical carrier terminal is shown on Fig. 7, in this case the OB terminal. The terminal is comprised of four channel units, two twin-channel units, group transmitting and receiving units, and a group oscillator. An oscillator in each of the twin channel units supplies carrier to the transmitting channel modulators. The same oscillator supplies transmitted carrier for two associated sidebands. The original carrier is balanced out in the transmitting modulator. This method results in a more accurate control of the transmitted carrier. level. The group oscillators supply the necessary frequencies to the

TABLE I

Location and Function	Filter Symbol	Filter Codes for Each System				
		Common	OA	OB	OC	OD
TERMINAL ONLY						
Transmitting low pass	None	168F				
Receiving low pass	None	169G				
Carrier pickoff (184kc)	F1	532A				
Carrier pickoff (192kc)	F2	532B				
Signal pickoff	None	169A				
Channel band pass	None	529A				
Channel band pass	None	529B				
Group transmitting	E	540A*				
Group receiving	A + D		530J	531B	530C	530F
Group receiving	B + D		531F	531C	530D	530G
TERMINAL AND REPEATER						
Directional	C		530H	530A	530B	530E
Line	G2	219S†				
	G G1	537A‡				
	G1	538A				
REPEATER ONLY						
Auxiliary	A + B			531A	531D	531E
	A		530K			
	B		530L			

* Except OA system. † Cut-apart region between 36 and 40 kc. ‡ Cut-apart region between 30 and 40 kc. 538A is a 537A filter with housing and protectors for pole mounting.

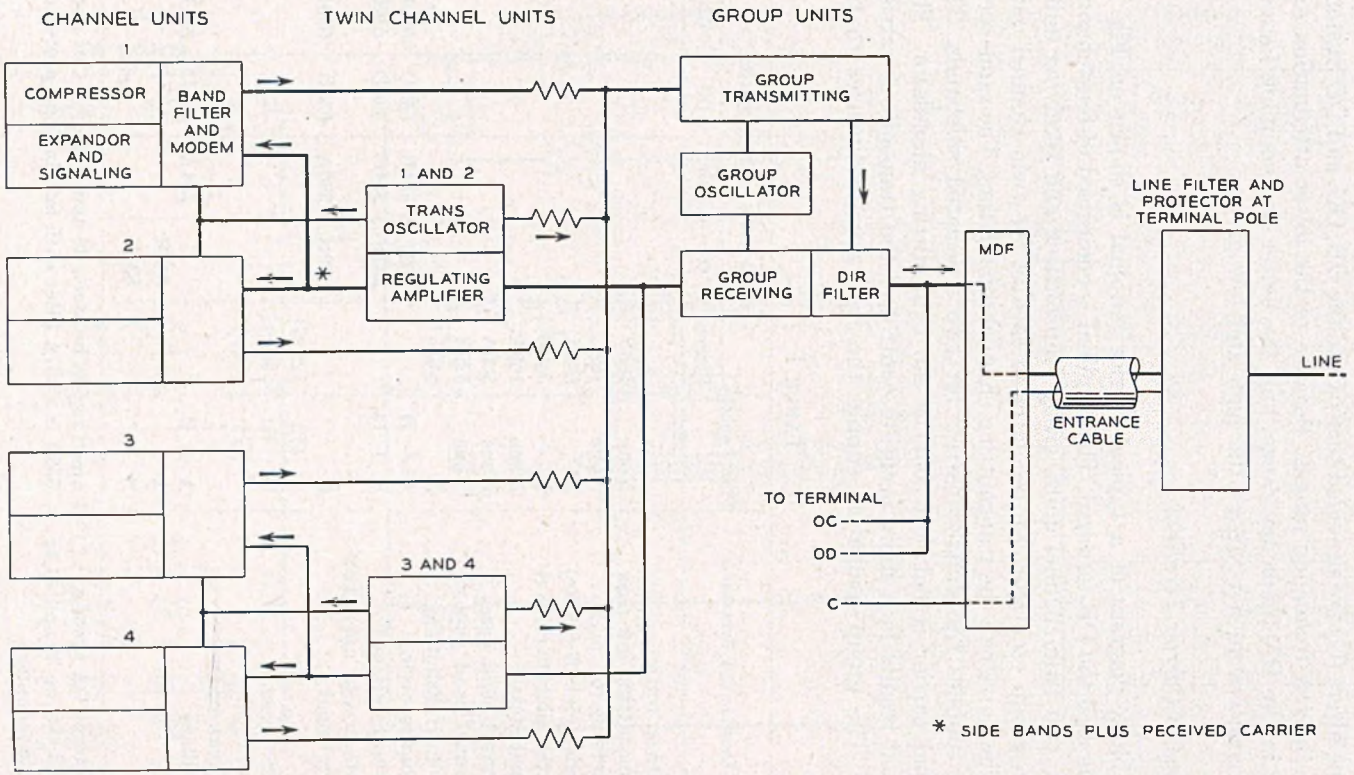

Fig. 7—Type-OB carrier terminal.

transmitting and receiving group units to translate the sidebands between the frequency range of the channel band filters and the correct line frequency allocation. The group receiving unit contains the directional filter for separating the four-channel transmitting and receiving groups at line frequencies. Multiple points are indicated for the connection of other O carrier systems on the same pair.

Channel Unit

A block diagram of the channel unit is shown on Fig. 8. As indicated by the dashed line, the channel unit is comprised of four parts which are interconnected by plugs and jacks. These are:

1. The Compressor Sub-Assembly. This unit contains the compressor and a terminating arrangement to permit the system to be used for four-wire termination, or for two-wire termination at non-gain locations, i.e., those without switching pad control.

2. The Expandor Sub-Assembly. This unit contains the expandor as well as the signal transmitting and receiving equipment.

3. The Carrier Frequency Sub-Assembly. This unit contains the transmitting and receiving modulators, and is arranged to receive the plug-in transmitting and receiving channel band filters.

4. The Transmitting and Receiving Band Filters. These are combined in a single plug-in unit.

Items 1 and 2 are practially identical to the corresponding sub-assemblies for N carrier. Each channel receives its carrier supply for the transmitting side from an oscillator in the twin channel unit. On the receiving side the carrier is obtained by selecting and amplifying the transmitted carrier.

The frequencies indicated on Fig. 8 are the same for all O systems, and apply to two of the four channels in the group. Figs. 4 and 5 show go and return channels in high and low frequency assignments in the same O system. However, as shown on Fig. 9 covering the OB system, the frequency assignments applying to the channel band filters are above any of the O line frequencies and are in the frequency range from 180 to 196 kc for both transmitting and receiving channel band filters.

Transmitting and receiving channel band filters are paired in a single plug-in unit. In order to reduce the number of kinds of paired channel band filters (transmitting and receiving in the same plug-in unit) the pairing has been done in a special way. If, for example, transmitting assignment 180–184 were paired with receiving assignment 180–184, etc., four different kinds of paired filters would result. Instead, assignment 180–184 is paired with assignment 192–196, and by making the

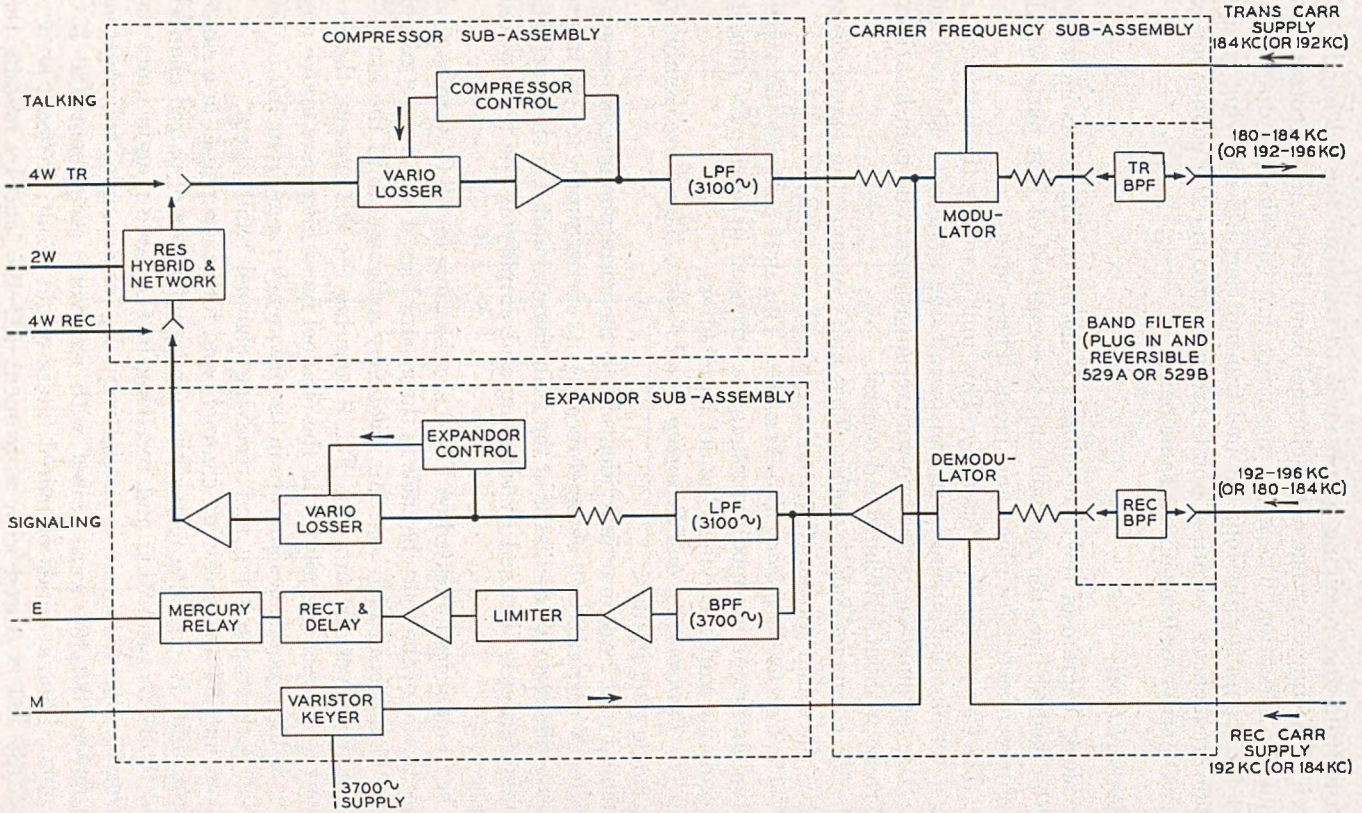

Fig. 8—Type-O channel unit.

plug-in filter reversible in its socket, this grouping can be made to serve two channels as follows:

$$\left\{\begin{matrix}\text{180–184 Transmitting}\\ \text{192–196 Receiving}\end{matrix}\right\} \text{ and } \left\{\begin{matrix}\text{192–196 Transmitting}\\ \text{180–184 Receiving}\end{matrix}\right\}$$

A similar paired filter serves

$$\left\{\begin{matrix}\text{184–188 Transmitting}\\ \text{188–192 Receiving}\end{matrix}\right\} \text{ and } \left\{\begin{matrix}\text{188–192 Transmitting}\\ \text{184–188 Receiving}\end{matrix}\right\}$$

Thus only two basic kinds of paired channel band filters are required, rather than four kinds. In these filters, as well as the reversible group filters, the filter designations are so arranged that when the filter is in place the proper filter designation is in view.

Twin Channel Unit

The twin channel unit is shown in somewhat more detail in Fig. 10. There are two kinds of twin channel units to serve the four channel assignments, and the frequencies shown on Fig. 10 correspond to those shown on Fig. 8. (and Fig. 9). A transmitting carrier adjustment permits the transmitted carrier level to be set properly in relation to the sideband levels. In order that the group regulators may function primarily on the carrier, and thus be substantially independent of voice or signaling sidebands, the carrier is transmitted approximately 6 db above the sideband level.

On the receiving side of the twin channel unit a regulating amplifier controls the received level of both sidebands. It does this from the carrier

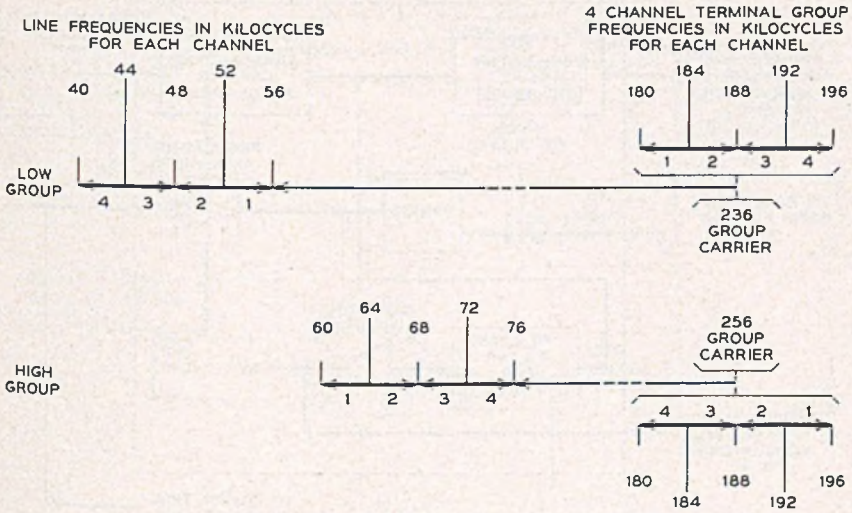

Fig. 9—Type-OB system frequencies.

picked off by a narrow band crystal filter. This same carrier is supplied to the receiving side of the channel units for demodulating the associated sidebands.

Group Transmitting Unit

The OB group transmitting unit is shown on Figure 11. It receives the four sidebands and two transmitted carriers and places them in the proper high or low line frequency assignment. The transmitting group unit, depending on the optional connection to the group oscillator (Fig. 11), can be either a high group transmitting unit or a low group transmitting unit.

For convenience the noise generator is contained in the group transmitting unit. On very quiet circuits this noise source provides a means of masking crosstalk. In ordinary usage the noise thus provided is not noticeable on the circuit, but is sufficient to reduce the chance of hearing intelligible crosstalk to a small value.

Group Receiving Unit

The OB group receiving unit is shown on Fig. 12. It is comprised of an amplifier and a regulator-modulator arrangement equipped with plug-in filters. The same basic arrangement is used for all receiving group units, as well as for all repeaters. Only the plug-in filters, and the frequencies from the associated oscillators are different. The directional

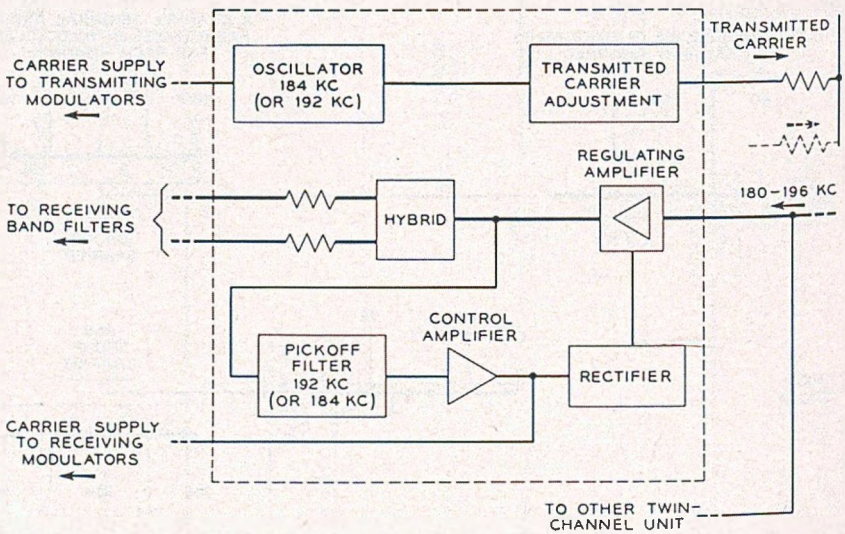

Fig. 10—Type-O twin channel unit.

filter is reversible as well as plug-in and thus serves either high or low groups. The receiving group band filter and its associated auxiliary filter have the same physical arrangement as in the repeater but they are never reversed.

A dc feedback type regulator controls the gain of the regulating amplifier, and operates principally on the two received carriers, although the sidebands are fed back also.

Group Oscillator

The group oscillator contains two oscillators for supplying the group transmitting and group receiving units. These oscillators are interchangeable (by strapping) and permit the group units to operate in either the high or low groups. For conveneince the 3700 cycle signaling oscillator, common to all four channels, is contained in the group oscillator.

Repeater

As indicated on Figs. 5 and 6, a repeater is provided for each four-channel system. An amplifier, regulator and modulator arrangement serves each direction. The directional bands are routed through the repeater by directional and auxiliary band pass filters as indicated on Figs. 13 and 14. At each repeater (except OA) the high- and low-frequency groups are "frogged" to improve transmission, particularly as

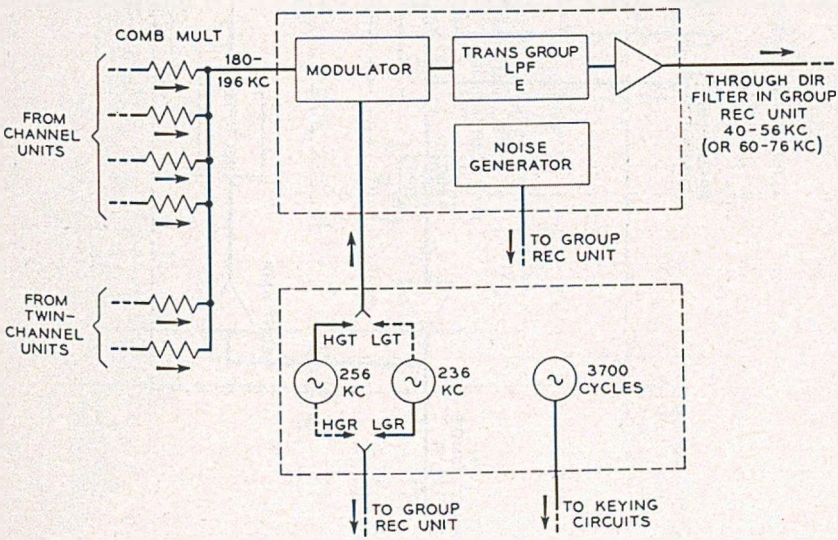

Fig. 11—Type-OB group transmitting unit and group oscillator unit.

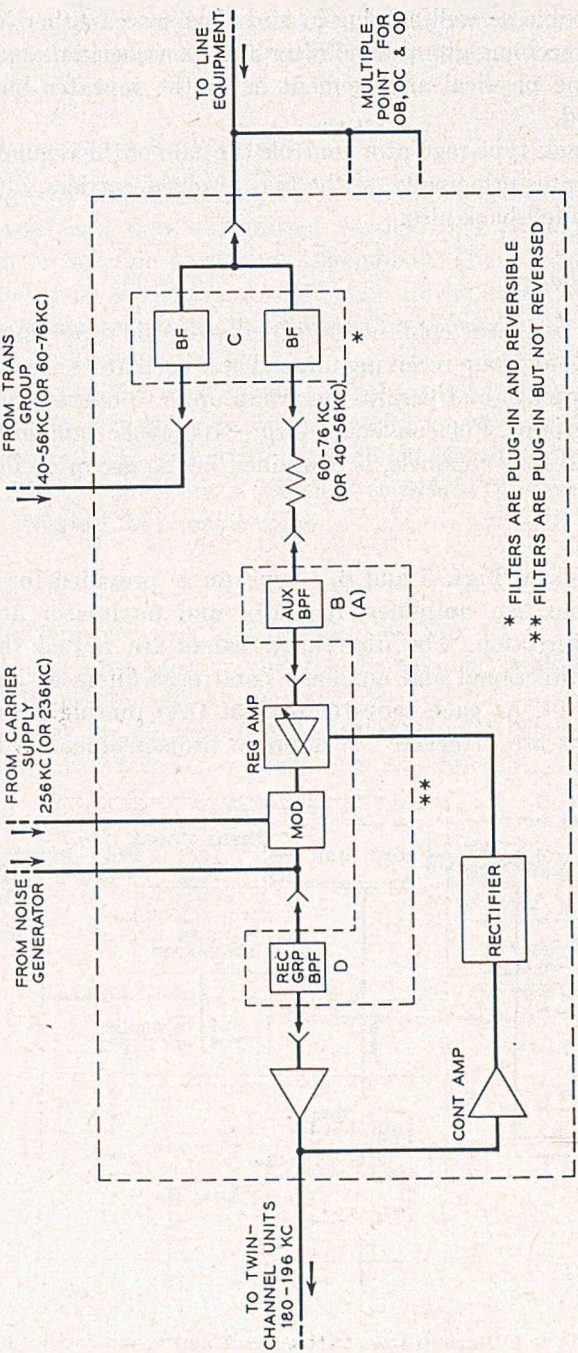

Fig. 12—Type-OB group receiving unit.

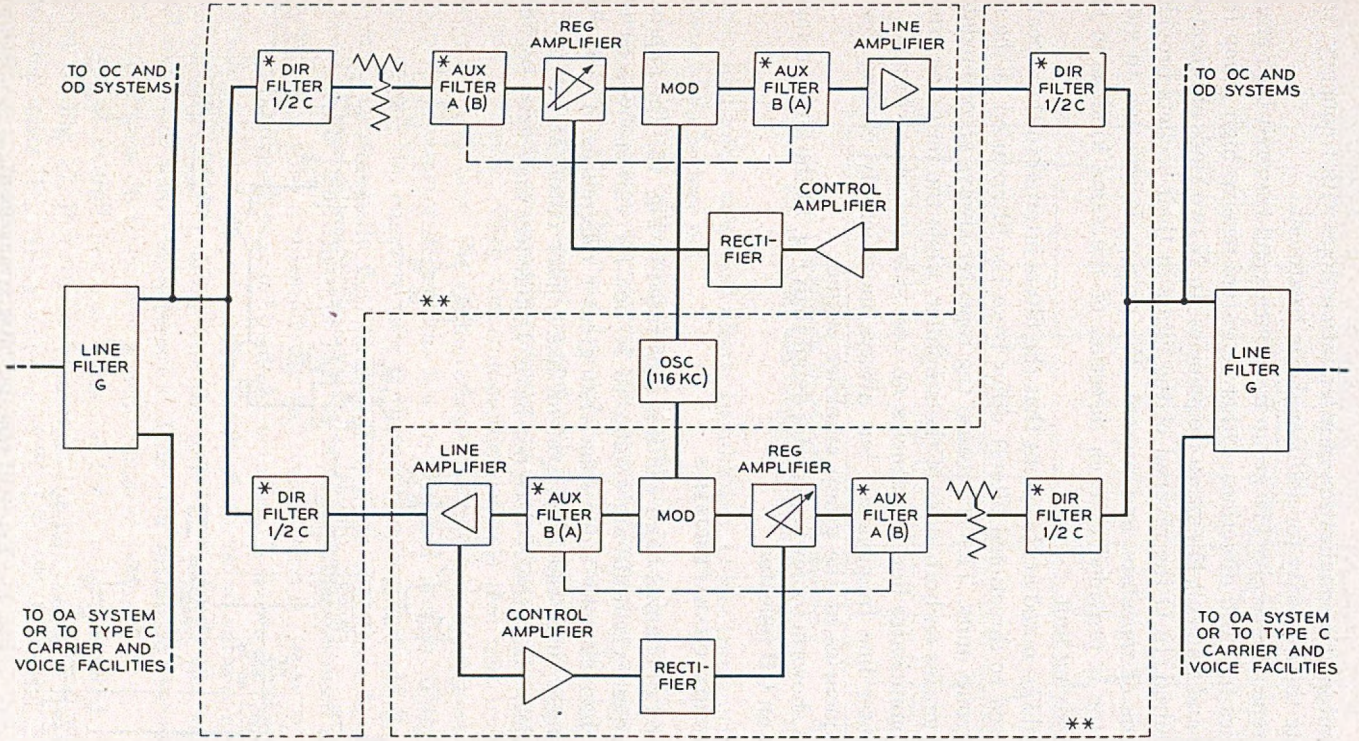

* FILTERS ARE PLUG-IN AND REVERSIBLE ** BASIC AMPLIFIER USED FOR OB, OC AND OD FOR REPEATERS AND GROUP RECEIVING UNITS

Fig. 13— Type-OB repeater.

regards automatic equalization of attenuation slope with frequency, and to obviate the necessity for additional line treatment.

Some repeaters receive low group frequencies and transmit high group frequencies for both directions. Other repeaters receive high group frequencies and transmit low group frequencies. In N two kinds of repeaters were required. In O the reversal of the filters in their sockets provides both kinds of repeaters, and presents the proper designation to view. A regulator is provided in each direction of the same kind as in the group receiving unit.

It should be noted at this point that the filters internal to the repeater (as opposed to directional filters) differ from the filters used in the receiving group units. This is because the repeater always accommodates line frequencies on both sides of the amplifier, while the receiving group unit accommodates line frequencies on one side (which correspond to the repeater line frequencies) but always must supply channel band filter frequencies at the group amplifier output.

Fig. 14 shows in somewhat greater detail than Fig. 13 the filter arrangement for an OB repeater.

TRANSMISSION CHARACTERISTICS

The overall channel band width is illustrated in Fig. 15. The approximate frequency cutoffs are similar to N but for various reasons the several channels may show somewhat greater differences. The O system, being a single sideband system, has a filter cutoff at low (voice) frequencies, which the N does not have. Differences may exist between

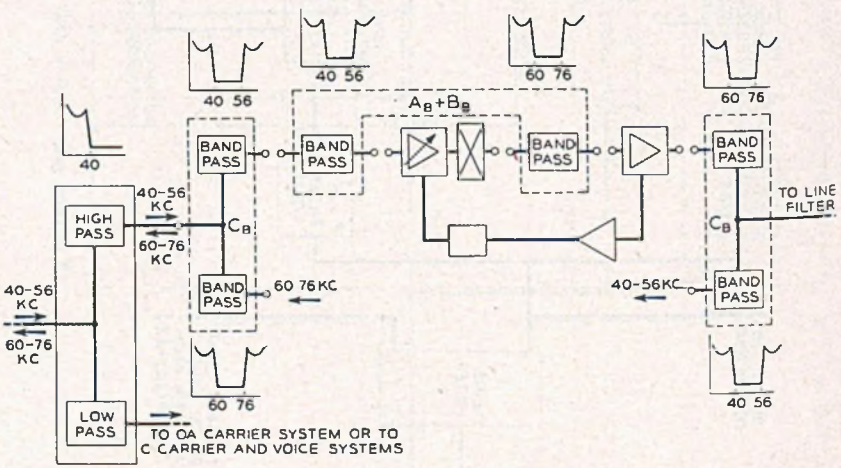

Fig. 14—Type-OB repeater filter arrangement.

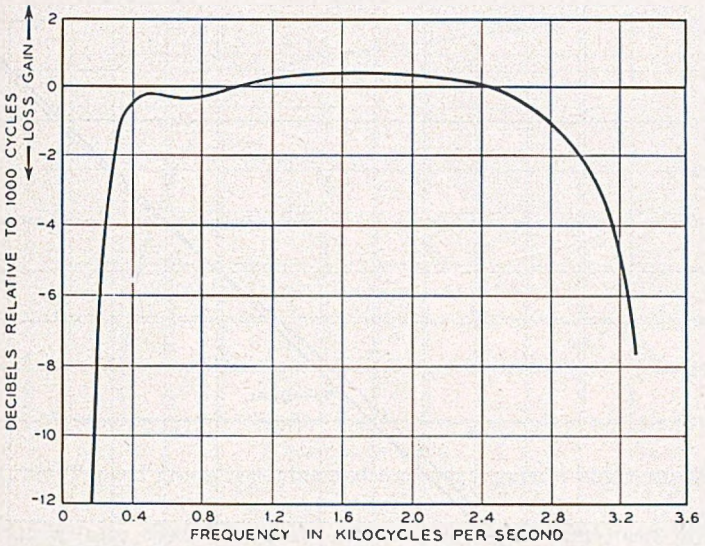

Fig. 15—Net loss frequency charactieristic.

upper and lower sideband filters. In addition, O has transmitting band filters while N does not.

A situation is of interest which applies to both N and O, as well as to any other system employing the type of compandor controlled from the voice energy. Different frequency characteristics will be obtained with the compandor operating and with the compandor controls locked. Neither of these necessarily corresponds to the operating condition with speech or music. With the compandor controls free and using single frequency test tone, the characteristic obtained is a combination of the frequency characteristics of the line and control circuits. With the controls locked, the characteristic is that of the line only. If the control circuit is substantially flat, there will be little distinction between the measurements. The curve of Fig. 15 is of the type obtained with free controls and with a substantially flat control circuit.

A typical overall channel load characteristic is shown on Fig. 16. This characteristic includes not only the load curve of various amplifiers, modulators, etc., but shows also the order of match of the compressor and expandor load characteristics. This is a match of curves having 2:1 slopes on a db basis over a wide range of volumes.

A typical overall net loss variation for a non-repeatered circuit is shown on Fig. 17. Principally because of the line regulator in the group receiving units (Fig. 18) a wide range of line loss is covered. A similar regulator is included in each repeater, and the extension of a system

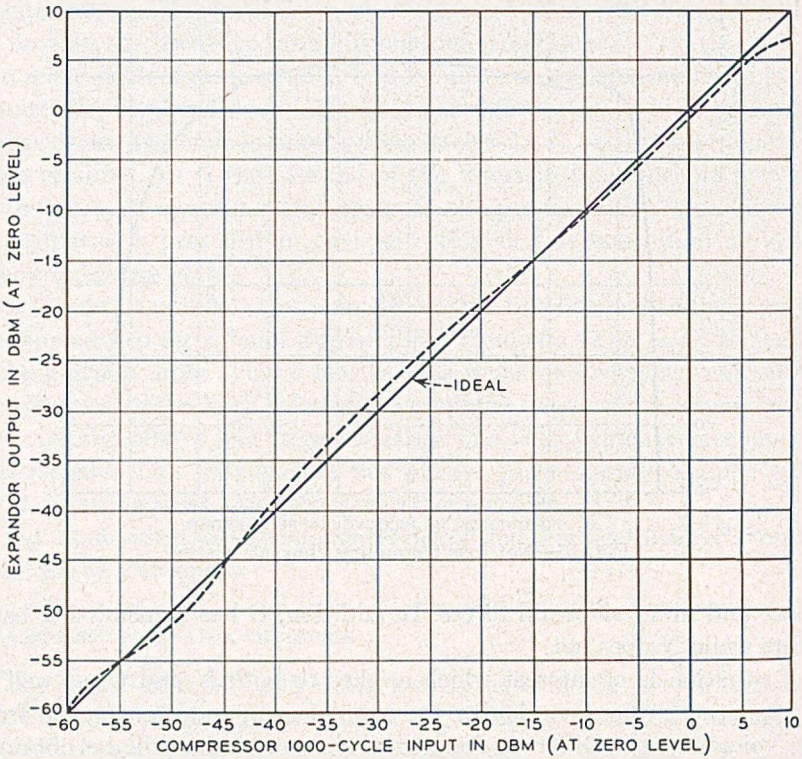

Fig. 16—Typical over-all channel load characteristic.

with repeaters will not result in a substantial change of the net loss variation, assuming the repeater section losses do not exceed the range of the regulators.

The line regulator is assisted by the twin channel regulator, for which a characteristic is shown on Fig. 19. This regulator is similar to the individual channel regulator of N, and serves two channels having a common carrier. This fact alone does not materially change the effectiveness of regulation since the carrier is adjacent to the sideband which

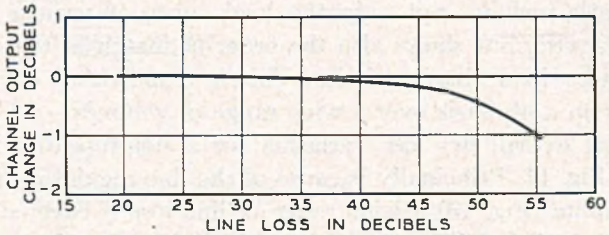

Fig. 17—Typical over-all channel net loss variation, nonrepeatered.

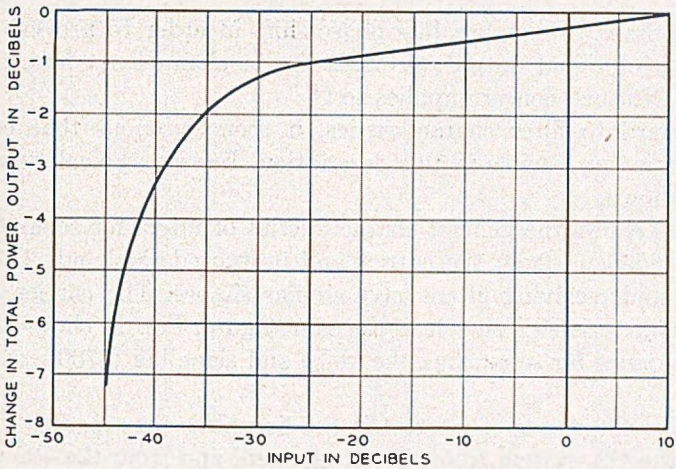

Fig. 18—Typical group receiving and repeater regulator characteristic.

it controls in any case. There are other important differences, however, between N and O channel regulators. In N the channel regulator follows the channel band filter and thus tends to compensate for its flat transmission variations. Also the N regulator is controlled from the demodulator dc output and thus compensates in some degree for demodulator variations. In O, the twin-channel control is ahead of both the channel band filter and the channel demodulator, and therefore does not make up their variations.

A statement might be interpolated at this point to emphasize that the relative advantages of single-sideband and double-sideband transmission are by no means easily listed and evaluated, since the differences are many and devious, some necessarily and some fortuitously. An example worthy of note is that in N it is necessary to be concerned about relative phase shift of the sidebands and in the instances of longer cir-

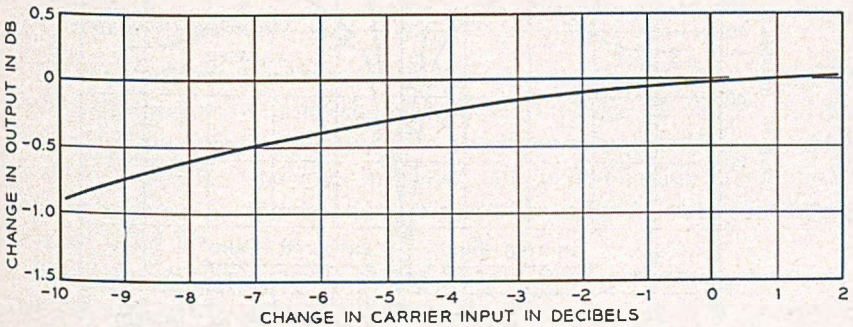

Fig. 19—Typical twin-channel regulator characteristic.

cuits, perhaps to equalize this phase shift in order to prevent serious reduction of signal output, or variation in channel net loss with frequency. No such concern applies to O.

In regard to filter characteristics, it seems obvious that complete coverage is not feasible in this description. Instead typical curves only will be shown.

Fig. 20 shows the general characteristics of filters for separating the wanted sideband from the carrier and unwanted sideband. The transmitting and receiving filters have similar shapes. The carrier pick-off filter characteristic is shown in the same figure. Fig. 21 shows the filter characteristics for separating the voice and signaling (3700 cycle) functions.

Another filter case of interest is the line filter for separating, for example, the OA system from the OB system, and from the OC and OD systems, as well, if they are employed. Fig. 22 shows the configuration and loss characteristics of the G1 (537A or 538A) filter. A C_B directional filter (530A) characteristic is shown on Figure 23. This filter assembly includes two filters to accommodate the OB high and low group assign-

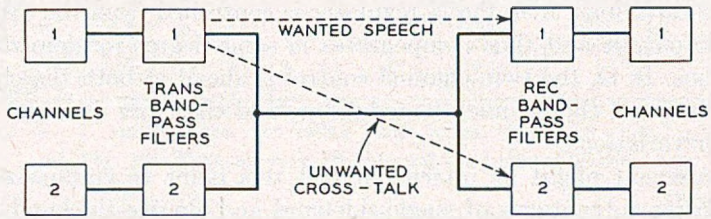

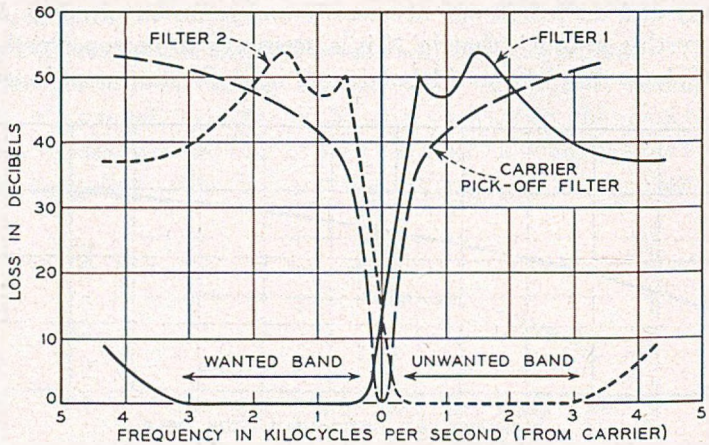

Fig. 20—Typical channel band and carrier pick-off filter characteristic.

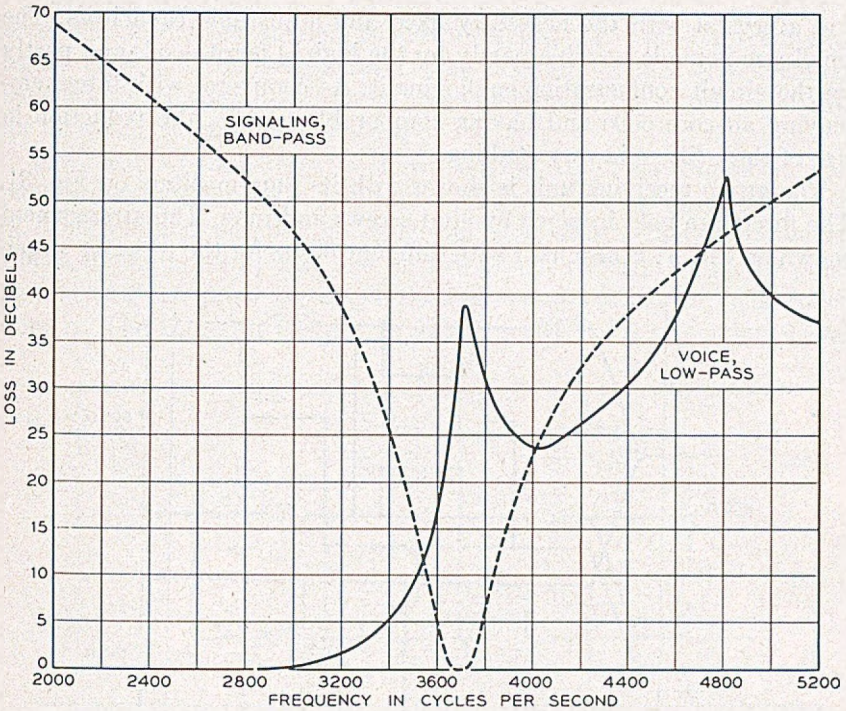

Fig. 21—Typical receiving low pass and signaling filter characteristics.

ments. Similar characteristics apply to the $A_B + B_B$ auxiliary filter (531A). The A and B characteristics are used in the group receiving filters $A_B + D_B$, (531B) and $B_B + D_B$, (531C). The D filter is a band-pass filter with relatively gradual cutoff to pass the 180–196 band for the channel filters, and has peaks at the group carrier frequencies of 236 kc and 256 kc. These filter characteristics are not shown.

PHYSICAL ARRANGEMENTS

A four-channel carrier terminal is shown on Fig. 24. This terminal includes four channel units shown in detail on Figs. 25, 26, 27 and 28. In Fig. 28 the unit is separated into the three sub-assemblies, of which as noted above, the two voice frequency sub-assemblies are substantially the same as for N carrier. The carrier sub-assembly with its plug-in channel band filters is shown on Fig. 29.

The interior arrangement of the plug-in unit containing the transmitting and receiving band filters is shown on Fig. 30. This assembly contains an adjustable ferrite inductance, a miniaturized transformer,

and a crystal with the necessary fixed and adjustable capacitors. The small size is made possible partly by the high Q ferrite coil, and partly by the circuit configuration employing it. As compared with filters employing air-core coils and having comparable cutoffs, the reduction in size of these filters is very striking.

The group receiving unit is shown with its plug-in filters on Fig. 31. The filters are held in place by stud screws and nuts. The arrangement shown on Fig. 31 is also used with different filters for the repeater ampli-

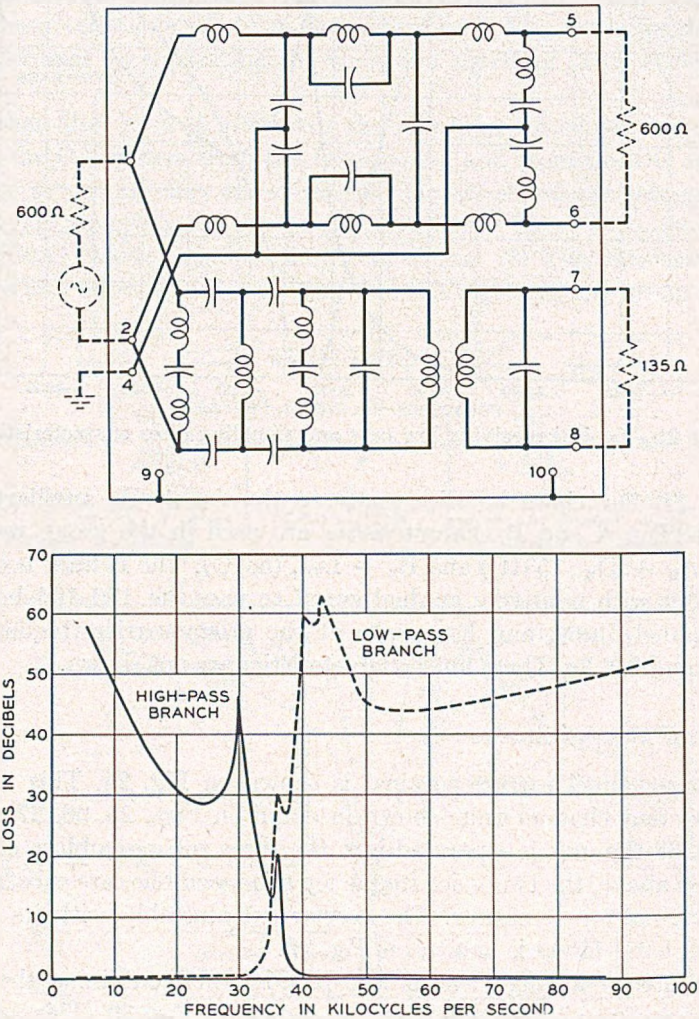

Fig. 22—Typical line filter characteristics (G1, 537A or 538A).

fiers. The filter construction is shown on Fig. 32. This filter employs ferrite coils and condensers, having no crystals because of percentage band width considerations. These filters employ a form of printed wiring for interconnection of components.

The terminal framework is shown on Fig. 33. This framework employs aluminum die-castings in contrast to the frabricated framework of N. This method permits the inclusion of a slide arrangement which guides the units into place, and insures proper registration of the plugs and jacks. Some units are above the framework; others are suspended from it. The same die-casting, inverted, serves both upper and lower

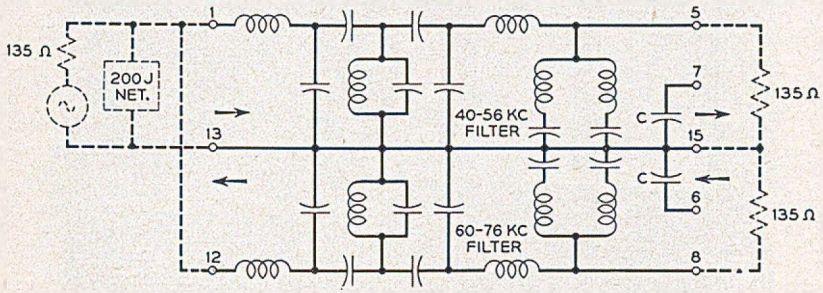

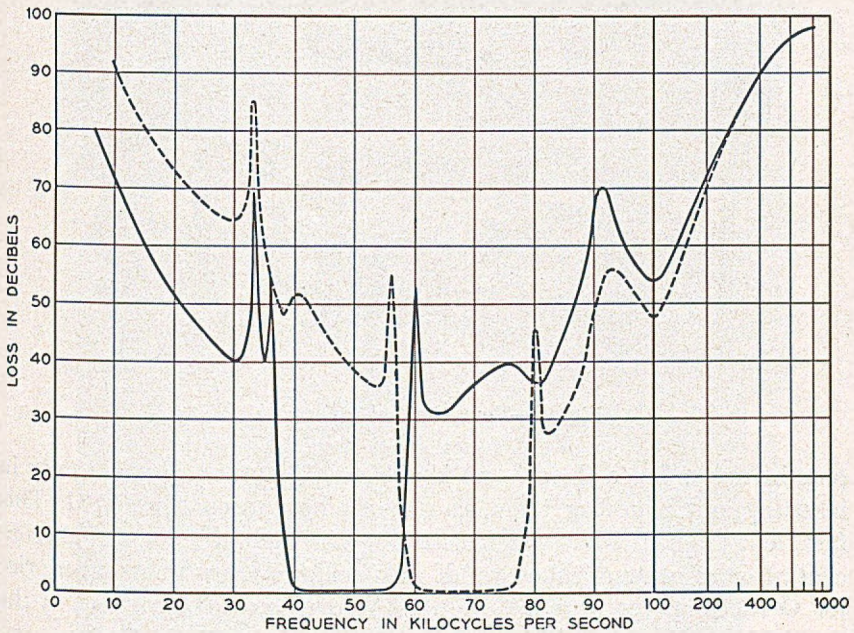

Fig. 23—Typical directional filter characteristics (C$_B$, 538A).

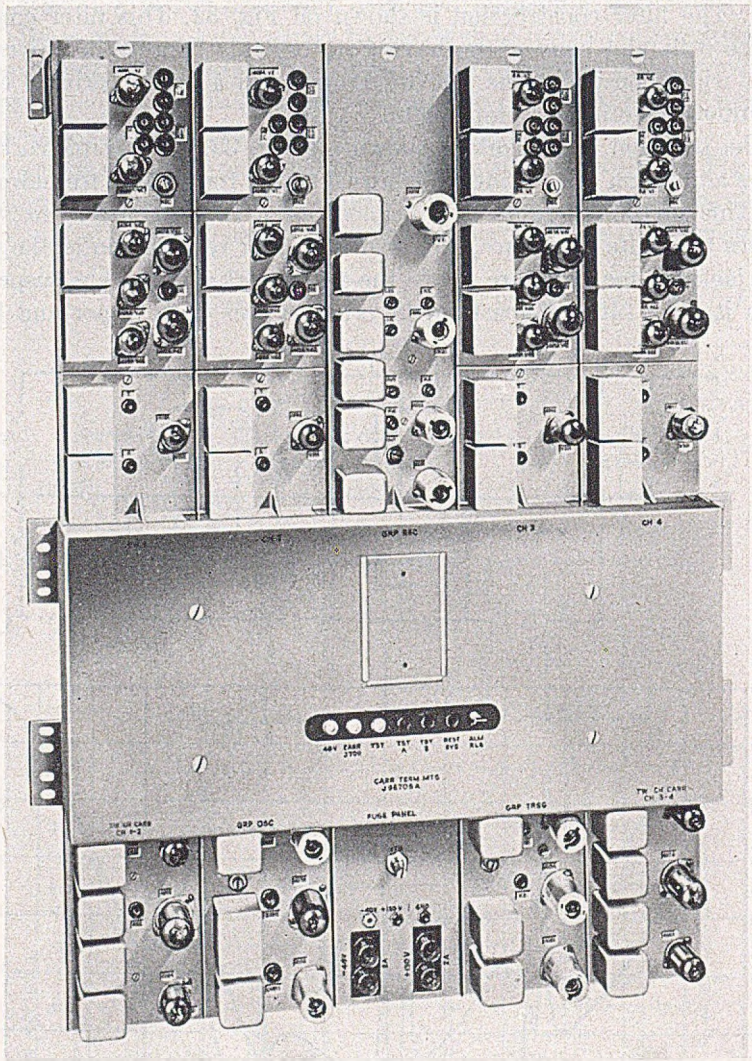

Fig. 24—Four-channel O terminal.

plug-in units. Since there is no interference between plug-in units in inserting and removing them, can covers have been eliminated. This fact, and the somewhat wider distribution of units having a high concentration of vacuum tubes, result in a relatively low temperature rise for O as compared with N. Blower facilities are not provided in the terminal.

Typical of the units suspended from the framework is the twin chan-

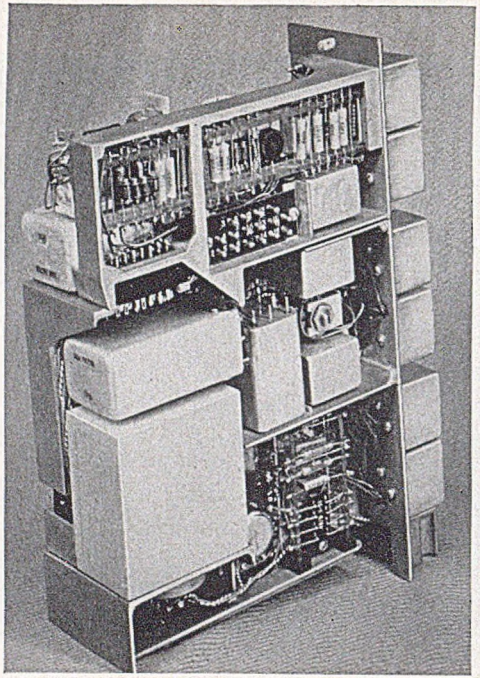

Fig. 25—Channel unit-left side view.

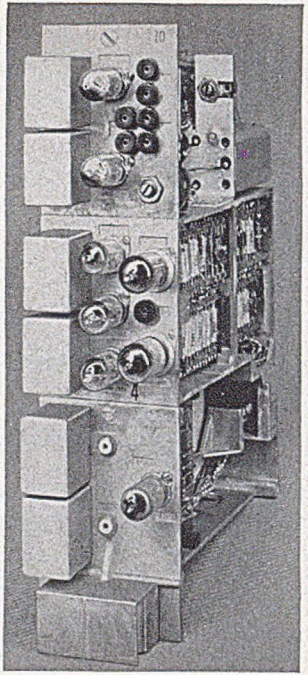

Fig. 26—Channel unit-front view.

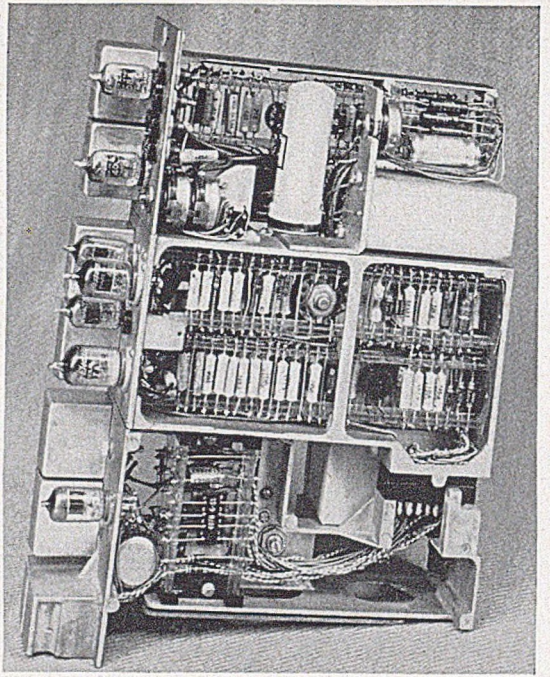

Fig. 27—Channel unit-right side view.

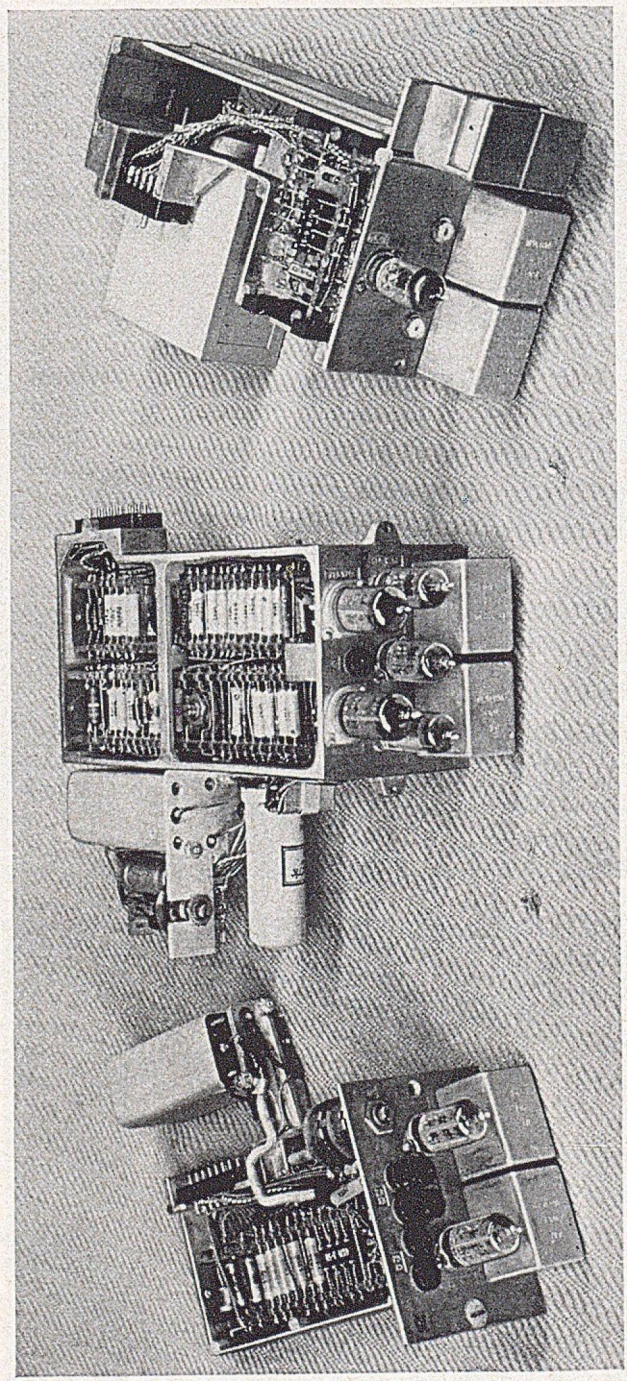

Fig. 28—Channel unit subassemblies.

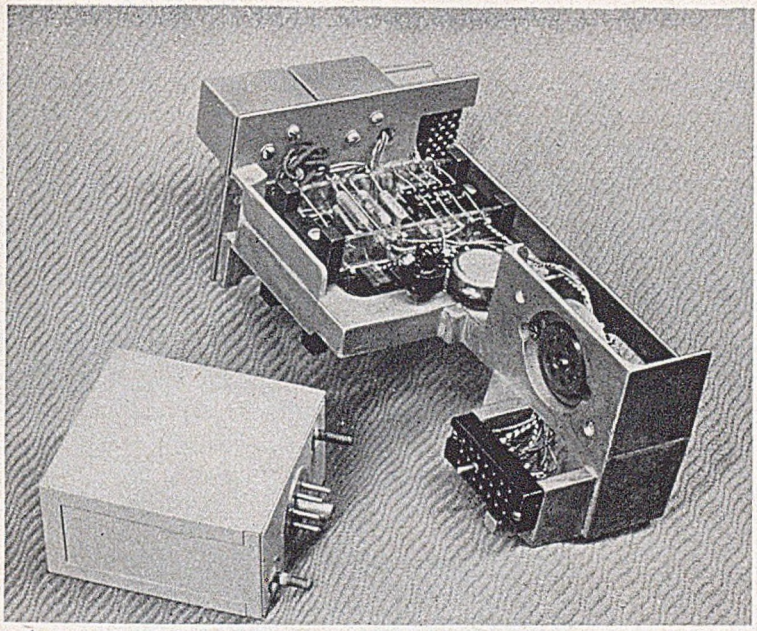

Fig. 29—Carrier subassembly and channel band filter.

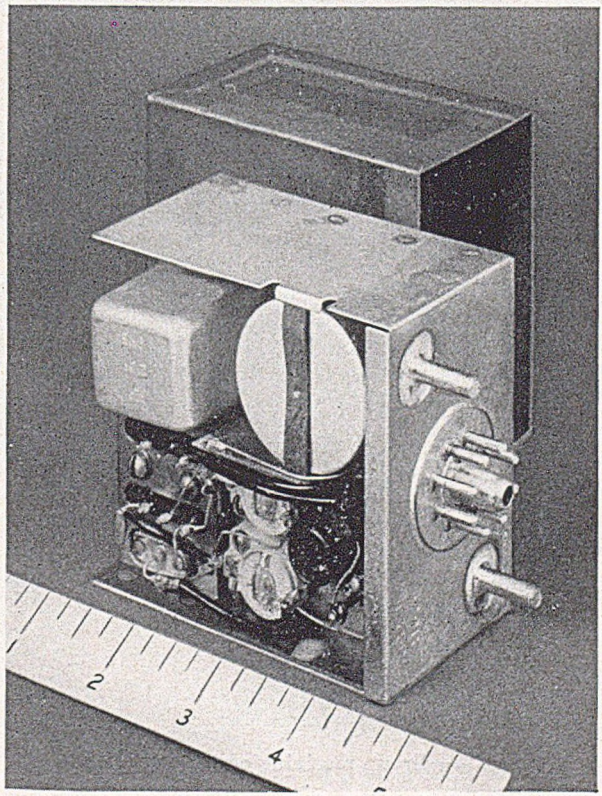

Fig. 30—Channel band filter-internal arrangement.

nel unit, shown on Fig. 34. The same basic die-casting is employed, with minor rearrangement of the die, for the two twin channel units, the group transmitting unit, and the group oscillator. The part of the slide arrangement associated with a plug-in unit is shown at the top of the twin channel unit.

All plug-in units are held in by a common cover (Fig. 24) which encloses the handles of the units. For additional support a rapid action fasterner holds the tops of the channel and receiving group units.

Repeaters may be either pole mounted or placed in a central office. A group of two repeaters is shown on Fig. 35. This assembly employs a framework, shown on Fig. 36, which includes the same slide die-casting as the terminal. A central unit (also plug-in) accommodates the two

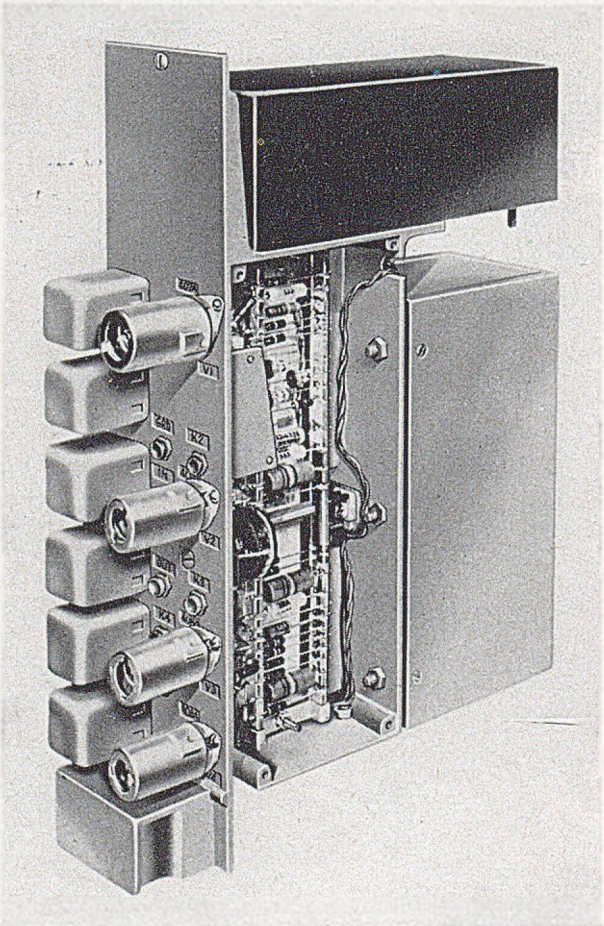

Fig. 31—Group receiving or repeater unit.

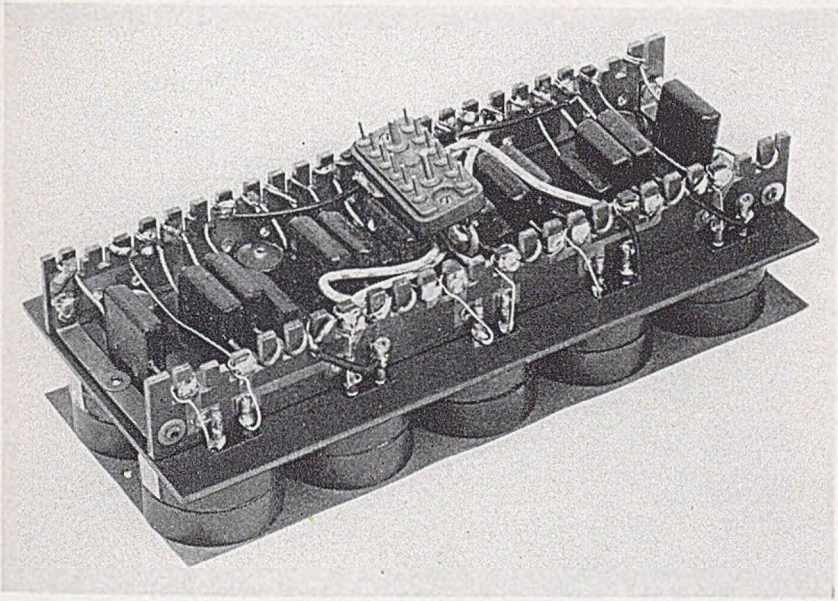

Fig. 32—Typical directional or auxiliary band filter—internal view.

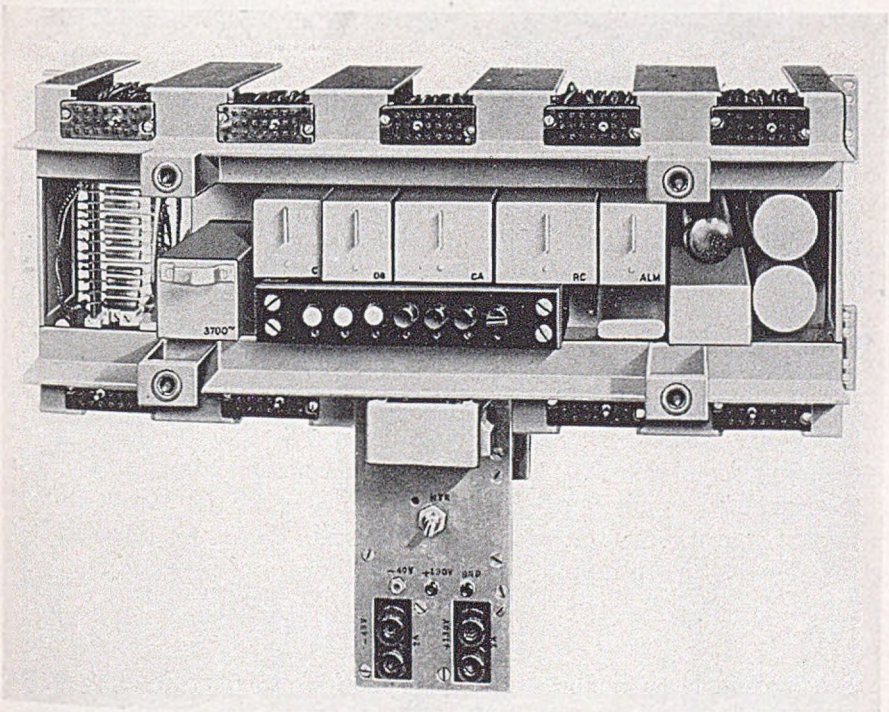

Fig. 33—Terminal framework.

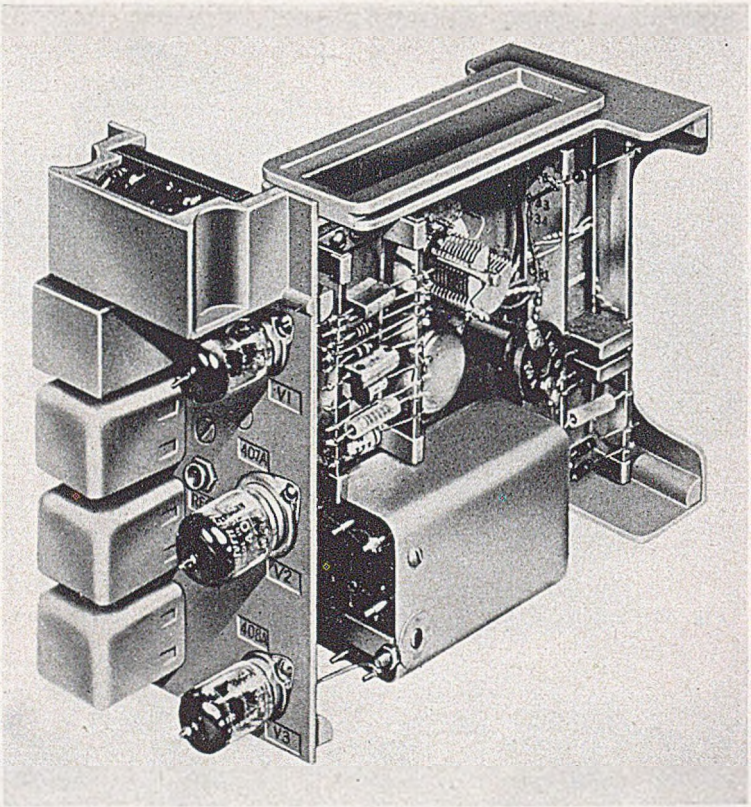

Fig. 34—Twin-channel unit.

plug-in group oscillators, which are also shown in the photograph, together with fuses, alarm lamps, etc.

Pole mounted repeaters are housed in a cabinet, similar to that used for N. Such a cabinet, equipped with four repeaters is shown on Fig. 37.

Since a maximum of four repeaters would have to be supplied by one pair of wires, it is not feasible to transmit power for the repeaters over line pairs. Instead the cabinet contains rectifiers and a line voltage regulator for obtaining 130 volts dc from commercial ac supply. For reserve power supply, a cabinet is available containing a 24-volt storage battery and a dynamotor to supply 130 volts dc to two repeaters (or two dynamotors to supply four repeaters) in case of power failure.

ALARMS

At terminals a common alarm, operating from carrier failure, performs the functions of: First, dropping all connected subscribers to prevent

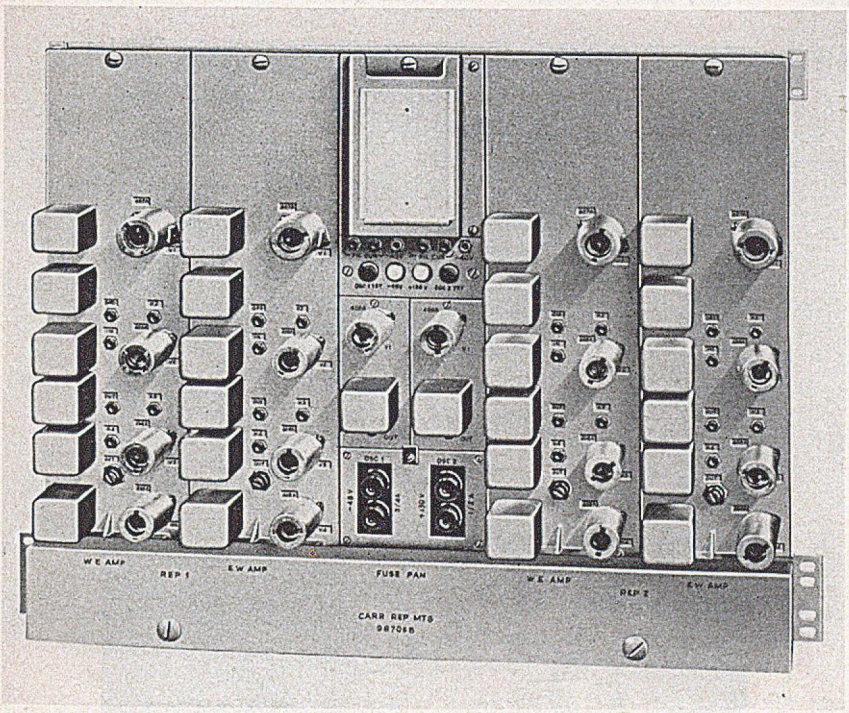

Fig. 35—Two repeater assembly.

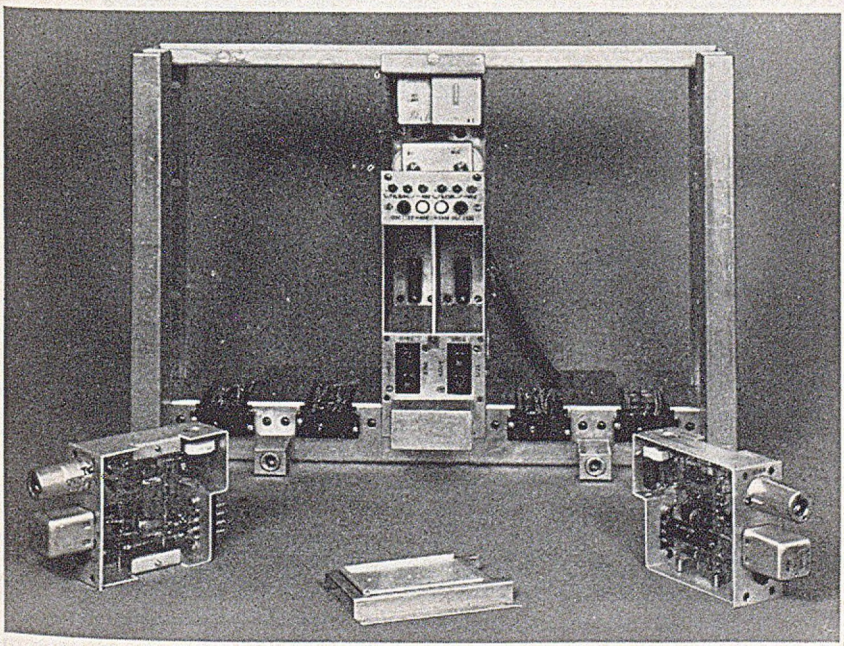

Fig. 36—Repeater framework with oscillators.

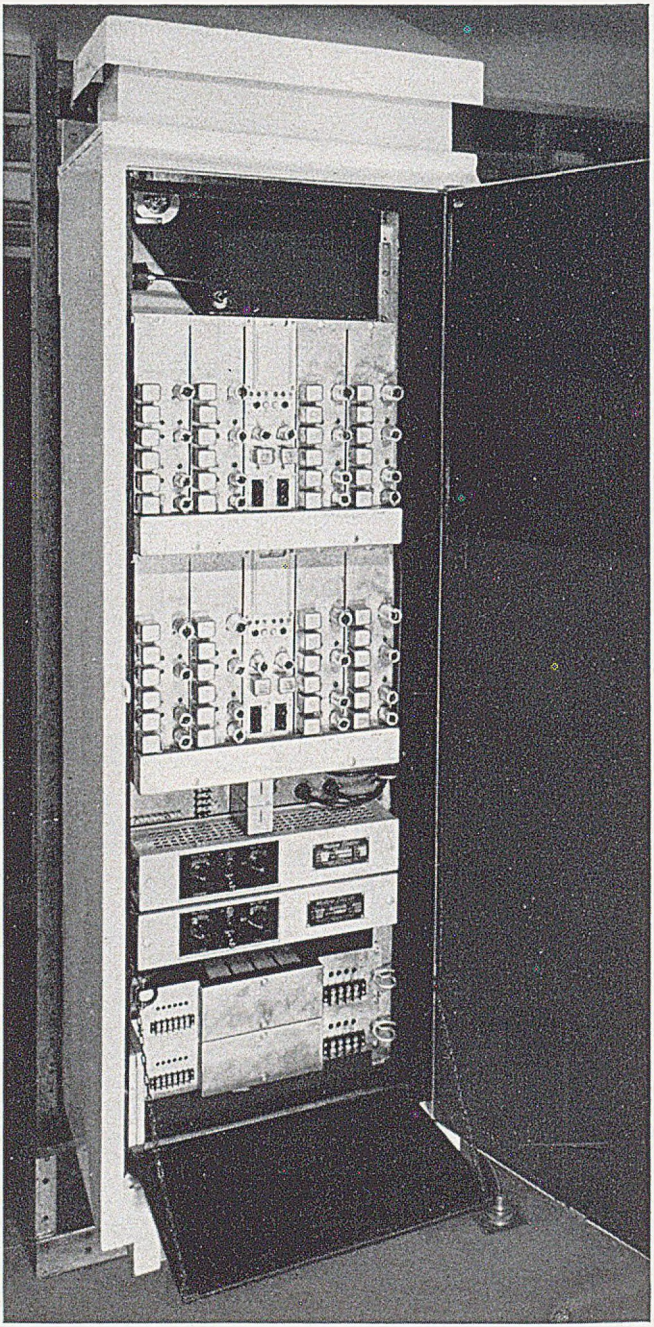

Fig. 37—Typical arrangement of pole mounted repeaters.

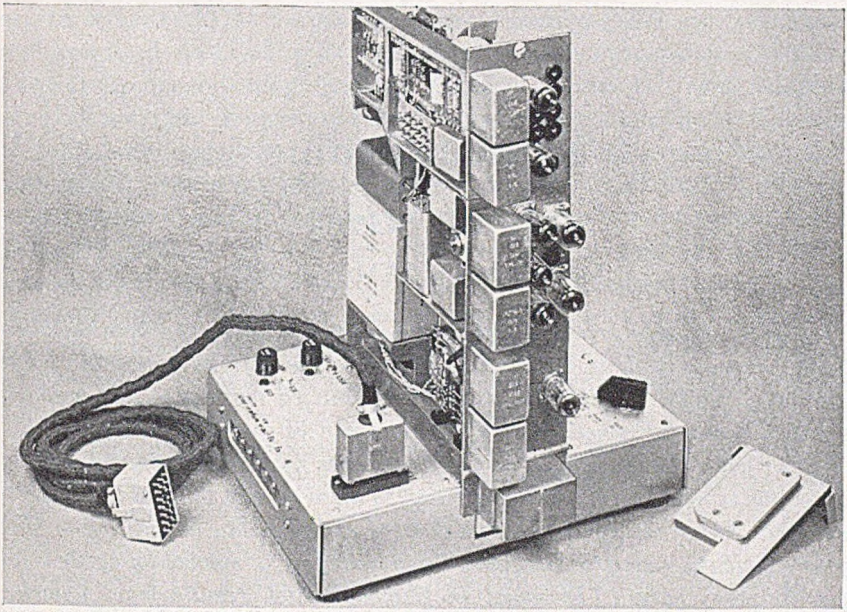

Fig. 38—Test stand.

their being held during the interval of failure; and second, to make all circuits busy at both terminals, to prevent false seizure by operators or automatic switching equipment. Since many O systems may be employed in situations where one terminal is unattended, facilities are included whereby, after failure, the system can be tested from either end, through the use of one of the signaling channels. If it is indicated that the system is operable it can be placed in service again without the necessity of a trip to the unattended terminal.

SPECIAL SIGNALING FEATURE

Arrangements are provided by which two O circuits can have their E and M signaling control leads interconnected without the use of the signaling converter, which is otherwise required. This feature is employed when two circuits are connected together on a permanent or semi-permanent basis to form a single trunk.

TESTING

To facilitate testing at terminal points a test stand (Fig. 38) has been provided which supports an O, or N, channel unit during test and adjustment. By a patch cord, the channel unit can be connected to its original framework if desired. Built in pin jacks permit bridging measurements to be made at selected points in the transmission circuit.

Efficient Coding

By B. M. OLIVER

(Manuscript received May 14, 1952)

This paper reviews briefly a few of the simpler aspects of communication theory, especially those parts which relate to the information rate of and channel capacity required for sampled, quantized messages. Two methods are then discussed, whereby such messages can be converted to a "reduced" form in which the successive samples are more nearly independent and for which the simple amplitude distribution is more peaked than in the original message. This reduced signal can then be encoded into binary digits with good efficiency using a Shannon-Fano code on a symbol-by-symbol (or pair-by-pair) basis. The usual inefficiency which results from ignoring the correlation between message segments is lessened because this correlation is less in the reduced message.

INTRODUCTION

The term coding, as applied to electrical communication, has several meanings. It means the representation of letters as sequences of dots and dashes. It means the representation of signal sample amplitudes as groups of pulses having two or more possible amplitudes as in pulse code modulation. Lately, it has also come to be the generic term for any process by which a message or message wave is converted into a signal suitable for a given channel. In this usage single-sideband modulation, frequency modulation and pulse code modulation are examples of encoding procedures, while microphones, teletypewriters and television cameras are examples of encoding devices.

This is a nice concept, but it is useful to distinguish between two classes of encoding processes and devices: those which make no use of the statistical properties of the signal, and those which do. In the first class, the encoding operation consists simply of a one-to-one conversion of the message into a new physical variable, as a microphone converts sound pressure into a proportional voltage or current, or of the one-to-one remapping of the message into a new representation without regard to probabilities, as by ordinary amplitude, frequency or pulse code modula-

tion. In ordinary PCM for example, the message samples are converted into groups of on-or-off pulses. The particular combination of pulses in any group depends only upon the amplitude of the particular sample, not upon any other property of the message, and the same time is allotted to each group, regardless of the probability of that group or of the amplitude it represents. Almost all the processes and devices used in present day communication belong to this first class. In the second class, the probabilities of the message are taken into account so that short representations are used for likely messages or likely subsequences, longer representations for less likely ones. Morse code, for example, uses short code groups for the common letters, longer code groups for the rare ones.

Processes of the first class we may call non-statistical coding processes, or simply modulation or remapping processes. The time of transmission is the same for all messages of the same length, and all messages are handled by the system with equal facility (or difficulty). These processes require no memory and have a small and constant delay. They are inefficient in their use of channel capacity.

Processes of the second class we may call statistical encoding processes. These processes in general require memory. The time of transmission of messages of the same length may be different so that if messages are to be accepted and delivered by the system at constant rates, variable delays may be necessary at the sending and receiving ends. They are more efficient in their use of channel capacity. It is with this second type of process that this paper is concerned, although processes of the first type may be used as component steps. Thus we consider systems of the type shown in Fig. 1, with the accent on the word "efficient".

TRANSMISSION CIRCUITS AND THEIR VOCABULARIES

Communication circuits or channels can, of course, differ in many respects. Either the peak signal power or the average signal power may be limited. The transmission may be uniform over the band or vary with frequency; it may be constant or subject to selective fading. The noise may be gaussian thermal or shot noise uniform across the band, or peaked at some frequency; or it may be largely impulse noise or erratic

SIGNAL = EFFICIENT DESCRIPTION OF MESSAGE

Fig. 1—Reversible statistical encoding.

static discharges. The best type of signal for one channel may be very poor for another.

In the following sections it is assumed that the channel transmission characteristic is flat in amplitude and delay over a definite band and zero outside. It is also assumed that the channel has a definite peak signal power limitation, and that the noise is white gaussian noise. Such a channel is no mere academic ideal. It is in fact quite closely approached in practice by many circuits. Moreover, the conclusions based on these assumptions can usually be modified or extended to other actual cases, such as that of noise with non-uniform spectral distribution (as for example the coaxial cable).

If the bandwidth of the channel is W, we can (using single sideband modulation, if necessary) transmit over it without distortion from frequency limitation signals containing frequencies from 0 to W (or $-W$ to W in the Fourier sense). Such a wave can assume no more than $2W$ *independent* amplitudes per second. Any set of samples of the wave taken at regular intervals $\frac{1}{2W}$ serves to specify the wave completely. The wave may be thought of as a series of $(\sin x)/x$ pulses centered on the samples and of proportional height, and indeed the wave may be reconstructed from the samples in this fashion. This is the well-known sampling theorem[1]. Thus a message source of bandwidth W can supply at most $2W$ independent symbols (samples) per second, and this same number can be transmitted as overlapping, but independently distinguishable pulses by a circuit of bandwidth W.

Since, as will appear later, channels which are to transmit signals resulting from efficient statistical encoding must be relatively invulnerable to noise, we shall assume that the pulses on the channel are quantized. This allows regenerative repeatering to be used to eliminate the accumulation of noise[1]. If there are b quantizing levels, and if the levels are sufficiently separated so that the probability of noise causing incorrect readings is negligibly small, then the capacity of the channel in bits/sec is[2]

$$C = 2W \log_2 b. \tag{1}$$

Such a circuit talks in an alphabet of b "letters" and uses a language in which all combinations of these letters are allowed. There are no forbidden or impossible "words". The circuit has a vocabulary of b one-letter words, b^2 two-letter words, b^n n-letter words. The basic inefficiency in present day electrical communication is that we build circuits with unrestricted vocabularies and then send signals over them which

use only a tiny fraction of this vocabulary. If all the letters of the written alphabet were used with equal probability and if all combinations of letters were allowed, then many words which are now long could be made shorter, and written text would be less than one third as long as English. Similarly, if we could arrange to let our circuits use their entire vocabulary with equal probability, they could describe our messages with much less time (or bandwidth) on the average.

EXCHANGE OF BANDWIDTH AND SIGNAL TO NOISE RATIO

It was the advent of wide band FM, and other modulation methods which exchange bandwidth for signal-to-noise ratio, which revealed the inadequacy of earlier concepts of information transmission and ultimately led to the development of modern communication theory, or information theory[2].

One of the more familiar results of this theory is the expression for the maximum capacity of a channel disturbed by white noise:

$$C = W \log_2 \left(1 + \frac{P}{N}\right) \tag{2}$$

in which C is the capacity in bits/sec, W is the bandwidth and P/N the ratio of average signal power to average noise power. This capacity can only be approached, never exceeded, and is only reached when the signal itself has the statistics of a white noise. The expression sets a limit for practical endeavor, and also gives the theoretical rate of exchange between W and P/N.

A practical quantized channel, operated so that the loss of information due to incorrectly received levels is negligible requires about 20 db more peak signal power than the average signal power of the ideal channel to attain the same capacity[1]. However, bandwidth and signal-to-noise ratio are still exchanged on the same basis. For example, a satisfactory television picture could be sent over a channel with, say, 100 levels. This would require a (peak) signal to rms noise ratio of some 40 + 20 = 60 db. The bandwidth could be halved by a sort of reverse PCM: by using one pulse to represent two picture elements. But there are 10,000 combinations of two samples each of which can have any of 100 values. Hence the new combination pulse would need 10,000 distinguishable levels and this would require a signal to noise ratio of 80 + 20 = (2 × 40) + 20 = 100 db.

It is evident that while bandwidth compression by non-statistical or straight signal remapping means is not an impossibility, it is neverthe-

less impractical when the signal to noise ratios are already high. What we should really try to do is make our descriptions of our messages more efficient so that less channel capacity is required in the first place. The saving can then be taken either in bandwidth or in signal-to-noise ratio, whichever fits the requirements of our channels best.

MESSAGES

Messages can either be continuous waves like speech, music, or television; or they can consist of a succession of discrete characters each with a finite set of possible values, such as English text. Because a finite bandwidth and a small added noise are both permissible, continuous signals can be converted to discrete signals by the processes of sampling and quantizing[1]. This permits us to talk about them as equivalent from the communication engineering viewpoint. Since many of the principles which follow are easier to think of with discrete messages and since quantization of the channel is assumed for reasons already stated, we shall think of our messages as always being available in discrete form.

Let S = the symbol (or sample) rate of the message

$W_0 = \frac{S}{2}$ = the original bandwith of the continuous message

ℓ = number of quantizing levels.

Then if all the message samples were independent and if all quantizing levels were equally likely, the information per sample would be

$$H_0 = \log_2 \ell \text{ bits} \tag{3}$$

the information rate would be

$$H_0' = S \log_2 \ell \text{ bits/sec} \tag{4}$$

and the message would use the full capacity of a channel with ℓ quantizing levels, and bandwidth $S/2$. Or by remapping k message samples (with the ℓ possible levels) into $\left(\frac{\log \ell}{\log b}\right) k$ samples, a channel with b levels and bandwidth $W = S/2 \left(\frac{\log \ell}{\log b}\right)$ could be loaded to full capacity.

However, it is not true that the successive samples of typical messages are independent, nor is it true that the various sample amplitudes are in general equiprobable. If these things *were* true, speech and music would sound like white noise, pictures would look like the snowstorm

a TV set produces on an idle channel. Written text would look like WPEIPTNKUH WFIOZ—: a random sequence of letters. The statistics of the message, in particular the correlations between the various samples, greatly reduce the number of sequences of given length which are at all likely. As a result the information rate is less, and fewer bits per second are required to describe the average message.

A sequence of M binary digits can describe any of 2^M possible messages. Conversely any of N messages can be described by $\log_2 N$ binary digits. The information rate, H, of a message source is therefore given by

$$H = \lim_{n\to\infty} \frac{\log N}{n} \text{ bits/symbol}$$

where N = number of message sequences of length n. If the successive symbols of the message are *independent* but *not equiprobable*, then a long sequence will contain x_1 symbols of type 1, x_2 of type 2, etc. The number of possible combinations of these symbols will be

$$N = \frac{n!}{\prod_j x_j!},$$

$$\text{so that } \log N = \log n! - \sum_j \log x_j!$$

For large enough n, all the x_j will be large also and we may write, by Stirling's approximation

$$\log N \to \log \sqrt{2\pi n} + n \log n - n - \sum_j [\log \sqrt{2\pi x_j} + x_j \log x_j - x_j]$$

But since $\sum x_j = n$, and since for large n, $x_j \to p(j)n$ where $p(j)$ is the probability of the j^{th} symbol, we have

$$\log N \to \log \sqrt{2\pi n} + n \log n - n \sum_j \log \sqrt{2\pi x_j} - n \sum_j p(j) \log p(j) - n \log n + n$$

$$H_1 = \lim_{n\to\infty} \frac{\log N}{n} = -\sum_j p(j) \log p(j) \tag{5}$$

which is the expression Shannon derives more rigorously[2]. H_1 is a maximum when all the $p(j)$ are equal to $1/\ell$. Then $H_1 = \log_2 \ell = H_0$. The more unequal the $p(j)$, i.e., the more peaked the probability distribution, the smaller H_1 becomes.

If the successive samples are not independent, the message source will pass through a sequence of states which are determined by the past of the message*. In each state there will be a set of *conditional* probabilities describing the choice of the next symbol. If the state is i and the conditional probability (in this state) of the next symbol being the j^{th} is $p_i(j)$, then the information produced by this selection is

$$H_i = -\sum_j p_i(j) \log p_i(j). \tag{6}$$

The average rate of the source is then found by averaging (6) over all states with the proper weighting; thus

$$H = \sum_i p(i)H_i = -\sum_i p(i)\sum_j p_i(j) \log p_i(j). \tag{7}$$

The greater the correlation between successive symbols or samples of a message, the more peaked the distributions $p_i(j)$ become on the average, and this results in a lower value for H. As Shannon points out, the information rate of a source, as given by (7), is simply the average uncertainty as to the next symbol when all the past is known. But in a properly operating communication channel the past of the message is available at both ends, so that it should be possible to signal over the channel at the rate H bits/message symbol, rather than H_0 as we now do. In present day communication systems we ignore the past and pretend each sample is a complete surprise.

By completely efficient statistical coding it should be possible to reduce the required channel capacity by the factor H/H_0. Whether or not this improvement can be actually reached in practice depends upon the amount of past required to uniquely specify the state of the message source. If long range statistical influences exist, then long segments of the past must be remembered. If there are m symbols in the past which determine the present state and each symbol has ℓ possible values, there will be ℓ^m states *possible* (although only 2^{mH} of these are at all probable for large m). If m is large the number of possible states becomes fan-

* In a philosophical sense the state of a message source may be dependent on many other factors besides the past of the message. If the source is a human being, for example, the state will depend on a large number of intangibles. If these could really be taken into account the resulting H for the message might be quite low. If the universe is strictly deterministic one might say that H is "really" always zero. When we describe the drawing of balls from the urn in terms of probabilities, we admit our ignorance as to the exact detail of the mixing operation which has occurred in the urn. Likewise the information rate of a source is a measure of our ignorance of the exact state of the source. From a communication engineering standpoint, the knowledge of the state of the source is confined to that given by the past of the message.

tastically large and complete statistical encoding becomes an economic impossibility if not a technical one.

Let B_i^k be a particular combination (the i^{th}) of k symbols in the past of the message. Each of these combinations at least partially determines the state of the system. Hence we can write an approximation to (7):

$$F_k = -\sum_i p(B_i^k) \sum_j p_{B_i^k}(j) \log p_{B_i^k}(j) \tag{8}$$

$F_k \to H$, as $k \to \infty$. If only m symbols in the past influence the present state, then k need only be as great as m, in order that $F_m = H$. In any case the sequence F_1, F_2, $\cdots$ F_k is monotone decreasing. Naturally one should always pick the k symbols in the past which exert the greatest effect upon the present state, i.e. which cause $p_{B_i^k}(j)$ to be as highly peaked as possible, on the average. In English these would be the immediately previous letters; in television, the picture elements in the immediate space-time vicinity of the present element.

Suppose we break the message up into blocks of length k. Each of these blocks may be considered to be a character in a new (and huge) alphabet. If we ignore any influences from previous blocks, i.e. if we consider the blocks to be independent, then the information per block will be simply

$$-\sum_i p(B_i^k) \log p(B_i^k). \tag{9}$$

Since there are k symbols per block, the information per symbol, G_k is

$$G_k = -\frac{1}{k} \sum_i p(B_i^k) \log p(B_i^k). \tag{10}$$

As $k \to \infty$, $G_k \to H$, since the amount of statistical influence ignored (between blocks) becomes negligible compared with that taken into account.

If d is the number of binary digits required to specify a message n symbols long, then as $n \to \infty$, $d/nH \to 1$. For large n there are thus 2^{nH} messages which are at all likely out of $2^{nH_0} = \ell^n$ possible sequences (in an ℓ letter alphabet). The probability that a purely random source will produce a message (i.e., a sequence with all the proper statistics) is therefore

$$p \cong 2^{-n(H_0 - H)} \tag{11}$$

for large n. Even if $H_0 - H$ is small, $p \to 0$ rapidly for large n. This is why white noise never produces anything resembling a picture on a television screen, for instance. For in television signals, $H_0 - H > 1$

even for very complicated picture material, and $n \cong 250{,}000$ for a single frame.

As given by (11), p, also represents the fraction of the possible signals on a channel of ℓ levels which are likely ever to be used by messages of length n without statistical encoding.

STATISTICALLY MATCHED CODES

Since a sequence of binary digits can be remapped by a non-statistical process into a channel with b quantizing levels, or indeed into a wide variety of other signalling alphabets, it suffices to consider statistical coding processes and codes which reduce the message to a sequence of binary digits. An efficient code is then one for which the average number of binary digits, H_c, per message symbol lies between H_0 and H. As the efficiency increases $H/H_c \to 1$, so this ratio may be taken as an efficiency index. With highly efficient processes, the sequences of binary digits produced will have little residual correlation, i.e., they will be nearly random sequences. Since the encoding process must be reversible the receiver must be able to recognize the beginnings and ends of code groups. Since we have at our disposal only zeros and ones, the divisions between code groups must either be marked by a special code group reserved for this purpose, or else the code must have the property that no short code group is duplicated as the beginning of a longer group.

A code which satisfies this latter requirement and which is capable of unity efficiency is the so-called Shannon-Fano code, developed independently by C. E. Shannon of Bell Telephone Laboratories and R. M. Fano of the Massachusetts Institute of Technology. This code is constructed as follows: One writes down all the possible message sequences of length k in order of decreasing probability. This list is then divided into two groups of as nearly equal probability as possible. One then writes *zero* as the first digit of the code for all messages in the top half, *one* as the first digit for all messages in the bottom half. Each of these groups is again divided into two subsets of nearly equal probability and a zero is written as the second digit if the message is in the top subsets, a one if it is in the bottom. The process is continued until there is only one message in each subset. Fig. 2a shows the code which results when this process is applied to a particularly simple probability distribution $p(B_i^k) = (1/2)^t$. Here each code group is a series of ones followed by a zero. The receiver knows a code group is finished as soon as a zero appears. Although the longer groups contain mostly ones, their probability is less and on the average as many zeros are sent as ones.

MESSAGE NO.	MESSAGE PROB.	CODE	STEP
1	1/2	0	(1)
2	1/4	1 0	(2)
3	1/8	1 1 0	(3)
4	1/16	1 1 1 0	(4)
5	1/32	1 1 1 1 0	(5)
6	1/64	1 1 1 1 1 0	
7			

(a)

MESSAGE NO.	MESSAGE PROB.	CODE	STEP
1	1/4	0 0	(2)
2	1/4	0 1	(1)
3	1/8	1 0 0	(3)
4	1/8	1 0 1	(2)
5	1/16	1 1 0 0	(4)
6	1/16	1 1 0 1	(3)
7	1/32	1 1 1 0 0	

(b)

MESSAGE NO.	MESSAGE PROB.	CODE	STEP
1	1/8	0 0 0	(3)
2	1/8	0 0 1	(2)
3	1/8	0 1 0	(3)
4	1/8	0 1 1	(1)
5	1/8	1 0 0	(3)
6	1/8	1 0 1	(2)
7	1/8	1 1 0	(3)
8	1/8	1 1 1	

(c)

Fig. 2—Shannon-Fano codes for three different distributions. The successive bisections are indicated by the dashed lines and the number gives the step at which that bisection took place.

If the successive message segments are independent, the code will generate a random sequence of zeros and ones. Fig. 2b shows the code which results with another distribution. Here the termination of each code group is more complicated but the non-duplicative property exists so the receiver can still identify the groups. Fig. 2c shows the code which results when all the $p(B_i^k)$ are equal. It is the ordinary binary code.

The length of each code group is equal to $\log 1/p(B_i^k)$, for the cases shown in the figures. This is true in general so long as it is possible to divide the list into subgroups which are of exactly equal probability.

When this is not possible, some code groups may be one digit longer as Shannon shows. The average number of digits per message symbol using this code is therefore given by

$$-1/k \sum_i p(B_i^k) \log p(B_i^k) \leq H_c \leq -1/k \sum_i p(B_i^k) [-1 + \log p(B_i^k)]$$

$$G_k \leq H_c \leq G_k + 1/k.$$

For large k, $H_c \to G_k \to H$ and the efficiency approaches unity. With small k, H_c increases both because the smaller list of messages cannot be so accurately divided repeatedly into equal probability subsets (so-called "granularity" trouble), and also because more statistics are ignored between the shorter blocks.

The ordinary binary code provides a statistical match between message source and channel only if the various message blocks B_i^k have equal probability $p(B_i^k) = 1/2^n$, and are mutually independent. With $k = 1$, $p(B_i^k) = p(j)$ and the "blocks" are merely the successive symbols.

Ordinary PCM is statistically matched only to a random message source with flat distribution.

If the messages from a source are characterized by frequent long runs of symbols of the same type (e.g., long runs of zeros) an obvious saving is possible by sending the value of the symbol only once, together with a code group which gives the length of the run. This is commonly known as run length coding. The remaining sections of the message (between runs) may then either be sent directly (i.e., merely remapped by a non-statistical process) or they may be encoded by some other statistical process, if this seems warranted. In the latter case we have a mixed coding procedure. The codes representing run lengths must either be set apart from the remainder of the signal by "punctuating" codes, or identifiable by some distinguishing characteristic.

Run length coding may be generalized to take care of other common sequences besides runs of a single symbol. Any commonly occurring sequence of symbols may be considered a "run" and treated in the same fashion. More complicated code groups will be required to specify the type of run, if a large variety is accommodated this way. Ultimately, the distinction between this type of coding and Shannon-Fano coding becomes rather nebulous, especially if a fixed maximum length of run is permitted, for then all possible messages of this length may be considered "runs" and simply encoded by the Shannon-Fano code.

No optimal general solution of the coding problem is known. That is, one cannot say in all cases exactly what coding procedure one should use with a given message source to produce the most efficient encoding for a given complexity of apparatus. Several procedures have been devised which seem suitable for certain types of messages and these are discussed in the following sections.

n-GRAMMING

The application of the Shannon-Fano code to a block of k symbols of a message in an ℓ letter alphabet requires that ℓ^k different codes be used. The receiver must be able to recognize each of these and to regenerate the proper message block when a particular code is received. If ℓ is on the order of 10 to 100 as is typically the case, we very quickly run out of room to house the receiver and money to build it with. On the other hand, if k is small, say on the order of 1 to 3, considerable statistical information between blocks is ignored. These considerations led to the development of a class of encoders known as n-grammers. The name stems from the fact that they operate on the n-gram statistics of the

message, to produce a reduced signal having more nearly independent symbols, but (in return) a highly peaked simple probability distribution which allows savings with Shannon-Fano coding on a symbol-by-symbol ($k = 1$) basis.

The simplest member of this class is the monogrammer. It is basically merely a re-ordering device. The operation may be best understood by the following example. Suppose someone supplied us with English text encoded into a quantized pulse signal as follows:

Symbol	Pulse height
Space	0
A	1
B	2
C	3
D	4
etc.	etc.

Now the letter frequencies in English are shown in Fig. 3. Merely to save average power in our channel we might wish to convert this signal into one in which the pulse height is not alphabetical, but in which the most common symbol is sent as a pulse of zero height, the next most common as a pulse of unit height, etc. In other words, we would like the following representation:

Symbol	Pulse height
Space	0
E	1
T	2
A	3
etc.	etc.

The device shown in Fig. 4 will accomplish this translation. The original signal is applied to the vertical deflecting plates of a cathode ray tube. The rest position of the spot corresponds to "space", i.e. no pulse. A pulse one unit high deflects the spot to *A*, a pulse two units high deflects the spot to *B*, etc.

Now in front of these spot positions we place a number of light attenuating filters. In front of the "space" position we place an opaque mask. Hence when the spot is deflected to "space" the photocell receives no light and no pulse is sent. In front of the "*E*" position we place a mask having one unit of transmission. So although *E* is received as a pulse 5 units high, it is sent as a pulse of unit height. In front of the

"T" position we place a mask with two units transmission, and so on. The signal amplitudes as received are thus re-ordered in the desired fashion.

The resulting signal has lower average power and this can sometimes be an advantage, particularly if several such signals are to be sent over a common channel by frequency division. In this case the extreme rarity of occurrence of high peak powers on all channels simultaneously means

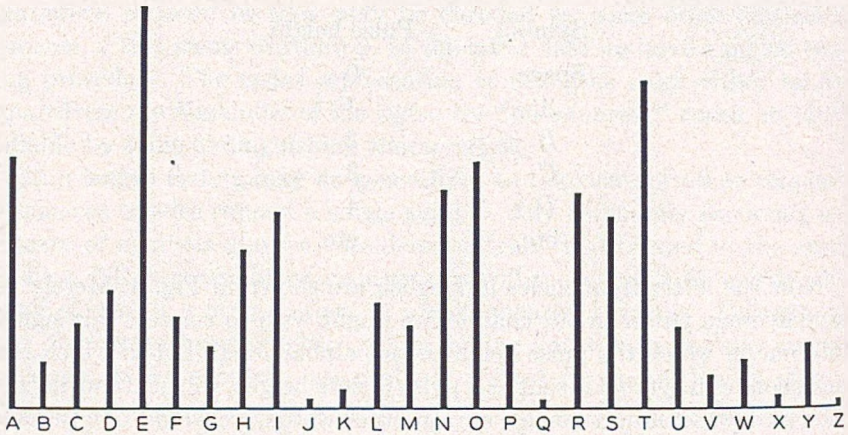

Fig. 3—Letter frequencies in English.

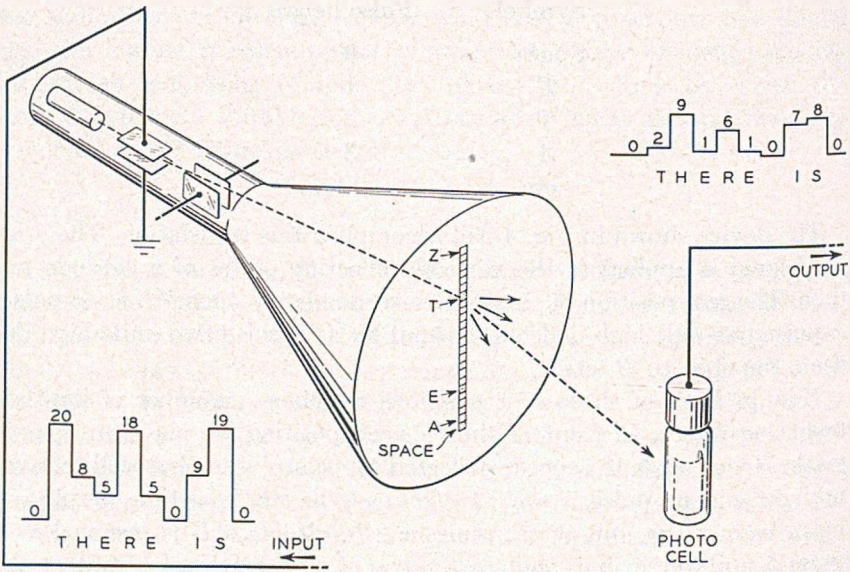

Fig. 4—The "Monogrammer."

that the system can be designed to have a lower *peak* power capacity. The signal out of the monogrammer can be remapped into binary digits using a Shannon-Fano code, pulse by pulse. However, this could have been done equally well with the original signal merely by rearranging the code groups in the coder tube. It is when we extend the principle to digrams and trigrams that the potentialities of the system become evident.

We can easily take account of the influence of the preceding message symbol. To do this we apply the signal to the vertical plates as before, and to the horizontal plates we apply the signal delayed by an amount equal to the time between successive pulses as shown in Fig. 5. Thus the beam is deflected *vertically* by the *present* message symbol, and *horizontally* by the *previous* message symbol. Whereas before we used a single column of optical filters chosen in accordance with the simple probabilities of the letters, we now have 27 columns, one for each letter and one for the space. The filters in each column are chosen in accordance with the *conditional* probabilities which apply when the corresponding letter was the previous symbol. For example, in the "Q" column (last letter Q), and the "U" row (present letter U) the mask would be opaque, since U is most common after Q. In general, the transmission of cell ij, in the i^{th} column and j^{th} row, is proportional to the rank of the entry for $p_i(j)$ when the entire distribution (conditioned on i) is ordered in a monotone decreasing sequence. The amplitude distribution of the output pulses

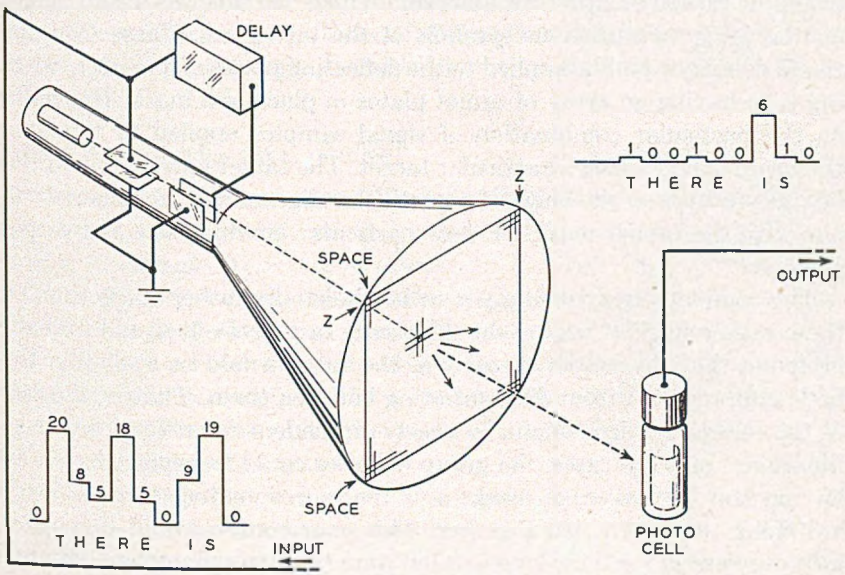

Fig. 5—The "Digrammer."

from the digrammer will be more peaked toward zero amplitude than that of the monogrammer. This is illustrated by the signals in the figures. At the receiver the same type of device, but with an inverse mask can be used to convert the signal back to its original form.

The digrammer can, with a little assistance, supply all the data required to prepare the encoding mask. If typical signals from the message source are applied to the cathode ray tube (without mask) for a long time, and a time exposure is made of the face of the tube, a lattice of spots will be obtained on the film. These spots will be dense where the high probability combinations occur and less dense elsewhere. The order of decreasing density in each column is noted, and the filter transmissions are arranged in the same order.

It is, of course, not necessary to use a phosphor, optical filters, and a photocell. An array of targets each of which connects to the appropriate tap on a load resistor might be simpler and more efficient. The cathode ray tube itself can be replaced with an appropriate diode switching network. Relay networks could be used for low-speed operation.

At the digrammer level we run out of new dimensions to use in the cathode ray tube. The principle can, however, be extended to trigramming and general n-gramming. For example, tetragramming could be accomplished by using a bank of ℓ^2 digrammers all in parallel, and all deflected by the present and previous samples. Only one of these tubes would be turned on at a time however. Which one this was would depend on the other two previous symbols of the tetragram. These (by additional delays) would be applied to the deflecting plates of a master switching tube having an array of target plates in place of a mask. Depending on the particular combination of signal samples applied to this tube, the beam would strike a particular target. The target current would then be used to turn on the beam of a particular digrammer tube, namely the one with the proper mask for that particular combination of two past symbols.

The complete array of equipment is admittedly rather staggering, but then, rather efficient coding should result. In practice it would probably be found that the masks of many of the tubes would be so similar that little gain resulted from differentiating between them. That is, the state of the message source might be nearly equivalent for several past combinations. In these cases, the group of tubes could be replaced with one having the best average mask, and the corresponding targets on the switching tube then tied together. This compromise would be particularly warranted for those tubes which were rarely used anyway. By these

tricks it should be possible to keep the growth of equipment down to something approaching 2^{nH} rather than ℓ^n.

The output signal from the n-grammer will be, as we have seen, a series of pulses with an amplitude distribution very peaked toward zero and small pulses. If ℓ ,the alphabet, is large, these pulses can be efficiently encoded into a Shannon-Fano code. For small alphabets, granularity trouble can be reduced by remapping the output pulses two-by-two into pulses of base ℓ^2, and then encoding these into the Shannon-Fano code.

The output signal from the n-grammer with English text as the input message is a pulse amplitude representation of the type of "reduced text" one gets by using running n-gram prediction on English, as described by Shannon[3].

More efficient encoding would result if the properly matched Shannon-Fano code for *each particular conditional distribution* were applied to the output pulses, rather than using the same code for all of them. The efficiency of the coding operation would then be close to F_n as given by (8) (take $k = n$). This would add a great deal to the complexity and with most signals it is felt the gain would be small. If all the conditional distributions were alike after ordering, the improvement would be nil.

English text was used as the message in describing the n-gramming technique to emphasize the fact that it is a powerful general method which works even when the conditional probability distributions of a message are disorderly, multimodal affairs. It is obviously suited to other types of messages as well. Its main drawback is the complexity of apparatus required.

PREDICTIVE-SUBTRACTIVE CODING

When the conditional probability distributions of a message are unimodal (or merely strongly peaked as a rule in the vicinity of a particular sample amplitude) it is not necessary to re-order the distributions in order to obtain a reduced message for coding. The distributions may then merely be shifted along the amplitude scale until their modes are near zero (or their second moments about zero are nearly minimum). This shifting can be accomplished by computing from the preceding $(n - 1)$ gram the amplitude at which this mode or mean is located, and then subtracting this computed amplitude (or the nearest quantizing level) from the actual amplitude of the present sample. The difference in each case is a symbol whose amplitude distribution is peaked in the vicinity of zero amplitude. Fig. 6 shows a block schematic of a system using pre-

dictive-subtractive coding. In an actual system the reduced signal would ordinarily be encoded into Shannon-Fano code groups before transmission over the channel.

If s_0 is the present sample amplitude, and s_1 , s_2 , $s_3 \cdots s_n$ are previous sample amplitudes we compute a predicted value, s_p , for the present sample which is given by

$$s_p = f(s_1 , s_2 , \cdots s_n) \pm \delta$$

where $\delta < \frac{1}{2}$ quantizing level. If the conditional probability distribution for the present sample is $p_{s_1 \cdots s_n}(s_0)$, then the difference, or output, or

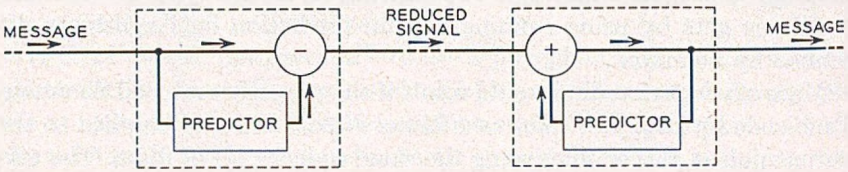

Fig. 6—Predictive-subtractive coding.

"error" signal, ϵ, will have the conditional distribution $p_{s_1 \cdots s_n}(\epsilon + s_p)$ for this particular case. The simple distribution is then the weighted average over all cases, i.e.

$$p(\epsilon) = \sum p(s_1 , s_2 , \cdots s_n) p_{s_1 \cdots s_n}(\epsilon + s_p)$$

where the sum is over all combinations of s_1 , $s_2 \cdots s_n$.

Predictive-subtractive coding has especial merit when a simple function can be used for computing s_p . This is often the case. When the function is simply a weighted sum of the past sample amplitudes, i.e. when

$$s_p = (as_1 + bs_2 + cs_3 + \cdots) \pm \delta$$

we have what is known as *linear prediction*. Of course, linear prediction can always be used, but it may not be good enough with some types of messages.

As Wiener has shown the coefficients a, b, c $\cdots$ which minimize $\overline{\epsilon^2}$ are readily computed. For simplicity, assume only two message samples, s_1 and s_2 , from the past are to be used. We then have

$$\epsilon = s_0 - s_p$$

$$\epsilon = s_0 - as_1 - bs_2$$

$$\epsilon^2 = s_0^2 + a^2 s_1^2 + b^2 s_2^2 - 2as_0 s_1 + 2ab\, s_1 s_2 - 2b\, s_0 s_2$$

Now

$$\overline{s_0^2} = \overline{s_1^2} = \overline{s_2^2} = A_0$$

$$\overline{s_0 s_1} = \overline{s_1 s_2} = A_1$$

$$\overline{s_0 s_2} = A_2$$

where A_0, A_1, and A_2 are the values of the auto-covariance of the message wave at displacements of 0, 1, and 2 sampling periods. Thus

$$\overline{\epsilon^2} = (1 + a^2 + b^2)A_0 + 2(ab - a)A_1 - 2bA_2 .$$

The autocorrelation (normalized auto-covariance) is given by $\phi_i = \frac{A_i}{A_0}$. A_0 is proportional to the average power in the message wave, so the ratio $\rho = \frac{\overline{\epsilon^2}}{A_0}$ is the ratio of the power in the error signal to the power in the original message wave. Thus:

$$\rho = (1 + a^2 + b^2) + 2(ab - a)\phi_1 - 2b\phi_2$$

$$\frac{\partial \rho}{\partial a} = 2a + 2(b - 1)\phi_1 = 0$$

$$\frac{\partial \rho}{\partial b} = 2b + 2a\phi_1 - 2\phi_2 = 0$$

from which

$$a = \frac{\phi_1(1 - \phi_2)}{1 - \phi_1^2}, \qquad b = \frac{\phi_2 - \phi_1^2}{1 - \phi_1^2}.$$

With these values of a and b:

$$\rho = 1 - \phi_1^2 - \frac{(\phi_1^2 - \phi_2)^2}{1 - \phi_1^2}.$$

If $\phi_2 = \phi_1^2$, then the expressions simplify to

$$a = \phi_1 , \qquad b = 0, \qquad \rho = 1 - \phi_1^2 .$$

As can easily be shown, if $\phi(x) = e^{-\alpha|x|}$, then all the coefficients except a are zero, and a has the value $e^{-\alpha}$. In other words, if the autocorrelation function is of exponential shape, the previous sample *alone* is needed

for linear prediction. Samples before this add no further information as to the location of the mean of the conditional distributions.*

It happens that in typical television signals the autocorrelation for small displacements shows a very nearly exponential behavior. Thus linear prediction on the basis of the previous picture element alone is a natural method for television, particularly in view of the simplicity of apparatus required.

Linear prediction is easily instrumented. Fig. 7 shows in block schematic form the essentials of a linear predictor. Samples of the message are applied to a delay line. Taps along this line separated by the intersymbol time of the message, or multiples thereof, make the desired past symbols available. The signals from these taps are merely attenuated by amounts corresponding to the coefficients $a, b, c \cdots$ and added. A differential summing amplifier is shown to allow for negative coefficients, and also to accomplish the subtraction of the predicted sample amplitude from the present sample amplitude.

A complete linear predictor-subtractor is nothing but a transversal (time domain) filter whose impulse response is

$$f(t) = \delta(t) - a\delta(t - \tau) - b\delta(t - 2\tau) \cdots$$

and whose equivalent frequency response is therefore

$$F(\omega) = 1 - ae^{-i\omega\tau} - be^{-2i\omega\tau} \cdots$$

where τ is the delay between taps. If, for example, simple previous value prediction is used ($a = 1; b, c \cdots = 0$)

$$F(\omega) = 1 - e^{-i\omega\tau} = 2i \sin \frac{\omega\tau}{2} e^{-\frac{i\omega\tau}{2}}.$$

---

* From the preceding expression for ρ, we see that $\rho = 0$ (i.e., perfect prediction is possible) if:

$$(\phi_1^2 - \phi_2)^2 = (1 - \phi_1^2)^2$$

$$\phi_1^2 - \phi_2 = \pm(1 - \phi_1^2)$$

$$\begin{cases} \phi_2 = 1 \\ \phi_2 = 2\phi_1^2 - 1. \end{cases}$$

If $\phi_2 = 1$, the message samples alternate between two independent but constant values. For this case $a = 0, b = 1$. If $\phi_2 = 2\phi_1^2 - 1$ the autocorrelation is a cosine wave so the message consists of samples of a sinusoid. In this case $a = 2\phi_1, b = -1$. If ϕ_1 is nearly unity, the sinusoid is of low frequency, and the prediction approaches "slope" prediction (i.e. extrapolation of a straight line through the last two samples).

In any case where perfect prediction is possible the wave is periodic and therefore $H = 0$.

It is often argued that linear prediction is therefore nothing more than pre-distortion (frequency-wise). If the message is unquantized and unsampled, and if the signal from the predictor is applied to the channel as straight amplitude or single side-band modulation, the allegation is certainly true. Pre-distortion is a perfectly valid way of improving the statistical match between message, and channel, and destination as the optimum filter theory of Weiner and Lee shows. On the other hand, when the message is sampled and quantized, and when the output of the linear predictor is further encoded into a sequence of binary digits, and these are possibly remapped onto a higher base for the channel, then the information is being handled digitally throughout, and the usual reasons for a certain type of predistortion no longer apply. The best linear predictor will usually be quite different for the two cases. Even though analogue operations (such as subtraction of amplitudes) are used for convenience, the quantization makes the operation discrete and hence equivalent to a digital process.

At the beginning of this section, we were a little vague as to whether the prediction should shift the modes or the means of the conditional distributions to zero amplitude. If the object of the prediction-subtraction operation is to minimize the *power* in the error signal, then certainly the means should be shifted to zero. The coefficients as determined from the autocorrelation function do this aside from quantizing granularity. They specify an optimum least-square predictor, i.e., one which tends to minimize $\overline{\epsilon_j^2} = \sum_j j^2 p(j)$.

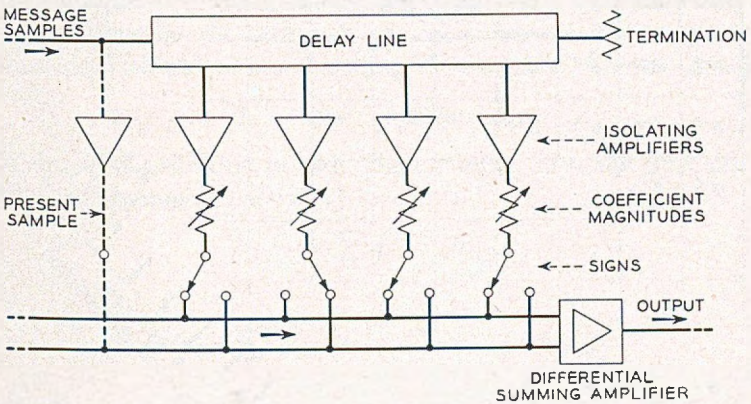

Fig. 7—A linear predictor.

Power reduction is an index of merit when many reduced signals are to be sent by frequency division over one channel, as we have said. When the object is to reduce the channel capacity required for a single message source, then it is the upper bound entropy of the reduced signal which should be minimized, not the power. That is we want $-\sum_j p(j) \log p(j)$ to be minimized. For certain types of signals this requires the modes to be shifted to zero, although this is by no means a general rule. Shifting the modes to zero may actually increase the entropy of the "reduced" signal over that of the original message, by adding too many new symbol levels, as the example in the last section shows.

If the original message has ℓ quantizing levels, the reduced message after predictive-subtractive coding will in general contain more than ℓ levels since an error of more than $\frac{\ell}{2}$ can be made in either direction. An n-gramming operation, on the other hand, never increases the alphabet.

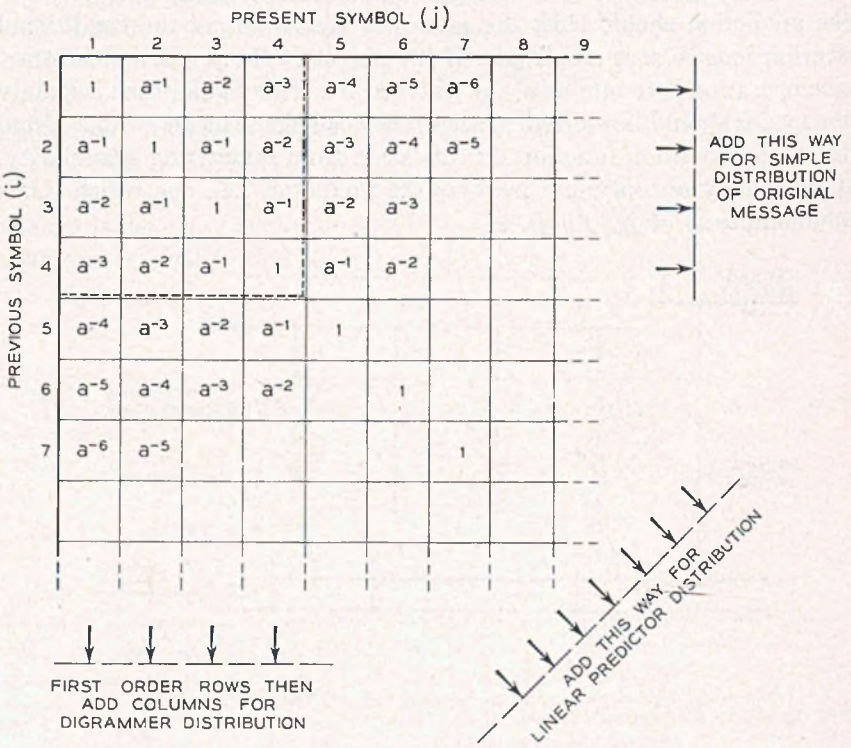

Fig. 8—Joint probability distribution (divide all coefficients by the sum over each array).

Other operations besides simple subtraction of the predicted symbol from the present symbol are of course possible. However, in most cases it would seem that if a more complicated operation were indicated, n-gramming would have provided a better start.

ILLUSTRATIVE EXAMPLE

Let us compare the operation of n-gramming and prediction-subtraction techniques on a hypothetical message. We will assume the message has digram statistics, but that longer range statistical influences either do not exist or are ignored. The statistics are then specified entirely by the joint probability distribution $p(i, j)$ of a pair of symbols. Let us assume that there are ℓ quantizing levels, and that

$$p(i, j) = Ka^{-|i-j|}$$

where a is a constant > 1, and K is given by

$$K = \left[\sum_{i,j} a^{-|i-j|}\right]^{-1}$$

K is the factor which assures that $\sum_{i,j} p(i, j) = 1$.

Thus the most likely level is that of the previous sample. A sample differing by one level is $1/a$ times as likely, one differing by m levels is a^{-m} times as likely. Figure 8 shows a plot of the *relative* values of $p(i, j)$ (neglecting the factor K). For $\ell = 4$, the total array would be the 4 x 4 portion enclosed by the dashed line. This sort of distribution is rather similar to those of typical television signals, as shown by preliminary measurements, although typical values of a have yet to be determined. With no statistical coding, the required channel capacity is

$$H_0 = \log_2 \ell \text{ bits/sample.}$$

If the simple distribution of individual samples is taken into account, the required channel capacity is reduced to

$$H_1 = -\sum p(i) \log p(i)$$

where

$$p(i) = \sum_j p(i, j) = \sum_i p(i, j) = p(j)$$

H_1 may be computed from the array of *relative* coefficients by adding the rows to form the sums

$$S_i = \frac{1}{K} \sum_j p(i, j) = \frac{p(i)}{K}.$$

In terms of these sums, we have

$$H_1 = \log \frac{1}{K} - K \sum_i S_i \log S_i .$$

Since, with the assumed distribution, the S_i are all nearly equal very little reduction in channel capacity is achieved by this step.

With linear prediction, the modes of the distributions ($i = j$) could be centered at zero merely by sending the difference between the present and previous sample (previous value prediction). This would give a reduced signal whose distribution may be found by adding the array along the diagonals. The required channel capacity is then given by:

$$H_L = -K\ell \log K\ell - 2\sum_{k=1}^{\ell-1} \frac{k(\ell-k)}{a^k} \log \frac{k(\ell-k)}{a^k}$$

The distribution of the signal from a digrammer is found by rearranging each row of the table in order of decreasing probability and then adding the resulting columns. Call these sums S_d . The digrammer output will thus require a channel capacity:

$$H_0 = -\sum_{d=1}^{\ell} KS_d \log KS_d$$

$$= \log \frac{1}{K} - K \sum_{d=1}^{\ell} S_d \log S_d$$

Lastly, the true rate of the source is given by

$$H = -\sum_i p(i) \sum_j p_i(j) \log p_i(j)$$

$$= \log \frac{1}{K} - H_1 + 2K \sum_{k=1}^{\ell-1} \frac{\ell - k}{a^k} k \log a$$

Values for the above quantities were computed for $a = z$ and $n = 2, 3, 4, 6, 8, 16, 32, \infty$. For the case of $a = 2$, we find that

$$K = [3\ell - 4(1 - 2^{-\ell})]^{-1}$$

and that as $\ell \to \infty$,

$$H_L , H_D , H \to \tfrac{4}{3} + \log_2 3 = 2.918 \text{ bits.}$$

The results are shown in the Table I and also are plotted in Fig. 9.

While H_0 and H_1 increase without limit as ℓ is increased, H_L , H_D, and H quickly approach a definite limit. This limit exists because we assumed that the decrease in joint probability as a function of *number*

TABLE I

Number of levels	H_0	H_1	H_L	H_D	H
1	0	0	0	0	0
2	1	1	1.252	0.918	0.918
3	1.585	1.583	1.777	1.437	1.422
4	2	1.995	2.074	1.764	1.750
6	2.583	2.575	2.381	2.157	2.131
8	3	2.988	2.552	2.370	2.343
16	4	3.99	2.768	2.678	2.641
32	5	$5 - \epsilon$	2.850	2.818	2.782
∞	$\log \infty$	$\log \infty$	2.918	2.918	2.918

(These figures were computed by slide rule so the fourth figure is not very significant.)

of levels off the diagonal was the same regardless of ℓ. In typical signals this is not true. The decrease is more apt to depend on *amplitude difference* and the finer the quantum step, the more levels a given difference represents. As a result, the probability will fall off less per level off the diagonal, and doubling ℓ will in general add one bit to H.

On the other hand, doubling the sampling rate will not in general double the required channel capacity, for the closer spaced samples will

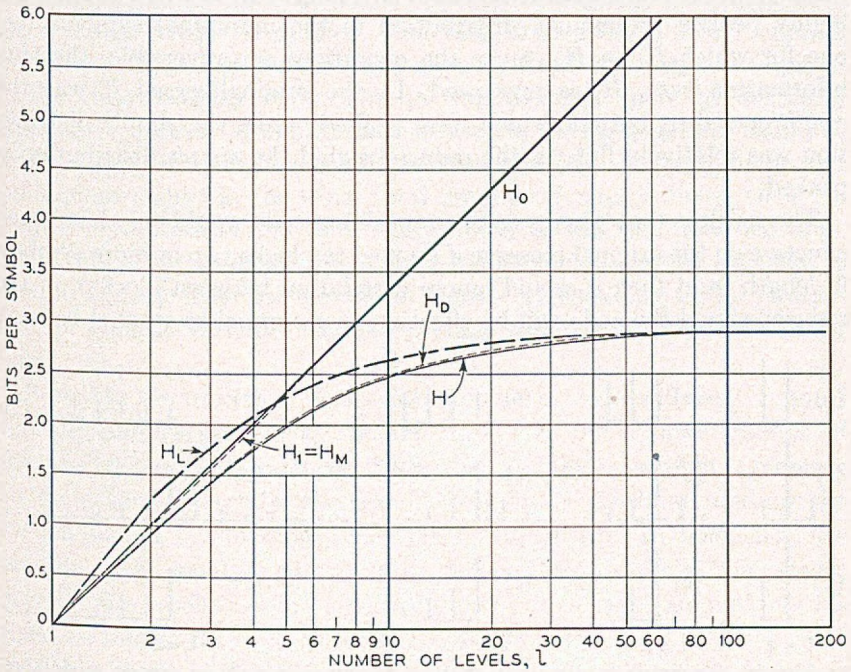

Fig. 9.

be more highly correlated. Thus in TV, doubling the horizontal resolution would not double the bandwidth for the same picture material if use were made of the statistics. (Of course, increased resolution in TV might encourage the use of more detailed scenes and this *would* increase the required bandwidth.)

It should also be noticed that for small ℓ, linear prediction actually makes matters worse. The increase in the number of levels in the error signal more than offsets the peaking of the distribution.

Since all the conditional distributions in this message are of similar shape (after ordering), H_D and H are almost the same, for all ℓ. The difference between H_L and H_D is slight except for small ℓ because the distribution we assumed is unimodal throughout.

Fig. 10 shows the simple probability distributions for (a) the original message, (b) the reduced signal from linear prediction, and (c) the reduced signal from the digrammer.

VARIABLE DELAY AND OTHER PROBLEMS

We have seen in the last two sections how it is possible to convert a message for which $H \ll H_0$ as a result primarily of intersymbol correlation, into a reduced signal for which $H \ll H_0$ as a result primarily of a highly peaked probability distribution in the individual symbols (i.e. one for which $H_1 \rightarrow H$). Since the operations are reversible, the true information rate, H, is preserved. In the original signal it was the *conditional* distributions which were peaked, while the simple distribution was relatively flat. In the reduced signal the *simple* distribution is peaked.

The result is that whereas a Shannon-Fano code would only have been effective on the original message if applied to blocks two or more symbols in length (and then it would ignore correlation between blocks), in the reduced signal the code will be effective on a symbol to symbol basis.

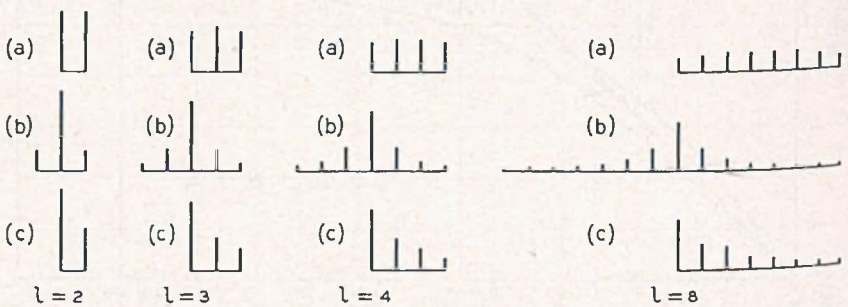

Fig. 10—Probability distributions: (a) Original, (b) After linear modal prediction, (c) After digramming.

The encoding of the reduced signal into binary digits presents no theoretical difficulties. A PCM type coder tube[4] with the appropriate Shannon-Fano groups built into it is all that is needed. The biggest practical complication arises out of the fact that the code groups are of different length. Some messages, such as written text, can be fed into the system as fast as it can handle them. The transmission time will then vary with the message complexity. Others, such as television are generated and must be accepted and delivered at a constant rate. One solution is then to take the binary digits in big and little batches as they come from the coder and store the surplus in a sort of pulse "surge tank" before they are sent over the channel at a regular rate. At the receiver, a similar sort of storage register is necessary as the pulses arrive over the channel at a regular rate and are used by the decoder at a varying rate. Devices which will perform this variable delay function satisfactorily for signals with relatively slow sampling frequency are available, and as the art progresses there is every reason to believe that high speed sampled signals like television can be handled also.

It will be noticed that the digramming or prediction operation, while it involves memory, does not introduce appreciable transmission delay. Each symbol of the reduced signal appears the moment the corresponding message sample is applied. The total transmission delay required for statistical coding thus depends upon how much variation is required in the variable delay units. This in turn depends upon the degree of stationarity in the "local information rate" of the message. For example, in television, if each line could be described (by the n-grammer and subsequent coder) in the same total number of binary digits, then the total delay variation and total delay would be less than one line time. Since this is not true, we either must have enough channel capacity to send in one line time the number of digits corresponding to the "worst" line, or enough variable delay to average the existing rate over many lines.

Probably the most practical solution is to provide sufficient channel capacity and variable delay to take care of all but a small fraction of the possible message sequences. Then when an unusual stretch of message continues long enough for the variable delay to be nearly all used up, the system should fail in some relatively harmless way. In television, the sampling rate could be momentarily reduced, for example. This would degrade the resolution in rare situations, but a small amount of this could be tolerated in return for transmission savings.

If long blocks of the message are efficiently encoded as a group, then an error in transmission may cause the whole block to be reproduced

incorrectly. If n-gramming or prediction is used, then an error in transmission will cause the receiver to function improperly not only for that symbol, but its further n-gram decoding or prediction will also be disturbed. Thus errors of transmission are either spread over definite blocks, or propagate for a considerable time rather than being confined to the particular symbols sent in error. In fact, if the encoding were completely efficient, all received sequences would be possible messages, and a single error could convert the received message from the proper one into a completely different but possible one. With *no* redundancy there is no way to recognize an error. It is for these reasons that we have assumed a rugged (quantized) channel. In view of the eight to ten db more average power required in a quantized channel to achieve the same channel capacity as an ideal channel of the same bandwidth, considerable statistical saving must be possible before statistical coding may be warranted. This initial handicap of course does not apply to channels already designed to work on a digital basis for other reasons. Lastly, the use of error correcting codes[5] is a possibility. In these codes a small amount of redundancy is introduced in a particularly efficient fashion. As a result, a certain frequency of transmission errors can be tolerated without causing errors in the reproduced message.

REFERENCES

1. Oliver, Pierce, and Shannon, "The Philosophy of PCM," *Proc. Inst. Radio Engrs.*, Nov. 1948.
2. C. E. Shannon, "A Mathematical Theory of Communication," *Bell System Tech. J.*, July and Oct. 1948; Shannon and Weaver, "The Mathematical Theory of Communication," University of Illinois Press, 1949.
3. C. E. Shannon, "Prediction and the Entropy of Printed English," *Bell System Tech. J.*, Jan. 1951.
4. R. W. Sears, "Electron Beam Deflection Tube for Pulse Code Modulation," *Bell System Tech. J.*, Jan. 1948; W. M. Goodall, "Television by Pulse Code Modulation," *Bell System Tech. J.*, Jan. 1951.
5. R. W. Hamming, "Error Detecting and Error Correcting Codes," *Bell System Tech. J.*, Apr. 1950.

Statistics of Television Signals

By E. R. KRETZMER

(Manuscript received February 28, 1952)

Measurements have been made of some basic statistical quantities characterizing picture signals. These include various amplitude distributions, autocorrelation, and correlation among successive frames. The methods of measurement are described, and the results are used to estimate the amount by which the channel capacity required for television transmission may be reduced through exploitation of the statistics measured.

INTRODUCTION

One of the teachings of information theory is that most communication signals convey information at a rate well below the capacity of the channels provided for them. The excess capacity is required to accommodate the redundancy, or repeated information, which the signals contain in addition to the actual information. Removal of some of this redundancy would reduce the channel capacity required for transmission, thus opening the way for possible bandwidth reduction. In order to remove redundancy, one must first understand it; the amount and nature of the redundancy can be completely defined in terms of various statistical parameters characterizing the signal.

It has been pointed out that the existence of redundancy is particularly evident in the case of television; moreover, its elimination is highly desirable because of the large bandwith presently required for transmission. Evidence of redundancy is found in the subject matter of television—the average scene or picture. Knowing part of a picture, one can generally draw certain inferences about the remainder; or, knowing a sequence of frames, one can, on the average, make a good guess or prediction about the next frame. In either case, knowledge of the past removes uncertainty as to the future, leaving less actual information to be transmitted.

Another way of looking at this is to visualize the picture as an array of approximately 210,000 dots, 500 vertically, 420 horizontally, corresponding, respectively, to the 500 scanning lines and 420 resolvable

picture elements per line of the standard television raster. Each dot can have, say, 100 distinguishable brightness values in a good-quality picture. The number of possible combinations is therefore approximately $100^{210,000}$ or $10^{420,000}$. At the usual rate of 30 frames per second it would take approximately $10^{419,991}$ years to transmit all these "pictures," which our present television system is fully prepared to transmit! The vast majority of these "pictures" will, of course, never be transmitted in this age because the average picture statistics virtually preclude the possiblity of their occurrence.

If all of the redundancy alluded to in the preceding paragraph were to be expressed in terms of statistics, the array of data would be staggering.* Redundancy encompassing even a small part of a single frame implies statistics of enormously high order because of the large number of possible past histories. The initial attention should therefore be focused on local redundancy, encompassing only a few adjoining picture elements. Accordingly, measurements have been made of the following statistical quantities.

1. *Simple probability distribution of signal amplitudes corresponding to picture brightness.* This encompasses only a single picture element, revealing the relative probabilities of this or any element's assuming the various possible brightness values, in the absence of any past-history information.

2. *Simple probability distribution of error amplitudes resulting from linear prediction of television signals.* Only the simplest type of linear prediction is considered here, so-called previous-value prediction, which predicts each picture element to have the same brightness value as the preceding one. The prediction error signal is simply the difference between the picture signal and a replica delayed by one Nyquist interval (one-half the reciprocal bandwidth or the time interval corresponding to the spacing between picture elements). The distribution of this error signal encompasses two picture elements (past history of one element) and therefore is a condensed version of the family of first-order joint probability distributions.

3. *Autocorrelation of typical pictures.* This statistical quantity is an even more streamlined version of various families of different-order joint probability distributions. Each family corresponds to just a single point on the autocorrelation curve; the ordinates of the curve represent the average correlation between picture elements spaced by various

* Complete statistics extending, say, over one frame period, would comprise one conditional probability distribution per picture element for each possible past history. With the approximate figures cited above, the number of distribution curves (many of which would be similar) is $210,000 \times 10^{419,999}$ or $10^{420,004.3}$.

distances. This correlation, say, between horizontally adjoining elements is simply the average product of the two brightness values of each pair of neighbors, relative to the average square of all brightness values.

The three quantities enumerated above contain a great deal of statistics in very compact form, but these statistics are essentially of a local and linear nature. They do not include the bulk of the large-scale redundancy, which is of a far-flung and nonlinear nature.

AUTOCORRELATION

For a function of time, f(t), the autocorrelation can be expressed as

$$\phi(\tau) = \overline{f(t)\, f(t + \tau)} \tag{1}$$

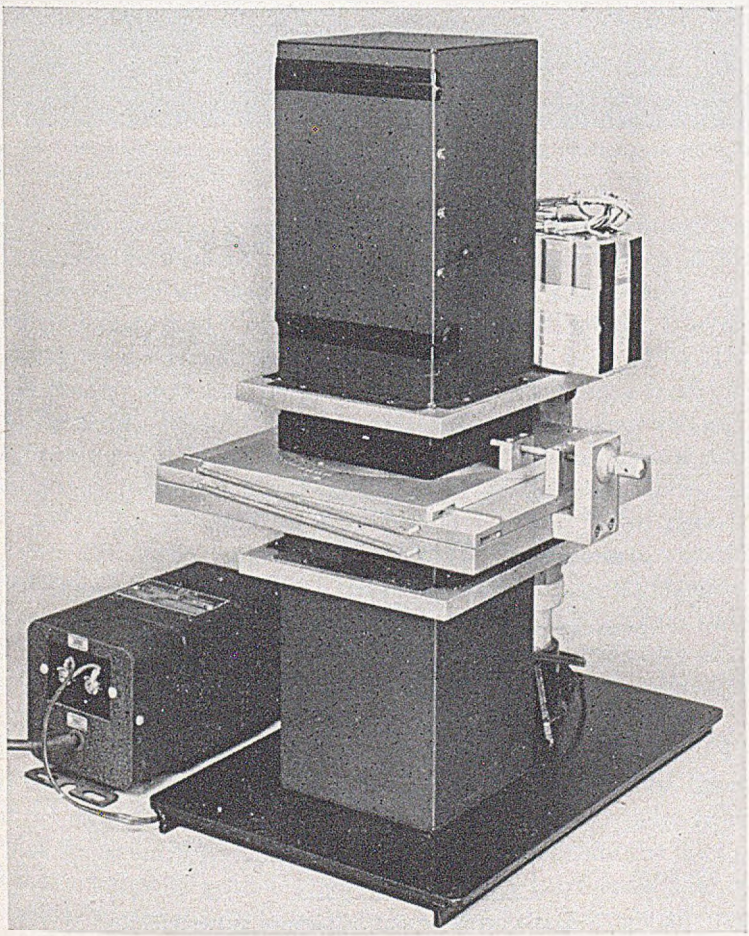

Fig. 1—Picture autocorrelator.

averaged over all time, for various values of the time shift τ. In the case of a picture transparency, the optical transmission is a function of two-dimensional space, expressible in polar coordinates as $T(s/\phi)$, and the autocorrelation can be expressed in analogous fashion. The time variable t is replaced by the space coordinate s/ϕ, and the correlation time shift τ is replaced by a space shift $\Delta s/\theta$, so that the new expression is

$$\phi(\Delta s/\theta) = \overline{T(s/\theta)\, T(s/\theta + \Delta s/\theta)}, \tag{2}$$

averaged over as much area as practicable. This space-domain autocorrelation is much easier to measure than the time-domain autocorrelation. We need merely measure the relative optical transmission of two identical cascaded transparencies, shifted from register by a variable

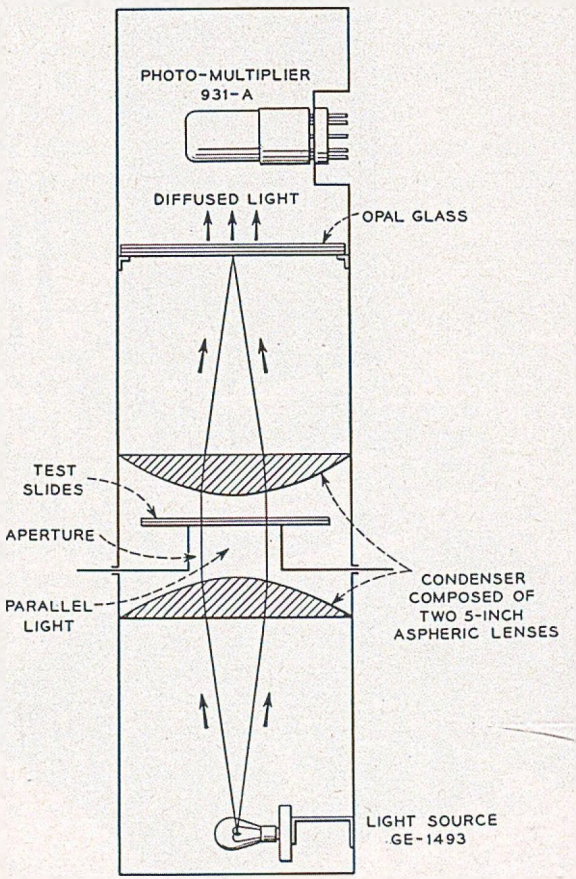

Fig. 2—Basic arrangement of picture autocorrelator.

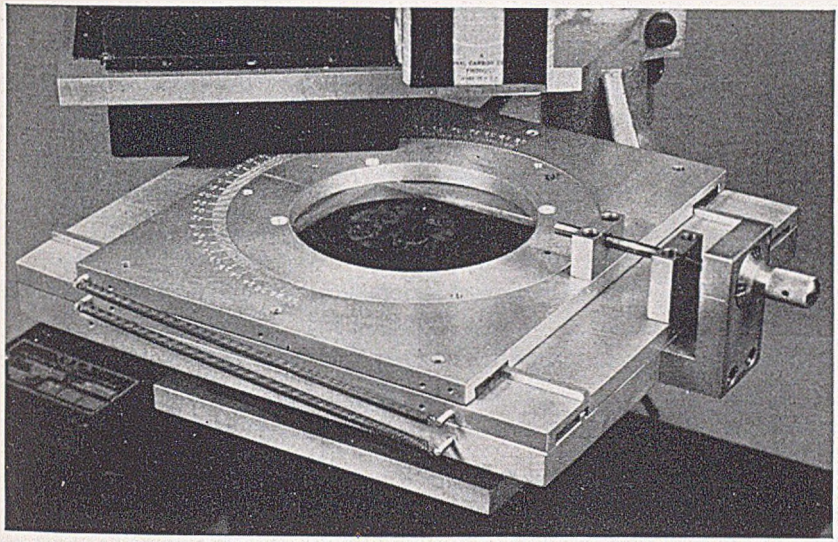

Fig. 3—Close-up view of slide holding assembly and shifting mechanism of picture autocorrelator.

amount. The averaging process is inherent in such a measurement.

The apparatus used to measure autocorrelation is shown in Figs. 1 and 2. The chamber at the bottom contains a light source of very constant intensity and a convex lens to collimate the light. The middle part, made of accurately machined aluminum, holds the two identical slides of the picture under test, and an aperture exposing a large circular area of the slides. The top chamber contains a collector lens and a photomultiplier tube which (on a microammeter not shown) gives a sensitive indication of the total light transmitted through the slides. Fig. 3 shows a close-up view of the slide-holding assembly. Two close-fitting graduated aluminum rings permit accurately determined rotation of both slides or one slide, and the micrometer drive permits translational displacements measurable to within one mil (moving the two slides by equal and opposite amounts); the separation between picture elements is approximately 7.5 mils horizontally and 5 mils vertically (for the $2\frac{1}{2}''$ by $3\frac{1}{4}''$ slide size used).

The light transmission is always a maximum when the two slides are in precise register ($\Delta s = 0$). For large shifts the transmission fluctuates about a nonzero asymptote. The nonzero asymptote results from the fact that the average transmission is always positive, and the fluctuation from the fact that large displacements introduce substantial amounts of new picture material into the aperture. Since these components tend to

obscure the correlation effects, it is useful to make additional measurements which enable us to subtract them out completely. This leaves us with a 'pure' autocorrelation $A(\Delta s/\underline{\theta})$, which is then normalized so as to have a peak value of unity. It is given by

$$A(\Delta s/\underline{\theta}) = \frac{T_2\left(\pm\frac{\Delta s}{2}/\underline{\theta}\right) - T_1\left(\frac{\Delta s}{2}/\underline{\theta}\right) T_1\left(-\frac{\Delta s}{2}/\underline{\theta}\right)}{T_2(0) - T_1^2(0)}, \quad (3)$$

where $T_2\left(\frac{\pm\Delta s}{2}/\underline{\theta}\right)$ is the transmission through the two cascaded slides shifted by equal and opposite amounts $\frac{\Delta s}{2}$ at an angle θ with the horizontal, and $T_1\left(\frac{\Delta s}{2}/\underline{\theta}\right)$ is the transmission of a single slide with displacement $\frac{\Delta s}{2}$ at the same angle θ.

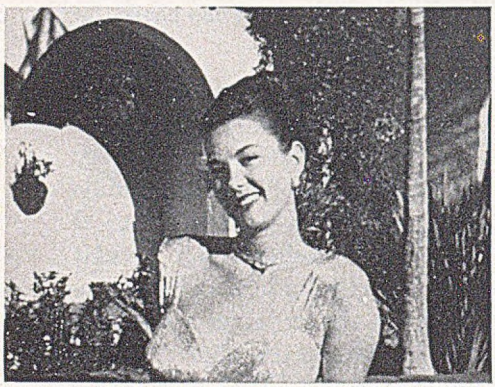

SCENE A

SCENE B

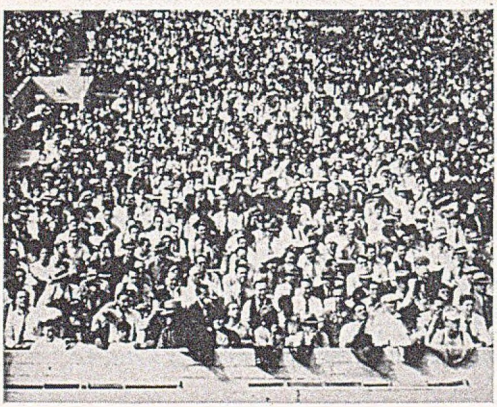

SCENE C

SCENE D

Fig. 4—Test pictures whose statistics are included in this article.

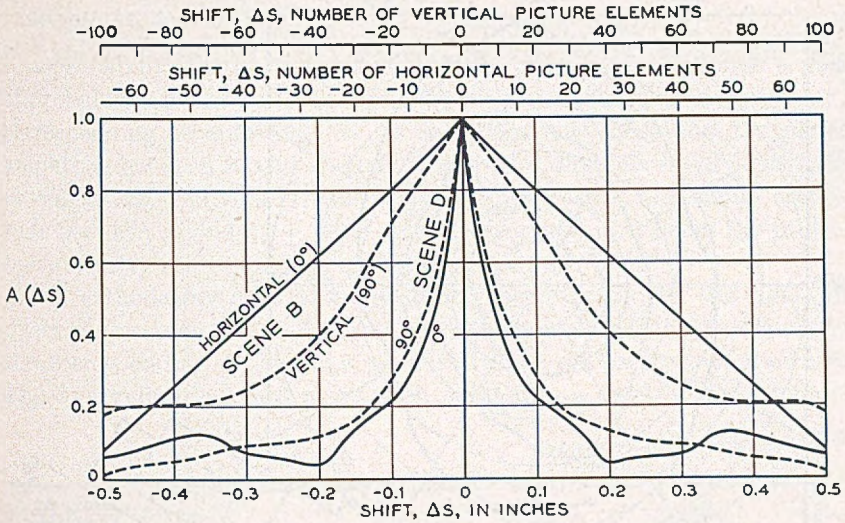

Fig. 5—Plots of autocorrelation in horizontal and vertical directions for two pictures.

Fig. 4 shows some pictures for which autocorrelation measurements have been made. The results can be presented in the various ways shown in Figs. 5, 6, and 7. Fig. 5 shows conventional plots of A versus Δs in the horizontal and vertical directions. Scene B is seen to have more correlation than Scene D, and curve shapes range from remarkably linear to somewhat like exponential. Fig. 6, giving contours of constant autocorrelation, brings out the variation with the angle θ. Scene A happens to have its greatest correlation in the vertical direction, but that was not found to be a general rule by any means; Scene B, for example, has its greatest correlation in the horizontal direction. No preferred directions appear to exist in general. In Fig. 7 attention is focused on the more local correlation, for small values of Δs. The average correlation among horizontally adjoining picture elements, designated by A_{10}, is seen to be approximately 0.99 for Scene B and only 0.75 for Scene C. A_{20} denotes the correlation for a horizontal spacing of two picture elements while A_{01} denotes the correlation among vertically adjoining picture elements.

It should be pointed out that the pictures which gave the above results were not band-limited to the standard 4-mc resolution. However, before the results were used quantitatively, the proper band limitation was applied mathematically. This has the effect of rounding off the peaks of the curves, decreasing the autocorrelation drop within the first Nyquist interval by up to approximately 24 per cent.

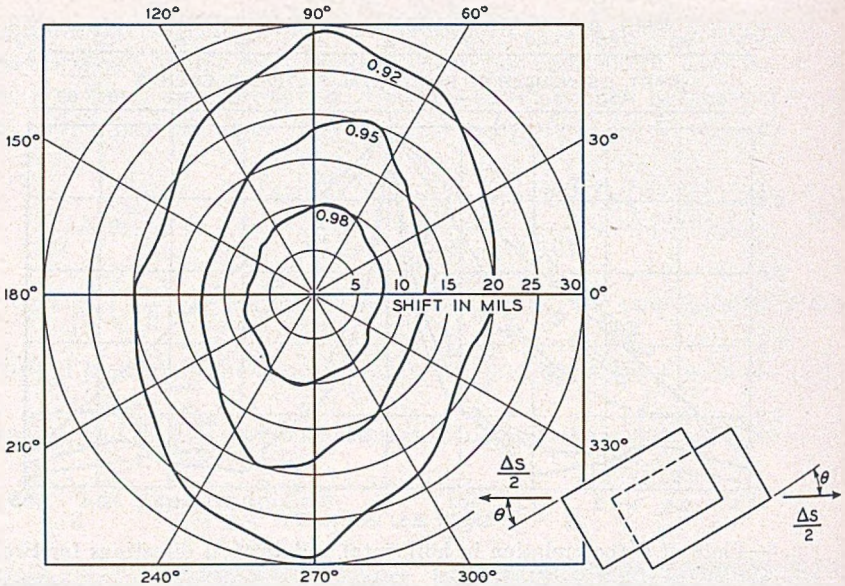

Fig. 6—Contours of constant autocorrelation for Scene A. In general there are no preferred directions of correlation.

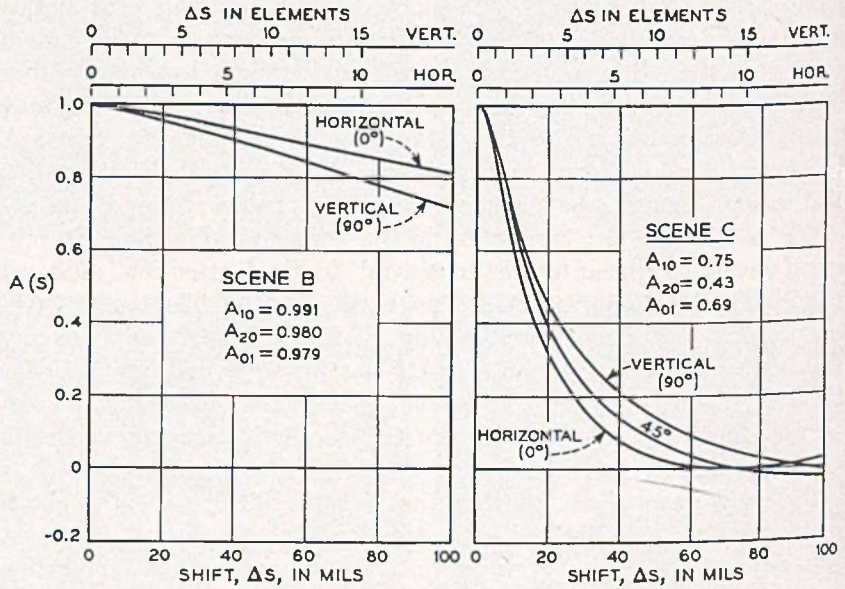

Fig. 7—Plots of autocorrelation for small shifts. A_{10} is the autocorrelation for a shift of one horizontal elemental distance, A_{20} for two horizontal elemental distances, and A_{01} for one vertical elemental distance. Alternatively A_{10} may be described as the average correlation between horizontally adjoining elements, etc.

PROBABILITY DISTRIBUTIONS

A probability distribution of amplitudes is generally shown as a plot of probability density versus signal amplitude. Probability density, say, corresponding to amplitude x_1, is the probability of finding the signal amplitude between x_1 and $x_1 + dx$, divided by the differential amplitude increment dx. Conversely, the probability of finding the signal amplitude between x_1 and $x_1 + dx$ is given by $p(x_1)dx$, $p(x)$ being the probability density corresponding to amplitude x.

If a cathode-ray spot is deflected, say horizontally, by the signal in question, its average dwell time at any point is directly proportional to the corresponding probability density. In the optical system shown in Fig. 8, a cylindrical lens maps each point into a vertical line which is

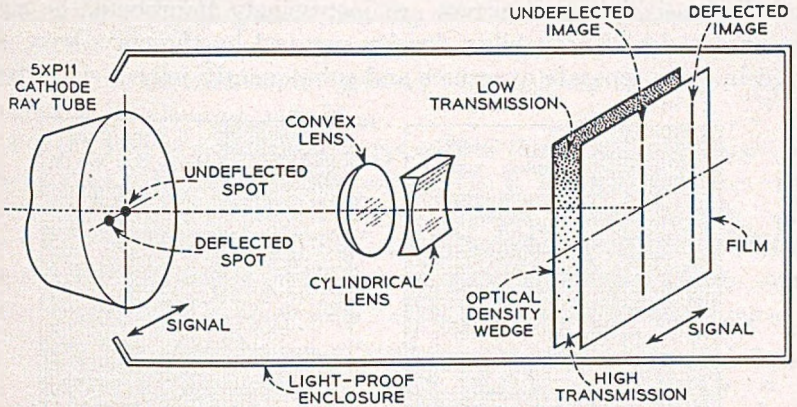

Fig. 8—Basic arrangement of probabiloscope.

then tapered in intensity by an optical density wedge before reaching a high-contrast photographic film. Depending on the dwell time at any amplitude level, the corresponding tapered line has enough average intensity to blacken the film up to a certain level. This level is proportional to log $p(x)$, since the density wedge is tapered exponentially so that the intensity of each tapered line of light reaching the film diminishes, say, by a factor of ten for each inch we travel up the line. The film in effect traces out a contour of constant exposure.

Two or three iterated photographic printings increase the effective gamma sufficiently to yield a contour of ample sharpness. This contour is then changed to a sharp line by a simple dark room trick: while the film is in the development tray, already fully developed, it is momentarily exposed to light. The blackened portion of the film is unaffected, the clear portion is fully blackened, while the transition contour, being partly opaque, is not fully blackened. By printing from this film we then

obtain a well-defined black-on-white curve of $p(x)$ versus x on a logarithmic probability scale. The logarithmic scale has the advantage of making the curve shape independent of exposure length and giving uniform relative accuracy over the entire range.

Fig. 9 shows some typical results obtained by means of the "probabiloscope." The two small curves are distributions of two different still pictures. The left-hand end corresponds to black, the right-hand end to peak white; the blanking intervals (slightly blacker than black) cause the peaks at the extreme left. (The signals did not contain any synchronizing pulses.) The tall and slender curve at the right of Fig. 9 is the distribution of errors resulting from previous-value prediction of one of the pictures in Fig. 4. The peak corresponds to zero error which is seen to be most probable, as it should be if the prediction criterion is good. Increasingly larger errors are increasingly improbable or rare. The six decades of probability density spanned by the curve were obtained in three separate exposures and subsequently joined, since stray

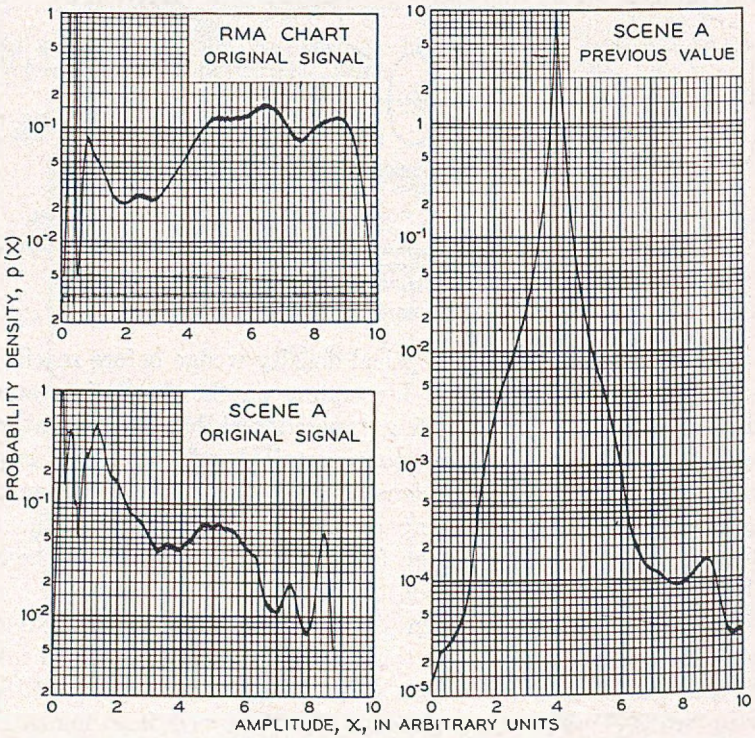

Fig. 9—Typical probability distributions as obtained from the probabiloscope. Curves at left are for video signals; right-hand curve is for difference between video signal and delayed replica.

light limits the useful range of the probabiloscope to approximately two decades. In obtaining those sections of the curve corresponding to the few and far-between large errors, a long exposure was used and the cathode-ray beam was blanked whenever passing through the range of zero or small errors. The vertical scale on all curves is determined solely by the density taper of the optical density wedge. If this scale is to represent true probability density, instead of a proportional quantity, it should be shifted up or down so as to make the area under the curve equal to unity.

APPLICATION OF RESULTS

The statistics measured can be put to various uses, such as in the design of better predicting or coding schemes. The most interesting application is probably in estimating the reduction in channel capacity which the measured statistics show to be theoretically possible. In other words, the results can give us various lower bounds to the redundancy of television signals.

For the sake of illustration, suppose that the signal is quantized into 64 amplitude levels. An ordinary television channel assumes all 64 levels to be equally likely, hence is prepared to accommodate $\log_2 64$ or 6 bits per sample. But the simple amplitude distribution of the signal is not flat, so that all 64 levels are *not* equally likely. The maximum possible associated average information content per sample is given by

$$H_{\max} = \sum_{i}^{64} p_i \log p_i , \tag{4}$$

where p_i is the simple probability of the signal's falling into the ith level. Since the 64 p_i's are unequal, $H_{\max}$ is necessarily less than 6 bits. For all available data the average value of $H_{\max}$ turns out to be approximately 5 bits, indicating a one-bit redundancy. The latter figure is essentially independent of quantization.

The prediction error signal still contains all the useful picture information. The maximum possible information content per sample (maximum in that all samples are assumed to be completely independent) is still given by (4) but in this case the 64 values of p_i are obtained from the peaked error distribution. The average* result from all available data turns out to be approximately 3.4 bits below the 6-bit ceiling, show-

* This average was computed by averaging the various redundancy values obtained for the individual pictures, rather than averaging all statistical data and then finding one corresponding average redundancy. The average computed here is more favorable and can be realized only if optimum coding is performed on a short-term basis rather than on the basis of one set of long-term statistics.

ing that the original signal must have contained at least 3.4 bits of redundancy.

The autocorrelation can also furnish a lower bound to the redundancy, as has been pointed out by P. Elias in his Letter to the Editor of the *Proceedings of the I.R.E.* for July, 1951. If, for example, the correlation A_{10}, between horizontally adjoining picture elements, is high, the corresponding lower-bound redundancy is very roughly equal to

$$R \approx -\tfrac{1}{2} \log_2 (1 - A_{10}) \text{ bits/sample.} \tag{5}$$

Alternatively, taking the Fourier transform of the autocorrelation yields the power spectrum $P(f)$, from which we can find the lower-bound redundancy through the relation

$$R = \frac{1}{2W} \int_0^W \log_2 P(f)\, df + \tfrac{1}{2} \log_2 W + \log_2 K \text{ bits/sample,} \tag{6}$$

where W = bandwidth in cps, and $\dfrac{1}{K} = \displaystyle\int_0^W P(f)\, df.$

Using either method, one obtains approximately 2.4 bits for the average* of the available data. This is an approximate bound, in that it applies strictly only to functions having gaussian amplitude distributions.

Suppose, then, that we have exposed an average redundancy of at least 3 bits per sample. This means a potential 3-bit reduction in the channel capacity required for television transmission. In a 6-bit system (64 amplitude levels) this means a 50 per cent reduction, and hence a potential halving of the bandwidth with the aid of an ideal coding scheme. It is true that the decorrelated signal is somewhat "frail," i.e., vulnerable to interference, so that it might be desirable to use a "rugged" system of the PCM variety for transmission. Thus, if a Shannon-Fano code were used, the 3-bit decorrelation should enable us to send television by an average of 3 on-off pulses per picture sample rather than 6. This represents a two-to-one saving over the usual PCM bandwidth. More spectacular reductions are likely to be achievable only by tapping the large-scale redundancies mentioned earlier.

FRAME-TO-FRAME CORRELATION

There is, of course, a great deal of interest in the possibility of utilizing the similarity between successive frames. Accordingly, adjacent-frame

* See previous footnote.

correlation was measured for two typical motion-picture films, by means of the apparatus described in the section on autocorrelation.* The results were 0.80 and 0.86, after correction for the 4-mc bandwidth limitation. This means that "previous-frame" prediction can remove only slightly more than one bit of redundancy per sample. More complicated schemes would presumably be more successful in taking advantage of the large frame-to-frame redundancy which undoubtedly exists.

ACKNOWLEDGMENT

Many of the ideas expressed in this paper are due to B. M. Oliver, whose resourcefulness is hereby gratefully acknowledged.

* The expression used in evaluating the correlation between frame 1 and frame 2 (any two frames) is

$$C_{12} = \frac{T_{12} - T_1^2}{T_{11} - T_1^2}, \tag{7}$$

where T_{12} is the optical transmission of frames 1 and 2 in cascade, T_1 is the average of the individual transmission of frames 1 and 2, and T_{11} is the average of the transmissions of two cascaded slides of frame 1 and two cascaded slides of frame 2, respectively. In all cascade transmission measurements, the two frames must be in precise register.

Experiments with Linear Prediction in Television

By C. W. HARRISON

(Manuscript received February 28, 1952)

The correlation present in a signal makes possible the prediction of the future of the signal in terms of the past and present. If the method used for prediction makes full use of the entire pertinent past, then the error signal—the difference between the actual and the predicted signal—will be a completely random wave of lower power than the original signal but containing all the information of the original.

One method of prediction, which does not make full use of the past, but which is nevertheless remarkably effective with certain signals and also appealing because of its relative simplicity, is linear prediction. Here the prediction for the next signal sample is simply the sum of previous signal samples each multiplied by an appropriate weighting factor. The best values for the weighting coefficients depend upon the statistics of the signal, but once they have been determined the prediction may be done with relatively simple apparatus.

This paper describes the apparatus used for some experiments on linear prediction of television signals, and describes the results obtained to date.

INTRODUCTION

Linear prediction is perhaps the most expedient elementary means of removing first order correlation in a television message. Before discussing the advantages and disadvantages of linear prediction, it might be well to consider what is generally meant by correlation in a television picture and why it should be removed.

Almost every picture that has recognizable features contains both linear and non-linear correlation. Each type of correlation helps in identifying one picture from another; however, linear prediction is only effective in removing linear correlation, and for this reason, future references to correlation will refer only to its linear properties. With television, a signal is obtained as the result of scanning; hence, the cor-

relation is evident in both space and time. Briefly, correlation is that relation which the "next" elemental part of the signal has with its past.

To leave correlation in a message is to be redundant, and this effectively loads the transmission medium with a lot of excess "words" not necessary to the description of the picture at the receiving end. It is then more "efficient" to send only the information necessary to identify the picture, and to restore the redundancy at the receiver.

EFFICIENT TRANSMISSION

The more *efficient* we are in sending pictures over a given transmission line, the more alarmed we become at the increasing amount of equipment that is required at the transmitting and receiving terminals. Certainly the design will be a compromise between the complexity of apparatus and the efficiency achieved. The ingenuity of engineers will be taxed along these lines for years to come; however basically, the general form of these systems will be similar to that shown in Fig. 1. Although not always separable, four essential operations are required-namely, decorrelating, encoding, decoding and correlating. The transmitting decorrelator and the encoder encompass the principal design problems, since the decoder and correlator at the receiving end perform the reverse operations which interpret the code and add in the redundancy that was removed.

Decorrelation involves prediction, and as the predictors are more nearly made to predict the future of the signal, the more the output signal from the decorrelator resembles random noise. The essential picture information is still present, which means that our original picture signal can be obtained at the receiving end without theoretical degradation. The basic job of the encoder is to match the picture information out of the decorrelator to the channel over which it is to be transmitted. There are several encoding operations. The first concerns the rate of information into the encoder, and that required out of it. In the case of television, there are flat, highly correlated areas as well as areas containing more concentrated detail. This means that the information

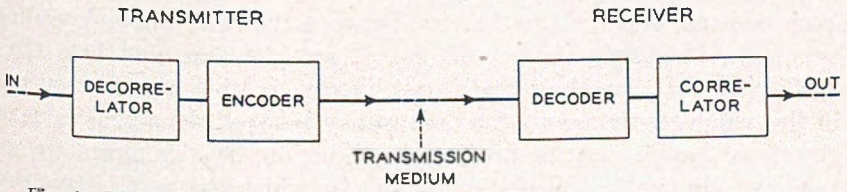

Fig. 1—Block diagram of an efficient transmission system employing reversible decorrelating and encoding means.

rate varies when the picture is scanned at the conventional uniform scanning rate. The output of the encoder feeds a transmission line that has a definite channel capacity, and if maximum efficiency is to be obtained from this transmission medium, then the rate of information into it must be held relatively uniform at a value near the channel capacity. It is the job of the encoder to take the varying rate of information from the decorrelator and feed it to the channel at a constant rate. At the receiving end, the decoder must take the constant rate of information and deliver it to the correlator at the variable rate as originally fed into the transmitter's encoder. Thus, to perform this task, a variable or elastic delay to run ahead or behind, depending on the information content of the picture being scanned, is an important part of the encoder. Over a long period of time, the variable delay would average out to some fixed value. This variable delay must never run out, even when the detail is concentrated. There are instances when this condition could not be met, such as an extended reproduction of a snow storm; however, with good design the system should fail "safe"—a slight degradation of picture quality. This condition can be made infrequent enough to cause little concern.

The encoder design must also account for noise as well as bandwidth of the channel and must consider the ultimate effect of an error that may be introduced by noise along the transmission line. As more redundancy is removed to get at the "essence" of the picture signal, the more important it is to guard this "essence," as mistakes presented to the receiver will propagate themselves longer in the absence of correlation. Errors can be minimized by rugged systems of modulation such as PCM, where the signal-to-noise ratio of the transmission line determines the base of the PCM system selected. In any event, the encoder must send the information so that the effect of errors will not appreciably disturb the picture.

DECORRELATION AND LINEAR PREDICTION

Fig. 2 illustrates, in a general way, a means of decorrelating the signal, $S_1(t)$. For purposes of explanation, the encoder and decoder have been omitted, and the transmission between the receiving and sending terminals, idealized. The predictors, P, are identical, and base their prediction, $S_p(t)$, on the signal's past history. In this way, the output of the computer represents the discrepancy between the actual value of the signal sample and the predictor's prediction. By this means we are sending only our mistakes—the amount by which the next picture element surprises us. For example, if the computer is so designed that it

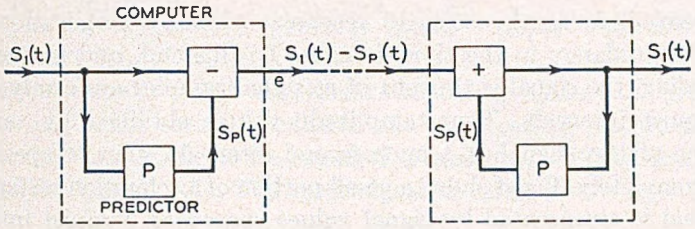

Fig. 2—Decorrelator and correlator showing reversible nature of this method of removing redundancy.

bases its prediction on the "previous frame," and we are transmitting a "still," there will be no surprises after the first frame and consequently no output signal. Certainly it is redundant to send the same picture more than once.

Linear prediction provides an easily instrumented means of removing redundancy. With linear prediction the next signal sample is simply the sum of the previous signal samples, each multiplied by an appropriate weighting factor. The best values for these weighting coefficients depend on the statistics of the signal.

Fig. 3 is a block diagram of a decorrelator employing linear prediction. The delayed versions of the input signal can be obtained from taps along the delay line. The weighting coefficients for each of the delayed signals are selected by loss in their respective paths as shown by the amplitude controls. The polarity of each signal can be determined by the switches. The output is simply the sum of these weighted signals.

If we consider the signal on a continuous basis (not quantized or sampled), linear predictors can be characterized as ordinary linear filters used to predistort the frequency spectrum of the signal. As such, they can be designed in the frequency or time domain. However as will

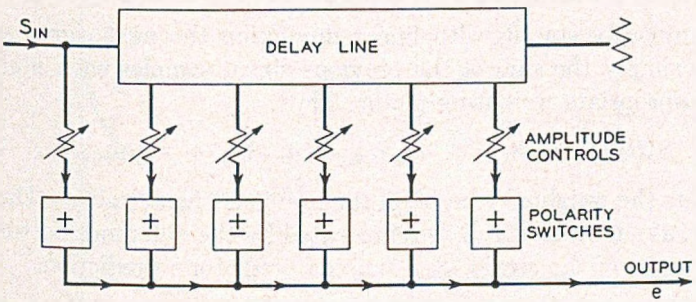

Fig. 3—General block diagram of decorrelator employing linear prediction. Linear prediction bases its prediction on the weighted sum of previous signal samples.

be shown, it is much easier to recognize circuit configurations that reduce redundancy in the time domain. To this end, and for purposes of encoding, the signal is thought of as signal samples uniformly spaced at Nyquist intervals. Thus, amplitude values obtained by sampling a 4.0 mc picture signal at $\frac{1}{8}$ microsecond intervals serve to specify the signal completely. Fig. 4 shows a small portion of a television raster where the signal is represented by signal values spaced at Nyquist intervals, τ. The coordinates shown are designated with respect to the "present value" of the signal, $S_{0,0}$. The positive coordinate directions are shown by the arrows. The past is represented by positive coordinates—the future by negative coordinates. In this way, the previous value of the signal

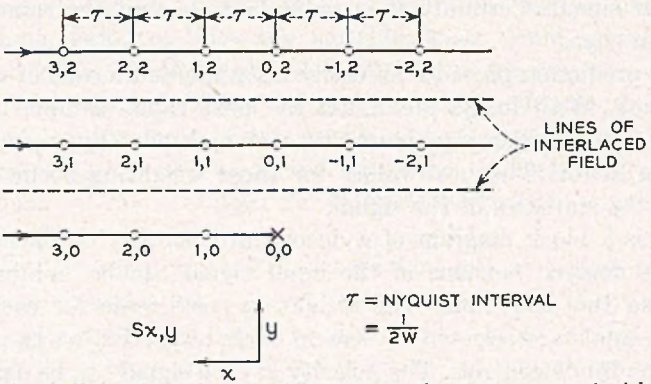

Fig. 4—A small portion of a television raster showing geometrical location of signal samples with relation to the "present value" of the signal, $S_{0,0}$.

taken one Nuquist interval before $S_{0,0}$ is designated by $S_{1,0}$ – the previous line samples by $S_{0,1}$, etc.

METHODS OF LINEAR PREDICTION

As previously stated, with linear prediction the next signal sample, $S_p(t)$, is simply the sum of the previous signal samples each multiplied by an appropriate weighting factor. Thus,

$$S_p(t) = a_{1,0}S_{1,0} + a_{2,0}S_{2,0} + a_{3,0}S_{3,0} + \cdots a_{m,n}S_{m,n}$$

represents the weighted sum of all the previous signal values. The error signal, e, as shown in Fig. 2, is represented by the difference between the present vaue of the signal, $S_{0,0}$ and the predictor's prediction.

$$e = S_{0,0} - S_p(t)$$

There are several specific types of linear prediction that deserve fur-

ther explanation—namely, "previous value," "slope," "previous line," "planar" and "circular."

"*Previous value*" prediction is illustrated in Fig. 5. Here the prediction is taken to be the signal amplitude of the preceding picture element. The previous amplitude of the signal, $S_{1,0}$ is subtracted from the present value of the signal, $S_{0,0}$. The error signal is given as

$$e = S_{0,0} - S_{1,0}$$

The filter characteristic can be expressed as

$$F(\omega) = \left(2 \sin \frac{\omega\tau}{2}\right) \epsilon^{i\left(\frac{\pi}{2} - \frac{\omega\tau}{2}\right)}$$

This method of prediction proves to be rather effective in reducing the average power for most television pictures. The expression for the filter characteristic given above shows that the peak amplitude can be twice that of the original signal.

"*Slope*" prediction is illustrated by Fig. 6. "Slope" prediction is so called because it is equivalent to passing a straight line through the two previous signal values, with the assumption that this line will pass through the next signal value. The predicted signal is given by

$$S_p = 2S_{1,0} - S_{2,0}$$

The frequency and phase characteristic is expressed as

$$F(\omega) = [4 \sin^2 \omega\tau]\epsilon^{i(\pi - \omega\tau)}$$

For this method of prediction, the peak amplitude of the error signal can be as much as four times the peak amplitude of the original signal.

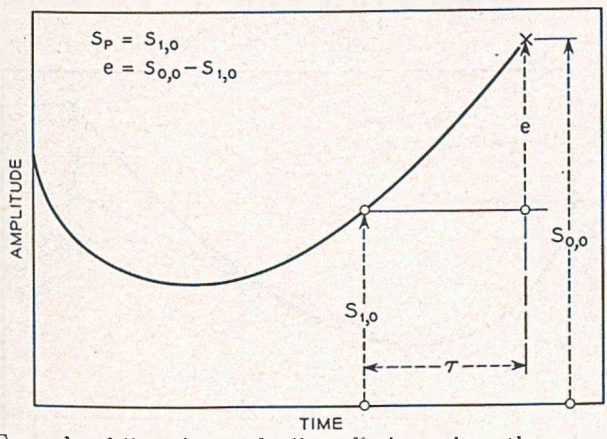

Fig. 5—Example of "previous value" prediction, where the error signal is the difference between the actual value of the signal and the previous value.

It is of interest to mention that "slope" prediction is equivalent to two "previous value" predictors in tandem. Three or more "previous value" predictors in tandem are equivalent to a binomial weighting of the previous values of the signal to form a predicted signal.

For example, the prediction for three "previous value" predictors in tandem is given by

$$S_p = 3S_{1,0} - 3S_{2,0} + S_{3,0}$$

For four "previous value" predictors in tandem

$$S_p = 4S_{1,0} - 6S_{2,0} + 4S_{3,0} - S_{4,0}$$

As can be seen from the above equations, further extension of "previous value" tandem operation results in a heavier weighting of picture elements further and further from the point to be predicted. For most pictures this leads to greater errors.

"*Previous line*" prediction, shown in Fig. 7, would be expected to be similar to previous value prediction, since a picture would presumably have approximately the same correlation vertically as it does horizontally. This would be the case except that our interlaced scanning system makes the previous line signal some 28 per cent further away from $S_{0,0}$ than the closest horizontal sample, $S_{1,0}$. The error signal, e, is given by where T is a line time. The error output has a maximum peak amplitude of twice the input.

$$e = S_{0,0} - S_{0,1}$$

The filter characteristic can be expressed as

$$F(\omega) = \left[2 \sin \frac{\omega T}{2}\right] \epsilon^{i\left(\frac{\pi}{2} - \frac{\omega T}{2}\right)}$$

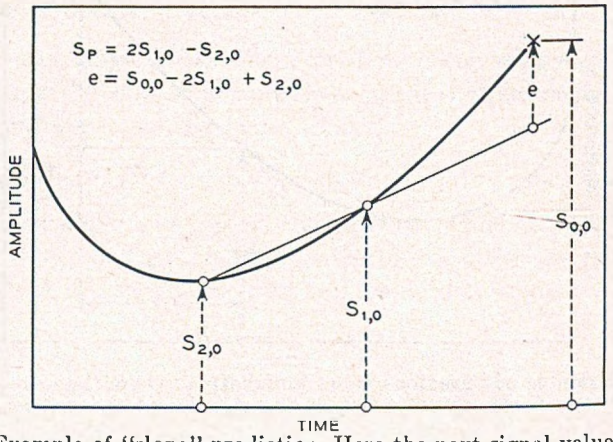

Fig. 6—Example of "slope" prediction. Here the next signal value is assumed to lie on a straight line that intersects the two previous signal values.

"*Planar*" prediction, shown in Fig. 8, is effectively tandem operation of "previous value" and "previous line" prediction. Planar prediction may also be thought of as the value represented by a plane above the present value of the signal when passed through three adjacent signal

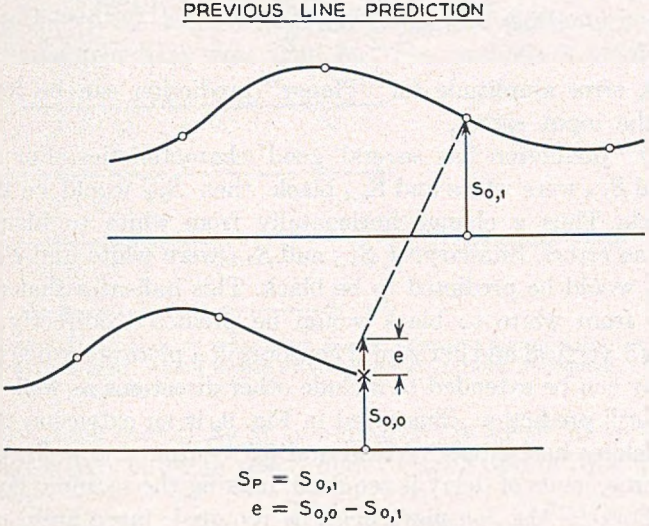

Fig. 7—Example of "previous line" prediction. Here the error signal is the difference between the actual value of the signal and the value of the signal on the line directly above.

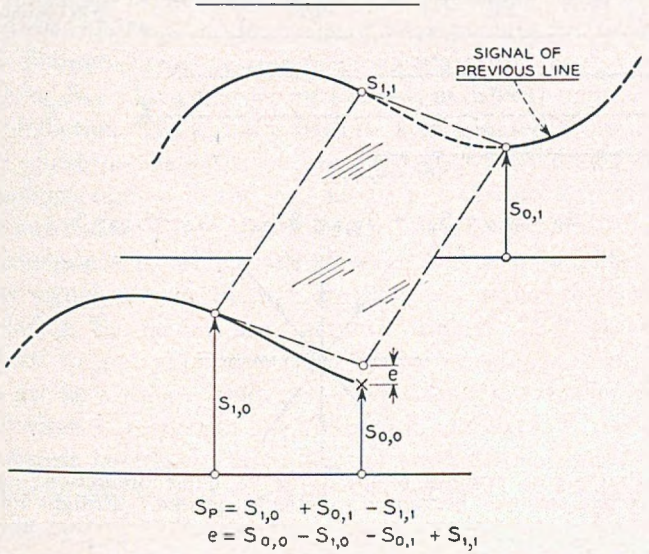

Fig. 8—An example of "planar" prediction. Here the prediction is represented by a plane that has been passed through three adjacent signal values.

values, namely $S_{1,0}$, $S_{0,1}$ and $S_{1,1}$. The predicted signal is given by

$$S_p = S_{1,0} + S_{0,1} - S_{1,1}.$$

The filter characteristic is given by

$$F(\omega) = 4 \sin \frac{\omega\tau}{2} \sin \frac{\omega T}{2} \epsilon^{i\left(\pi - \frac{\omega}{2}(T+\tau)\right)}$$

The peak error amplitude for "Planar" prediction can be four times that of the input signal.

"Planar" prediction has several good characteristics. For example, if $S_{1,1}$ and $S_{1,0}$ were white and $S_{0,1}$ black, then $S_{0,0}$ would be predicted to be black. Thus a change horizontally from white to black would produce no errors. Similary, if $S_{1,1}$ and $S_{0,1}$ were white and $S_{1,0}$ black, then $S_{0,0}$ would be predicted to be black. This indicates that a change vertically from white to black would be predicted correctly. In this manner, all vertical and horizontal contours in a picture are deleted. This philosophy can be extended to include other directions as well.

"Circular" prediction, illustrated in Fig. 9, is an extension of planar, since it deletes horizontal, vertical and 52° contours as well. A total of 190.5 microseconds of delay is required, making the required equipment more elaborate. Also, as more delay is required, more noise is added.

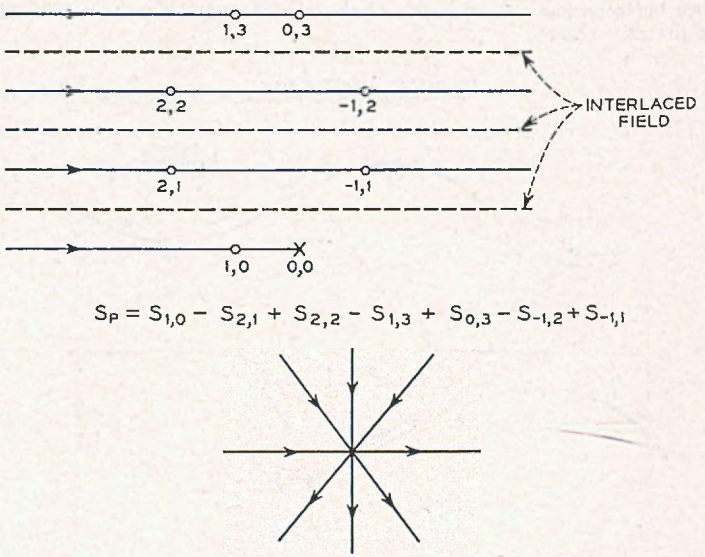

Fig. 9—Past signal samples required for "circular prediction"—a type of prediction which removes horizontal, vertical, and ±52° straight line picture contours.

Therefore, indefinite extension of this straight line contour deleting philosophy is not a paying means of prediction, at least not at the present state of the art of wide band delay lines. Furthermore, the increasing diameter of the circle for extension of circular prediction would decrease its accuracy for finely concentrated detail.

Fig. 10 shows the relative position of picture elements nearest $S_{0,0}$ if a wide band field delay were available. The methods of prediction dis-

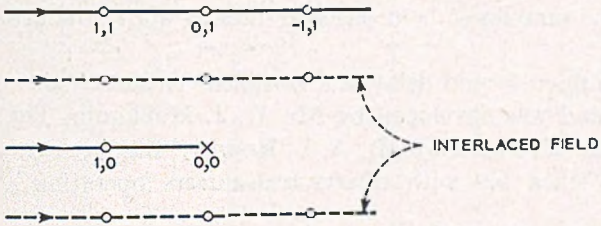

Fig. 10—Small portion of television raster showing signal samples, including those of previous field, which would enable time extrapolation-space interpolation as a method of prediction.

cussed have been essentially an extrapolation in space; however, with a field delay, interpolation in space, and extrapolation in time would also be possible.

EXPERIMENTAL CIRCUITRY

Experimentally, those types of predictors that involve only a few Nyquist intervals of delay are easiest to mechanize. Fig. 11 shows a simplified schematic of a decorrelator that enables an evaluation of linear prediction schemes having error signals given by $e = a_{0,0}S_{0,0} \pm a_{1,0}S_{1,0} \pm a_{2,0}S_{2,0}$. This enables an evaluation of "previous value" and "slope" prediction. The signal is fed into a terminated delay line having taps at Nyquist intervals. Each of these signals is individually attenuated by the potentiometers in the cathode circuit of the cathode followers. Each output is then fed to its respective polarity switch. The D.P.D.T. switch determines to which side of the differential amplifier, V_4, the particular signal is sent. Since more than one signal may require the same polarity, the signals are combined through "L" type resistance attenuators to prevent interaction between signals. The D.P.D.T. switches are so arranged that the other signals are unaffected when a polarity switch is reversed. The differential amplifier, V_4, is a cathode coupled circuit having the advantage of two identical grids which produce opposing effects in the output. The output is then matched to the line by the cathode follower, V_5. In this way we can transmit (1) the

original picture signal with either polarity and any amplitude, (2) the picture signal delayed by one or two Nyquist intervals with either polarity and any amplitude or (3) any linear combination of (1) or (2).

Fig. 12 is a block diagram of the experimental set-up used to investigate prediction methods that involve previous value and previous line samples such as "planar," etc. The input is fed into a manually variable delay having 0.1 Nyquist interval steps. This delay line acts like a vernier for the 63.5 microsecond line delay. Effectively, it enables the previous line samples to be positioned directly above the previous value samples.

The 63.5 microsecond delay is a so-called "acoustic" or "ultrasonic" delay line and was developed by Mr. H. J. McSkimin. The associated circuitry was developed by Mr. A. L. Hopper.* Storage is accomplished by a fused silica bar with quartz transducers operating at a carrier

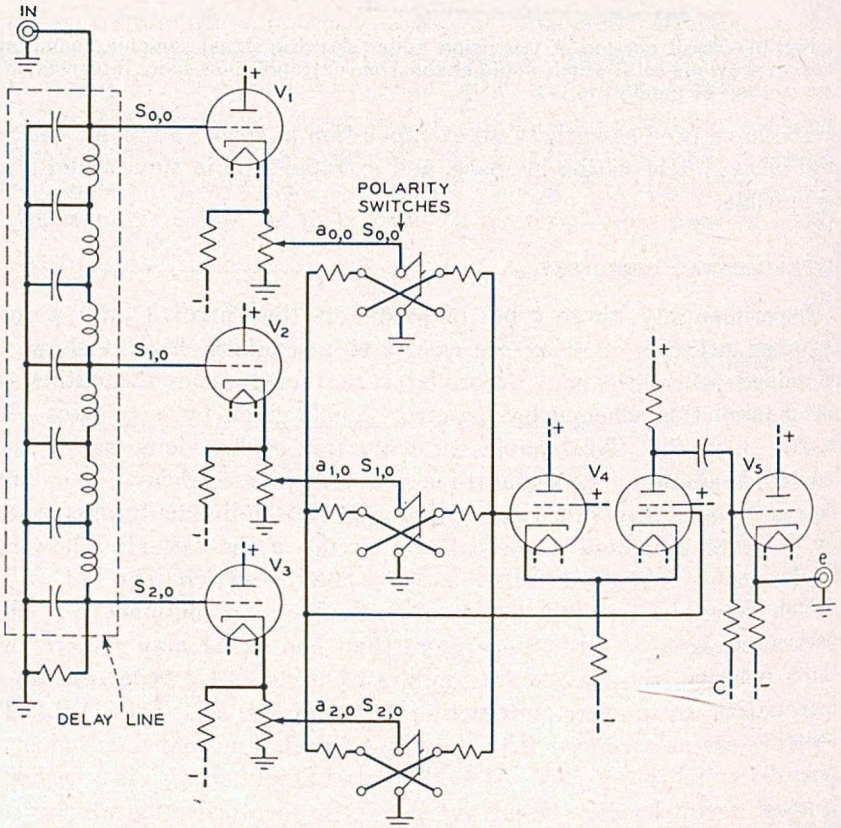

Fig. 11—Simplified schematic for "previous value" and "slope" prediction.

* A. L. Hopper, "Storing Video Information," *Electronics*, 24, pp. 122–125, June, 1951.

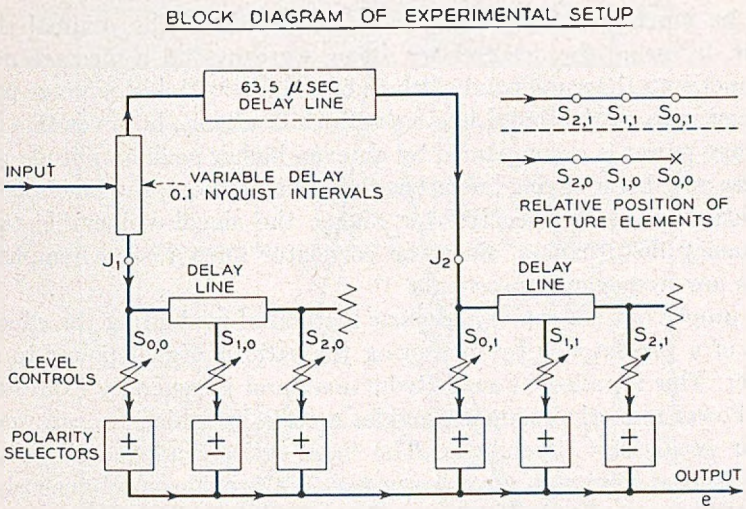

Fig. 12—Block diagram of experimental apparatus used to investigate methods of prediction involving combinations of previous signal values along a line with those on the line directly above.

frequency of 54.0 mc. The over-all video bandwidth is flat (± 0.1 db) to 5.0 mc. Nonlinear distortion is approximately one percent when the peak-to-peak signal to r.m.s. noise is 58 db. To give an idea of its complexity, two such units with their associated power supplies require a seven-foot relay rack for housing. The signal at J_1 represents the input picture signal, even though it may be delayed by a small fraction of a Nyquist interval from the actual input signal. The signal at J_2 is the same signal as found at J_1 but delayed by one line time. Each of these signals is fed into terminated delay lines to enable additional signal samples to be obtained. The geometrical location of these signal samples is illustrated in the upper right section of Fig. 12. Here, six signals are obtained instead of three as were required for "previous value" and "slope" prediction. These signals are weighted and polarized in the same manner as the three signals shown in Fig. 11. The output is the sum of these weighted signals and is given by

$$e = a_{0,0}S_{0,0} + a_{1,0}S_{1,0} + a_{2,0}S_{2,0} + a_{0,1}S_{0,1} + a_{1,1}S_{1,1} + a_{2,1}S_{2,1}\,.$$

The coefficients may assume positive or negative values.

MEASUREMENTS

It is obvious that if we are able to predict the value of most signal samples closely (which we will be able to do if there is a large amount of correlation in the picture), then the average amplitude of our mistakes

will be much less than the average amplitude of the original signal. Thus, by using the decorrelator alone, we can send a message over a channel with the same bandwidth as before but with less average power. At first, this might sound like a worthwhile saving; however this lower average power is accompanied by an even higher peak amplitude which makes any direct saving less attractive. Furthermore, the low frequency attentuation of the decorrelator makes the signal vulnerable to low frequency disturbances, since the correlator must restore (emphasize) these low frequency components.

A proper but *not entirely adequate* method of evaluating the effectiveness of a predictor is by measuring the ratio of signal power to error power. This is called "Power Reduction" and is generally expressed in db. Power reduction simply provides a scale by which we can weigh a linear predictor's capabilities. The "not entirely adequate" refers to the fact that minimum error power may not provide simultaneously the lowest amount of redundancy for that given type of prediction.

As an example, Fig. 13 shows the power reduction for the relative weighting of the previous horizontal signal sample as compared to the present value of the signal, for three pictures-later to be described as Scene A, B and C. The top-most curve is for Scene B, which is a simple, soft picture that contains very little detail. For this picture, the minimum error power coincides (within measurable limits) with the minimum redundancy. For Scene A and particularly Scene C, minimum error power is considerably different than that for minimum redundancy. This difference between minimum error power and minimum redundancy also applies to decorrelators using other types of predictors as well. Minimum redundancy may also be a misleading criterion of a predictor's performance, since the value of the prediction must depend on the particular type of encoder used, and some types of encoding will require certain types of redundant information to be retained.

The following pictures are representations of the error signal as photographed from a 10-inch laboratory monitor. The signals were band limited to 4.3 mc. Fig. 14 represents the "original" for three scenes called A, B and C. These pictures represent, to a first approximation, the gamut of pictures normally expected to be transmitted. They are by no means the best or the worst pictures than can be imagined; however any system should be able to reproduce these pictures without appreciable distortion. For example, Scene C should be capable of being sent continuously without the elastic delay running out, etc.

Fig. 15 shows how the error signal appears for "previous value" prediction. "Previous value" prediction is excellent for flat white or dark

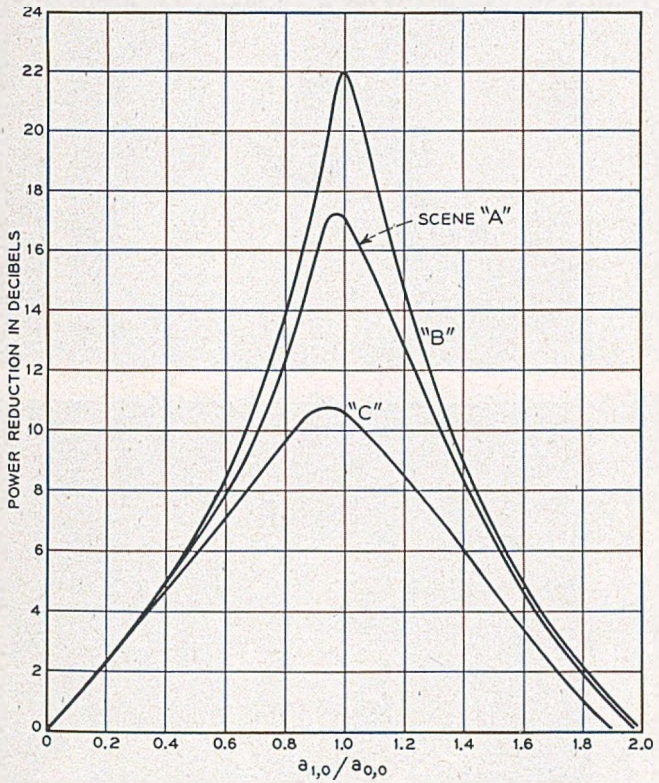

Fig. 13—Power reduction for various weighting coefficients for the previous horizontal sample.

areas as can be observed in the background of Scene A. Where the separation of a white to black area is made, the error signal is large. It is this large error signal that informs the receiver of this change in brightness, and until another change occurs, the error output is again zero. This type of performance produced the flat grey appearance of the background. In this way, the picture represents only changes in brightness—a first difference type of picture.

It may be noted that horizontal contour lines have vanished leaving only vertical contours which pertain to the brightness changes that have occurred. This effect is especially evident in Scene C. The power reductions given in the lower left hand corner of these pictures are consistent with their complexity.

Fig. 16 shows the error signal appearance for "slope" prediction. When compared to the error signal for "previous value" prediction a finer vertical granularity is observed, and this is attributed to sudden

Fig. 14—Three pictures as photographed from the face of a kinescope. Scene "A" is a picture of average complexity. Scene "B" is a simple, rather soft picture. Scene "C" is a complex, highly detailed picture. Roughly, these pictures represent the gamut of pictures normally expected to be transmitted.

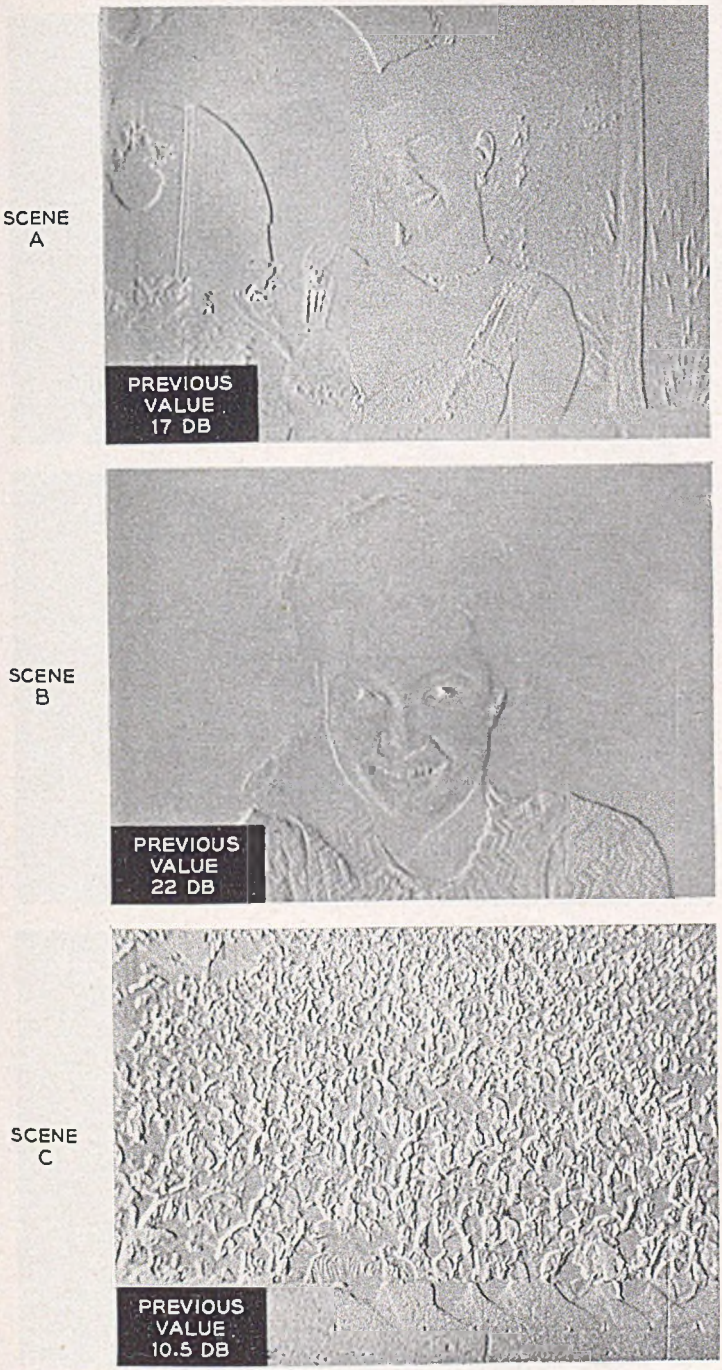

Fig. 15—Three pictures showing the appearance of the error signal when using "previous value" prediction. Note the absence of horizontal contours.

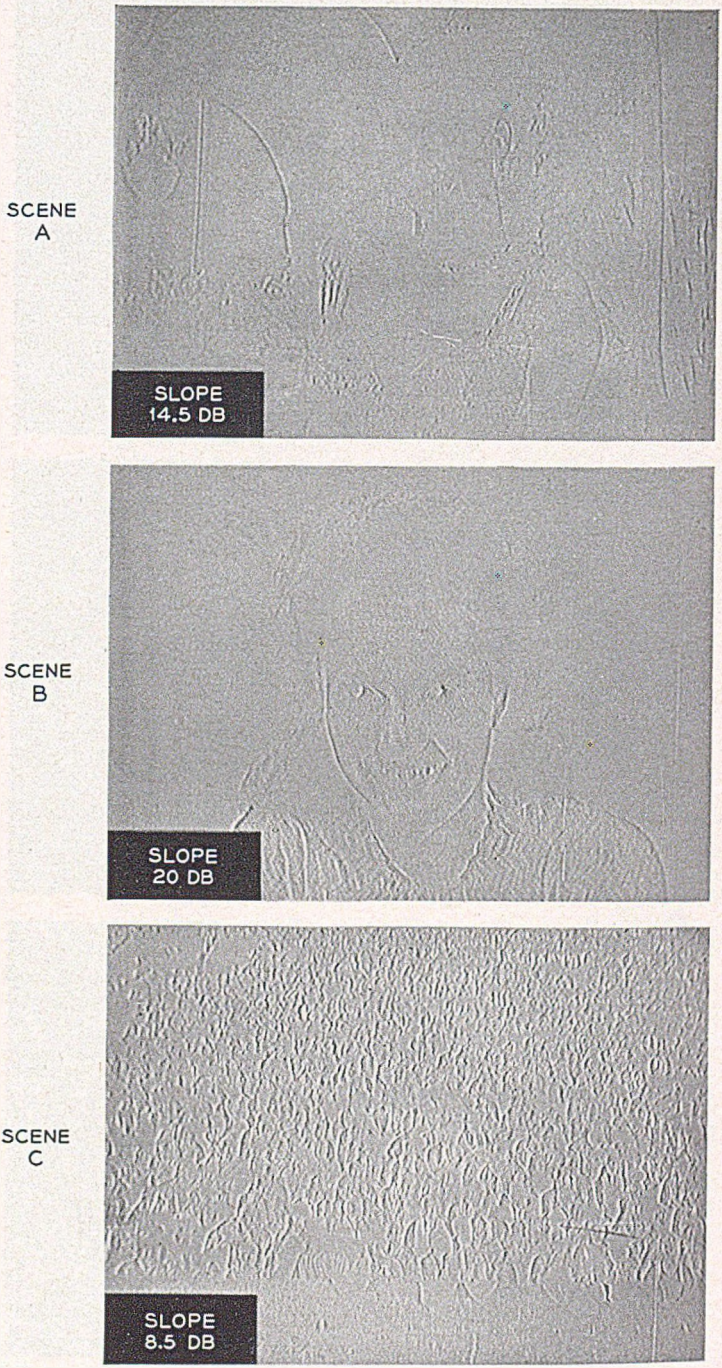

Fig. 16—Three pictures showing the appearance of the error signal when using "slope" prediction.

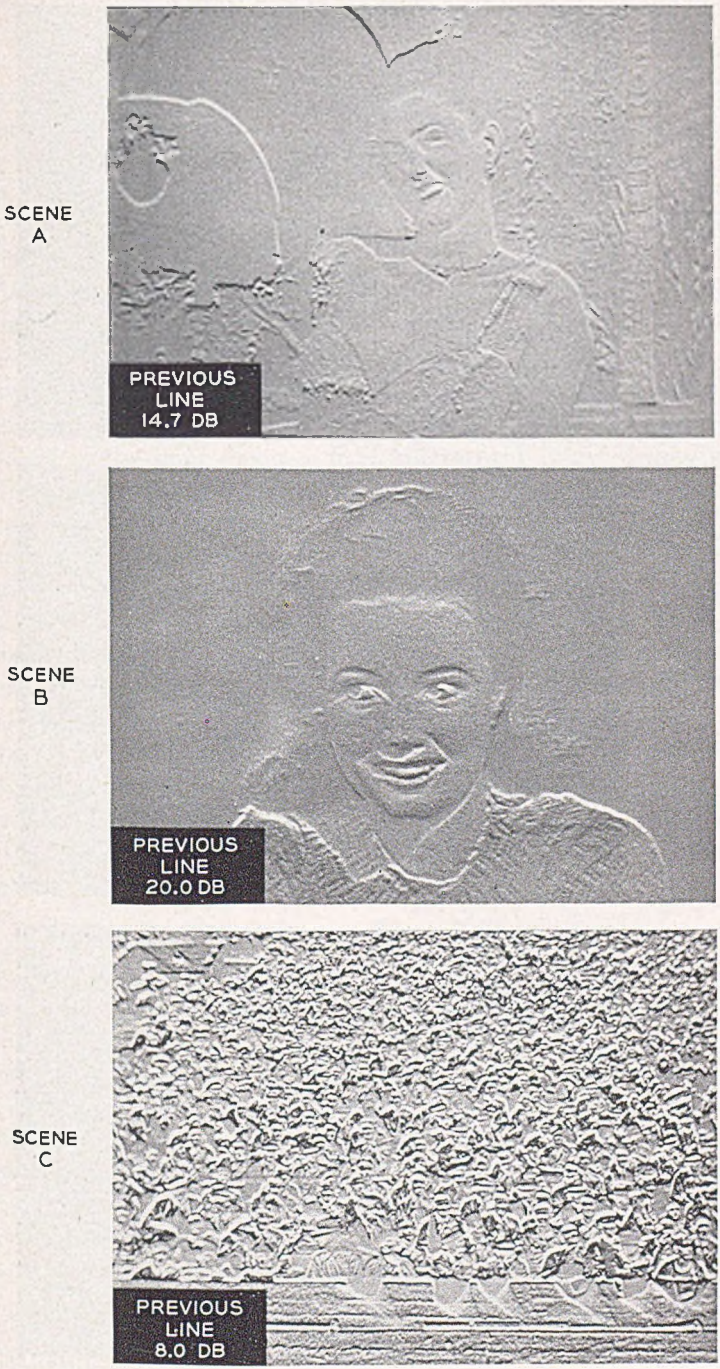

Fig. 17—Three pictures showing the appearance of the error signal when using "previous line" prediction. Note the absence of vertical contours.

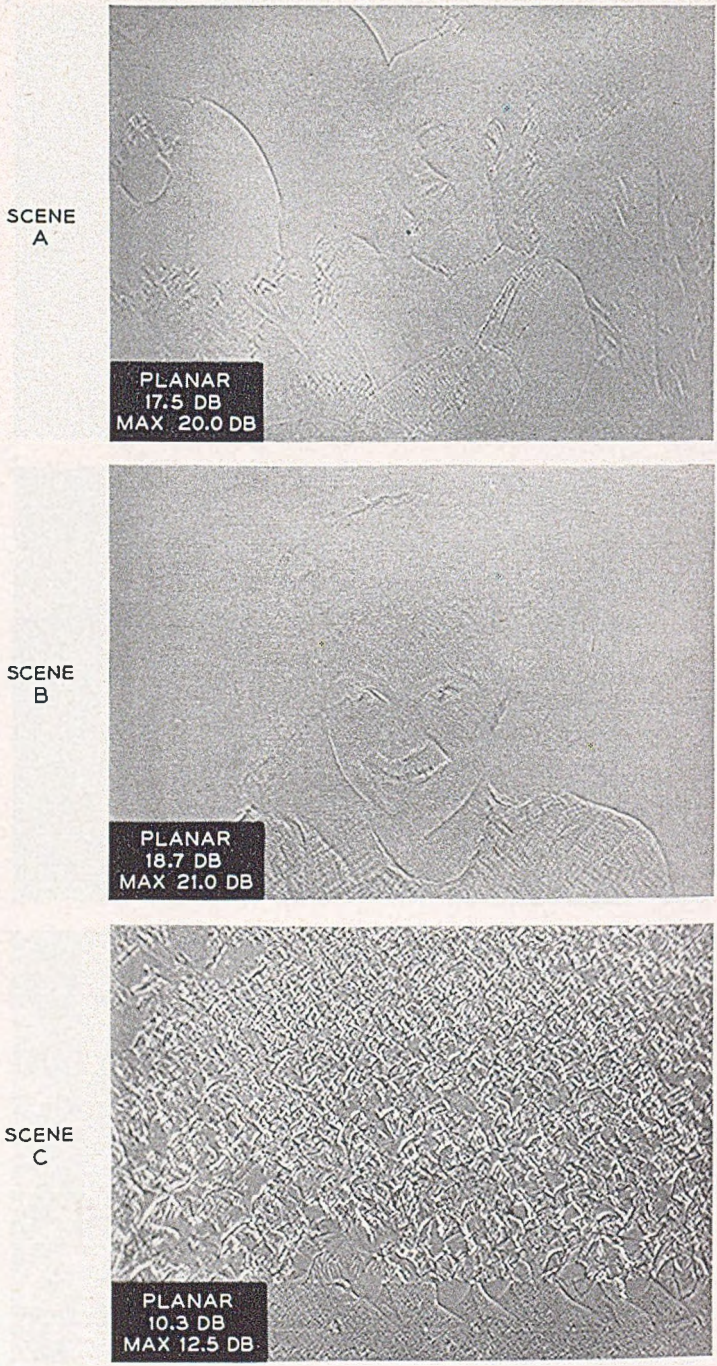

Fig. 18—Three pictures showing the appearance of the error signal when using "planar" prediction. Note the absence of horizontal and vertical contours.

changes in brightness. In the case of "previous value" prediction a sudden change in brightness produces only one error, where for "slope," two errors result. This, to some extent, accounts for the lesser amount of power reduction measured for these scenes.

Fig. 17 shows the appearance of the error signal for "previous line" prediction in the three scenes. Where vertical contour lines are predominately left after "previous value" prediction shown in Fig. 15, horizontal contours, are more prevalent now. It can be noted that the power reduction for "previous line" prediction is less than that for "previous value" prediction. This is due principally to the increased distance of the previous line sample from $S_{0,0}$. If the closest horizontal sample was taken at the same distance from the present value of the signal as the previous line sample, then the power reduction using these signal values individually for prediction would be essentially the same for most pictures.

Fig. 18 shows the error signal appearance for "planar" prediction. Here, vertical as well as horizontal contours are deleted. In Scene A the tree trunk has almost completely vanished. In Scene B the picture has an extremely flat appearance. Scene C exhibits the lack of horizontal and vertical contours best, since only sloping contours are left. The power reduction figures at the lower left hand corner also show values for minimum error power. For most pictures, the error power can be reduced by a factor of one-half again over the planar coefficients by modifying the weighting coefficients. The coefficients for this modified planar case are given by

$$S_p = \tfrac{2}{3}S_{1,0} + \tfrac{2}{3}S_{0,1} - \tfrac{1}{3}S_{1,1}$$

These coefficients generally produce an error signal with less power than the coefficients used for "planar" prediction.

While all pictures contain redundancy, the error signals from these simple linear predictors shown in Figs. 15, 16, 17 and 18 can visually be noted still to contain large amounts of redundancy. The contours of the models and of the various objects are readily identifiable. Were all redundancy removed, the picture would be completely chaotic and would appear very much like random noise, although greater efficiency in transmission would be achieved. For richer rewards, more sophisticated methods of prediction will be required.

ACKNOWLEDGMENT

The author wishes to acknowledge with grateful appreciation the invaluable guidance of Dr. B. M. Oliver. It was principally through his efforts that this study was made possible.

Generalized Telegraphist's Equations for Waveguides

By S. A. SCHELKUNOFF

(Manuscript received April 30, 1952)

In this paper Maxwell's partial differential equations and the boundary conditions for waveguides filled with a heterogeneous and non-isotropic medium are converted into an infinite system of ordinary differential equations. This system represents a generalization of "telegraphist's equations" for a single mode transmission to the case of multiple mode transmission. A similar set of equations is obtained for spherical waves. Although such generalized telegraphist's equations are very complicated, it is very likely that useful results can be obtained by an appropriate modal analysis.

From a purely mathematical point of view the problem of electromagnetic wave propagation inside a metal waveguide reduces to obtaining that solution of Maxwell's equations which satisfies certain boundary conditions *along* the waveguide and certain terminal conditions at the ends of the waveguide. If the medium inside the waveguide is homogeneous and isotropic and if the cross-section of the waveguide is either rectangular or circular or elliptic, the desired solution is obtained by the method of separating the variables. The method works for some other special cross-sections. It works also if the medium inside a rectangular waveguide consists of homogeneous, isotropic strata parallel to one of its faces. Similarly, it works if the medium inside a circular waveguide consists of coaxial, homogeneous, isotropic layers. But in general if the medium is either nonhomogeneous or non-isotropic or both, the method does not work. The mathematical reason for this is that the solution is of a more complicated form than a simple production of functions, each depending on a single coordinate. Any function that one usually encounters in physical problems, and therefore a solution of Maxwell's equations, may be expanded in a series of orthogonal functions. Sets of such functions are provided by the solutions for waveguides filled with homogeneous media. Such functions already satisfy the proper boundary conditions and the problem is to obtain series which also satisfy

Maxwell's equations. From the physical point of view this method represents a conversion of Maxwell's equations into generalized "telegraphist's equations."

Thus it is already known that Maxwell's partial differential equations *and* the boundary conditions *along* a waveguide are convertible into a set of independent ordinary differential equations, each resembling telegraphist's equations for electric transmission lines.[1] Each equation describes a "mode of propagation" in terms of concepts well known in electric circuit theory. A waveguide can be considered as an infinite system of transmission lines. If the medium inside the waveguide is homogeneous and isotropic and if the surface impedance of the boundary is zero, the method of separating the variables enables us to obtain a set of "normal", that is, *uncoupled* modes of propagation. Any irregularity or "discontinuity" in the waveguide provides a coupling between some, or all, modes of propagation. The irregularity may be in a boundary of the waveguide or in the dielectric within it. A heterogeneous dielectric may be considered as a homogeneous dielectric with distributed irregularities.[2] Similarly a heterogeneous non-isotropic dielectric may be considered as a homogeneous isotropic dielectric with distributed irregularities. Such irregularities provide a distributed coupling between the various modes appropriate to homogeneous isotropic waveguides. Our problem is to calculate the coupling coefficients. The generalized telegraphist's equations, obtained in this manner, are very complicated in that they represent an infinite number of coupled transmission modes. They are useful, however, in suggesting a physical picture of wave propagation under complicated conditions, and can be used in approximate analysis when we can ignore all but the most tightly coupled modes. For example, this picture was successfully employed by Albersheim[3] in studying the effect of gentle bending of a waveguide on propagation of circular electric waves. In this case it was important to consider the coupling between only two modes, TE_{01} and TM_{11}, which have the same cutoff frequency in a straight waveguide. More recently, Stevenson obtained exact equations for waves in horns of arbitrary shape.[4] His equations express the propagation of the axial components of E and H. The various modes are coupled through the boundary of the horn. In

[1] S. A. Schelkunoff, "Transmission Theory of Plane Electromagnetic Waves," *Proc. Inst. Radio Engrs.*, Nov. 1937, pp. 1457–1492.

[2] S. A. Schelkunoff, "Electromagnetic Waves," D. van Nostrand Co., (1943), pp. 92–93.

[3] W. J. Albersheim, "Propagation of TE_{01} Waves in Curved Waveguides," *Bell System Tech. J.*, Jan. 1949, pp. 1–32.

[4] A. F. Stevenson, "General Theory of Electromagnetic Horns," *J. Appl. Phys.*, Dec. 1951, pp. 1447–1460.

the present paper we shall consider waveguides of *constant* cross-section and *conical* horns of arbitrary shape filled with a heterogeneous and non-isotropic dielectric and derive the equations for propagation of the generalized voltages and currents representing the *transverse* field components. The various modes are coupled through the medium. It is very likely that our equations can be generalized to include the coupling through the boundary.

To understand the mechanism of coupling between the various modes through the medium consider Maxwell's equations

$$\text{curl } E = -j\omega B, \qquad \text{curl } H = {}^{c}J + j\omega D, \tag{1}$$

where ${}^{c}J$ is the density of conduction current while the other letter symbols have the usual meanings. In the most general linear case the components of B and D are linear functions of the components of H and E respectively, with the coefficients depending on the coordinates. These equations can always be rewritten as follows

$$\text{curl } E = -j\omega\mu H - M, \qquad \text{curl } H = j\omega\epsilon E + J, \tag{2}$$

where M and J are the densities of magnetic and electric polarization currents.[5]

$$M = j\omega(B - \mu H), \qquad J = {}^{c}J + j\omega(D - \epsilon E), \tag{3}$$

and μ, ϵ are constants (not necessarily those of vacuum). If M and J were given, they would act as sources exciting various modes of propagation in a homogeneous, isotropic waveguide. If M and J are functions of H and E, they can still be considered as the sources, acting on power borrowed from the wave, of the various modes. Thus M and J will provide the coupling between the modes existing in a homogeneous, isotropic waveguide.

Thus in order to derive the generalized telegraphist's equations we shall first consider the various modes of propagation in a homogeneous isotropic wave guide. Each mode is described by a transverse field distribution pattern[6] $T(u, v)$, where u and v are orthogonal coordinates of a point in a typical cross-section. This function is a solution of the following two-dimensional partial differential equation

$$\Delta T = \frac{1}{e_1 e_2}\left[\frac{\partial}{\partial u}\left(\frac{e_2}{e_1}\frac{\partial T}{\partial u}\right) + \frac{\partial}{\partial v}\left(\frac{e_1}{e_2}\frac{\partial T}{\partial v}\right)\right] = -\chi^2 T, \tag{4}$$

[5] See Reference 2.

[6] S. A. Schelkunoff, "Electromagnetic Waves," D. van Nostrand Co. (1943), Chapter 10.

where χ is the separation constant and e_1, e_2 are the scale factors in the expression for the elementary distance

$$ds^2 = e_1^2\, du^2 + e_2^2\, dv^2. \tag{5}$$

In the case of TM waves the T-function must vanish on the boundary of zero impedance. This boundary condition restricts χ to a doubly infinite set of values χ_{mn} with the corresponding functions T_{mn}. In the case of TE waves the normal derivative of the T-function must vanish on the boundary of zero impedance. Since we have to consider both types of waves simultaneously, we shall distinguish between them by enclosing the *subscripts in parentheses* for TM waves and *in brackets* for TE waves. The double subscript designation of various modes has been standardized only for rectangular and circular waveguides. For waveguides of other shapes the standard is to use a single subscript by arranging the modes in the order of their cutoff frequencies. For convenience, we shall use this convention in the general case and denote TM modes by $T_{(n)}(u, v)$, and TE modes by $T_{[n]}(u, v)$. The corresponding cutoff constants will be $\chi_{(n)}$ and $\chi_{[n]}$. In what follows it is understood that whenever the T-functions should be designated by double subscripts, our single letter subscripts should be considered as symbols for ordered double subscripts.

The transverse field components may be derived from the potential and stream functions,[7] V and Π for TM waves and U and Ψ for TE waves. Thus

$$E_t = -\operatorname{grad} V - \operatorname{flux} \Psi, \qquad H_t = \operatorname{flux} \Pi - \operatorname{grad} U, \tag{6}$$

where the components of the gradient and flux of a scalar function W are

$$\begin{aligned} \operatorname{grad}_u W &= \frac{\partial W}{e_1\, \partial u}, & \operatorname{grad}_v W &= \frac{\partial W}{e_2\, \partial v}, \\ \operatorname{flux}_u W &= \frac{\partial W}{e_2\, \partial v}, & \operatorname{flux}_v W &= -\frac{\partial W}{e_1\, \partial u}. \end{aligned} \tag{7}$$

The T-functions corresponding to the various modes *of the same variety* are orthogonal; that is, the following integrals over the cross-section vanish,

$$\iint T_{(n)} T_{(m)}\, dS = 0, \qquad \iint T_{[n]} T_{[m]}\, dS = 0, \qquad \text{if } m \neq n. \tag{8}$$

It should be stressed that $T_{(n)}$ and $T_{[m]}$ are not, in general, orthogonal.

[7] See Reference 6.

Similarly the gradients of the T-functions of the same variety as well as the fluxes, are orthogonal,

$$\begin{aligned}\iint (\text{grad } T_{(n)}) \cdot (\text{grad } T_{(m)})\, dS &= \iint (\text{flux } T_{(n)}) \cdot (\text{flux } T_{(m)})\, dS \\ = \iint (\text{grad } T_{[n]}) \cdot (\text{grad } T_{[m]})\, dS &= \iint (\text{flux } T_{[n]}) \cdot (\text{flux } T_{[m]})\, dS = 0,\end{aligned} \tag{9}$$

if $m \neq n$. The following gradients and fluxes of the T-functions are orthogonal for all m and n,

$$\begin{aligned}\iint (\text{grad } T_{(n)}) \cdot (\text{flux } T_{[m]})\, dS &= \iint (\text{grad } T_{[n]}) \cdot (\text{flux } T_{(m)})\, dS \\ &= \iint (\text{grad } T_{(n)}) \cdot (\text{flux } T_{(m)})\, dS = 0.\end{aligned} \tag{10}$$

On the other hand, grad $T_{[m]}$ and flux $T_{[n]}$ are not, in general, orthogonal.

If all modes are present, the potential and stream functions are

$$\begin{aligned} V &= -V_{(n)}(z)T_{(n)}(u, v), & \Pi &= -I_{(n)}(z)T_{(n)}(u, v), \\ \Psi &= -V_{[n]}(z)T_{[n]}(u, v), & U &= -I_{[n]}(z)T_{[n]}(u, v), \end{aligned} \tag{11}$$

where the tensor summation convention is used: whenever the same letter subscript is used in a product, it should receive all values in a given set and the resulting products should be added. The negative signs have been inserted in order to avoid a preponderance of negative signs in later equations. Substituting in (9), we have

$$\begin{aligned} E_t &= V_{(n)} \text{ grad } T_{(n)} + V_{[n]} \text{ flux } T_{[n]}\,, \\ H_t &= -I_{(n)} \text{ flux } T_{(n)} + I_{[n]} \text{ grad } T_{[n]}\,. \end{aligned} \tag{12}$$

The T-functions for the various modes are determined by equation (4) and the boundary conditions except for arbitrary factors related to the power levels of the modes. If we choose these constants in such a way that

$$\iint (\text{grad } T) \cdot (\text{grad } T)\, dS \equiv \chi^2 \iint T^2\, dS = 1, \tag{13}$$

then the complex power carried by the wave is given by an expression similar to that in an ordinary transmission line,

$$P = \tfrac{1}{2} V_{(n)} I^*_{(n)} + \tfrac{1}{2} V_{[n]} I^*_{[n]}\,. \tag{14}$$

Hence, the V's and I's correspond to the voltages and currents in coupled transmission lines.

In an expanded form equations (12) are

$$E_u = V_{(n)} \frac{\partial T_{(n)}}{e_1 \partial u} + V_{[n]} \frac{\partial T_{[n]}}{e_2 \partial v}, \qquad E_v = V_{(n)} \frac{\partial T_{(n)}}{e_2 \partial v} - V_{[n]} \frac{\partial T_{[n]}}{e_1 \partial u},$$
$$H_v = I_{(n)} \frac{\partial T_{(n)}}{e_1 \partial u} + I_{[n]} \frac{\partial T_{[n]}}{e_2 \partial v}, \qquad H_u = -I_{(n)} \frac{\partial T_{(n)}}{e_2 \partial v} + I_{[n]} \frac{\partial T_{[n]}}{e_1 \partial u}. \tag{15}$$

To these we add the following expansions for the longitudinal components of E and H

$$E_z = \chi_{(n)} V_{z,(n)}(z) T_{(n)}(u, v), \qquad H_z = \chi_{[n]} I_{z,[n]}(z) T_{[n]}(u, v). \tag{16}$$

Equations of this form satisfy automatically the boundary conditions on E_z and H_z. The multipliers χ_n have been inserted arbitrarily in order to make the physical dimensions of the second factors to correspond to those of voltage and current.

Let us now write Maxwell's equations in an expanded form

$$\frac{\partial E_z}{e_2 \partial v} - \frac{\partial E_v}{\partial z} = -j\omega B_u, \qquad \frac{\partial H_z}{e_2 \partial v} - \frac{\partial H_v}{\partial z} = j\omega D_u,$$
$$\frac{\partial E_u}{\partial z} - \frac{\partial E_z}{e_1 \partial u} = -j\omega B_v, \qquad \frac{\partial H_u}{\partial z} - \frac{\partial H_z}{e_1 \partial u} = j\omega D_v, \tag{17}$$
$$\frac{\partial (e_2 E_v)}{\partial u} - \frac{\partial (e_1 E_u)}{\partial v} = -j\omega e_1 e_2 B_z, \qquad \frac{\partial (e_2 H_v)}{\partial u} - \frac{\partial (e_1 H_u)}{\partial v} = j\omega e_1 e_2 D_z.$$

Substituting from (15) and (16) in the left column of (17), we find

$$\chi_{(n)} V_{z,(n)} \frac{\partial T_{(n)}}{e_2 \partial v} - \frac{dV_{(n)}}{dz} \frac{\partial T_{(n)}}{e_2 \partial v} + \frac{dV_{[n]}}{dz} \frac{\partial T_{[n]}}{e_1 \partial u} = -j\omega B_u, \tag{18}$$

$$-\chi_{(n)} V_{z,(n)} \frac{\partial T_{(n)}}{e_1 \partial u} + \frac{dV_{(n)}}{dz} \frac{\partial T_{(n)}}{e_1 \partial u} + \frac{dV_{[n]}}{dz} \frac{\partial T_{[n]}}{e_2 \partial v} = -j\omega B_v, \tag{19}$$

$$V_{(n)} \frac{\partial^2 T_{(n)}}{\partial u \partial v} - V_{[n]} \frac{\partial}{\partial u} \left(\frac{e_2}{e_1} \frac{\partial T_{[n]}}{\partial u} \right) - V_{(n)} \frac{\partial^2 T_{(n)}}{\partial v \partial u} - V_{[n]} \frac{\partial}{\partial v} \left(\frac{e_1}{e_2} \frac{\partial T_{[n]}}{\partial v} \right)$$
$$= -j\omega e_1 e_2 B_z. \tag{20}$$

In view of (4) the last equation reduces to

$$\chi_{[n]}^2 V_{[n]} T_{[n]} = -j\omega B_z. \tag{21}$$

Multiplying (18) by $[-\partial T_{(m)}/e_2\,\partial v]\,dS$, (19) by $[\partial T_{(m)}/e_1\,\partial u]\,dS$, adding, and integrating over the cross-section, we obtain

$$-\chi_{(m)}V_{z,(m)} + \frac{dV_{(m)}}{dz} = j\omega \iint \left(B_u \frac{\partial T_{(m)}}{e_2\,\partial v} - B_v \frac{\partial T_{(m)}}{e_1\,\partial u} \right) dS\,. \quad (22)$$

In the first term the summation convention should be ignored. Multiplying (18) by $[\partial T_{[m]}/e_1\,\partial u]\,dS$, (19) by $[\partial T_{[m]}/e_2\,\partial v]\,dS$, adding, and integrating we find

$$\frac{\partial V_{[m]}}{dz} = -j\omega \iint \left(B_u \frac{\partial T_{[m]}}{e_1\,\partial u} + B_v \frac{\partial T_{[m]}}{e_2\,\partial v} \right) dS. \quad (23)$$

Multiplying (21) by $T_{[m]}\,dS$ and integrating, we have

$$V_{[m]} = -j\omega \iint B_z T_{[m]}\,dS. \quad (24)$$

Subjecting the right column of (17) to a similar treatment, we obtain three additional equations. Summarizing, we have

$$\frac{\partial V_{(m)}}{dz} = j\omega \iint \left(B_u \frac{\partial T_{(m)}}{e_2\,\partial v} - B_v \frac{\partial T_{(m)}}{e_1\,\partial u} \right) dS + \chi_{(m)}V_{z,(m)}\,, \quad (25)$$

$$\frac{\partial I_{(m)}}{dz} = -j\omega \iint \left(D_u \frac{\partial T_{(m)}}{e_1\,\partial u} + D_v \frac{\partial T_{(m)}}{e_2\,\partial v} \right) dS, \quad (26)$$

$$\frac{dV_{[m]}}{dz} = -j\omega \iint \left(B_u \frac{\partial T_{[m]}}{e_1\,\partial u} + B_v \frac{\partial T_{[m]}}{e_2\,\partial v} \right) dS, \quad (27)$$

$$\frac{dI_{[m]}}{dz} = j\omega \iint \left(-D_u \frac{\partial T_{[m]}}{e_2\,\partial v} + D_v \frac{\partial T_{[m]}}{e_1\,\partial u} \right) dS + \chi_{[m]}I_{z,[m]}\,, \quad (28)$$

$$V_{[m]} = -j\omega \iint B_z T_{[m]}\,dS, \qquad I_{(m)} = -j\omega \iint D_z T_{(m)}\,dS. \quad (29)$$

In the last terms of equations (25) and (28) the summation convention should be ignored.

If the components of B and D are linear functions of the components of H and E respectively, then with the aid of (15) and (16) they can be expressed as linear functions of $V_{(n)}$, $V_{[n]}$, $I_{(n)}$, $I_{[n]}$, $V_{z,(n)}$, $I_{z,[n]}$. Solving (29) for $V_{z,(n)}$ and $I_{z,[n]}$ and making the appropriate substitutions in (25), (26), (27), (28), we obtain the generalized telegraphist's

equations in the following form

$$\begin{aligned}
\frac{dV_{(m)}}{dz} &= -Z_{(m)(n)}I_{(n)} - Z_{(m)[n]}I_{[n]} - {}^{V}T_{(m)(n)}V_{(n)} - {}^{V}T_{(m)[n]}V_{[n]}, \\
\frac{dI_{(m)}}{dz} &= -Y_{(m)(n)}V_{(n)} - Y_{(m)[n]}V_{[n]} - {}^{I}T_{(m)(n)}I_{(n)} - {}^{I}T_{(m)[n]}I_{[n]}, \\
\frac{dV_{[m]}}{dz} &= -Z_{[m][n]}I_{[n]} - Z_{[m](n)}I_{(n)} - {}^{V}T_{[m][n]}V_{[n]} - {}^{V}T_{[m](n)}V_{(n)}, \\
\frac{dI_{[m]}}{dz} &= -Y_{[m][n]}V_{[n]} - Y_{[m](n)}V_{(n)} - {}^{I}T_{[m][n]}I_{[n]} - {}^{I}T_{[m](n)}I_{(n)}.
\end{aligned} \tag{30}$$

The transfer impedances Z, the transfer admittances Y, the voltage transfer coefficients ${}^{V}T$, and the current transfer coefficients ${}^{I}T$ between various modes are in general functions of z. They are constants if the properties of the waveguide are independent of the distance along it; in this case the problem of solving the generalized telegraphist's equations reduces to solving an infinite system of linear algebraic equations and the corresponding characteristic equation.

Similar equations may be derived for spherical waves either in an unlimited medium or in a medium bounded by a perfectly conducting conical surface of arbitrary cross-section. If the latter is circular and if the flare angle is 180°, we have a plane boundary. Hence, the case of spherical waves in a non-homogeneous medium is included. In the spherical case we shall use the general orthogonal system of coordinates (r, u, v) where r is the distance from the center and (u, v) are orthogonal angular coordinates. In this system the elements of length ds and area dS are given by

$$ds^2 = dr^2 + r^2(e_1^2\,du^2 + e_2^2\,dv^2), \qquad dS = r^2 d\Omega, \qquad d\Omega = e_1 e_2\,du\,dv. \tag{31}$$

The transverse field components may be expressed in a form similar to that for waveguides

$$rE_t = -\operatorname{grad} V - \operatorname{flux} \Pi, \qquad rH_t = \operatorname{flux} \Pi - \operatorname{grad} U, \tag{32}$$

where grad and flux of a typical scalar function are defined by equations (10). Instead of (11) we have

$$\begin{aligned}
V &= -V_{(n)}(r)T_{(n)}(u, v), \qquad \Pi = -I_{(n)}(r)T_{(n)}(u, v), \\
\Psi &= -V_{[n]}(r)T_{[n]}(u, v), \qquad U = -I_{[n]}(r)T_{[n]}(u, v),
\end{aligned} \tag{33}$$

where the T-functions satisfy equation (4) and appropriate boundary conditions. These functions, their gradients and fluxes are orthogonal.

They are assumed to be normalized as follows

$$\iint (\text{grad } T)\cdot(\text{grad } T)\, d\Omega = \chi^2 \iint T^2\, d\Omega = 1\,, \tag{34}$$

where $d\Omega$ is an elementary solid angle. Hence, equation (14) will again represent the complex power flow in the direction of propagation.

The various field components may then be expressed as follows

$$rE_u = V_{(n)} \frac{\partial T_{(n)}}{e_1\, \partial u} + V_{[n]} \frac{\partial T_{[n]}}{e_2\, \partial v}\,, \qquad rE_v = V_{(n)} \frac{\partial T_{(n)}}{e_2\, \partial v} - V_{[n]} \frac{\partial T_{[n]}}{e_1\, \partial u}\,,$$

$$rH_v = I_{(n)} \frac{\partial T_{(n)}}{e_1\, \partial u} + I_{[n]} \frac{\partial T_{[n]}}{e_2\, \partial v}\,, \qquad rH_u = -I_{(n)} \frac{\partial T_{(n)}}{e_2\, \partial v} + I_{[n]} \frac{\partial T_{[n]}}{e_1\, \partial u}\,, \tag{35}$$

$$r^2E_r = \chi_{(n)}\, V_{r,(n)}\, T_{(n)}\,, \qquad r^2H_r = \chi_{[n]}\, I_{r,[n]}\, T_{[n]}\,.$$

It should be noted that the physical dimensions of $V_{r,(n)}$ and $I_{r,[n]}$ are not those of voltage and current. Substituting in Maxwell's equations and using transformations similar to those in the case of plane waves, we find

$$\frac{dV_{(m)}}{dr} = j\omega \iint \left(rB_u \frac{\partial T_{(m)}}{e_2\, \partial v} - rB_v \frac{\partial T_{(m)}}{e_1\, \partial u} \right) d\Omega + \chi_{(m)} r^{-2}\, V_{r,(m)}\,,$$

$$\frac{dI_{(m)}}{dr} = -j\omega \iint \left(rD_u \frac{\partial T_{(m)}}{e_1\, \partial u} + rD_v \frac{\partial T_{(m)}}{e_2\, \partial v} \right) d\Omega,$$

$$\frac{dV_{[m]}}{dr} = -j\omega \iint \left(rB_u \frac{\partial T_{[m]}}{e_1\, \partial u} + rB_v \frac{\partial T_{[m]}}{e_2\, \partial v} \right) d\Omega, \tag{36}$$

$$\frac{dI_{[m]}}{dr} = j\omega \iint \left(- rD_u \frac{\partial T_{[m]}}{e_2\, \partial v} + rD_v \frac{\partial T_{[m]}}{e_1\, \partial u} \right) d\Omega + \chi_{[m]} r^{-2} I_{r,[m]}\,,$$

$$V_{[m]} = -j\omega \iint (r^2 B_r) T_{[m]}\, d\Omega, \qquad I_{(m)} = -j\omega \iint (r^2 D_r) T_{(m)}\, d\Omega.$$

Returning to the plane wave case and assuming the following general linear relations

$$B_u = \mu_{uu}H_u + \mu_{uv}H_v + \mu_{uz}H_z\,, \qquad D_u = \epsilon_{uu}E_u + \epsilon_{uv}E_v + \epsilon_{uz}E_z\,,$$

$$B_v = \mu_{vu}H_u + \mu_{vv}H_v + \mu_{vz}H_z\,, \qquad D_v = \epsilon_{vu}E_u + \epsilon_{vv}E_v + \epsilon_{vz}E_z\,, \tag{37}$$

$$B_z = \mu_{zu}H_u + \mu_{zv}H_v + \mu_{zz}H_z\,, \qquad D_z = \epsilon_{zu}E_u + \epsilon_{zv}E_v + \epsilon_{zz}E_z\,,$$

we find

$$B_u = I_{(n)}\left[-\mu_{uu}\frac{\partial T_{(n)}}{e_2\,\partial v} + \mu_{uv}\frac{\partial T_{(n)}}{e_1\,\partial u}\right] + I_{[n]}\left[\mu_{uu}\frac{\partial T_{[n]}}{e_1\,\partial u} + u_{uv}\frac{\partial T_{[n]}}{e_2\,\partial v}\right] + I_{z,[n]}\mu_{uz}\chi_{[n]}T_{[n]},$$

$$B_v = I_{(n)}\left[-\mu_{vu}\frac{\partial T_{(n)}}{e_2\,\partial v} + \mu_{vv}\frac{\partial T_{(n)}}{e_1\,\partial u}\right] + I_{[n]}\left[\mu_{vu}\frac{\partial T_{[n]}}{e_1\,\partial u} + \mu_{vv}\frac{\partial T_{[n]}}{e_2\,\partial v}\right] + I_{z,[n]}\mu_{vz}\chi_{[n]}T_{[n]},$$

$$B_z = I_{(n)}\left[-\mu_{zu}\frac{\partial T_{(n)}}{e_2\,\partial v} + \mu_{zv}\frac{\partial T_{(n)}}{e_1\,\partial u}\right] + I_{[n]}\left[\mu_{zu}\frac{\partial T_{[n]}}{e_1\,\partial u} + \mu_{zv}\frac{\partial T_{[n]}}{e_2\,\partial v}\right] + I_{z,[n]}\mu_{zz}\chi_{[n]}T_{[n]}, \tag{38}$$

$$D_u = V_{(n)}\left[\epsilon_{uu}\frac{\partial T_{(n)}}{e_1\,\partial u} + \epsilon_{uv}\frac{\partial T_{(n)}}{e_2\,\partial v}\right] + V_{[n]}\left[\epsilon_{uu}\frac{\partial T_{[n]}}{e_2\,\partial v} - \epsilon_{uv}\frac{\partial T_{[n]}}{e_1\,\partial u}\right] + V_{z,(n)}\epsilon_{uz}\chi_{(n)}T_{(n)},$$

$$D_v = V_{(n)}\left[\epsilon_{vu}\frac{\partial T_{(n)}}{e_1\,\partial u} + \epsilon_{vv}\frac{\partial T_{(n)}}{e_2\,\partial v}\right] + V_{[n]}\left[\epsilon_{vu}\frac{\partial T_{[n]}}{e_2\,\partial v} - \epsilon_{vv}\frac{\partial T_{[n]}}{e_1\,\partial u}\right] + V_{z,(n)}\epsilon_{vz}\chi_{(n)}T_{(n)},$$

$$D_z = V_{(n)}\left[\epsilon_{zu}\frac{\partial T_{(n)}}{e_1\,\partial u} + \epsilon_{zv}\frac{\partial T_{(n)}}{e_2\,\partial v}\right] + V_{[n]}\left[\epsilon_{zu}\frac{\partial T_{[n]}}{e_2\,\partial v} - \epsilon_{zv}\frac{\partial T_{[n]}}{e_1\,\partial u}\right] + V_{z,(n)}\epsilon_{zz}\chi_{(n)}T_{(n)}.$$

Substituting from equations (38) into equations (25) to (29) we obtain

$$\frac{dV_{(m)}}{dz} = -j\omega I_{(n)}\iint\left[\mu_{uu}\frac{\partial T_{(n)}}{e_2\,\partial v}\frac{\partial T_{(m)}}{e_2\,\partial v} + \mu_{vv}\frac{\partial T_{(n)}}{e_1\,\partial u}\frac{\partial T_{(m)}}{e_1\,\partial u} - \mu_{uv}\frac{\partial T_{(n)}}{e_1\,\partial u}\frac{\partial T_{(m)}}{e_2\,\partial v} - \mu_{vu}\frac{\partial T_{(n)}}{e_2\,\partial v}\frac{\partial T_{(m)}}{e_1\,\partial u}\right]dS$$

$$+ j\omega I_{[n]}\iint\left[\mu_{uu}\frac{\partial T_{[n]}}{e_1\,\partial u}\frac{\partial T_{(m)}}{e_2\,\partial v} - \mu_{vv}\frac{\partial T_{[n]}}{e_2\,\partial v}\frac{\partial T_{(m)}}{e_1\,\partial u} + \mu_{uv}\frac{\partial T_{[n]}}{e_2\,\partial v}\frac{\partial T_{(m)}}{e_2\,\partial v} - \mu_{vu}\frac{\partial T_{[n]}}{e_1\,\partial u}\frac{\partial T_{(m)}}{e_1\,\partial u}\right]dS \tag{39}$$

$$+ j\omega I_{z,[n]}\iint\left[\mu_{uz}\frac{\partial T_{(m)}}{e_2\,\partial v} - \mu_{vz}\frac{\partial T_{(m)}}{e_1\,\partial u}\right]\chi_{[n]}T_{[n]}\,dS + \chi_{(m)}V_{z,(m)},$$

$$\frac{dI_{(m)}}{dz} = -j\omega V_{(n)} \iint \left[\epsilon_{uu} \frac{\partial T_{(n)}}{e_1\,\partial u} \frac{\partial T_{(m)}}{e_1\,\partial u} + \epsilon_{vv} \frac{\partial T_{(n)}}{e_2\,\partial v} \frac{\partial T_{(m)}}{e_2\,\partial v} + \epsilon_{uv} \frac{\partial T_{(n)}}{e_2\,\partial v} \frac{\partial T_{(m)}}{e_1\,\partial u} + \epsilon_{vu} \frac{\partial T_{(n)}}{e_1\,\partial u} \frac{\partial T_{(m)}}{e_2\,\partial v} \right] dS$$

$$+ j\omega V_{[n]} \iint \left[-\epsilon_{uu} \frac{\partial T_{[n]}}{e_2\,\partial v} \frac{\partial T_{(m)}}{e_1\,\partial u} + \epsilon_{vv} \frac{\partial T_{[n]}}{e_1\,\partial u} \frac{\partial T_{(m)}}{e_2\,\partial v} + \epsilon_{uv} \frac{\partial T_{[n]}}{e_1\,\partial u} \frac{\partial T_{(m)}}{e_1\,\partial u} - \epsilon_{vu} \frac{\partial T_{[n]}}{e_2\,\partial v} \frac{\partial T_{(m)}}{e_2\,\partial v} \right] dS \tag{40}$$

$$- j\omega V_{z,(n)} \iint \left[\epsilon_{uz} \frac{\partial T_{(m)}}{e_1\,\partial u} + \epsilon_{vz} \frac{\partial T_{(m)}}{e_2\,dv} \right] \chi_{(n)} T_{(n)}\, dS,$$

$$\frac{dV_{[m]}}{dz} = j\omega I_{(n)} \iint \left[\mu_{uu} \frac{\partial T_{(n)}}{e_2\,dv} \frac{\partial T_{[m]}}{e_1\,\partial u} - \mu_{vv} \frac{\partial T_{(n)}}{e_1\,\partial u} \frac{\partial T_{[m]}}{e_2\,\partial v} - \mu_{uv} \frac{\partial T_{(n)}}{e_1\,\partial u} \frac{\partial T_{[m]}}{e_1\,\partial u} + \mu_{vu} \frac{\partial T_{(n)}}{e_2\,\partial v} \frac{\partial T_{[m]}}{e_2\,\partial v} \right] dS$$

$$- j\omega I_{[n]} \iint \left[\mu_{uu} \frac{\partial T_{[n]}}{e_1\,\partial u} \frac{\partial T_{[m]}}{e_1\,\partial u} + \mu_{vv} \frac{\partial T_{[n]}}{e_2\,\partial v} \frac{\partial T_{[m]}}{e_2\,\partial v} + \mu_{uv} \frac{\partial T_{[n]}}{e_2\,\partial v} \frac{\partial T_{[m]}}{e_1\,\partial u} + \mu_{vu} \frac{\partial T_{[n]}}{e_1\,\partial u} \frac{\partial T_{[m]}}{e_2\,\partial v} \right] dS \tag{41}$$

$$- j\omega I_{z,[n]} \iint \left[\mu_{uz} \frac{\partial T_{[m]}}{e_1\,\partial u} + \mu_{vz} \frac{\partial T_{[m]}}{e_2\,\partial v} \right] \chi_{[n]} T_{[n]}\, dS,$$

$$\frac{dI_{[m]}}{dz} = j\omega V_{(n)} \iint \left[-\epsilon_{uu} \frac{\partial T_{(n)}}{e_1\,\partial u} \frac{\partial T_{[m]}}{e_2\,\partial v} + \epsilon_{vv} \frac{\partial T_{(n)}}{e_2\,\partial v} \frac{\partial T_{[m]}}{e_1\,\partial u} - \epsilon_{uv} \frac{\partial T_{(n)}}{e_2\,\partial v} \frac{\partial T_{[m]}}{e_2\,\partial v} + \epsilon_{vu} \frac{\partial T_{(n)}}{e_1\,\partial u} \frac{\partial T_{[m]}}{e_1\,\partial u} \right] dS$$

$$- j\omega V_{[n]} \iint \left[\epsilon_{uu} \frac{\partial T_{[n]}}{e_2\,\partial v} \frac{\partial T_{[m]}}{e_2\,\partial v} + \epsilon_{vv} \frac{\partial T_{[n]}}{e_1\,\partial u} \frac{\partial T_{[m]}}{e_1\,\partial u} - \epsilon_{uv} \frac{\partial T_{[n]}}{e_1\,\partial u} \frac{\partial T_{[m]}}{e_2\,\partial v} - \epsilon_{vu} \frac{\partial T_{[n]}}{e_2\,\partial v} \frac{\partial T_{[m]}}{e_1\,\partial u} \right] dS \tag{42}$$

$$+ j\omega V_{z,(n)} \iint \left[-\epsilon_{uz} \frac{\partial T_{[m]}}{e_2\,\partial v} + \epsilon_{vz} \frac{\partial T_{[m]}}{e_1\,\partial u} \right] \chi_{(n)} T_{(n)}\, dS + \chi_{[m]} I_{z,[m]},$$

$$I_{z,[n]} \iint j\omega \mu_{zz} \chi_{[n]} T_{[n]} T_{[m]}\, dS = -V_{[m]} + I_{(p)} \iint j\omega \left[\mu_{zu} \frac{\partial T_{(p)}}{e_2\,\partial v} - \mu_{zv} \frac{\partial T_{(p)}}{e_1\,\partial u} \right] T_{[m]}\, dS \tag{43}$$

$$- I_{[p]} \iint j\omega \left[\mu_{zu} \frac{\partial T_{[p]}}{e_1\,\partial u} + \mu_{zv} \frac{\partial T_{[p]}}{e_2\,\partial v} \right] T_{[m]}\, dS,$$

$$V_{z,(n)} \iint j\omega\epsilon_{zz}\chi_{(n)}T_{(n)}T_{(m)}\,dS = -I_{(m)}$$

$$- V_{(p)} \iint j\omega \left[\epsilon_{zu}\frac{\partial T_{(p)}}{e_1\,\partial u} + \epsilon_{zv}\frac{\partial T_{(p)}}{e_2\,\partial v}\right] T_{(m)}\,dS \qquad (44)$$

$$+ V_{[p]} \iint j\omega \left[-\epsilon_{zu}\frac{\partial T_{[p]}}{e_2\,\partial v} + \epsilon_{zv}\frac{\partial T_{[p]}}{e_1\,\partial u}\right] T_{(m)}\,dS.$$

If we solve the last two equations for $I_{z,[n]}$ and $V_{z,(n)}$ and substitute in the preceding four equations, we shall obtain the telegraphist's equations in their final form (30). Thus, let

$$\begin{aligned} {}^{z}Z_{[m][n]} &= \iint j\omega\mu_{zz}\chi_{[n]}T_{[n]}T_{[m]}\,dS, \\ {}^{z}Y_{(m)(n)} &= \iint j\omega\epsilon_{zz}\chi_{(n)}T_{(n)}T_{(m)}\,dS. \end{aligned} \qquad (45)$$

From these coefficients we obtain another set

$$\begin{aligned} {}^{z}Z_{[n][m]} &= \text{normalized co-factor of } {}^{z}Z_{[m][n]}, \\ {}^{z}Z_{(n)(m)} &= \text{normalized co-factor of } {}^{z}Y_{(m)(n)}. \end{aligned} \qquad (46)$$

Then,

$$\begin{aligned} I_{z,[n]} &= -V_{[m]}{}^{z}Y_{[n][m]} \\ &\quad + I_{(p)}{}^{z}Y_{[n][m]} \iint j\omega \left[\mu_{zu}\frac{\partial T_{(p)}}{e_2\,\partial v} - \mu_{zv}\frac{\partial T_{(p)}}{e_1\,\partial u}\right] T_{[m]}\,dS \\ &\quad - I_{[p]}{}^{z}Y_{[n][m]} \iint j\omega \left[\mu_{zu}\frac{\partial T_{[p]}}{e_1\,\partial u} + \mu_{zv}\frac{\partial T_{[p]}}{e_2\,\partial v}\right] T_{[m]}\,dS, \end{aligned} \qquad (47)$$

$$\begin{aligned} V_{z,(n)} &= -I_{(m)}{}^{z}Z_{(n)(m)} \\ &\quad - V_{(p)}{}^{z}Z_{(n)(m)} \iint j\omega \left[\epsilon_{zu}\frac{\partial T_{(p)}}{e_1\,\partial u} + \epsilon_{zv}\frac{\partial T_{(p)}}{e_2\,\partial v}\right] T_{(m)}\,dS \\ &\quad + V_{[p]}{}^{z}Z_{(n)(m)} \iint j\omega \left[-\epsilon_{zu}\frac{\partial T_{[p]}}{e_2\,\partial v} + \epsilon_{zv}\frac{\partial T_{[p]}}{e_1\,\partial u}\right] T_{(m)}\,dS. \end{aligned}$$

Before substituting in equations (39) to (42), the summation index m in (47) should be changed to avoid conflict with m in the former equations. It does not seem necessary to make these final substitutions in their most general form. The results are very complicated and in practice the various coefficients are not independent. Some coefficients may

vanish; others may be small. In isotropic media, $\mu_{uu} = \mu_{vv} = \mu_{zz} = \mu$, $\epsilon_{uu} = \epsilon_{vv} = \epsilon_{zz} = \epsilon$ and the mutual coefficients vanish. In gyromagnetic media subjected to a strong magnetic field in the z-direction, the permeability coefficients of superposed *ac* fields are[8]

$$\mu_{uu} = \mu_{vv} = \mu, \qquad \mu_{vu} = -\mu_{uv}, \qquad \mu_{zu} = \mu_{zv} = \mu_{uz} = \mu_{vz} = 0. \tag{48}$$

If the entire waveguide is filled with such a medium, assumed to be homogeneous, equations (43) and (44) become

$$\begin{aligned} I_{z,[n]}\, j\omega\mu_{zz}\chi_{[n]} \iint T_{[n]}T_{[m]}\, dS &= -V_{[m]}\,, \\ V_{z,(n)}\, j\omega\epsilon\chi_{(n)} \iint T_{(n)}T_{(m)}\, dS &= -I_{(m)}\,. \end{aligned} \tag{49}$$

In view of the orthogonality of the T-functions and the normalization conditions (13), we have

$$I_{z,[m]} = -\frac{\chi_{[m]}}{j\omega\mu_{zz}}\, V_{[m]}\,, \qquad V_{z,(m)} = -\frac{\chi_{(m)}}{j\omega\epsilon}\, I_{(m)}\,, \tag{50}$$

where the summation convention is waived. In this case all the transfer coefficients in equations (30) vanish,

$$\begin{aligned} {}^{v}T_{(m)(n)} = {}^{v}T_{(m)[n]} = {}^{v}T_{[m][n]} = {}^{v}T_{[m](n)} = {}^{I}T_{(m)(n)} = {}^{I}T_{(m)[n]} \\ = {}^{I}T_{[m](n)} = {}^{I}T_{[m][n]} = 0. \end{aligned} \tag{51}$$

The transfer impedances and admittances are

$$\begin{aligned} Z_{(m)(n)} &= 0, \quad \text{if } n \neq m, \\ &= j\omega\mu + \frac{\chi^2_{(m)}}{j\omega\epsilon}, \quad \text{if } n = m; \\ Z_{(m)[n]} &= -j\omega\mu_{uv} \iint \left[\frac{\partial T_{[n]}}{e_1\,\partial u}\,\frac{\partial T_{(m)}}{e_1\,\partial u} + \frac{\partial T_{[n]}}{e_2\,\partial v}\,\frac{\partial T_{(m)}}{e_2\,\partial v}\right] e_1e_2\, du\, dv; \\ Y_{(m)(n)} &= 0, \quad \text{if } n \neq m, \\ &= j\omega\epsilon, \quad \text{if } n = m; \\ Y_{(m)[n]} &= 0, \quad \text{all } m, n; \\ Z_{[m][n]} &= j\omega\mu_{uv} \iint \left[\frac{\partial T_{[n]}}{\partial v}\,\frac{\partial T_{[m]}}{\partial u} - \frac{\partial T_{[n]}}{\partial u}\,\frac{\partial T_{[m]}}{\partial v}\right] du\, dv, \quad \text{if } n \neq m, \\ &= j\omega\mu, \quad \text{if } n = m; \end{aligned} \tag{52}$$

[8] C. L. Hogan, "The Ferromagnetic Faraday Effect at Microwave Frequencies and Its Applications—The Microwave Gyrator, *Bell System Tech. J.*, Jan. 1952, p. 9.

$$Z_{[m](n)} = j\omega\mu_{uv} \iint \left[\frac{\partial T_{(n)}}{e_1 \partial u} \frac{\partial T_{[m]}}{e_1 \partial u} + \frac{\partial T_{(n)}}{e_2 \partial v} \frac{\partial T_{[m]}}{e_2 \partial v} \right] e_1 e_2 \, du \, dv;$$

$$Y_{[m][n]} = 0, \quad \text{if } n \neq m,$$

$$= j\omega\epsilon + \frac{\chi^2_{[m]}}{j\omega\mu_{zz}}, \quad \text{if } n = m;$$

$$Y_{[m](n)} = 0, \quad \text{all } m, n.$$

We note that $Z_{(m)[n]} = -Z_{[n](m)}$; $Z_{[m][n]} = -Z_{[n][m]}$, $(n \neq m)$.

In rectangular waveguides we choose cartesian coordinates; then $e_1 = e_2 = 1$, $u = x$, $v = y$ and

$$T_{(pq)} = 1_{pq} \chi^{-1}_{(pq)} (ab)^{-1/2} \sin \frac{p\pi x}{a} \sin \frac{q\pi y}{b},$$

$$T_{[st]} = 1_{st} \chi^{-1}_{[st]} (ab)^{-1/2} \cos \frac{s\pi x}{a} \cos \frac{t\pi y}{b}, \tag{53}$$

$$\chi^2_{(pq)} = \chi^2_{[pq]} = \frac{p^2\pi^2}{a^2} + \frac{q^2\pi^2}{b^2} \equiv \chi^2_{pq},$$

where $1_{pq} = 2$ if neither p nor q is equal to zero and $1_{0q} = 1_{p0} = \sqrt{2}$. Hence

$$Z_{(pq)[st]} = j\omega\mu_{xy} \frac{1_{pq} 1_{st} \pi^2}{a^2 b^2 \chi_{pq} \chi_{st}} \times \iint \left[(b/a) sp \sin \frac{s\pi x}{a} \cos \frac{p\pi x}{a} \cos \frac{t\pi y}{b} \sin \frac{q\pi y}{b} + (a/b) tq \cos \frac{s\pi x}{a} \sin \frac{p\pi x}{a} \sin \frac{t\pi y}{b} \cos \frac{q\pi y}{b} \right] dx \, dy$$

$$= j\omega\mu_{xy} \frac{1_{pq} 1_{st} pq[(s/a)^2 + (t/b)^2][1 - (-)^{s+p}][1 - (-)^{q+t}]}{\chi_{pq} \chi_{st} (s^2 - p^2)(q^2 - t^2)}, \tag{54}$$

$$\text{if } s \neq p, \; q \neq t,$$

$$= 0, \quad \text{if } s = p \text{ or } q = t;$$

$$Z_{[pq][st]} = j\omega\mu_{xy} \frac{1_{pq} 1_{st} (p^2 t^2 - q^2 s^2)[1 - (-)^{s+p}][1 - (-)^{q+t}]}{\chi_{pq} \chi_{st} (s^2 - p^2)(q^2 - t^2) ab},$$

$$\text{if } s \neq p, \; q \neq t,$$

$$= 0, \quad \text{if } s = p \text{ or } q = t, \text{ but not if } s = p \text{ and } q = t,$$

$$= j\omega\mu, \quad \text{if } s = p \text{ and } q = t.$$

Some of the mutual impedances vanish; thus

$$Z_{(pq)[st]} = 0, \tag{55}$$

if either $p + s$ *or* $q + t$ *is even.* If $p + s$, as well as $q + t$, is odd,

$$Z_{(pq)[st]} = \frac{4 \cdot 1_{pq} 1_{st} j\omega\mu_{xy} pq[(s/a)^2 + (t/b)^2]}{\chi_{pq}\chi_{st}(s^2 - p^2)(q^2 - t^2)}. \tag{56}$$

Similarly

$$Z_{[pq][st]} = 0, \tag{57}$$

if either $p + s$ *or* $q + t$ *is even,* provided $p \neq s$ and $q \neq t$. If $p + s$, as well as $q + t$, is odd,

$$Z_{[pq][st]} = \frac{4 \cdot 1_{pq} 1_{st}(p^2t^2 - q^2s^2) j\omega\mu_{xy}}{\chi_{pq}\chi_{st}(s^2 - p^2)(q^2 - t^2)ab}. \tag{58}$$

Consider now the set of modes which includes $TE_{[10]}$. This set includes $TE_{[01]}$ modes and all the other modes which are coupled to either of these modes. Noting that there are no $TM_{(p0)}$ and $TM_{(0q)}$ modes, we obtain the following table in which those modes which do not belong to the set are marked with a bar:

$$\begin{aligned}
&TE_{[10]}\ ,\ TE_{[01]}\ ,\\
&\overline{TE}_{[20]}\ ,\ \overline{TE}_{[11]}\ ,\ \overline{TE}_{[02]}\ ,\ \overline{TM}_{(11)}\ ,\\
&TE_{[30]}\ ,\ TE_{[21]}\ ,\ TE_{[12]}\ ,\ TE_{[03]}\ ,\ TM_{(21)}\ ,\ TM_{(12)}\ ,\\
&\overline{TE}_{[40]}\ ,\ \overline{TE}_{[31]}\ ,\ \overline{TE}_{[22]}\ ,\ \overline{TE}_{[13]}\ ,\ \overline{TE}_{[04]}\ ,\ \overline{TM}_{(31)}\ ,\ \overline{TM}_{(22)}\ ,\ \overline{TM}_{(13)}\ ,
\end{aligned} \tag{59}$$

From the preceding equations we obtain the coupling impedances,

$$\begin{aligned}
&Z_{[10][01]} = \frac{8}{\pi^2} j\omega\mu_{xy}\ ,\ Z_{[01][10]} = -\frac{8}{\pi^2} j\omega\mu_{xy}\ ,\\
&Z_{[10][30]} = Z_{[30][10]} = Z_{[01][03]} = Z_{[03][01]} = 0,\\
&Z_{[30][01]} = -Z_{[01][30]} = Z_{[10][03]} = -Z_{[03][10]} = \frac{8}{3\pi^2} j\omega\mu_{xy}\ ,\\
&Z_{[21][10]} = -Z_{[10][21]} = \frac{8\sqrt{2}}{3\pi^2} j\omega\mu_{xy}[1 + 4(b/a)^2]^{-1/2},\\
&Z_{[01][12]} = -Z_{[12][01]} = \frac{8\sqrt{2}}{3\pi^2} j\omega\mu_{xy}[1 + 4(a/b)^2]^{-1/2},\\
&Z_{[10][12]} = Z_{[12][10]} = Z_{[01][21]} = Z_{[21][01]} = 0,\\
&Z_{[10](21)} = -Z_{(21)[10]} = \frac{16\sqrt{2}}{3\pi^2} j\omega\mu_{xy}[4 + (a/b)^2]^{-1/2},
\end{aligned} \tag{60}$$

$$Z_{[01](12)} = -Z_{(12)[01]} = \frac{16\sqrt{2}}{3\pi^2} j\omega\mu_{xy}[4 + (b/a)^2]^{-1/2},$$

$$Z_{(12)[10]} = Z_{[10](12)} = Z_{(21)[01]} = Z_{[01](21)} = 0.$$

The principal effect of the gyromagnetic medium on the $TE_{[10]}$ and $TE_{[01]}$ modes may be understood by taking into account their mutual coupling but ignoring their coupling to other modes. The equations of propagation become

$$\begin{aligned}
\frac{dV_{[10]}}{dz} &= -j\omega\mu I_{[10]} - j\omega\mu_{xy}(8/\pi^2)I_{[01]}, \\
\frac{dI_{[10]}}{dz} &= -\left(j\omega\epsilon + \frac{\pi^2}{j\omega\mu_{zz}a^2}\right)V_{[10]}, \\
\frac{dV_{[01]}}{dz} &= j\omega\mu_{xy}(8/\pi^2)I_{[10]} - j\omega\mu I_{[01]}, \\
\frac{dI_{[01]}}{dz} &= -\left(j\omega\epsilon + \frac{\pi^2}{j\omega\mu_{zz}b^2}\right)V_{[01]}.
\end{aligned} \tag{61}$$

For exponentially propagated waves we have

$$\begin{aligned}
V_{[10]} &= \hat{V}_{[10]}e^{-j\beta z}, \qquad V_{[01]} = \hat{V}_{[01]}e^{-j\beta z}, \\
I_{[10]} &= \hat{I}_{[10]}e^{-j\beta z}, \qquad I_{[01]} = \hat{I}_{[01]}e^{-j\beta z}.
\end{aligned} \tag{62}$$

When the mutual permeability is zero, we have two independent modes whose phase constants are

$$\beta_{10} = \left(\omega^2\mu\epsilon - \frac{\mu\pi^2}{\mu_{zz}a^2}\right)^{1/2}, \qquad \beta_{01} = \left(\omega^2\mu\epsilon - \frac{\mu\pi^2}{\mu_{zz}b^2}\right)^{1/2}. \tag{63}$$

The phase constants of the perturbed modes may be expressed in terms of the unperturbed constants and the coefficient of coupling. When the losses are neglected, the mutual permeability is a pure imaginary. In this case it is convenient to define a *real* coupling coefficient

$$k = \frac{j8\mu_{xy}}{\pi^2\mu}. \tag{64}$$

Substituting from (62) in (61) and using (64), we find

$$\begin{aligned}
\beta\hat{V}_{[10]} &= \omega\mu\hat{I}_{[10]} - j\omega\mu k\hat{I}_{[01]}, \qquad \beta\hat{I}_{[10]} = \left(\omega\epsilon - \frac{\pi^2}{\omega\mu_{zz}a^2}\right)\hat{V}_{[10]}, \\
\beta\hat{V}_{[01]} &= j\omega\mu k\hat{I}_{[10]} + \omega\mu\hat{I}_{[01]}, \qquad \beta\hat{I}_{[01]} = \left(\omega\epsilon - \frac{\pi^2}{\omega\mu_{zz}b^2}\right)\hat{V}_{[01]}.
\end{aligned} \tag{65}$$

Eliminating $\hat{V}_{[10]}$ and $\hat{V}_{[01]}$, we have

$$\begin{aligned}(\beta^2 - \beta_{10}^2)\hat{I}_{[10]} &= -jk\beta_{10}^2\hat{I}_{[01]}\,,\\ (\beta^2 - \beta_{01}^2)\hat{I}_{[01]} &= jk\beta_{01}^2\hat{I}_{[10]}\,.\end{aligned} \tag{66}$$

Multiplying term by term, we obtain the characteristic equation

$$\beta^4 - (\beta_{10}^2 + \beta_{01}^2)\beta^2 + (1 - k^2)\beta_{10}^2\beta_{01}^2 = 0. \tag{67}$$

Solving, we have

$$\beta^2 = \tfrac{1}{2}(\beta_{10}^2 + \beta_{01}^2) \pm \tfrac{1}{2}[(\beta_{10}^2 - \beta_{01}^2)^2 + 4k^2\beta_{10}^2\beta_{01}^2]^{1/2}. \tag{68}$$

The effect of coupling is to increase the larger phase constant and decrease the smaller one; that is, to make the slower wave slower, and the faster wave faster.

Let us assume $a > b$; then $\beta_{10} > \beta_{01}$. Taking the upper sign in (68) and substituting in the second equation of the set (66), we have

$$\frac{\hat{I}_{[01]}}{\hat{I}_{[10]}} = \frac{jk(\beta_{01}/\beta_{10})}{p + (p^2 + k^2)^{1/2}}, \qquad p = \frac{1}{2}\left(\frac{\beta_{10}}{\beta_{01}} - \frac{\beta_{01}}{\beta_{10}}\right). \tag{69}$$

From (65) and (69) we find

$$\frac{\hat{V}_{[01]}}{\hat{V}_{[10]}} = \frac{\beta_{10}^2}{\beta_{01}^2}\frac{\hat{I}_{[01]}}{\hat{I}_{[10]}} = \frac{jk(\beta_{10}/\beta_{01})}{p + (p^2 + k^2)^{1/2}}. \tag{70}$$

Hence, the ratio of the power carried in the $TE_{[01]}$ mode to that in the $TE_{[10]}$ mode is

$$\frac{P_{01}}{P_{10}} = \frac{\hat{V}_{[01]}\hat{I}_{[01]}^*}{\hat{V}_{[10]}\hat{I}_{[10]}^*} = \frac{k^2}{[p + (p^2 + k^2)^{1/2}]^2}. \tag{71}$$

This ratio increases as k increases and p decreases.

If the phase constants of the uncoupled modes are equal, then $p = 0$ and $P_{01} = P_{10}$ for all values of the coupling coefficient. In this case (68) becomes

$$\beta^2 = \beta_{10}^2(1 \pm k) \quad \text{or} \quad \beta = \beta_{10}(1 \pm k)^{1/2}. \tag{72}$$

In terms of the original constants,

$$\beta = \left[\left(\mu \pm \frac{8}{\pi^2}\,j\mu_{xy}\right)\left(\omega^2\epsilon - \frac{\pi^2}{\mu_{zz}a^2}\right)\right]^{1/2}. \tag{73}$$

The cutoff frequencies of both normal modes are seen to be independent of either the transverse permeability or the mutual permeability. Since

μ_{xy} is a pure imaginary, it effectively increases the transverse permeability for one mode and decreases it for the other.

To evaluate the effect of higher order TE and TM modes on wave propagation we may substitute from (68) in all terms of the characteristic equation for telegraphist's equations except the first two diagonal terms and recalculate the β's. Alternatively we may replace $TE_{[10]}$ and $TE_{[01]}$ modes by the normal modes just obtained, recalculate the coupling coefficients, and evaluate the effect of the mode with the greatest coupling to the modes under consideration.

Photoelectric Properties of Ionically Bombarded Silicon

By EDWIN F. KINGSBURY and RUSSELL S. OHL

(Manuscript received March 25, 1952)

In the course of investigation of the rectifying properties of silicon very interesting photoelectric properties were found. The first photo-cells were cut from bulk silicon in which a natural potential barrier was found. A typical spectral characteristic of such a cell is shown. This early work was followed by the discovery of the ionic bombardment method of producing photo active silicon surfaces. The effects of the temperature of the target and of the energy of the bombarding particles in the photoelectric properties is illustrated by characteristic curves. Relative equi-energy spectral response characteristics as a function of wavelength are illustrated. The photon efficiency as a function of wavelength of a typical cell is shown.

INTRODUCTION

Because of the importance that barriers have come to assume in the general field of semiconductors the authors have been urged to publish results of their early experiments in this field. These experiments were undertaken in the course of a search for semiconductive material suitable for use as point contact rectifiers.

Before March 1941[1] one of the writers discovered a well-defined barrier having a high degree of photovoltaic response. The barrier was found only in melts of some lots of commercially available high-purity silicon. This barrier showed a high photovoltaic sensitivity to radiation from incandescent lamps.

The existence of this natural barrier was first observed in rods cut from melts for resistivity measurements. These rods showed a high degree of photovoltaic response, were found to have a high thermoelectric coefficient, and had good rectifying properties.[1] The fact that one end of the rod developed a negative potential when illuminated or heated and that when supplied with a negative potential showed low resistance to current flow across the barrier led to the terminology of *n*-type

silicon. The material of opposite type was named p-type. Material of the n-type is now known to derive its electrical properties from the presence in the crystal lattice of electron donor impurities, for example phosphorus, while p-type derives its electrical properties from the presence of electron acceptor impurities, such as boron. In this paper some of the results of investigations of the natural barrier are reported; however, the photovoltaic properties of induced barriers obtained by the ionic bombardment of p-type silicon will be given more detail treatment.

EARLY RESULTS

The approximate location of the natural barrier found in early melts is shown in Fig. 1. The barrier was generally located in the melt perpendicular to the axis of the melting crucible or more accurately to the direction of the temperature gradient. Plates and rods containing sections of the photoactive barrier, Fig. 1a, were cut from the melt and mounted on convenient supports for laboratory tests. Fig. 1c shows a magnified section of one of these barriers.[2]

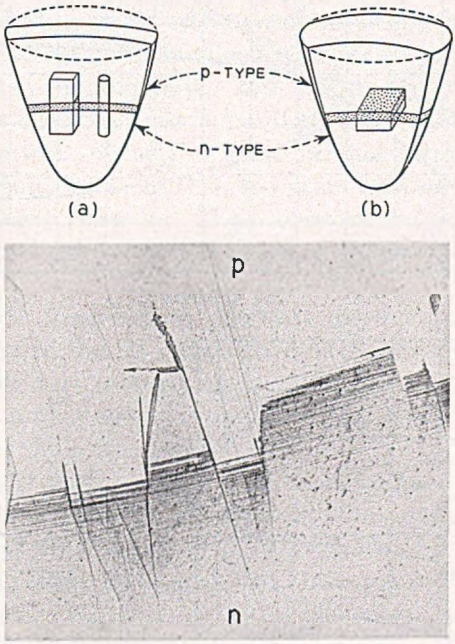

Fig. 1—(a) Drawing of melt showing position of photovoltaic barrier and photo cells with natural barrier. (b) Drawing of melt showing surface type photo cell made from natural barrier. (c) Magnified, etched section of slowly cooled silicon showing the transition between p and n silicon forming the barrier which consists of intermeshed striae of these two varieties.

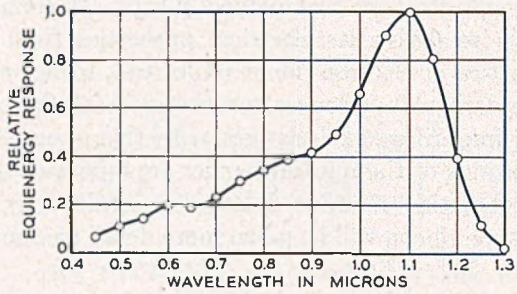

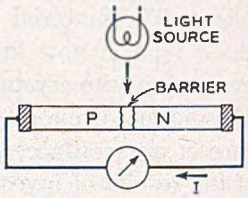

(a)

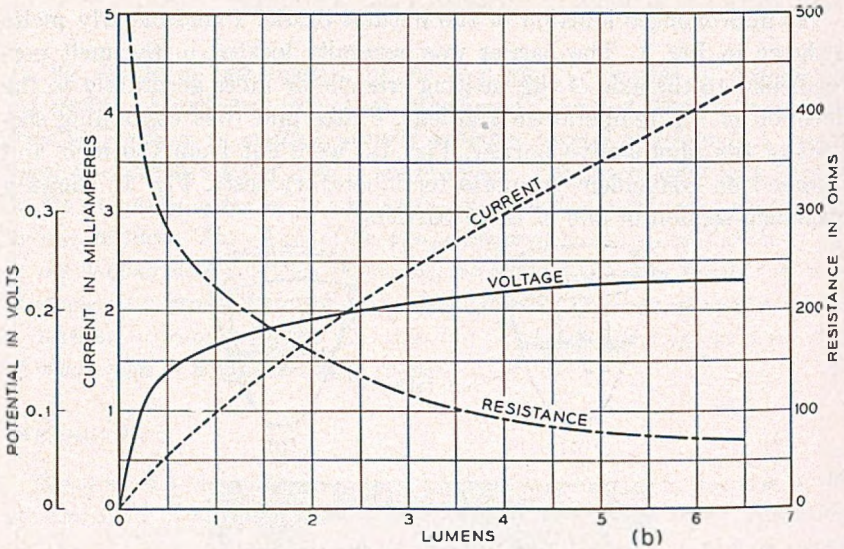

(b)

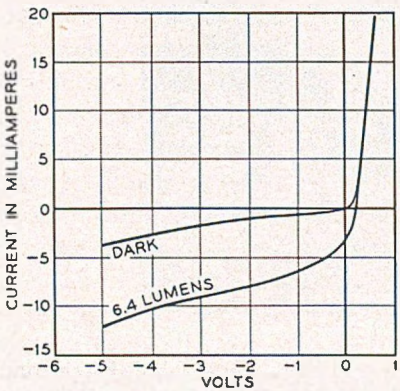

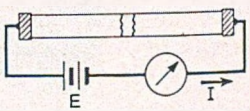

(c)

Fig. 2a—Spectral response of internal barrier in silicon.
Fig. 2b—Voltage and current photosensitivity of internal barrier in silicon.
Fig. 2c—Rectification characteristic of internal barrier, dark and illuminated.

A typical spectral response curve of such a barrier is shown in Fig. 2a while Fig. 2b gives its open circuit voltage, short-circuit current and resistance when illuminated by a tunsten light of 2848°K color temperature. This cell resistance was taken as equal to that of an added series resistance which reduced the short-circuit photocurrent to one-half. The value so obtained is somewhat higher than the corresponding ratio of the voltage and current given in the figure. Fig. 2c gives the behavior as a rectifier in the dark and with a stated light on the barrier.

Cells whose barrier was near the surface were made by cutting close to the natural one as shown in Fig. 1b. This cut exposed large photoactive areas. Surface barrier activity was occasionally found on the top surface of some melts. These surface type cells showed a wider spectral response toward the visible than the internal barrier type. This was found to be due to the spectral absorption characteristics of the bulk silicon. A further discussion of this appears later in the paper.

These early barrier cells showed remarkable stability under severe temperature conditions. For instance, they could be heated to redness in air and quenched in water with no serious change in their characteristics. They were tested in liquid nitrogen, under water and in oil without injury. They could be illuminated with direct sunlight with no injury to their response characteristics other than the temporary effect of the increased temperature. Several of these internal barrier cells have been in use in test circuits for more than ten years with no serious change in their photoresponse properties. These observations seemed to indicate clearly that a very high degree of stability could be expected from silicon photocells.

However, there were serious practical disadvantages to the early cells. Those shown in Fig. 1a were active near the exposed barrier itself which was usually a strip along the surface about $\frac{1}{2}$ mm wide. On the other hand, the surface types as shown in Fig. 1b showed irregular responsiveness over the surface area.

From these early studies it was clear that if a good method could be found to activate large areas of silicon surfaces uniformly, cells could be made which might compete with other kinds of surface barrier type cells already available. The search for such a process resulted in the ionic bombardment method of activating silicon surfaces. Such surfaces also have desirable rectifying properties.[3]

METHOD OF PREPARATION

Hyper-purity silicon was used for bombardment type cells to avoid the formation of natural barriers due to minute impurities and to give

better control of the sensitivity. After being cast in a fused silica crucible, the roughly cylindrical piece was ground to a cylinder about $1\frac{1}{2}''$ diameter, a process which removed crucible contamination and gave a convenient size for slicing into wafers about 0.025″ thick. The two faces were then made approximately flat and parallel after which one was left rough and the other ground and polished down to a good optical surface. In most cases the discs were then cleaned by soaking for approximately fifteen minutes in a solution of hydrofluoric acid, rinsed in distilled water and dried.

The activation consisted of exposing the polished face to a uniform beam of positive ions of helium at a pressure of 10^{-3} to 10^{-4} mm of

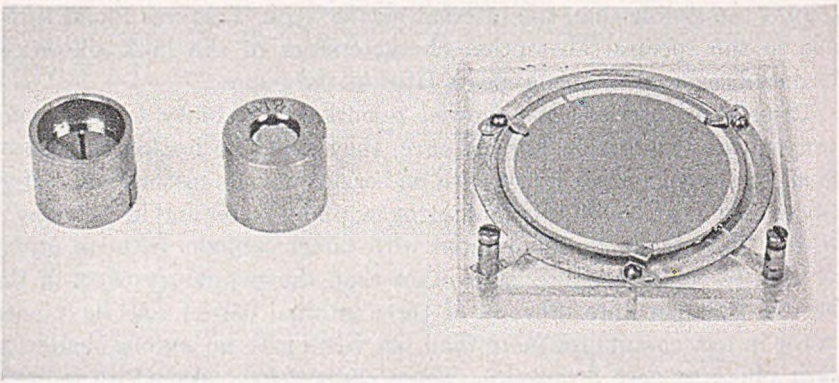

Fig. 3—Intermediate and large size photocells made by ion bombardment. Back of the intermediate also shown.

mercury. The energy of the particles used in different units ranged from 100 to 30,000 electron volts. During this bombardment the silicon surface was kept at a favorable temperature, about 395°C.

After activation, collector electrodes of evaporated rhodium were applied. Cells of three sizes have been constructed, two of which are shown in Fig. 3, the intermediate and the large one, of exposed active areas about 0.40 and 8.0 sq. cm. respectively. A small one had an area around 0.005 sq. cm. Most of the measurements reported in this paper have been made with the intermediate size.

EFFECT OF ION VELOCITY

That ion velocity has a profound effect on the voltage current characteristic of bombarded surfaces is shown in Fig. 5. These characteristics were obtained by placing a tungsten point contact under 10 gm of force,

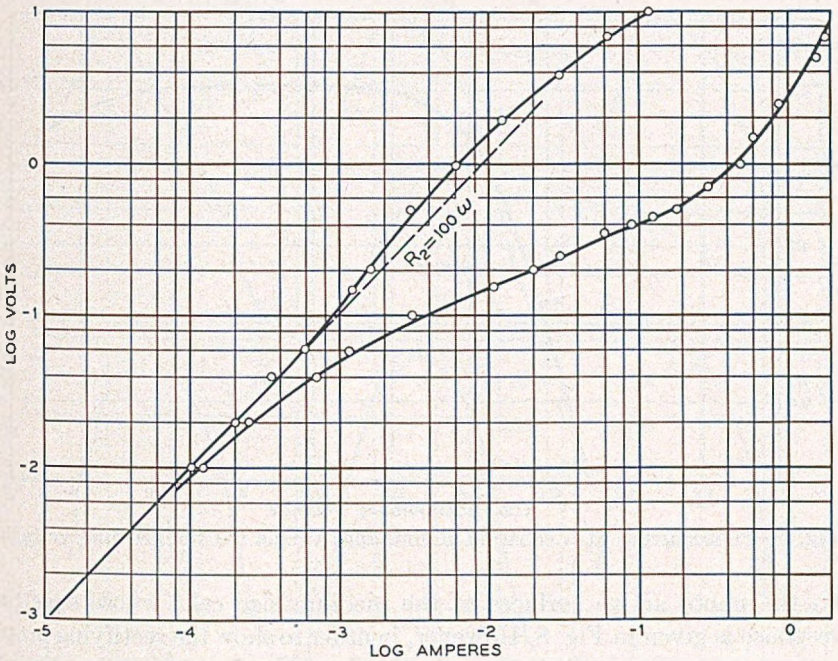

Fig. 4—Rectification characteristic of the large photocell.

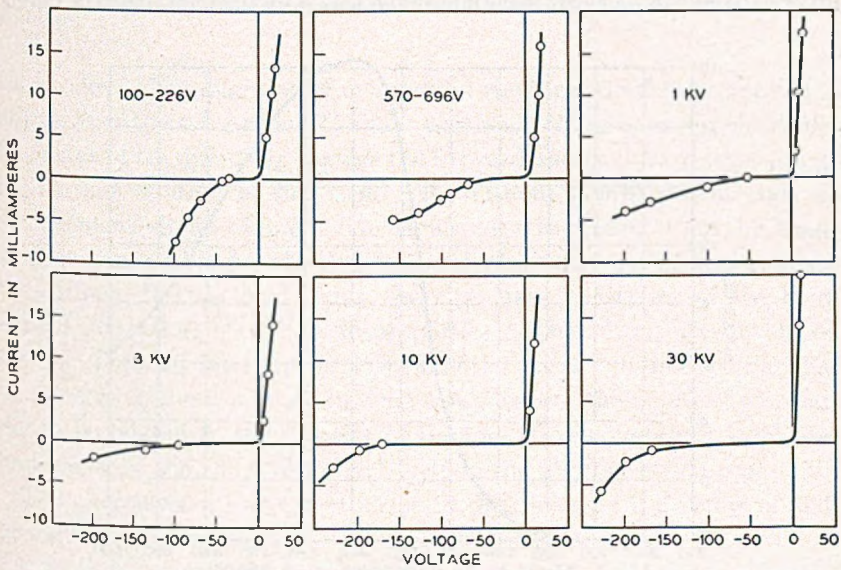

Fig. 5—Effect of bombardment voltage on the rectification of the intermediate cells.

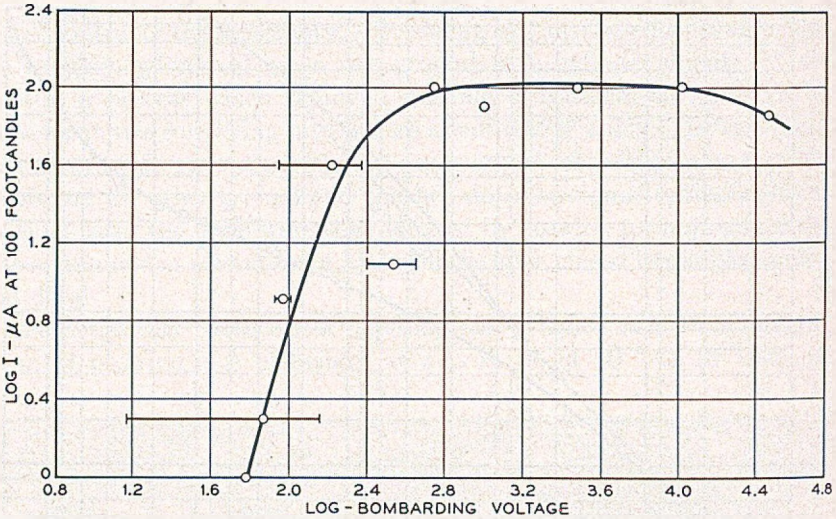

Fig. 6—Photocurrent at a constant illuminance versus the bombarding voltage.

on the photo active surfaces of the medium size cells whose spectral response is given in Fig. 8. However, in order to show the rectifying property of the barrier without the complication of a point contact, a disc of hyper-purity silicon $1\frac{1}{2}''$ in diameter and about 0.025″ thick was given an optical polish on both faces. One face was bombarded with 30-kv ions.

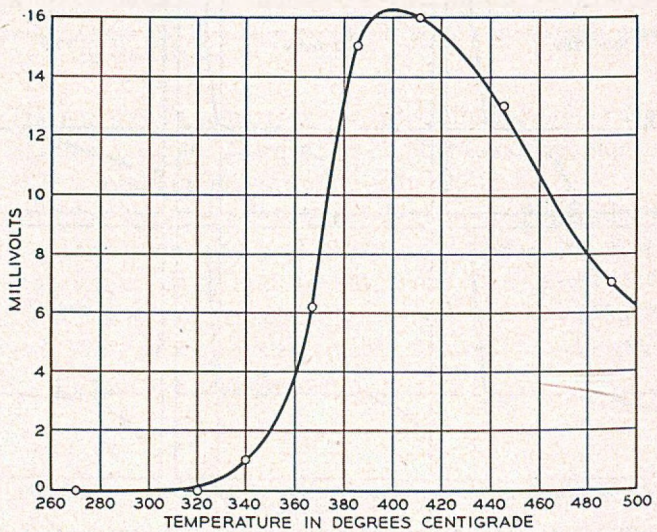

Fig. 7—Photovoltage at a constant illumination versus temperature of the bombarded silicon surface.

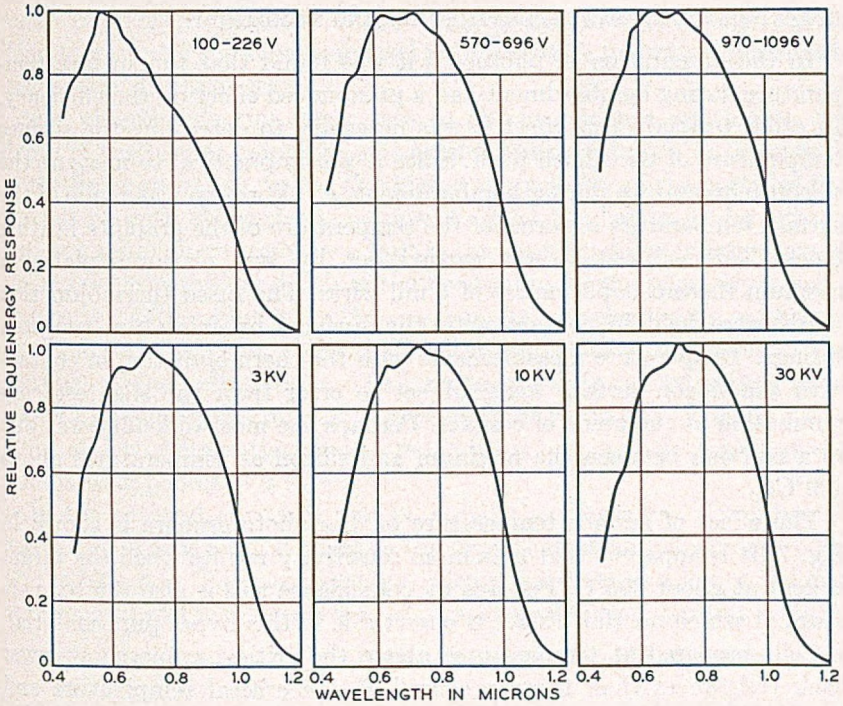

Fig. 8—Spectral response of the intermediate size cells at various bombarding voltages.

Electrodes $1\frac{1}{8}''$ in diameter of evaporated rhodium metal were applied in like manner to each surface. Contact was made to the collector electrodes by means of tin discs. Fig. 4 gives the forward and backward log voltage-log current relation of this large cell. Without bombardment such an arrangement shows ohmic conductivity so it is evident that the treatment is responsible for the development of a potential barrier beneath the surface. It is believed from the high dark resistivity of the bombarded layer that the intrinsic properties of the silicon are developed therein. Thus an intrinsic -p type potential barrier is produced similar to a degree to the n-p junction. One would expect the depth of this barrier to be related to the velocity of the ions. Consequently a study has been made of the effect of ion velocity on the photoelectric properties.

The photoelectric current at constant illuminance for a series of cells prepared by bombardment with ions of different energies is shown in Fig. 6. It is remarkable how quickly and completely the current sensitivity saturates at approximately 500 volts.

EFFECT OF SURFACE TEMPERATURE DURING BOMBARDMENT

In the preparation of photocells it was found that the surface temperature during bombardment had a pronounced effect on the efficiency. In order to study this effect it was necessary to determine the surface temperature of the silicon itself. Since it was impractical to measure the silicon temperature during bombardment, a calibration was made of the surface temperature in terms of the temperature of the graphite heating block. This calibration was carried out by two platinum/platinum rhodium thermocouples made of 5-mil wires. The fused thermojunction beads were held in contact with the surfaces by miniature tungsten springs. Temperature measurements with the thermojunction in contact with the silicon surface were subject to error from the slightest contamination at the point of contact. Perhaps the most difficulty was due to a reaction between the platinum and silicon at temperatures above 400°C.

The effect of surface temperature on the photoresponse is shown in Fig. 7. It is apparent that maximum sensitivity results when the target is kept at about 395°C. Perhaps by coincidence this is also the temperature at which no Hall Effect is observable in this hyper-pure material.

Cells prepared at temperatures above the critical value show lower back resistances than those prepared at the critical temperature and conversely those at temperatures below the critical value have higher back resistances but a much reduced photoresponse.

EFFECT OF TOTAL BOMBARDING CHARGE

The photoresponsiveness improves as the total bombarding charge is increased until it has reached about 600 microcoulombs per sq. cm. Further bombardment produces no appreciable improvement. In certain exploratory tests a total charge of about 9000 microcoulombs at 30 kv has been applied. Under these severe conditions the surface may show small areas having a slightly etched appearance.

No extensive tests have been made to determine the effect of the rate of application of the bombarding charge. The apparatus was designed for use at a rate of about 5 microamperes per sq. cm. It is known however, that between the limits of about 2.5 and 10 microamperes per sq. cm. the effects are subject only to the total charge or the total number of ions which strike the silicon surface.

EFFECT OF BOMBARDMENT VOLTAGE IN SPECTRAL RESPONSE

Six spectral curves are shown in Fig. 8 which illustrate the result obtained with the intermediate size cells over the bombardment voltage

range previously mentioned. The peak of the lowest voltage cell is definitely toward the blue compared with the other five whose maximum is constant at about 0.725 μ.

One objective in this study was to obtain evidence relating to the depth of the barrier below the silicon surface as a function of the energy of the bombarding particles. The higher the velocity of the particles the further beneath the surface one would expect the barrier to be located and as a result there might be a shift in the spectral characteristic toward the red with increasing depth of the barrier due to the relatively greater absorption at the blue end. There is however, a selective or secondary maximum at the peak which sharpens it and nullifies the effect of the warping of the entire curve. The blue to red shift can be shown as in Fig. 9 by plotting the ratio of the responses in Fig. 8 at 0.50 μ and 1.0 μ. Thus at low voltage the blue to red ratio is high and decreases as the bombarding potential is raised.

In the spectral curves it will be noted that there are a number of secondary humps located near the top of the curves and extending down on the blue side. There is a strong tendency for them to occur at definite wavelengths and to be evenly spaced regardless of the bombarding voltage.

SPECTRAL MEASUREMENTS ON THE LARGE CELLS AND THE EFFECT OF MATERIAL COMPOSITION

For the large cells, two grades of silicon were used both prepared by pyrolytic reduction of $SiCl_4$ and called "hyper-pure". These will be

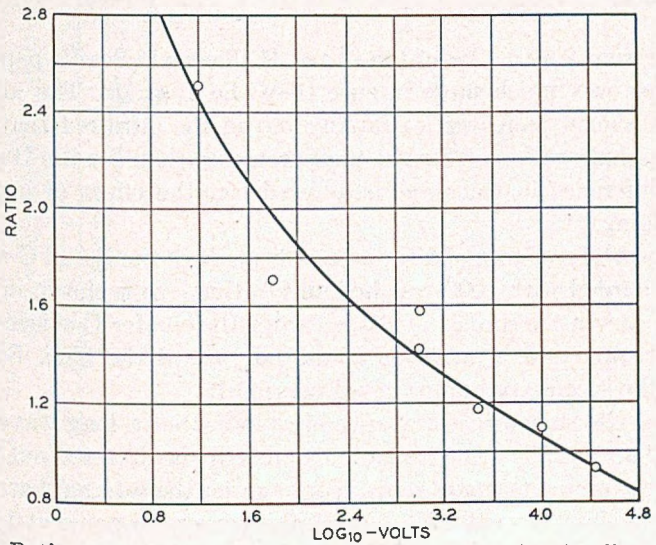

Fig. 9—Ratio of blue to near infra-red response versus bombarding voltage.

designated B and C, the former being from the same source as "silicon B" referred to in the paper by Scaff et al.[2] A typical analysis is given therein. The C silicon was from another source and a spectroscopic analysis indicated it was somewhat more impure than B thus agreeing with observed differences in its electrical and optical characteristics. An optical variation of considerable interest is shown in Fig. 10 where the spectral transmittance of the two grades of silicon is compared in the infra-red for polished plates each 0.0195″ thick.

The transmittance of B decreases a little with increasing wavelength but C goes down much more. Both however, start to get transparent at about the same point, 1.1 μ and also show corresponding absorption bands superimposed on the main curve. Briggs[4] has compared the trans-

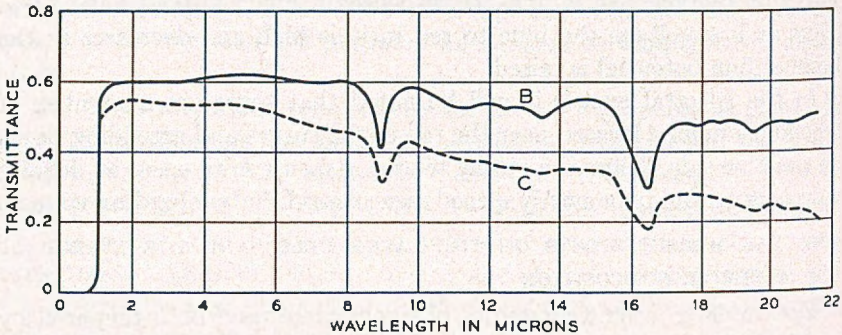

Fig. 10—Spectral transmittance of B and C grades of silicon, polished plates, 0.0195″ thick.

mittance from 2 μ to 12 μ of the A and B silicons in Scaff's paper where the former was much more impure than the C grade. The absorption of the A silicon increased so rapidly out in the infra-red that a much thinner sample was used for the measurements than for the B material. If this difference in thickness is allowed for, the effect of impurity is very striking.

The spectral response of large area cells made of the B and C materials and bombarded with 1000-volt helium positive ions is shown in Fig. 11. The two curves are similar in shape except the one for C silicon is somewhat narrower and in addition is shifted toward the blue. Both have some of the secondary humps noted previously.

All the cells shown in this paper have indicated a long wave limit of about 1.2 μ. Actually some response can usually be detected out to about 1.3 μ. Measurements made some years ago on the internal barrier units also gave a limit around 1.3 μ but relatively more response at 1.2 μ with peaks close to 1.10 μ. This difference is reasonable because light was

projected along the barrier plane and not normal to it as in the latest units, so that with the rapidly increasing transparency in this region, less infra-red radiation was lost. However, the blue was rapidly attenuated.

When illuminated by tungsten light of 2848°K color temperature, the large B cells gave 2160 microamps per lumen and the C unit 638. Correcting for a surface reflectance of 0.385, the net sensitivities would be 3510 and 1040. These measurements were made with between 4- and 5-footcandles illuminance on the cells, a region in which the response is proportional to the intensity. At much higher values of illuminance there was some falling off of response so that the effective sensitivity was a little lower. The above measurements were made on a ten ohm microammeter which is too low a resistance to affect the linearity. The intermediate cells ran approximately 3000 microamps per lumen in the most sensitive region of bombardment without correction for surface reflection and at 10- to 20-footcandles for the same tungsten lamp using a meter of 76 ohms.

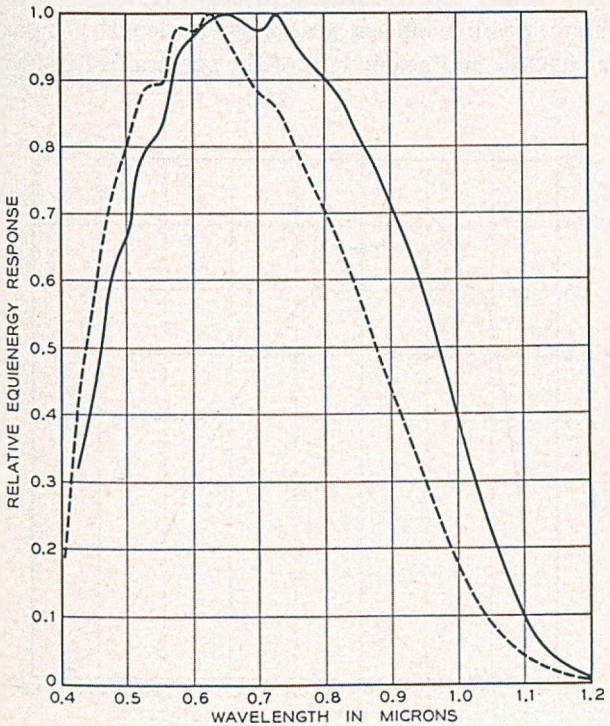

Fig. 11—Spectral response of large size photocells of B and C grades of silicon.

PHOTON EFFICIENCY

It is of interest to examine the spectral photon efficiency of a cell made by bombardment. As an example, there may be taken the 3-kv cell whose spectral response is shown in Fig. 8. When illuminated by a tungsten light of 2848°K color temperature at 10-foot candles, a sensitivity of 3090 microamps per lumen was secured. Allowing for a surface reflectance loss of 0.385, this value becomes 5020 for the radiation actually absorbed. From these data the sensitivity in microamps per microwatt at the peak 0.725 μ, calculates to be 0.388 and the photon efficiency, i.e., the electrons per photon, 0.66. Fig. 12 gives the efficiency through the spectrum. Note that the efficiency rises some on the short wave side shifting the peak of the equi-energy curve (Fig. 8) over to 0.625 μ. This increase is evident from the fact that if the equi-energy curve decreased linearly from the peak at 0.725 μ to zero at 0 μ, the photon efficiency would remain constant and equal to that at 0.725 μ. For the purpose of the above calculation, the curve in Fig. 8 has been taken as going to zero at about 0.40 μ, a fact experimentally checked. If unity is considered to be the maximum possible efficiency at any wavelength, 72 per cent of it is attained at 0.625 μ and nearly half of the spectral range is 50 per cent or higher.

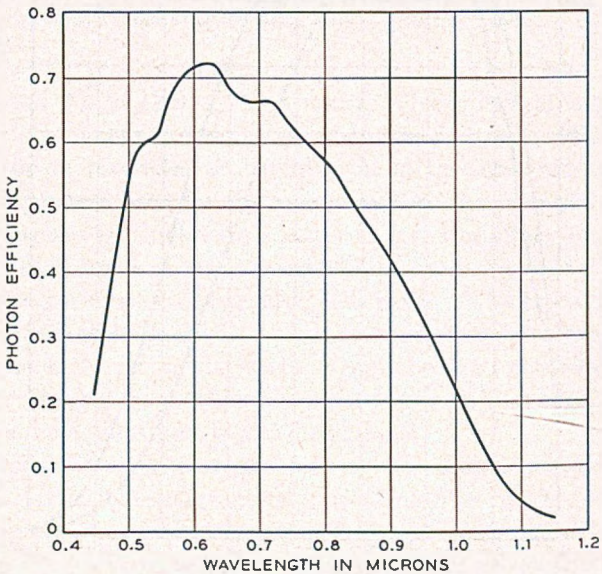

Fig. 12—Spectral photon efficiency of the 3-kv cell of Fig. 8.

CONCLUDING REMARKS

These experiments have served not only to introduce us to some of the phenomena involved in semiconductor barriers but have also yielded photo cells having desirable properties. These cells have a high degree of stability and will stand treatment ruinous to most other cells. They have a very high current sensitivity to tungsten light and daylight. They require no associated battery and can be made in large areas. Unlike the material used in many types of photo cells, silicon does not have the disadvantage of scarcity. All tests to date indicate that an indefinitely long life may be expected even under extreme illumination. Fig. 11 suggests that it may be possible to control to some extent the spectral response in the region from the deep blue into the infra-red. The long wave limit is set by the edge of the absorption characteristic.

REFERENCES

1. U. S. Patent No. 2,402,839, Filed Mar. 27, 1941.
   U. S. Patent No. 2,402,662, Filed May 27, 1941.
   U. S. Patent No. 2,443,542, Filed May 27, 1941.
2. J. H. Scaff, H. C. Theuerer and E. E. Schumacher; also W. G. Pfann and J. H. Scaff, *Trans. A. I. M. E.*, **185**, pp. 383–392, 1949.
3. R. S. Ohl, *Bell System Tech. J.*, Jan., 1952. Also see this paper for more details regarding the method of preparing silicon.
4. H. B. Briggs, *Phys. Rev.*, **77**, pp. 727–728, Mar. 1, 1950.

Abstracts of Bell System Technical Papers* Not Published in This Journal

Mechanical Properties of Discrete Polymer Molecules. W. O. Baker[1], W. P. Mason[1] and J. H. Heiss[1]. *J. Polymer Sci.*, **8**, pp. 129–155, Feb., 1952. (Monograph 1937).

Post-War Achievements of Bell Laboratories: II. O. E. Buckley[1]. *Bell Tel. Mag.*, **30**, No. 4, pp. 224–237, 1951–1952.

A Portable, Direct-Reading Microwave Noise Generator. E. L. Chinnock[1]. *Proc. Inst. Radio Engrs.*, **40**, pp. 160–164, Feb., 1952. (Monograph 1939).

This paper discusses the factors which influenced the design of a directly calibrated portable microwave noise source, utilizing a fluorescent lamp. The variation of the noise power output and the impedance match as a function of the operating temperature are considered, and the portable unit is described.

The Quantum Theory. K. K. Darrow[1]. *Sci. Am.*, **186**, pp. 47–54, Mar., 1952. (Monograph 1940).

Concerning the early years of this fundamental concept of modern physics—how Max Planck formulated it at the turn of the century and how others enlarged it up to 1923.

Performance of Ultrasonic Vitreous Silica Delay Lines. M. D. Fagan[1]. *Tele-Tech*, **11**, pp. 43–45, 138+, Mar., 1952. (Monograph 1951).

Results of tests at 10 and 60 mc with resistive terminations of 75 to 1000 ohms. Low terminating impedance values yield wide bands but involve higher insertion losses.

Phase Transition of $ND_4D_2PO_4$. B. T. Matthias[1]. *Phys. Rev.*, v. **85**, p. 141, Jan. 1, 1952.

Engineering Local Television Facilities and Their Operation. B. D.

---

* Certain of these papers are available as Bell System Monographs and may be obtained on request to the Publication Department, Bell Telephone Laboratories, Inc., 463 West Street, New York 14, N. Y. For papers available in this form, the monograph number is given in parentheses following the date of publication, and this number should be given in all requests.

[1] Bell Telephone Laboratories.

WICKLINE[4] and J. E. FARLEY[4]. *Elec. Eng.*, **71**, pp. 252–257, Mar., 1952.

All the means of electrical communication are called into play when a city-wide coverage of an event is to be televised. How telephone and television facilities were utilized on the day that Chicago welcomed General MacArthur is explained in this article.

Echo Distortion in the FM Transmission of Frequency-Division Multiplex. W. J. ALBERSHEIM[1] and J. P. SCHAFER[1]. *Proc. Inst. Radio Engrs.*, **40**, pp. 316–328, March, 1952.

The composite multiplex signals generated by frequency-division methods long standard in telephone communication can be transmitted by the new transcontinental broad-band FM radio relays. Signal intermodulation by echoes must be minimized. Such intermodulation is investigated in this paper experimentally and analytically. Two types of echoes are considered: (1) weak echoes with delays exceeding 0.1 microseconds, caused mainly by mismatched long lines; and (2) powerful echoes with delays shorter than 0.01 microseconds, caused by multipath transmission, and leading to selective fading. By use of random noise signals, the distortion is evaluated as a function of various parameters of the echo, the base-band, and the rf modulation.

Motion of a Ferromagnetic Domain Wall in Fe_3O_4. J. K. GALT[1]. *Phys. Rev.*, **85**, pp. 664–669, Feb. 15, 1952.

Experiments have been made on a sample of Fe_3O_4 cut from a single crystal in such a way that its ferromagnetic domain pattern includes an individual domain wall whose motion can be studied. This sample has a permeability which is high (about 5000) at low frequencies and drops off rapidly above 1000 cycles. A hysteresis loop and data on wall velocity vs applied field were also taken. The data are discussed in terms of recent developments in the theory of the ferromagnetic domain wall. It appears that this theory explains our data satisfactorily, and that in using it to explain our data we determine some of the fundamental magnetic constants of Fe_3O_4. We are also able to gain some insight into domain wall motion in ferrites generally in this way.

The Drift Mobility of Electrons in Silicon. J. R. HAYNES[1] and W. C. WESTPHAL[1]. *Phys Rev.*, **85**, p. 680, Feb. 15, 1952.

Formulas for the Group Sequential Sampling of Attributes. H. L. JONES[4]. *Ann. Math. Statistics*, **23**, pp. 72–87, March, 1952.

Some Fundamental Properties of Transmission Systems. F. B. LLEWELLYN[1]. *Proc. Inst. Radio Engrs.*, **40**, pp. 271–283, March, 1952.

The problem of the minimum loss in relation to the singing point is investigated for generalized transmission systems that must be stable for any combina-

[1] Bell Telephone Laboratories.
[4] Illinois Bell Telephone Company.

tion of passive terminating impedances. It is concluded that the loss may approach zero db only in those cases where the image impedances seen at the ends of the system are purely resistive. Moreover, in such cases, the method of overcoming the transmission loss, whether by conventional repeaters or by series and shunt negative impedance loading, or otherwise, is quite immaterial to the external behavior of the system as long as the image impedances are not changed. The use of impedance-correcting networks provides one means of insuring that the phase of the image impedance of the over-all system approaches zero. General relations are derived which connect the image impedance and the image gain of an active system with its over-all performance properties.

The Arithmetic of Ménage Numbers. J. RIORDAN[1]. *Duke Math. Jl.*, **19**, pp. 27–30, March, 1952.

A Recurrence Relation for Three-Line Latin Rectangles. J. RIORDAN[1]. *Am. Math. Monthly*, **59**, pp. 159–162, March, 1952.

Capacitors and Communications. Inductive Coordination of Lines. A. R. WAEHNER[5] and W. E. BLOECKER[2]. *Elec. Light and Power*, **30**, pp. 105–108, 114, March, 1952.

Although the use of capacitors on power lines has been expanding, their use has caused relatively few cases of noise on communication lines and these have been satisfactorily corrected. The causes of trouble and remedial measures were the subject of a recent, joint E.E.I.-Bell System study described here.

Book Reviews

ANTENNAS: THEORY AND PRACTICE. By Sergei A. Schelkunoff and Harald T. Friis, 639 + xxii pages, John Wiley and Sons, Inc., New York (1952). Price: $10.00.

This is a recent addition to Wiley's Applied Mathematics Series edited by I. S. Sokolnikoff. It contains a thorough and balanced treatment of electromagnetic radiation and electrical properties of various types of antennas. In these days of rapid expansion of microwave engineering it would have been easy to neglect the older and less glamorous long-wave and short-wave antennas. The authors are to be congratulated on their impartiality. The exposition is lucid. While the entire quantitative theory of antennas is based on Maxwell's equations, unnecessary mathematics is conspicuous by its absence, and physical explanations are abundant.

The book begins with a long chapter on Physical Principles of Radiation. This chapter is almost a book within the book. It touches upon the most important ideas and problems of antenna analysis and contains a number of simple but useful formulas. Circuit and field concepts are compared, and the similarities as well as the differences between them are exhibited. Maxwell's equations are stated in a form which is particularly easy to understand. In this form, one

[1] Bell Telephone Laboratories.
[2] American Telephone and Telegraph Company.
[5] Line Material Company.

equation expresses a relation between the average electric intensity tangential to a given curve and the time rate of change of the average magnetic intensity normal to a surface bounded by this curve. The other equation expresses a complementary relation. The reader will be impressed by a simple physical picture from which the authors are able to derive the expression for the radiation field of a short antenna. In this chapter they discuss the effect of heat loss and impedance mismatch on the efficiency of antennas. Among other topics will be found directive radiation and reception, large antenna arrays, horns, reflectors, and lenses.

After this extended general introduction a more detailed analysis of various problems begins. Chapter 2 is devoted to Maxwell's equations and Chapter 3 to plane waves on conductors and in free space. The main topic in Chapter 4 is the derivation of the expressions for the complete field surrounding a short antenna from Maxwell's equations. The authors have made a special effort to show the connection between this field and the oscillating charge in the antenna.

Applications of this basic theory begin with Chapter 5 devoted to directive radiation. This chapter is concerned with radiation patterns of various arrays and with calculation of radiated power. A novel method, the *method of momonts* (pp. 162–195), is likely to prove valuable when spatial distributions of antenna current are complicated (as in the case of shunt-fed antennas). Chapter 6 explains methods for calculating directivites and effective areas of antennas. Some ground effects are considered briefly in Chapter 7. In Chapter 8, the discussion of current distributions in antennas made up of thin wires is particularly thorough. First, simple approximations are developed; then the effects of various factors are carefully examined. Various reciprocity and circuit equivalence theorems, so useful in antenna analysis, are collected in Chapter 9.

Beginning with Chapter 10 the general theory is applied to specific antenna types. Thus, small antennas are treated in Chapter 10; quarter-wave, half-wave and full-wave antennas in Chapter 11; general dipole antennas in Chapters 12 and 13; rhombic antennas in Chapter 14; miscellaneous types of wire antennas in Chapter 15; horn antennas in Chapter 16; slot antennas in Chapter 17; reflectors in Chapter 18; and lenses in Chapter 19.

Practical engineers will be delighted with the appendices which contain in a compact form some of the most useful information about transmission lines, dipole antennas, antenna arrays, optimum horns, and lenses. Teachers will welcome the numerous problems scattered throughout the book.

ADVANCED ANTENNA THEORY. By Sergei A. Schelkunoff, 216 + xii pages, John Wiley and Sons, Inc., New York (1952). Price: $6.50.

This book is a recent addition to Wiley's Applied Mathematics Series edited by I. S. Sokolnikoff. It is concerned with recent advances in antenna theory and is divided into six chapters. General expressions in spherical coordinates are derived for electromagnetic fields in free space and in the presence of conducting cones and thin wires diverging from a common point. In Chapter 2 these expressions are applied to dipole antennas, vee antennas, end-fed antennas, etc. Chapter 3 gives an account of Stratton and Chu's theory of spheroidal antennas. Integral equations in antenna theory and Hallen's method of their solution are treated in Chapters 4 and 5. The book is concluded with a chapter on natural oscillations in antennas. A substantial number of problems and several interesting appendices will be found at the end.

Contributors to this Issue

Sidney Darlington, B.S., Harvard University, 1928; B.S. in E.E., Massachusetts Institute of Technology, 1929; Ph.D., Columbia University, 1940. Bell Telephone Laboratories, 1929–. Dr. Darlington has been engaged in research in applied mathematics with emphasis on network theory.

Paul G. Edwards, B.E.E., Ohio State University, 1924; E.E., Ohio State University, 1929. Western Union Telegraph Company, 1919–22; American Telephone and Telegraph Company, 1922–34; Bell Telephone Laboratories, 1934–. His main concern in the Laboratories has been with toll transmission problems, including voice frequency and carrier systems. Member of the I.R.E., A.I.E.E., Sigma Xi, Tau Beta Pi, and Eta Kappa Nu.

C. W. Harrison, B.S. in E.E., Purdue University, 1938; M.S., Lehigh University, 1940. Bamberger Broadacasting Company, 1939–41. Bell Telephone Laboratories, 1941–. Mr. Harrison is a member or the televison research group. He formerly designed radio receivers and, later, microwave relay repeaters. Member of the I.R.E.

John L. Hysko, B.S. in E.E., Cooper Union, 1921. U. S. Army, 1918–19. Bell Telephone Laboratories, 1919–. Mr. Hysko's principal activities in the Laboratories have been in the development of amplitude-modulation and frequency-shift carrier telegraph systems for land line, radio teletypewriter and submarine cable applications.

Edwin F. Kingsbury, B.S., Colgate University, 1910. United Gas Improvement Company, 1910–18. U. S. Army, 1918–19. Eastman Kodak Company, 1919–20. Bell Telephone Laboratories, 1920–51. Mr. Kingsbury retired in 1951 after a career which was primarily concerned with television research and development, especially that part dealing with photoelectric and electrooptical problems. Member of the Franklin Institute, the Optical Society of America, and Phi Beta Kappa; Fellow of the American Physical Society and the American Association for the Advancement of Science.

ERNEST R. KRETZMER, B.S., Worcester Polytechnic Institute, 1944; M.S., Massachusetts Institute of Technology, 1946; Sc.D., Massachusetts Institute of Technology, 1949. As a member of the Electrical Engineering Department at Massachusetts Institute of Technology, Dr. Kretzmer taught from 1944–46 and conducted research there from 1946–49. Bell Telephone Laboratories, 1949–. He works in the televison research group, where he has been principally concerned with decorrelation of television signals. Member of I.R.E. and Sigma Xi.

L. R. MONTFORT, E.E., University of Virginia, 1926; American Telephone and Telegraph Company 1926–34; Bell Telephone Laboratories, 1934–. Mr. Montfort has been concerned with the engineering of carrier systems. This has included field work with new systems and field tests prior to the design of new systems. During the end of World War II and for a short time thereafter, he assisted in the engineering and testing of microwave radio systems. Member of A.I.E.E., Tau Beta Pi, Theta Tau, and Sigma Phi Epsilon.

RUSSELL S. OHL, B.S. in Electro-Chemical Engineering, Pennsylvania State College, 1918; U. S. Army, 1918 (2nd Lieutenant, Signal Corps); Vacuum tube development, Westinghouse Lamp Company, 1919–21; Instructor in Physics, University of Colorado, 1921–1922. Department of Development and Research, American Telephone and Telegraph Company, 1922–27; Bell Telephone Laboratories, 1927–. Mr. Ohl has been engaged in various exploratory phases of radio research, the results of which have led to numerous patents. For the past ten or more years he has been working on some of the problems encountered in the use of millimeter radio waves. Member of American Physical Society and Alpha Chi Sigma and Senior Member of the I.R.E.

B. M. OLIVER, B.A., Stanford University, 1935; M.S., California Institute of Technology, 1936; Ph.D., California Institute of Technology, 1939. Bell Telephone Laboratories, 1939–52. During World War II, Dr. Oliver was engaged in radar research and the rest of his employment before leaving the laboratories was in the television research group. Member of I.R.E. and Phi Beta Kappa.

WILTON T. REA, B.S., Princeton University, 1926; American Telephone and Telegraph Company, 1926–34; Bell Telephone Laboratories, 1934–. Except for the years 1941–45, when he worked on military projects. Mr. Rea has been principally concerned with telegraphy. As Tele-

graph Development Engineer, he is in charge of the development of telegraph and telephotograph systems. Senior member of I.R.E. and member of A.I.E.E. and Phi Beta Kappa.

L. C. Roberts, A.B., Harvard University, 1916; B.S. in E.E., Harvard University, 1919; B.S. in E.E., Massachusetts Institute of Technology, 1918; American Telephone and Telegraph Company, 1917–34; Bell Telephone Laboratories, 1934–. Mr. Roberts has been primarily concerned with the development of dc and carrier telegraph except during World War II when he worked on multichannel and single-channel radio teletypewriter developments. Member of A.I.E.E.

S. A. Schelkunoff, B.A., M.A. in Mathematics, The State College of Washington, 1923; Ph.D. in Mathematics, Columbia University, 1928. Engineering Department, Western Electric Company, 1923–25; Bell Telephone Laboratories, 1925–26. Department of Mathematics, State College of Washington, 1926–29. Bell Telephone Laboratories, 1929–. Dr. Schelkunoff has been engaged in mathematical research, especially in the field of electromagnetic theory.